

EARLY TRANSITION METAL COMPLEXES CONTAINING TRIDENTATE AMIDO
LIGANDS. A SYSTEMATIC APPROACH TO ZIEGLER-NATTA CATALYSIS.

by

LAN-CHANG LIANG

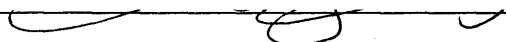
M.S. in Chemistry, National Sun Yat-sen University, Taiwan, R.O.C.
(1992)

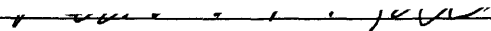
B.S. in Chemistry, National Sun Yat-sen University, Taiwan, R.O.C.
(1990)

Submitted to the Department of Chemistry
in Partial Fulfillment of the Requirements
for the Degree of

DOCTOR OF PHILOSOPHY
at the
MASSACHUSETTS INSTITUTE OF TECHNOLOGY
September 1999

© Massachusetts Institute of Technology, 1999

Signature of Author  Department of Chemistry
June 28, 1999

Certified by  Richard R. Schrock
Thesis Supervisor

Accepted by _____ Robert W. Field
Chairman, Departmental Committee on Graduate Students in Chemistry

This doctoral thesis has been examined by a Committee of the Department of Chemistry as follows:

Professor Christopher C. Cummins _____
Chairman

Professor Richard R. Schrock _____
Thesis Supervisor

Professor Stephen J. Lippard _____

To my parents,
Hsiu-Ling, and Jia-Yu

EARLY TRANSITION METAL COMPLEXES CONTAINING TRIDENTATE AMIDO
LIGANDS. A SYSTEMATIC APPROACH TO ZIEGLER-NATTA CATALYSIS.

by
LAN-CHANG LIANG

Submitted to the Department of Chemistry, September 1999
in Partial Fulfillment of the Requirements
for the Degree of Doctor of Philosophy in Chemistry

ABSTRACT

Chapter 1

The synthesis of group 4 complexes containing diamido/ether ligands, $[(RN-o-C_6H_4)_2O]^{2-}$ ($[RNON]^{2-}$; R = Cy, Bde, Mes), is presented. These ligands are obtained straightforwardly from the reaction of $O(o-C_6H_4NH_2)_2$ with cyclohexanone, 1,2-bis(chlorodimethylsilyl)ethane, and mesityl bromide, respectively. The reactions between *in situ* prepared $Li_2[RNON]$ (R = Cy, Bde, Mes) and $TiCl_2(NMe_2)_2$ yield $[RNON]Ti(NMe_2)_2$ (R = Cy, Bde, Mes), which subsequently reacts with Me_3SiCl to give $[RNON]TiCl_2$ (R = Cy, Bde) and $[MesNON]TiCl(NMe_2)$. Zirconium and hafnium dichloride complexes, $[RNON]MCl_2$ (M = Zr, R = Cy, Mes; M = Hf, R = Mes), are readily obtained from the reactions between $H_2[RNON]$ and $M(NMe_2)_4$ followed by addition of Me_3SiCl . Several dialkyl complexes containing $[CyNON]^{2-}$ and $[MesNON]^{2-}$ are readily prepared by alkylation of the dichlorides, including β -hydrogen containing dialkyl complexes. An X-ray study of $[MesNON]HfNp_2$ reveals an approximately square pyramidal structure with one neopentyl ligand on the apical position. Decomposition of $[CyNON]Zr(CH_2CHR_2)_2$ (R = H, Me) in the presence of PMe_3 yields $[CyNON]Zr(\eta^2-C_2H_2R_2)(PMe_3)_2$. Activated $[CyNON]ZrMe_2$ and $[MesNON]ZrMe_2$ react with 1-hexene catalytically, but β hydrogen elimination or β hydrogen transfer relative to chain propagation is significant in either case. $H_2[BdeNON]$ reacts with ZrR_4 (R = CH_2Ph , CH_2SiMe_3) and $Zr(NMe_2)_4$ to give $Zr[BdeNON]_2$ and $[BdeNON]Zr(NMe_2)_2(HNMe_2)$, respectively. Addition of pyridine or 2,4-lutidine to $[BdeNON]Zr(NMe_2)_2(HNMe_2)$ produces $[BdeNON]Zr(NMe_2)_2(L)$ (L = py, lut), which is readily converted to $[BdeNON]ZrCl_2(py)$ with Me_3SiCl . Addition of one equivalent of Cp^*Li or two equivalents of $RMgCl$ (R = CH_2SiMe_3 , CH_2CMe_2Ph) to $[BdeNON]ZrCl_2(py)$ yields $[BdeNON]ZrCp^*Cl$ and $[BdeNON][BdeNON']Zr_2R_2$, respectively. An X-ray study of $[BdeNON][BdeNON']Zr_2(CH_2SiMe_3)_2$ shows it to contain a bridging methine between the two zirconium centers as a consequence of double C-H activation of $SiCH_3$ in $[BdeNON]^{2-}$.

Chapter 2

A series of tridentate amido ligands including diamido/ether $[(RNCH_2CH_2)_2O]^{2-}$ ($[RN_2O]^{2-}$; R = t-Bu, Ad, Ph, Ar; Ar = 2,6-C₆H₃Me₂), diamidoamine $[(C_6F_5NCH_2CH_2)_2NR]^{2-}$ ($[Ar^FN_2NR]^{2-}$; R = H, Me), and triamido $[(ArylNCH_2CH_2)_2N]^{3-}$ ($[ArylN_2N]^{3-}$; Aryl = Ar^F, Mes) are employed for the synthesis of group 5 complexes. TaMe₅ reacts with H₂[RN₂O] (R = t-Bu, Ad, Ph, Ar) and H₂[MesN₂NH] to yield $[RN_2O]TaMe_3$ and $[MesN_2N]TaMe_2$, respectively. Reaction between TaMe₅ and H₂[Ar^FN₂NH] yields $[Ar^FN_2NH]TaMe_3$, which subsequently eliminates methane to give $[Ar^FN_2N]TaMe_2$. The NMR spectra of $[Ar^FN_2N]TaMe_2$ reveal a quintet resonance for the methyl ligands as a consequence of the interaction with four fluorine atoms in the C₆F₅ rings. An X-ray study of $[Ar^FN_2N]TaMe_2$ shows it to have a trigonal bipyramidal structure with $[Ar^FN_2N]^{3-}$ being virtually planar and a close contact between tantalum and *ortho* fluorine atoms (average 2.432 Å). Dimethyl $[MesN_2N]MMe_2$ (M = Ta, Nb) can be synthesized directly from metal pentachlorides, H₂[MesN₂NH], and five equivalents of MeLi or MeMgI. Reaction between MeLi and $[Ar^FN_2NH]TaMe_3$ followed by addition of MeOTf yields $[Ar^FN_2NMe]TaMe_3$. Several cationic tantalum dimethyl complexes are isolated. An X-ray study of $\{[Ar^FN_2NH]TaMe_2\}\{MeB(C_6F_5)_3\}$ reveals a *mer* structure for the diamidoamine ligand with the amino nitrogen being only modestly distorted from planarity. No reaction is observed between 1-hexene and the cationic tantalum complexes reported in this chapter.

Chapter 3

The catalyst design for α -olefin polymerization involves group 4 complexes containing diamidoamine ligands, $[(MesNCH_2CH_2)_2NR]^{2-}$ ($[MesN_2NR]^{2-}$; R = H, alkyl). Reaction between Zr(NMe₂)₄ and H₂[MesN₂NH] produces $[MesN_2NH]Zr(NMe_2)_2$. The NH proton in $[MesN_2NH]Zr(NMe_2)_2$ can be removed by MeLi; subsequent addition of MeI, PhCH₂Br, or C₆F₅CH₂Br produces $[MesN_2NR]Zr(NMe_2)_2$ (R = Me, Bn, Bn^F). Dihalide $[MesN_2NR]ZrX_2$ (R = H, Me, Bn, Bn^F; X = Cl, I) is readily obtained by treatment of $[MesN_2NR]Zr(NMe_2)_2$ with MeI or Me₃SiCl; subsequent alkylation yields mono- or dialkyl complexes such as $[MesN_2NH]ZrMe_2$, $[MesN_2NH]ZrNpCl$, and $[MesN_2NMe]ZrMe_2$. The dimethyl $[MesN_2NH]MMe_2$ (M = Ti, Zr, Hf) can also be synthesized by formation of an adduct between H₂[MesN₂NH] and metal tetrachlorides followed by addition of four equivalents of methyl Grignard reagents. Deprotonation followed by electrophilic alkylation of the amino nitrogen in $[MesN_2NH]MMe_2$ yields $[MesN_2NR]MMe_2$ (M = Ti, R = Me; M = Zr, R = Me, Bn, Bn^F). An analogous dibenzyl $[MesN_2NMe]Zr(CH_2Ph)_2$ is obtained in a similar manner. X-ray studies of $[MesN_2NH]ZrMe_2$ and $[MesN_2NMe]ZrMe_2$ reveal a *mer* structure for these diamidoamine ligands and the amino nitrogen in $[MesN_2NMe]^{2-}$ is virtually tetrahedral. Activated $[MesN_2NR]ZrMe_2$ (R = H, Me, Bn, Bn^F) complexes are active

catalysts for polymerization of 1-hexene. The number average molecular weight of poly(1-hexene) obtained with $[\text{Ph}_3\text{C}][\text{B}(\text{C}_6\text{F}_5)_4]$ activated $[\text{MesN}_2\text{NH}]\text{ZrMe}_2$ maximizes at ~ 17000 , while that with $[\text{MesN}_2\text{NMe}]\text{ZrMe}_2$ at ~ 28000 . Molecular weight distribution is found in the range of 1.1-1.5. Controlled polymerization with the $[\text{MesN}_2\text{NMe}]\text{ZrMe}_2$ initiator reveals that the cationic species is active up to $30\text{ }^\circ\text{C}$.

Thesis Supervisor: Dr. Richard R. Schrock

Title: Frederick G. Keyes Professor of Chemistry

TABLE OF CONTENTS

	page
Title Page	1
Signature Page	2
Dedication	3
Abstract	4
Table of Contents	7
List of Figures	10
List of Schemes	11
List of Tables	12
List of Abbreviation Used in Text	13
 General Introduction	 16
 Chapter 1 Synthesis of Group 4 Complexes Containing Diamido/ether Ligands	
Introduction	19
Specific Goals	20
Results	
1.1 Synthesis of $H_2[RNON]$ ($R = Cy, Bde, Mes$).	21
1.2 Entry into titanium chemistry; reactions involving $TiCl_2(NMe_2)_2$.	23
1.3 Reactions between $[RNON]Ti(NMe_2)_2$ and Me_3SiCl ($R = Cy, Bde, Mes$).	24
1.4 Entry into zirconium and hafnium chemistry; reactions involving $M(NMe_2)_4$ ($M = Zr, Hf$).	25
1.5 Synthesis of dialkyl complexes containing $[CyNON]^{2-}$ and $[MesNON]^{2-}$.	28
1.6 X-ray structure of $[MesNON]HfNp_2$.	30
1.7 Alkylation of dichloride complexes containing $[BdeNON]^{2-}$.	32
1.8 X-ray structure of $[BdeNON][BdeNON']Zr_2(CH_2SiMe_3)_2$.	34
1.9 Reaction between $H_2[BdeNON]$ and ZrR_4 ($R = Bn, CH_2SiMe_3$).	36
1.10 Thermal stability of alkyl complexes.	37
1.11 Decomposition of $[CyNON]ZrR_2$ ($R = Et, i-Bu$) in the presence of PMe_3 .	38
1.12 Generation of cations and their reactions with 1-hexene.	39
Discussion	42
Conclusions	44
Experimental Section	

E.1.1	[CyNON] ²⁻ ligand system.	46
E.1.2	[BdeNON] ²⁻ ligand system.	56
E.1.3	[MesNON] ²⁻ ligand system.	62
Chapter 2	Synthesis of Group 5 Complexes Containing Tridentate Amido Ligands	
Introduction		71
Specific Goals		72
Results		
2.1	Design and synthesis of triamines.	73
2.2	Synthesis of diamine/ether ligands, H ₂ [RN ₂ O] (R = t-Bu, Ad, i-Pr, Ph, 2-t-BuC ₆ H ₄).	74
2.3	Reactions between TaMe ₅ and H ₂ [MesN ₂ NH] or H ₂ [RN ₂ O] (R = t-Bu, Ad, Ph, Ar).	75
2.4	Reaction between TaMe ₅ and H ₂ [Ar ^F N ₂ NH].	77
2.5	X-ray structure of [Ar ^F N ₂ N]TaMe ₂ .	79
2.6	Deprotonation-alkylation of [Ar ^F N ₂ NH]TaMe ₃ .	82
2.7	Direct synthesis of dialkyl tantalum and niobium complexes containing [MesN ₂ N] ³⁻ .	83
2.8	Synthesis of mixed-alkyl complexes.	85
2.9	Observation and isolation of cationic tantalum complexes.	85
2.10	X-ray structure of {[Ar ^F N ₂ NH]TaMe ₂ } {MeB(C ₆ F ₅) ₃ }.	87
2.11	Reaction between LiNMe ₂ and cationic {[Ar ^F N ₂ NH]TaMe ₂ } ⁺ .	90
2.12	Reaction between PhNH ₂ and [Ar ^F N ₂ N]TaMe ₂ .	91
Discussion		93
Conclusions		98
Experimental Section		
E.2.1	[MesN ₂ N] ³⁻ ligand system.	100
E.2.2	[RN ₂ O] ²⁻ ligand system (R = alkyl, aryl).	102
E.2.3	[Ar ^F N ₂ NH] ²⁻ or [Ar ^F N ₂ N] ³⁻ ligand system.	113
Chapter 3	Synthesis of Group 4 Complexes Containing Diamidoamine Ligands and the Polymerization of 1-Hexene by Activated Zirconium Dimethyl Complexes	
Introduction		120
Specific Goals		121
Results		
3.1	Synthesis of H ₂ [MesN ₂ NH].	121

3.2	Synthesis of [MesN ₂ NH]ZrCl ₂ .	122
3.3	Alkylation of [MesN ₂ NH]ZrCl ₂ .	123
3.4	Synthesis of zirconium dialkyl complexes involving deprotonation-alkylation sequence.	124
3.5	Comparison of the thermal stability of dimethyl [MesN ₂ NR]ZrMe ₂ (R = H, Me, Bn, Bn ^F).	126
3.6	Synthesis of zirconium dialkyl complexes involving triflate intermediates.	127
3.7	X-ray structures of [MesN ₂ NH]ZrMe ₂ and [MesN ₂ NMe]ZrMe ₂ .	128
3.8	Direct synthesis of group 4 dialkyl complexes containing [MesN ₂ NR] ²⁻ (R = H, alkyl).	132
3.9	Polymerization of 1-hexene by activated [MesN ₂ NR]ZrMe ₂ (R = H, Me, CH ₂ Ph, CH ₂ C ₆ F ₅). Preliminary information obtained from NMR experiments.	134
3.10	Bulk polymerization of 1-hexene by trityl activated [MesN ₂ NR]ZrMe ₂ (R = H, Me).	134
3.11	Thermal stability investigation of the propagating species.	136
	Discussion	139
	Conclusions	147
	Experimental Section	148
Appendix	X-ray Crystallographic data: Structural Parameters and Atomic Coordinates.	164
References		175
Acknowledgments		185

List of Figures

	Page
Chapter 1	
Figure 1.1 An ORTEP drawing of the structure of [MesNON]HfNp ₂ , with selected bond lengths, bond angles, and dihedral angles.	31
Figure 1.2 The structure of {cyclo-ZrCHSiMe ₂ NSiMe ₃ [N(SiMe ₃) ₂]} ₂ .	33
Figure 1.3 An ORTEP drawing of the structure of [BdeNON][BdeNON']Zr ₂ (CH ₂ SiMe ₃) ₂ , with selected bond lengths and bond angles.	35
Figure 1.4 The olefin region of the ¹ H NMR spectrum of the reaction between 1-hexene (50 equivalents) and {[CyNON]ZrMe(NMe ₂ Ph)}[B(C ₆ F ₅) ₄] at 0 °C.	39
Figure 1.5 The olefin region of the ¹ H NMR spectrum (C ₂ D ₂ Cl ₄ , 120 °C) of low molecular weight polypropylene prepared from MAO activated rac-[ethylene(1-indenyl) ₂]ZrCl ₂ .	40
Figure 1.6 The ¹ H NMR spectra (500 MHz) of the reactions between 1-hexene (60 equivalents) and [Ph ₃ C]{B(C ₆ F ₅) ₄ } activated [CyNON]ZrMe ₂ (top) or [MesNON]ZrMe ₂ (bottom) in C ₆ D ₅ Br at 0 °C.	41
Chapter 2	
Figure 2.1 An ORTEP drawing of the structure of [Ar ^F N ₂ N]TaMe ₂ , with selected bond lengths, bond angles, and dihedral angles.	80
Figure 2.2 An ORTEP drawing of the structure of {[Ar ^F N ₂ NH]TaMe ₂ }{MeB(C ₆ F ₅) ₃ }, with selected bond lengths and bond angle in the anion.	88
Figure 2.3 An ORTEP drawing of the structure of cationic {[Ar ^F N ₂ NH]TaMe ₂ } ⁺ , with selected bond lengths, bond angles, and dihedral angles.	89
Figure 2.4 The coordinate system for trigonal bipyramidal complexes. The three p orbitals parallel to the x axis correspond to the three p orbitals on the nitrogen atoms.	94
Chapter 3	
Figure 3.1 An ORTEP drawing of the structure of [MesN ₂ NH]ZrMe ₂ , with selected bond lengths, bond angles, and dihedral angles.	129
Figure 3.2 An ORTEP drawing of the structure of [MesN ₂ NMe]ZrMe ₂ , with selected bond lengths, bond angles, and dihedral angles.	130

List of Schemes

	Page
General Introduction	
Scheme 0.1 Representation of a family of tridentate amido ligands.	17
Chapter 1	
Scheme 1.1 The diamido/ether ligands employed in this study.	21
Scheme 1.2 Synthesis of the diamido/ether ligands.	22
Chapter 2	
Scheme 2.1 A portion of the ^{13}C NMR spectra of $[\text{Ar}^{\text{F}}\text{N}_2\text{N}]\text{TaMe}_2$ (22 °C, CD_2Cl_2); only the TaMe and one CH_2 resonances are shown. Top: proton-coupled fluorine-coupled ^{13}C NMR spectrum ($J_{\text{CF}} = 5.0$ Hz). Bottom: proton-coupled fluorine-decoupled ^{13}C NMR spectrum.	78
Chapter 3	
Scheme 3.1 Synthesis of $[\text{MesN}_2\text{NMe}]\text{ZrMe}_2$ <i>via</i> triflate intermediates.	127
Scheme 3.2 Representative literature examples of five coordinate group 4 complexes containing the diamido/ N_{donor} ligands.	140
Scheme 3.3 The proposed fluxional process in $[\text{t-BuNON}]\text{MMe}_2$ ($\text{M} = \text{Ti}, \text{Zr}$)	140
Scheme 3.4 Proposed resonance contributors of the presumed cationic monoalkyl zirconium complex containing the diamidoamine ligands.	146

List of Tables

	Page
Chapter 1	
Table 1.1 Synthesis of dialkyl complexes according to equation 1.9.	29
Chapter 2	
Table 2.1 A comparison of core bond lengths and angles in five coordinate Ta and Zr complexes containing tridentate amido ligands having a <i>mer</i> structure.	81
Table 2.2 Synthesis of cationic tantalum dimethyl complexes according to equation 2.16.	86
Chapter 3	
Table 3.1 A comparison of some bond lengths and angles in the five-coordinate diamido/ N_{donor} complexes with a <i>mer</i> geometry.	131
Table 3.2 Characterization of the poly(1-hexene) prepared with $[\text{MesN}_2\text{NR}]\text{ZrMe}_2$ initiators.	135
Table 3.3 Poly(1-hexene) prepared with trityl-activated $[\text{MesN}_2\text{NMe}]\text{ZrMe}_2$ under controlled conditions.	137
Table 3.4 Comparison of the poly(1-hexene) data obtained with $[\text{ArN}_2\text{O}]\text{ZrMe}_2$, $[\text{ArN}_2\text{S}]\text{ZrMe}_2$, and $[\text{MesN}_2\text{NR}]\text{ZrMe}_2$ ($\text{R} = \text{H}, \text{Me}$) initiators.	144

List of Abbreviations Used in the Text

Ad	1-Adamantyl
Anal.	Analysis
Ar	2,6-dimethylphenyl
Ar ^F	pentafluorophenyl
Aryl	generalized aromatic groups
Bn	Benzyl
Bn ^F	2,3,4,5,6-pentafluorobenzyl
br	broad
Calcd.	Calculated
C _{ipso}	ipso carbon atom in an aromatic ring
C _m	<i>meta</i> carbon atom in an aromatic ring
C _o	<i>ortho</i> carbon atom in an aromatic ring
C _p	Cyclopentadienyl
C _p	<i>para</i> carbon atom in an aromatic ring
Cp*	Pentamethylcyclopentadienyl
Cy	Cyclohexyl
C _α	carbon atom(s) attached on transition metals
cat.	catalytic amount
cm ⁻¹	wavenumber
DME	1,2-Dimethoxyethane
d	doublet
deg; (°)	degree
EI	Electron Impact
Et	Ethyl
eV	electron volt
equiv.	equivalent(s)
F _m	fluorine atom on C _m
F _o	fluorine atom on C _o
F _p	fluorine atom on C _p
<i>fac</i>	<i>facial</i>
GPC	Gel Permeation Chromatography
g	grams
H _m	proton atom on C _m

H _o	proton atom on C _o
H _p	proton atom on C _p
HRMS	High Resolution Mass Spectroscopy
Hz	Hertz; sec ⁻¹
h	hour(s)
IR	Infrared
i-Bu	iso-Butyl
i-Pr	iso-Propyl
<i>J</i>	coupling constant in Hertz
L	generalized 2e neutral ligands
M	generalized transition or main group metals
MAO	methylaluminoxane, (MeAlO) _n
Me	Methyl
Me _o	Methyl group on C _o
Me _p	Methyl group on C _p
Mes	Mesityl; 2,4,6-trimethylphenyl
M _n	number average molecular weight
M _w	weight average molecular weight
m	multiplet
min	minute(s)
<i>mer</i>	<i>meridional</i>
NMR	Nuclear Magnetic Resonance
N _{amide}	Nitrogen donor in an amido ligand
N _{amine}	Nitrogen donor in an amino ligand
N _{ax}	Nitrogen atom(s) on axial position(s)
N _{donor}	Nitrogen-based donor ligands, including sp ² - and sp ³ - hybridized nitrogen atom(s)
N _{eq}	Nitrogen atom(s) on equatorial position(s)
N _{imide}	Nitrogen donor in an imido ligand
Np	Neopentyl; 2,2-dimethylpropyl
n-Bu	n-Butyl
OAc	Acetate
ORTEP	Oak Ridge Thermal Elipsoid Plot
OTf	Triflate; trifluoromethanesulfonate; CF ₃ SO ₃
OTs	Tosylate; <i>p</i> -toluenesulfonate; <i>p</i> -CH ₃ C ₆ H ₄ SO ₃
<i>o</i> -	<i>ortho</i>

Ph	Phenyl
ppm	parts per million
py	pyridine
<i>p</i> -	<i>para</i>
q	quartet
R	generalized alkyl groups, including hydrogen and aryl sometimes when specified
rac-	racemic-
rac-BINAP	racemic-2,2'-bis(diphenylphosphino)-1,1'-binaphthyl
s	singlet
st.	stretch
THF	tetrahydrofuran
T _c	coalescence temperature
t	triplet
t-Bu	tert-Butyl
X	generalized 2e monoanionic ligands
[RN ₂ L] ²⁻	dianionic diamido/donor ligands containing ethylene backbone and amido substituent R; [(RNCH ₂ CH ₂) ₂ L] ²⁻ (L = O, S, NR', PR'; R, R' = alkyl, aryl)
[RNLN] ²⁻	dianionic diamido/donor ligands containing <i>o</i> -phenylene backbone and amido substituent R; [(RN- <i>o</i> -C ₆ H ₄) ₂ L] ²⁻ (L = O, S, NR', PR'; R, R' = alkyl, aryl)
Δδ	difference in chemical shift (Hz) for a static state structure
Å	Angstrom; 10 ⁻¹⁰ m
δ	chemical shift downfield from tetramethylsilane
η	descriptor for hapticity

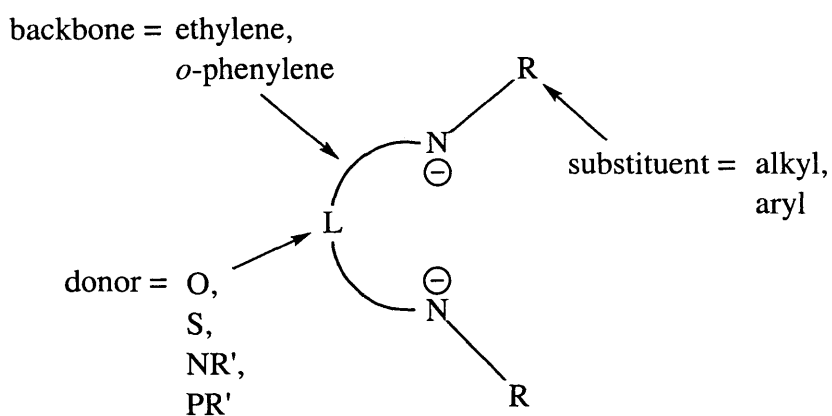
General Introduction

Since the structure of "the iron sandwich" was discovered in 1952,^{1,2} Cp and its derivatives (mostly Cp*) have been used tremendously in organometallic chemistry.³⁻⁹ Subsequently, a rich harvest in Cp chemistry from an unusual number of interdisciplinary chemists has been reaped.³⁻¹⁹ The search for alternatives to Cp-based ligand systems which can facilitate the isolation of new transition-metal, lanthanide, and actinide complexes has been of great interest in the last decade.²⁰⁻²² Particularly successful have been the sterically bulky chelating $[(R_2PCH_2SiMe_2)_2N]^-$,²³ $[(RNCH_2CH_2)_3N]^{3-}$,²⁴⁻²⁷ and $[(RNCH_2)_3CR']^{3-}$ ²⁸⁻³¹ amide ligands which form a variety of complexes across the d- and f-block elements.

Group 4 metallocenes have been the catalysts to produce polyolefins commercially since the early 1990s.^{8,32-35} The search for alternative ligands for group 4 metallocenes has focused on nitrogen-containing ligands such as porphyrins,³⁶⁻³⁸ tetraaza macrocycles,³⁹⁻⁴² tetradentate Schiff bases,⁴³⁻⁴⁶ *o*-phenylenediamides,⁴⁷ (hydroxyphenyl)oxazolines,⁴⁸ and benzamidinates.⁴⁹ However, no significant ethylene polymerization activities have been reported. The polymerization activity of putative $[Cp_2ZrR]^+$ with ethylene is high, but that with α -olefins is relatively slow. A linked Cp-amide complex such as $\{[(\eta^5-C_5Me_4)SiMe_2(N-t-Bu)]TiR\}^+$ incorporates α -olefins more readily,⁵⁰ presumably due to the more accessible coordination sphere and higher electrophilicity of the cation. Chelating diamide ligands have shown to stabilize the propagating species during the polymerization. Activated $(ArylNCH_2CH_2CH_2NAryl)_2TiMe_2$ ⁵¹ and $[t-BuNON]ZrMe_2$ ^{52,53} reveal the living polymerization of 1-hexene under appropriate conditions.

We became interested in investigating tridentate amido chemistry for early transition metals. Scheme 0.1 illustrates the family of the tridentate amido ligands. A systematic ligand design involves the variation of amido substituents, ligand backbones, and the donor atom/groups. Abbreviations $[RN_2L]^{2-}$ and $[RNLN]^{2-}$ (R = alkyl, aryl; L = O, S, NR', PR') are used to represent the diamido/donor ligands which contain ethylene and *o*-phenylene backbone, respectively. The ligands employed in this thesis focus on diamido/ether and diamidoamine derivatives. The

synthesis of group 4 and 5 complexes is presented. In group 5 chemistry, trianionic triamido ligands, $[\text{RN}_2\text{N}]^{3-}$ and $[\text{RNNN}]^{3-}$, are also investigated (only $[\text{RN}_2\text{N}]^{3-}$ is discussed). Activated dimethyl complexes are primarily used to investigate the catalytic activity of α -olefin polymerization. 1-Hexene is chosen to be the monomer for polymerization on the basis of the precise control of its stoichiometry and the better solubility of poly(1-hexene) in common solvents as compared to poly(ethylene).



Scheme 0.1. Representation of a family of tridentate amido ligands.

Chapter 1 begins with the synthesis of group 4 complexes containing diamido/ether ligands followed by the catalytic reactions of the activated zirconium dimethyl complexes with 1-hexene. Chapter 2 covers group 5 chemistry based on tridentate amido ancillaries, including the diamido/ether, diamidoamine, and triamido ligands. In chapter 3, the synthesis of group 4 complexes containing diamidoamine ligands is presented, as well as the polymerization of 1-hexene by activated zirconium dimethyl complexes. The goals of this thesis are two-fold: (1) to demonstrate that the organometallic chemistry derived from the diamido/donor ligand system can be as abundant and as significant as metallocene chemistry, with the advantage that the former is far easier to functionalize; (2) to show that the catalytic polymerization activity of these tridentate

amido complexes with 1-hexene can be fine-tuned by changing the steric and electronic properties of the ligands and by employing different transition metals. A great deal of chemistry in this thesis focuses on structure investigation in both solid state and in solution in order to understand the relationship between the structures of these organometallic complexes and polymerization catalysis.

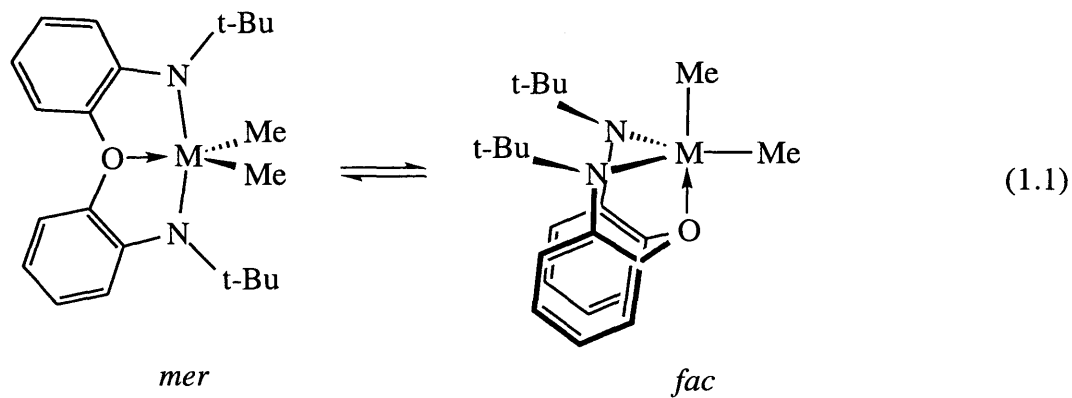
Chapter 1

Synthesis of Group 4 Complexes Containing Diamido/ether Ligands

INTRODUCTION

Our research group has focused on the chemistry of triamidoamine complexes,²⁴ largely of Mo or W.⁵⁴⁻⁵⁸ While the well-defined apical pocket enables the stabilization of otherwise elusive molecular structures (e.g., trigonal monopyramid)^{59,60} and provides the opportunity to investigate its reactivity (e.g., dinitrogen chemistry),⁶¹⁻⁶⁴ it seems to limit the scope of chemistry that can only occur in the pocket if the triamidoamine does not get involved. One way to increase the reactivity is to cut off the "linker" amino nitrogen and still maintain the original trianionic format by employing three monodentate amido ligands. Early transition metal complexes containing three N-t-butyl anilides have proven significant,⁶⁵⁻⁶⁸ particularly for the cleavage of dinitrogen.^{69,70} Another way involves the removal of one amido "arm" to open the coordination sites from the tripodal claw. The ligand thus becomes tridentate diamido/donor with a decrease of formal charge by one from the triamidoamine ligand. Group 4 complexes that contain the diamido/ether ligands of the type $[\text{ArylN}_2\text{O}]^{2-}$ and $[\text{t-BuNON}]^{2-}$ have shown activity for α -olefin polymerization.^{52,71,72} Perhaps the most important and attractive feature is that the zirconium complexes of $[\text{t-BuNON}]^{2-}$ are shown to polymerize 1-hexene in a living fashion, even after a given quantity of 1-hexene is consumed.⁵³

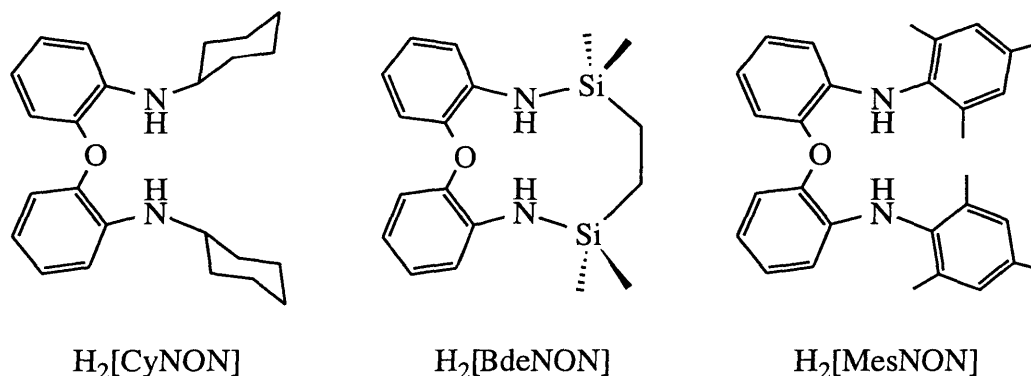
X-ray studies showed the structures of five coordinate $[t\text{-BuNON}]\text{ZrMe}_2$ and $\text{B}(\text{C}_6\text{F}_5)_3$ -activated $[t\text{-BuNON}]\text{ZrMe}_2$ to be distorted trigonal bipyramid in which the amido nitrogens occupy equatorial positions and the two Me groups are inequivalent (a *fac* form in equation 1.1). However, the two Me groups in $[t\text{-BuNON}]\text{ZrMe}_2$ equilibrate rapidly on the NMR time scale in solution, even at -80°C , presumably *via* a *mer* structure with C_2 or C_{2v} symmetry.⁵² We began to suspect that the success of $[t\text{-BuNON}]\text{ZrMe}_2$ in polymerization is because of the steric crowding of the *t*-butyl groups, that a *fac* structure is required for the development of active species for α -olefin polymerization, and that the substituent on the amido nitrogens may not necessarily be an alkyl. We set out to test these ideas by preparing several diamido/ether ligands in which the ligand backbone is the same as that in $[t\text{-BuNON}]^{2-}$ so as to *only* understand the nature of the amido substituents.



SPECIFIC GOALS

A set of ligands employed in this study is shown in Scheme 1.1. $\text{H}_2[\text{CyNON}]$ was designed with the intent of realizing the importance of the steric crowding imposed by *t*-butyl groups in $[t\text{-BuNON}]^{2-}$. (An analogous iso-propyl ligand was also investigated at about the same time of this study.⁷³) $\text{H}_2[\text{BdeNON}]$ was designed to impede the fluxional exchange process between *fac* and *mer* structures in solution by connecting the two equatorial nitrogens in a *fac* form. It was assumed that the oxygen coordination is strong enough to maintain the tridentate

feature for the diamido/ether ligand and that the N...N linker is short enough to preclude the axial methyl ligand (in a *fac* form shown in equation 1.1) from penetrating underneath it. The ultimate goal of this specific design is to "fix" the diamido/donor structure to be *fac*. Mesityl derived $H_2[MesNON]$ provides an opportunity to examine the polymerization activity by affording different steric and electronic properties from *t*-butyl. The benefit of the arylated derivatives is that they can be far more easily fine-tuned sterically and electronically as compared to their alkyl counterparts. Preliminary study only focuses on mesityl which is reasonably bulky, although more sterically demanding substituents may be available.



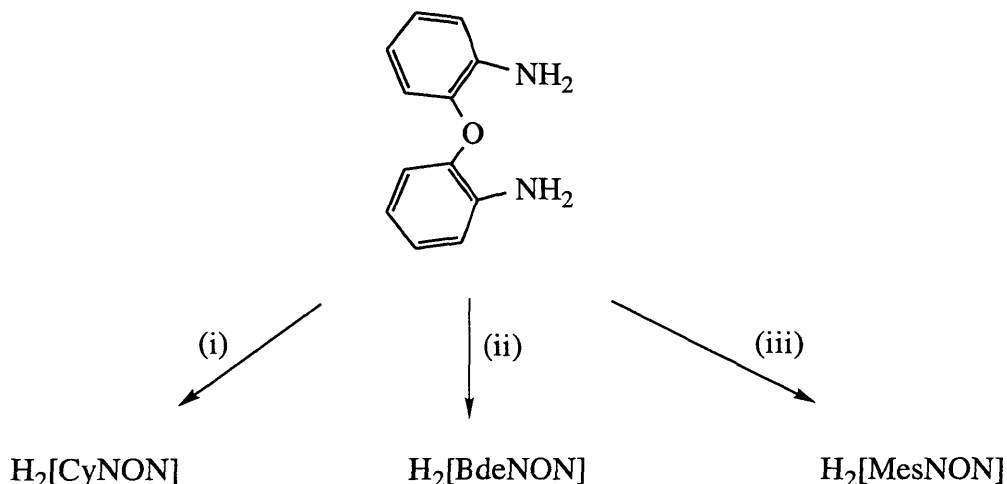
Scheme 1.1. The diamido/ether ligands employed in this study.

RESULTS

1.1 Synthesis of $H_2[RNON]$ (R = Cy, Bde, Mes).

Scheme 1.2 summarizes the synthesis of these diamido/ether ligands. Condensation between cyclohexanone and $O(o-C_6H_4NH_2)_2$ in acetic acid in the presence of excess zinc at 65 °C cleanly affords $H_2[CyNON]$ in ~90% yield. A similar condition has been reported for the synthesis of aniline derivatives.⁷⁴ $H_2[CyNON]$ is an air stable, yellow viscous oil that is soluble in common solvents; it occasionally crystallizes at room temperature after several weeks.

Lithium anilide $O(o\text{-C}_6\text{H}_4\text{NHLi})_2$ was prepared *in situ* by addition of two equivalents of $n\text{-BuLi}$ to $O(o\text{-C}_6\text{H}_4\text{NH}_2)_2$; it subsequently reacted with 1,2-bis(chlorodimethylsilyl)ethane in THF with a high dilution technique⁷⁵ to give crystalline $\text{H}_2[\text{BdeNON}]$ in ~70% yield. Without the high dilution technique, the desirable product was obtained in a relatively low yield (~20%), presumably due to the formation of oligomeric chains.



Scheme 1.2. Synthesis of the diamido/ether ligands. Conditions: (i) 2 equiv. cyclohexanone, excess Zn, AcOH, 65 °C. (ii) 2 equiv. $n\text{-BuLi}$, THF, -78 °C; $\text{ClMe}_2\text{SiCH}_2\text{CH}_2\text{SiMe}_2\text{Cl}$, THF, 25 °C. (iii) 2 equiv. MesBr, cat. $\text{Pd}_2(\text{dba})_3$, cat. rac-BINAP, excess NaO-*t*-Bu, toluene, 95 °C.

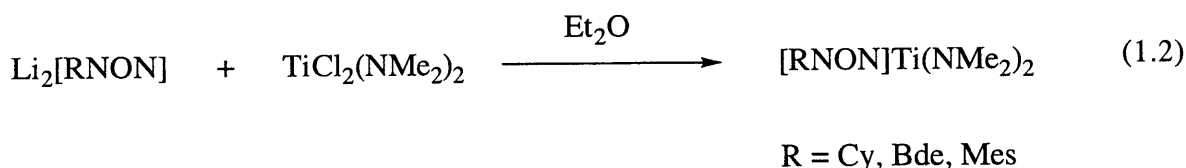
$\text{H}_2[\text{MesNON}]$ can be synthesized in ~70% yield by a palladium catalyzed C-N bond-forming reaction between $O(o\text{-C}_6\text{H}_4\text{NH}_2)_2$ and two equivalents of mesityl bromide in a condition similar to those reported by Buchwald and co-workers.⁷⁶ The aniline arylation reaction appears to be slow; it requires a more vigorous condition to lead to a complete conversion as compared to its aliphatic amine analogues.⁷⁷ Pale yellow solid $\text{H}_2[\text{MesNON}]$ is stable in the air and soluble in essentially all regular solvents.

All NMR data of these compounds are consistent with C_{2v} symmetric structures. For instance, the ^1H NMR spectrum of $\text{H}_2[\text{BdeNON}]$ exhibits one singlet resonance at 0.70 ppm for

CH₂ and one singlet at 0.03 ppm for SiCH₃. The ¹H NMR spectrum of H₂[MesNON] shows one singlet resonance at 2.09 ppm for the *ortho* mesityl methyl groups. IR spectroscopy confirms the NH absorption for these molecules, e.g., 3412 cm⁻¹ for H₂[CyNON]. Satisfactory molecular ion signals are observed from high resolution mass spectroscopy for these compounds.

1.2 Entry into titanium chemistry; reactions involving TiCl₂(NMe₂)₂.

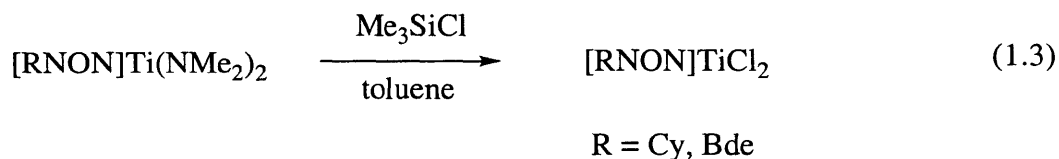
Attempts to synthesize titanium complexes containing the diamido/ether ligands mentioned above involving salt metathesis between TiCl₄(THF)₂ and Li₂[RNON] (R = Cy, Bde, Mes) or aminolysis between Ti(NMe₂)₄ and H₂[RNON] were not successful. A general entry into titanium chemistry for these tridentate amido ligands employs TiCl₂(NMe₂)₂.⁷⁸ Addition of two equivalents of *n*-BuLi to H₂[RNON] in diethyl ether followed by addition of TiCl₂(NMe₂)₂ leads to [RNON]Ti(NMe₂)₂ as purple to red crystalline solids in moderate to high yields (equation 1.2).



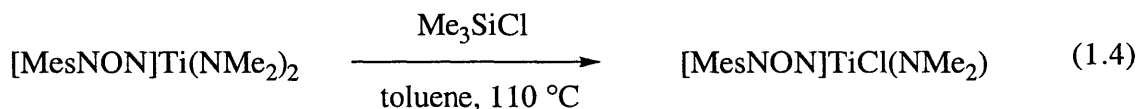
The NMR data of [CyNON]Ti(NMe₂)₂ and [MesNON]Ti(NMe₂)₂ are consistent with C_{2v} symmetric structures. The two dimethylamide ligands in [RNON]Ti(NMe₂)₂ (R = Cy, Mes) are equivalent at room temperature on the ¹H NMR time scale, suggesting a *mer* geometry for the diamido/ether ligands or a *fac* in which the two NMe₂ ligands undergo a fluxional exchange process shown in equation 1.1. The ¹H NMR spectrum of [BdeNON]Ti(NMe₂)₂, however, exhibits two singlet resonances at 3.26 and 2.63 ppm for the NMe₂ ligands and two diastereotopic resonances at 1.21 and 0.94 ppm for the methylene groups (in a CH^AH^B pattern), indicating a mirror plane that bisects the [BdeNON]²⁻ ligand and a *fac* structure for the [BdeNON]²⁻ ligand in which the oxygen donor is bound to the metal.

1.3 Reactions between $[\text{RNON}]\text{Ti}(\text{NMe}_2)_2$ and Me_3SiCl ($\text{R} = \text{Cy}, \text{Bde}, \text{Mes}$).

The reactions between $[\text{RNON}]\text{Ti}(\text{NMe}_2)_2$ ($\text{R} = \text{Cy}, \text{Bde}$) and an excess (3 equivalents) of Me_3SiCl in toluene lead to $[\text{RNON}]\text{TiCl}_2$ in high yields (equation 1.3). The formation of $[\text{BdeNON}]\text{TiCl}_2$ is complete at room temperature in hours, while that of $[\text{CyNON}]\text{TiCl}_2$ requires 3 days at 105 °C in order for a complete conversion of $[\text{CyNON}]\text{Ti}(\text{NMe}_2)_2$. The NMR data of $[\text{CyNON}]\text{TiCl}_2$ and $[\text{BdeNON}]\text{TiCl}_2$ are all consistent with those observed for their bis(dimethylamide) analogues, i.e., C_{2v} symmetry for $[\text{CyNON}]\text{TiCl}_2$ and C_s symmetry for $[\text{BdeNON}]\text{TiCl}_2$.

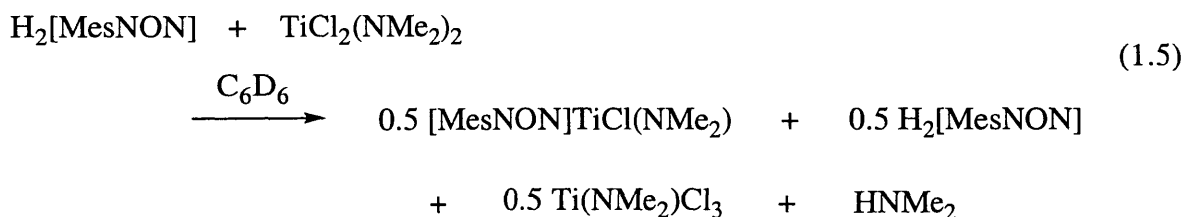


The formation of $[\text{MesNON}]\text{TiCl}_2$ seems to be more difficult. The reaction between $[\text{MesNON}]\text{Ti}(\text{NMe}_2)_2$ and an excess amount of Me_3SiCl in toluene at 110 °C leads to red crystalline $[\text{MesNON}]\text{TiCl}(\text{NMe}_2)$ in quantitative yield (equation 1.4). This reaction requires 6 days for a complete conversion. Attempts to employ more harsh conditions did not efficiently give $[\text{MesNON}]\text{TiCl}_2$ in a considerable yield, although the dichloride can be spectroscopically observed in a mixture containing $[\text{MesNON}]\text{TiCl}(\text{NMe}_2)$ after months.



Attempt to synthesize $[\text{MesNON}]\text{TiCl}_2$ by aminolysis between $\text{TiCl}_2(\text{NMe}_2)_2$ and $\text{H}_2[\text{MesNON}]$ yields a mixture which contains $\text{H}_2[\text{MesNON}]$ and $[\text{MesNON}]\text{TiCl}(\text{NMe}_2)$ in a ratio of 1:1 according to its ^1H NMR spectrum. $[\text{MesNON}]\text{TiCl}(\text{NMe}_2)$ can be selectively crystallized from the mixture as red rocks in 48% yield. A rationalized reaction is shown in

equation 1.5. Attempts to react $[\text{MesNON}]\text{Ti}(\text{NMe}_2)_2$ with ethereal HCl led to protonation of $[\text{MesNON}]^{2-}$ ligand.

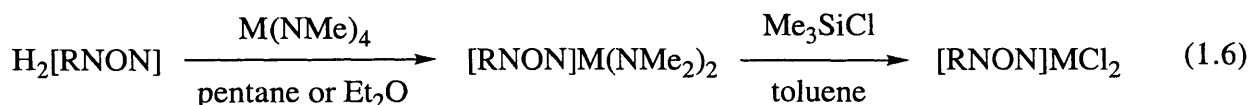


The ^1H NMR spectrum of $[\text{MesNON}]\text{TiCl}(\text{NMe}_2)$ exhibits three singlet resonances at 2.37, 2.15, and 1.98 ppm for the mesityl methyl groups, and one singlet resonance at 2.58 ppm for the dimethylamide ligand. It is likely that the structure of $[\text{MesNON}]\text{TiCl}(\text{NMe}_2)$ contains only one mirror plane which bisects the $[\text{MesNON}]^{2-}$ ligand and that the mesityl rings in $[\text{MesNON}]^{2-}$ do not rotate readily on the NMR time scale. The possibility of a dimeric structure that contains two bridging chlorides cannot be eliminated.

1.4 Entry into zirconium and hafnium chemistry; reactions involving $\text{M}(\text{NMe}_2)_4$ ($\text{M} = \text{Zr}, \text{Hf}$).

$\text{H}_2[\text{CyNON}]$ and $\text{H}_2[\text{MesNON}]$ react with $\text{Zr}(\text{NMe}_2)_4$ ⁷⁹ in pentane or diethyl ether at room temperature to give $[\text{CyNON}]\text{Zr}(\text{NMe}_2)_2$ and $[\text{MesNON}]\text{Zr}(\text{NMe}_2)_2$, respectively, in quantitative yields according to their ^1H NMR spectra. $[\text{MesNON}]\text{Zr}(\text{NMe}_2)_2$ seems to be more crystalline than the cyclohexyl analogue, as the former can be isolated as colorless cubic crystals quantitatively while the latter can be isolated in only ~70% yield. Subsequent addition of an excess (~3 to 4 equivalents) of Me_3SiCl to $[\text{RNON}]\text{Zr}(\text{NMe}_2)_2$ in toluene yields $[\text{RNON}]\text{ZrCl}_2$ in high yields ($\text{R} = \text{Cy}, \text{Mes}$; equation 1.6). When the synthesis of $[\text{CyNON}]\text{ZrCl}_2$ is performed in diethyl ether, $[\text{CyNON}]\text{ZrCl}_2(\text{OEt}_2)$ is obtained according to its ^1H NMR spectrum (3.53 ppm for OCH_2CH_3 and 0.63 ppm for OCH_2CH_3 in C_6D_6). However, the coordinated diethyl ether disappears upon recrystallization of the dichloride in toluene, perhaps as a consequence of formation of $\{[\text{CyNON}]\text{ZrCl}_2\}_2$ in the solid state. Analogous hafnium complexes can be synthesized in a

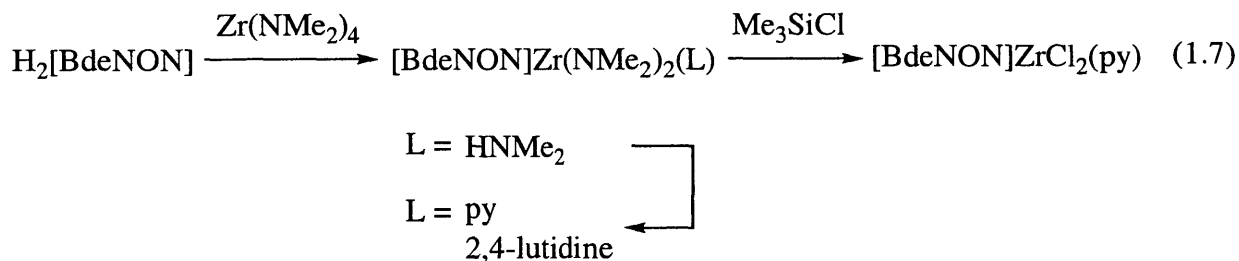
similar manner. For instance, [MesNON]HfCl₂ is obtained in two steps in ~70% overall yield. In general, the isolation of pure dichloride complexes can be achieved simply by treatment of a concentrated toluene solution of a reaction mixture with pentane to precipitate the dichloride products.



In contrast to the chemistry found for [CyNON]²⁻ and [MesNON]²⁻, [BdeNON]²⁻ seems to require an external base to stabilize its zirconium complexes. Reaction between H₂[BdeNON] and Zr(NMe₂)₄ in pentane leads to a dimethylamine adduct, [BdeNON]Zr(NMe₂)₂(HNMe₂), as colorless crystals in ~90% yield (equation 1.7). The coordinated dimethylamine appears to be strongly bound to zirconium since it remains unchanged under dynamic vacuum (~30 mTorr) at 100 °C over a period of 24 hours.

Several attempts to convert [BdeNON]Zr(NMe₂)₂(HNMe₂) to a dichloride complex with excess Me₃SiCl or MeI lead to a decomposition from which H₂[BdeNON] is observed by ¹H NMR spectroscopy, presumably due to the protonation of HNMe₂. The NH proton in [BdeNON]Zr(NMe₂)₂(HNMe₂) can be removed by n-BuLi in diethyl ether to give what we formulate as {[BdeNON]Zr(NMe₂)₃}Li(OEt)_x according to its ¹H NMR spectrum. Addition of an excess of Me₃SiCl to this ethereal complex results in intractable materials which are essentially insoluble in ordinary solvents. The dimethylamine ligand in [BdeNON]Zr(NMe₂)₂(HNMe₂), however, can be replaced by pyridine or 2,4-lutidine to give a pyridine or lutidine adduct in quantitative yields (equation 1.7). Attempts to employ 2,6-lutidine were not successful. Subsequent addition of an excess of Me₃SiCl to [BdeNON]Zr(NMe₂)₂(py) affords [BdeNON]ZrCl₂(py) in 92% yield. Attempts to synthesize a base-free zirconium dichloride

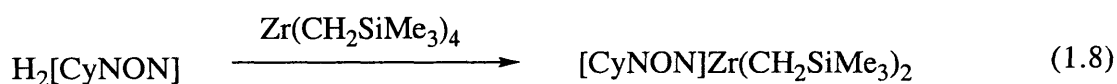
complex involving $\text{ZrCl}_4(\text{THF})_2$ and $\text{Li}_2[\text{BdeNON}]$ or $\text{ZrCl}_2(\text{CH}_2\text{SiMe}_3)_2$ and $\text{H}_2[\text{BdeNON}]$ were not successful.



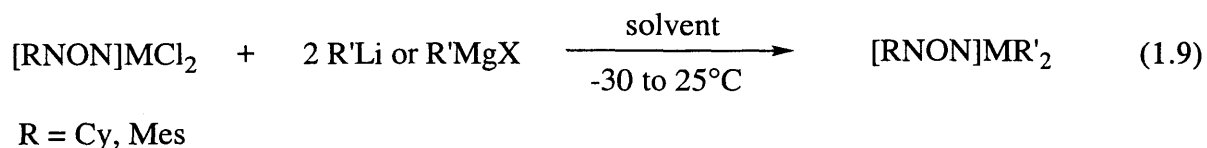
At room temperature, the ^1H NMR spectrum of $[\text{BdeNON}]\text{Zr}(\text{NMe}_2)_2(\text{HNMe}_2)$ exhibits a broad singlet resonance centered at 2.86 ppm ascribed to the two dimethylamide ligands. Variable temperature study shows that this broad signal splits into two sharp singlet resonances at temperatures $< -20\text{ }^\circ\text{C}$ but becomes one sharp singlet at temperatures $> 60\text{ }^\circ\text{C}$, suggesting a hindered rotation for the two dimethylamide ligands. The estimated activation energy ΔG^\ddagger for this hindered rotation is $\sim 14.03\text{ Kcal mol}^{-1}$ ($T_c = 30\text{ }^\circ\text{C}$, $\Delta\delta = 237.5\text{ Hz}$).^{80,81} A similar phenomenon is also observed for the pyridine or lutidine adduct. In $[\text{BdeNON}]\text{Zr}(\text{NMe}_2)_2(\text{L})$ ($\text{L} = \text{pyridine}$ or $2,4\text{-lutidine}$), two broad singlet resonances are observed for the two dimethylamide ligands in the ^1H NMR spectra at room temperature ($\text{L} = \text{pyridine}$, centered at 3.04 and 2.76 ppm; $\text{L} = 2,4\text{-lutidine}$, centered at 3.19 and 2.71 ppm). Variable temperature NMR experiment of $[\text{BdeNON}]\text{Zr}(\text{NMe}_2)_2(\text{py})$ indicates a rotational activation energy ΔG^\ddagger of $\sim 16.05\text{ Kcal/mol}$ ($T_c = 65\text{ }^\circ\text{C}$, $\Delta\delta = 147.0\text{ Hz}$)^{80,81} about the two Zr-NMe_2 bonds. All NMR data of $[\text{BdeNON}]\text{Zr}(\text{NMe}_2)_2(\text{L})$ and $[\text{BdeNON}]\text{ZrCl}_2(\text{py})$ are consistent with structures that have a mirror plane. These complexes are all proposed to have a pseudo-octahedral structure which contains a *fac* $[\text{BdeNON}]^{2-}$ with the oxygen donor being trans to the nitrogen atom in the coordinated dimethylamine, pyridine, or lutidine.

1.5 Synthesis of dialkyl complexes containing [CyNON]²⁻ and [MesNON]²⁻.

The reaction between H₂[CyNON] and Zr(CH₂SiMe₃)₄ in toluene or benzene at room temperature yields pale yellow crystalline [CyNON]Zr(CH₂SiMe₃)₂ in 70% yield (equation 1.8). In contrast, attempts to react H₂[CyNON] with ZrBn₄ or ZrNp₄ (Bn = CH₂Ph, Np = CH₂CMe₃; 70 °C for 3.5 days and 70 °C for 7 days, respectively) lead to a mixture which contains the desired products according to their ¹H NMR spectra; however, attempts to selectively recrystallize the products proved difficult.



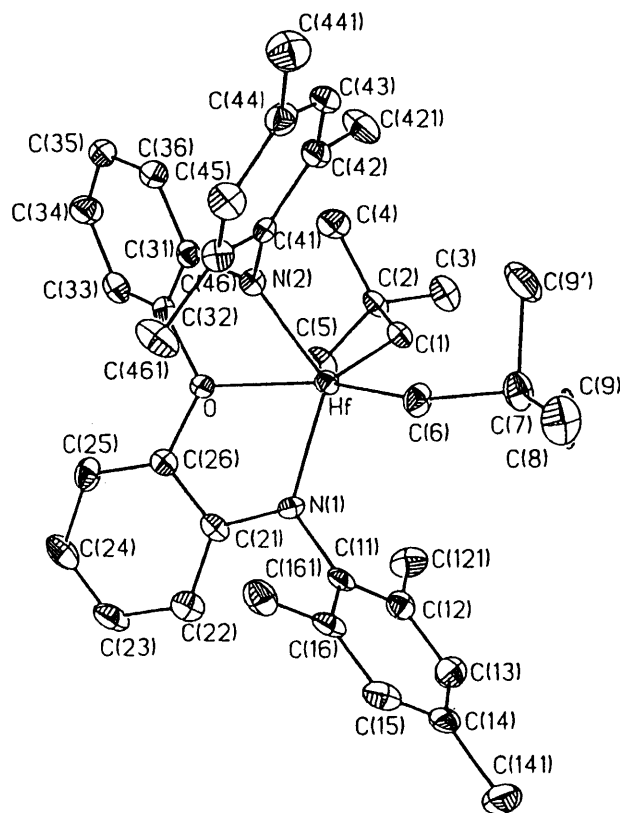
Dialkyl complexes are best obtained by alkylation of the dichloride complexes. [RNON]MCl₂ reacts with magnesium or lithium reagents in diethyl ether or toluene to give the corresponding dialkyl complexes, [RNON]MR'₂ (R = Cy, Mes), in moderate to excellent yields (equation 1.9, Table 1.1). Alkylation of [MesNON]TiCl(NMe₂) was not attempted since it does not parallel the other reactions discussed here. The choice of alkylating reagent appears to be important in certain cases. For instance, attempts to prepare [CyNON]ZrMe₂ with MeMgCl instead of MeMgI led to a mixture which made purification of the product relatively more difficult. The ¹H and ¹³C NMR spectra of the dialkyl complexes are all consistent with structures that have two mirror planes. Variable temperature NMR studies of [CyNON]ZrMe₂ and [MesNON]ZrMe₂ exhibit only one sharp singlet resonance for the two methyl ligands at temperatures between -80 and 90 °C. The ¹H NMR spectrum (500 MHz, -80 to 90 °C) of [MesNON]ZrMe₂ reveals one singlet resonance for *ortho* mesityl methyl groups, which is in contrast to the inequivalent *ortho* methyl groups observed for [MesNON]TiCl(NMe₂). The ¹³C NMR spectra of [MesNON]ZrPh₂ and [MesNON]HfPh₂ reveal four resonances for the phenyl ligands, suggesting that the two phenyl ligands are equivalent on the NMR time scale; the ipso carbons are found as a singlet resonance at 191.70 and 205.28 ppm, respectively.

**Table 1.1.** Synthesis of dialkyl complexes according to equation 1.9.

$[\text{RNON}]\text{MCl}_2$	$\text{R}'\text{Li}/\text{R}'\text{MgX}$	Solvent	$[\text{RNON}]\text{MR}'_2$	Yield (%)
$[\text{CyNON}]\text{TiCl}_2$	MeMgI	Et_2O	$[\text{CyNON}]\text{TiMe}_2$	47
$[\text{CyNON}]\text{TiCl}_2$	(i-Bu)MgCl	Et_2O	$[\text{CyNON}]\text{Ti}(\text{i-Bu})_2$	72
$[\text{CyNON}]\text{TiCl}_2$	NpLi	Et_2O	$[\text{CyNON}]\text{TiNp}_2$	80
$[\text{CyNON}]\text{ZrCl}_2$	MeMgI	Et_2O	$[\text{CyNON}]\text{ZrMe}_2$	100
$[\text{CyNON}]\text{ZrCl}_2$	EtMgBr	Et_2O	$[\text{CyNON}]\text{ZrEt}_2$	61
$[\text{CyNON}]\text{ZrCl}_2$	(i-Bu)MgCl	PhCH_3	$[\text{CyNON}]\text{Zr}(\text{i-Bu})_2$	70
$[\text{CyNON}]\text{ZrCl}_2$	NpLi	Et_2O	$[\text{CyNON}]\text{ZrNp}_2$	50
$[\text{CyNON}]\text{ZrCl}_2$	BnMgCl	PhCH_3	$[\text{CyNON}]\text{ZrBn}_2$	70
$[\text{CyNON}]\text{ZrCl}_2$	$(\text{CH}_2\text{CH}=\text{CH}_2)\text{MgBr}$	Et_2O	$[\text{CyNON}]\text{Zr}(\text{CH}_2\text{CH}=\text{CH}_2)_2$	50
$[\text{MesNON}]\text{ZrCl}_2$	MeMgI	Et_2O	$[\text{MesNON}]\text{ZrMe}_2$	85
$[\text{MesNON}]\text{ZrCl}_2$	NpLi	Et_2O	$[\text{MesNON}]\text{ZrNp}_2$	83
$[\text{MesNON}]\text{ZrCl}_2$	PhMgBr	Et_2O	$[\text{MesNON}]\text{ZrPh}_2$	92
$[\text{MesNON}]\text{HfCl}_2$	MeMgI	Et_2O	$[\text{MesNON}]\text{HfMe}_2$	88
$[\text{MesNON}]\text{HfCl}_2$	EtMgBr	Et_2O	$[\text{MesNON}]\text{HfEt}_2$	88
$[\text{MesNON}]\text{HfCl}_2$	(i-Bu)MgBr	Et_2O	$[\text{MesNON}]\text{Hf}(\text{i-Bu})_2$	79
$[\text{MesNON}]\text{HfCl}_2$	NpLi	Et_2O	$[\text{MesNON}]\text{HfNp}_2$	93
$[\text{MesNON}]\text{HfCl}_2$	PhMgBr	Et_2O	$[\text{MesNON}]\text{HfPh}_2$	95

1.6 X-ray structure of [MesNON]HfNp₂.

A single crystal of [MesNON]HfNp₂ was grown from a saturated solution of diethyl ether, benzene, and pentane at -30 °C. An X-ray study of [MesNON]HfNp₂ shows it to have an approximate square pyramidal structure for the HfC₂N₂O core with the C(1) atom on the apical position (Figure 1.1). The hafnium center is a little shifted above the equatorial plane and the bond angles between Hf-C(1) and the four equatorial atoms are in the range from 107.0° to 110.4°, except 97.5° for O-Hf-C(1) as a consequence of the steric repulsion between the two neopentyl ligands. The two amido nitrogens are sp²-hybridized as evidenced by the sum of the angles around them (N(1) = 359.6° and N(2) = 359.8°). The mesityl rings lie perpendicular to the plane of the *o*-phenylene backbone with the dihedral angles of 90.7° and 89.5°. The dihedral angle between O-Hf-N(1) and O-Hf-N(2) is ~145.6°, which is larger than the corresponding angles in the *fac* structures of [ArN₂O]TiBn₂ (137°; Ar = 2,6-C₆H₃Me₂) and [ArN₂S]ZrMe₂ (140°) but smaller than those in the square pyramid of [i-PrNSN]ZrMe₂ (154°) and [(2,6-*i*-Pr₂-C₆H₃)N₂O]HfEt₂ (160°).^{72,83} The Hf-C(6) bond distance (2.225(7) Å) is slightly longer than Hf-C(1) (2.210(7) Å), presumably because C(6) is virtually trans to the oxygen donor (O-Hf-C(6) = 155.1(3)°). The hafnium center lies on the plane of O/C(1)/C(6) (dihedral angle Hf/O/C(1)/C(6) = 179.6°). The orientation of the *t*-butyl groups on C(1) and C(6) suggests steric crowding between the [MesNON]²⁻ and neopentyl ligands. Nevertheless, the Hf-O, Hf-N_{amide}, and Hf-C_α bond distances are all within ~0.02 Å difference from those for [(2,6-*i*-Pr₂-C₆H₃)N₂O]HfEt₂.



Bond Lengths

Hf-N(1)	2.114(6)
Hf-N(2)	2.093(6)
Hf-O	2.332(5)
Hf-C(1)	2.210(7)
Hf-C(6)	2.225(7)

Bond Angles

C(1)-Hf-C(6)	107.4(3)
N(1)-Hf-N(2)	127.7(2)
Hf-N(1)-C(11)	122.0(5)
Hf-N(2)-C(41)	125.0(4)
O-Hf-C(1)	97.5(2)
O-Hf-C(6)	155.1(3)

Dihedral Angles^a

N(2)/O-Hf-N(1)	145.6	C(1)/O-Hf-C(6)	179.0
Hf-N(1)-C(11)-C(16)	90.7	Hf-N(2)-C(41)-C(42)	89.5

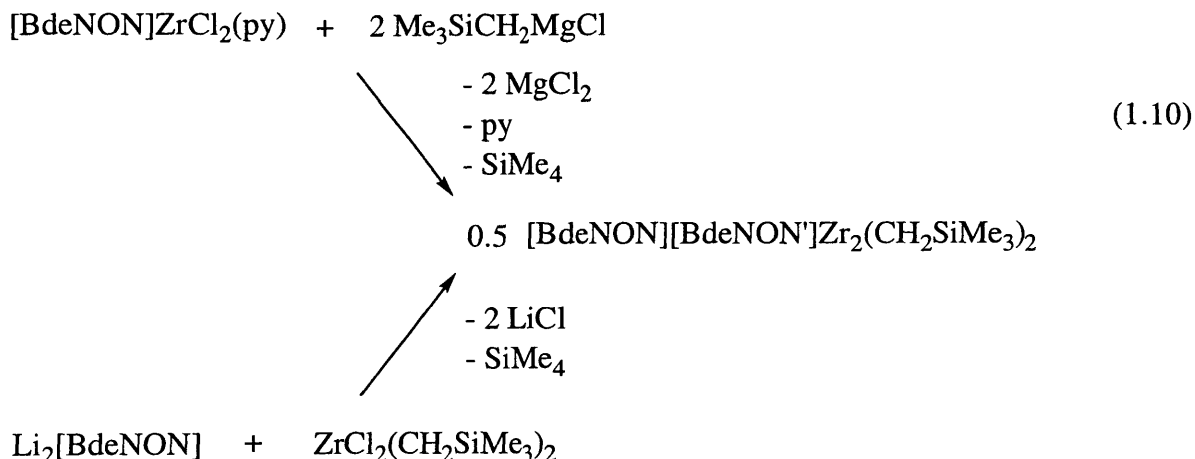
Figure 1.1. An ORTEP drawing (35% probability level) of the structure of [MesNON]HfNp₂, with selected bond lengths (Å), bond angles (deg), and dihedral angles (deg). ^a Obtained from a Chem 3D model.

1.7 Alkylation of dichloride complexes containing [BdeNON]²⁻.

Attempts to alkylate [BdeNON]TiCl₂ or [BdeNON]ZrCl₂(py) with one or two equivalents of magnesium or lithium reagents (such as MeLi, MeMgCl, BnMgCl) did not prove successful. These reactions are highly intractable and no isolated compounds can be identified so far. Salt metathesis presumably takes place immediately upon treatment of the dichloride complexes with alkylation reagents as evidenced by the observation of color change and salt precipitation from the reaction solutions. Typically, a diethyl ether solution of dark purple [BdeNON]TiCl₂ becomes red or orange, and yellow [BdeNON]ZrCl₂(py) turns to brown. It is likely that the hypothetical [BdeNON]MR_{2-n}Cl_n (M = Ti, Zr; n = 0, 1) or [BdeNON]ZrR_{2-n}Cl_n(py) is unstable and tends to decompose. Attempts to observe the presumed alkyl complexes by ¹H NMR spectroscopy at -30 °C were not successful.

The reaction between two equivalents of Me₃SiCH₂MgCl and [BdeNON]ZrCl₂(py) in diethyl ether at -35 °C yields a pale yellow crystalline solid in ~50% isolated yield. (The yield is calculated on the basis of the formula obtained below.) This crystalline compound can also be obtained in ~70% isolated yield by addition of Li₂[BdeNON] to ZrCl₂(CH₂SiMe₃)₂ in diethyl ether at -35 °C. (The fact that these two reactions produce the same product has been confirmed by preparing a mixture solution of the two reaction products followed by examining this mixture solution by ¹H NMR spectroscopy which shows identical spectrum to either original one.) Low symmetry is recognized for this compound according to its complex ¹H and ¹³C NMR spectra which make identification almost impossible. An X-ray study (see Section 1.8) establishes the connection of this molecule and shows it to contain two zirconium metal centers with no symmetry. Consistent with the equal stoichiometry employed for the starting materials, the bimetallic zirconium complex contains essentially two [BdeNON]²⁻ ligands with one of them being transformed by double C-H activation of one of the silicon-bound methyl groups to result in a methine bridging between the two zirconium metal centers. Therefore, this transformed ligand is formally a tetraanion. The double C-H activation is consistent with the structure that contains only two (instead of four) trimethylsilylmethyl ligands as a consequence of liberating two equivalents of

tetramethylsilane. The two trimethylsilylmethyl ligands are found to coordinate to the same metal. These reactions are summarized in equation 1.10, where [BdeNON'] stands for



the transformed ligand with a formal charge of -4. The bridging methine group shows a singlet resonance at 5.42 ppm in the ^1H NMR spectrum and a doublet centered at 163.59 ppm (with $^1J_{\text{CH}} = 106$ Hz) in the ^{13}C NMR spectrum. A similar reaction between $[\text{BdeNON}]\text{ZrCl}_2(\text{py})$ and two equivalents of $\text{PhMe}_2\text{CCH}_2\text{MgCl}$ yields orange crystalline $[\text{BdeNON}][\text{BdeNON}']\text{Zr}_2(\text{CH}_2\text{CMe}_2\text{Ph})_2$ in ~50% yield, which reveals a singlet resonance at 4.88 ppm for the bridging methine in the ^1H NMR spectrum. These NMR data should be compared with those found for a bridging methine group in $\{\text{cyclo-ZrCHSiMe}_2\text{NSiMe}_3[\text{N}(\text{SiMe}_3)_2]\}_2$ (Figure 1.2; 7.08 ppm for ZrCHZr , 201.4 ppm for

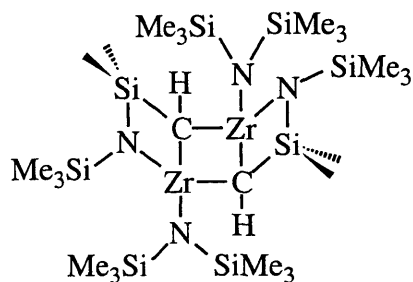
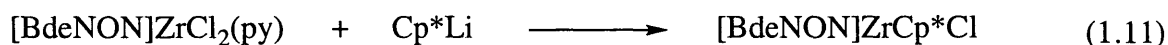


Figure 1.2. The structure of $\{\text{cyclo-ZrCHSiMe}_2\text{NSiMe}_3[\text{N}(\text{SiMe}_3)_2]\}_2$; see reference 84.

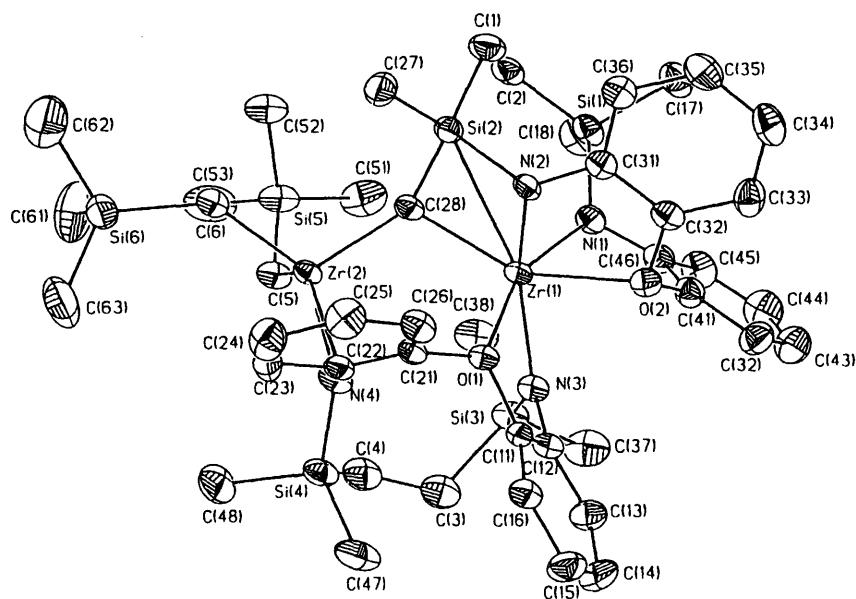
ZrCHZr), which is obtained by thermolysis (60 °C, 0.01 mm) of mononuclear dialkyl $[(\text{Me}_3\text{Si})_2\text{N}]_2\text{ZrR}_2$ (R = Me, Et, CH_2SiMe_3) reported by Andersen.⁸⁴ Therefore, we propose that the bimetallic complexes $[\text{BdeNON}][\text{BdeNON}']\text{Zr}_2\text{R}_2$ (R = CH_2SiMe_3 , $\text{CH}_2\text{CMe}_2\text{Ph}$) are thermodynamic products from the hypothetical $[\text{BdeNON}]\text{ZrR}_2$ which is analogous to $[(\text{Me}_3\text{Si})_2\text{N}]_2\text{ZrR}_2$, that the intermolecular decomposition of $[\text{BdeNON}]\text{ZrR}_2$ may be too fast and intractable if R is a methyl, and that the decomposition may be prohibited by employing an alkyl which is significantly more crowded than the trimethylsilylmethyl ligand.

We set out to test this hypothesis by applying pentamethylcyclopentadienyl as the sterically demanding ligand if it is π bound to the metal. Addition of one equivalent of Cp^*Li to dichloride $[\text{BdeNON}]\text{ZrCl}_2(\text{py})$ yields yellow crystalline $[\text{BdeNON}]\text{ZrCp}^*\text{Cl}$ in ~50% yield (equation 1.11). The NMR data of $[\text{BdeNON}]\text{ZrCp}^*\text{Cl}$ indicate a mirror plane that bisects the $[\text{BdeNON}]^{2-}$ ligand. The Cp^* ring is η^5 bound to the zirconium center and rotates readily on the NMR time scale, as evidenced by a singlet resonance at 1.66 ppm for $\text{C}_5(\text{CH}_3)_5$ in the ^1H NMR spectrum and a quartet resonance centered at 11.49 ppm for $\text{C}_5(\text{CH}_3)_5$ in the ^{13}C NMR spectrum.



1.8 X-ray structure of $[\text{BdeNON}][\text{BdeNON}']\text{Zr}_2(\text{CH}_2\text{SiMe}_3)_2$.

Figure 1.3 shows the structure of this bimetallic zirconium complex. Pseudo-octahedral and pseudo-tetrahedral structures are found for the two zirconium centers. The Zr-O, Zr-N_{amide}, Zr-C _{α} bond lengths are all typical of zirconium complexes containing a diamido/ether ligand.^{52,72,73} A *fac* geometry can be recognized in the Zr(1) core with the dihedral angle between N(1)-Zr(1)-O(2) and N(2)-Zr(1)-O(2) being 68.9°. This angle is much smaller than those found in



Bond Lengths

Zr(1)-N(1)	2.109(3)	Zr(1)-N(2)	2.114(3)
Zr(1)-N(3)	2.154(4)	Zr(1)-O(1)	2.365(3)
Zr(1)-O(2)	2.374(3)	Zr(1)-C(28)	2.236(4)
Zr(1)-Si(2)	2.884(2)	Zr(2)-C(28)	2.141(4)
Zr(2)-N(4)	2.082(4)	Zr(2)-C(5)	2.229(4)
Zr(2)-C(6)	2.253(4)	Zr(2)-C(22)	2.768(4)

Bond Angles

O(1)-Zr(1)-O(2)	82.27(9)	N(1)-Zr(1)-N(2)	95.85(13)
Zr(1)-C(28)-Zr(2)	116.0(2)	C(5)-Zr(2)-C(6)	104.4(2)
C(11)-O(1)-C(21)	117.4(3)	C(32)-O(2)-C(41)	116.1(3)
Zr(2)-N(4)-C(22)	102.2(2)		

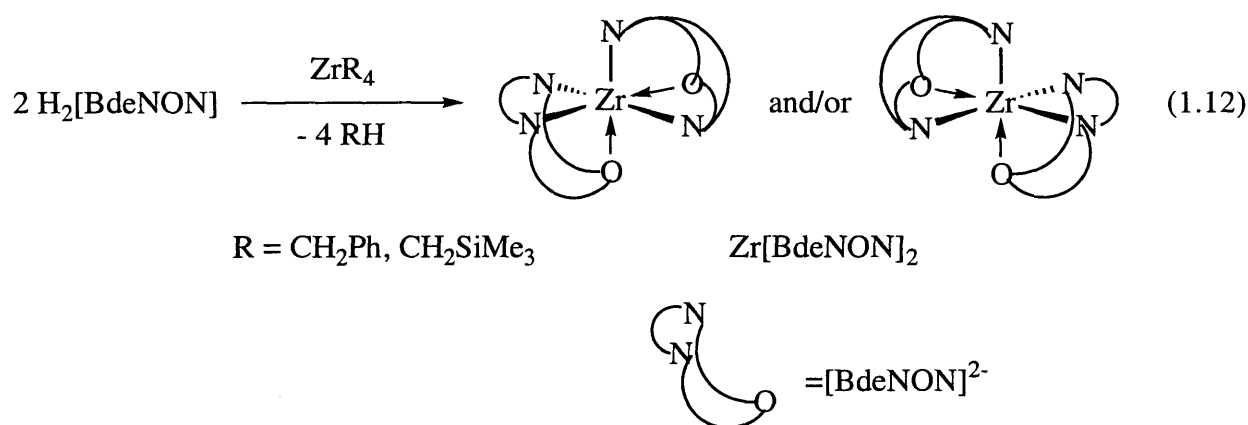
Figure 1.3. An ORTEP drawing (35% probability level) of the structure of [BdeNON][BdeNON']Zr₂(CH₂SiMe₃)₂, with selected bond lengths (Å) and bond angles (deg).

the *mer* structure of [i-PrNON]ZrMe₂ (176°)⁷³ and the *fac* of [t-BuNON]ZrMe₂ (124°),⁵² presumably due to inter-ligand interaction in this bimetallic compound. The bond lengths between the bridging methine carbon and the two zirconium metal centers (2.236(4) and 2.141(4) Å) are comparable with those found in Andersen's {cyclo-ZrCHSiMe₂NSiMe₃[N(SiMe₃)₂]}₂ (2.21(2) and 2.16(2) Å).⁸⁴ The Zr(1)-C(28)-Zr(2) angle (116.0(2)°) in [BdeNON][BdeNON']Zr₂(CH₂SiMe₃)₂, however, is ~22° larger than the corresponding angle in {cyclo-ZrCHSiMe₂NSiMe₃[N(SiMe₃)₂]}₂ (93.9(5)°) due to the longer O(1)···N(4) bridge in the former as compared to the single-carbon bridge in the latter (Figure 1.2). All of the amido nitrogens in [BdeNON][BdeNON']Zr₂(CH₂SiMe₃)₂ are virtually planar as evidenced by the sum of bond angles around them (~357°), except N(2) (sum = 349.2°), presumably due to the coordination of bridging methine to the same metal, i.e., Zr(1), thereby bringing Si(2) to be close to Zr(1) (Zr(1)-Si(2) = 2.884(2) Å). The donor atoms O(1) and O(2) are both bound to Zr(1) and cis to one another with the O(1)-Zr(1)-O(2) angle of 82.27(9)°. The two oxygen donors adopt two types of geometry. The sum of the angles around O(1) is ~356° while that around O(2) is ~331°, suggesting their being virtually planar and tetrahedral, respectively. The *o*-phenylene backbone containing C(22) is found to partially bind to Zr(2) with Zr(2)-C(22) distance of 2.768 (4) Å and Zr(2)-N(4)-C(22) angle of 102.2(2)°. These numbers are comparable with those found for η²-benzyl groups in ZrBn₄.⁸⁵

1.9 Reaction between H₂[BdeNON] and ZrR₄ (R = Bn, CH₂SiMe₃).

H₂[BdeNON] reacts with ZrR₄ (R = Bn, CH₂SiMe₃) in toluene or benzene to yield a two-component mixture of ZrR₄ and Zr[BdeNON]₂ in a ratio of 1:1 according to the ¹H NMR spectra. Alternatively, Zr[BdeNON]₂ can be obtained in quantitative yields by addition of two equivalents of H₂[BdeNON] to ZrR₄. No sign of formation of [BdeNON]ZrR₂ (R = Bn, CH₂SiMe₃) can be observed by ¹H NMR spectroscopy even if the reaction is conducted in coordinating solvents (such as diethyl ether or THF) with the hope that solvent molecules might

occupy at least one of the coordination sites to sterically prevent the binding of a second $\text{H}_2[\text{BdeNON}]$ to zirconium metal center. In contrast to the other monometallic $[\text{BdeNON}]^{2-}$ complexes reported here, $\text{Zr}[\text{BdeNON}]_2$ exhibits four resonances for SiCH_3 and twelve resonances for *o*-phenylene carbons in the ^{13}C NMR spectrum, consistent with a C_2 symmetric structure in which the two oxygen donors are cis to one another. The cis orientation of the two oxygen donors in $\text{Zr}[\text{BdeNON}]_2$ is similar to that observed for $\text{Zr}(1)$ in $[\text{BdeNON}][\text{BdeNON}']\text{Zr}_2(\text{CH}_2\text{SiMe}_3)_2$. The C_2 axis lies on the O-Zr-O plane and bisects the O-Zr-O angle. Two possible enantiomeric structures are shown in equation 1.12.



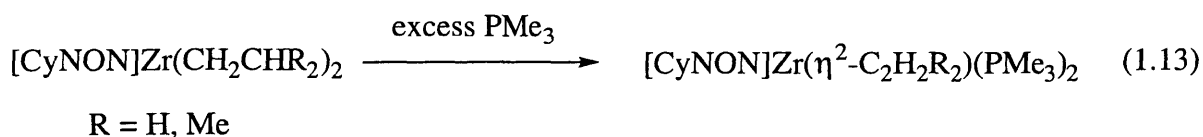
1.10 Thermal stability of alkyl complexes.

The dimethyl, dineopentyl, dibenzyl, diphenyl, and bis(trimethylsilylmethyl) complexes reported here are all stable in solution at room temperature for days without detectable decomposition according to their ^1H NMR spectra. A toluene- d_8 solution of $[\text{CyNON}]\text{Zr}(\text{CH}_2\text{SiMe}_3)_2$ (~ 0.16 M) showed $< 5\%$ decomposition after being heated to 100°C for three days. In contrast, orange $[\text{CyNON}]\text{Ti}(\text{i-Bu})_2$ (~ 8 mM in C_6D_6) decomposed at room temperature over a period of several hours. Solutions of $[\text{CyNON}]\text{Zr}(\text{i-Bu})_2$ (~ 7 mM in C_6D_6) showed no signs of decomposition at room temperature after 24 hours, but decomposed readily at 100°C with a rapid color change from colorless to deep red. The ^1H NMR spectrum of this deep

red solution indicates the presence of both isobutane and isobutene, consistent with β hydride abstraction. $[\text{CyNON}]\text{ZrEt}_2$ decomposes readily over a period of one hour at room temperature. Therefore, the thermal stability of these β -hydrogen containing complexes follows the order of $[\text{CyNON}]\text{Zr}(\text{i-Bu})_2 > [\text{CyNON}]\text{Ti}(\text{i-Bu})_2 > [\text{CyNON}]\text{ZrEt}_2$. Synthesis of $[\text{CyNON}]\text{TiEt}_2$ has not yet been successful. Similar phenomena were also observed for the $[\text{MesNON}]^{2-}$ complexes. For instance, $[\text{MesNON}]\text{HfEt}_2$ (~6 mM in C_6D_6) and $[\text{MesNON}]\text{Hf}(\text{i-Bu})_2$ (~6 mM in C_6D_6) do not show detectable decomposition at room temperature for several days, while attempts to synthesize their zirconium analogues have not been successful.

1.11 Decomposition of $[\text{CyNON}]\text{ZrR}_2$ ($\text{R} = \text{Et}, \text{i-Bu}$) in the presence of PMe_3 .

Decomposition of $[\text{CyNON}]\text{ZrEt}_2$ in neat PMe_3 yields $[\text{CyNON}]\text{Zr}(\eta^2\text{-C}_2\text{H}_4)(\text{PMe}_3)_2$ as an orange solid in ~70% yield (equation 1.13). The coordinated ethylene shows a singlet at 1.23 ppm in the ^1H NMR spectrum. The room temperature ^{31}P NMR spectrum of $[\text{CyNON}]\text{Zr}(\eta^2\text{-C}_2\text{H}_4)(\text{PMe}_3)_2$ exhibits two resonances at -25.31 and -60.86 ppm; the latter of which corresponds to free PMe_3 . Variable temperature ^{31}P NMR spectra reveal that these two resonances coalesce at ~70 °C, consistent with rapid exchange of coordinated and free phosphine. A similar reaction between $[\text{CyNON}]\text{Zr}(\text{i-Bu})_2$ and neat PMe_3 requires a temperature of 50 °C over a period of three days. $[\text{CyNON}]\text{Zr}(\eta^2\text{-C}_2\text{H}_2\text{Me}_2)(\text{PMe}_3)_2$ appears to be sensitive to light and this reaction must be conducted in the dark. It is obvious that the required condition for the decomposition of $[\text{CyNON}]\text{Zr}(\text{i-Bu})_2$ is more vigorous than that of $[\text{CyNON}]\text{ZrEt}_2$, consistent with less accessibility of β hydrogens in the former due to the steric shielding from the β methyl groups. Similar reactions are also observed for the iso-propyl substituted diamido/ether complexes.⁷³



1.12 Generation of cations and their reactions with 1-hexene.

The reaction between $[\text{CyNON}]\text{ZrMe}_2$ and $[\text{HNMe}_2\text{Ph}][\text{B}(\text{C}_6\text{F}_5)_4]$ in $\text{C}_6\text{D}_5\text{Br}$ at $-35\text{ }^\circ\text{C}$ yields a single species, for which ^1H NMR spectrum at $0\text{ }^\circ\text{C}$ exhibits a singlet resonance at 0.65 ppm with an intensity of three, consistent with the formation of a cationic $\{[\text{CyNON}]\text{ZrMe}(\text{NMe}_2\text{Ph})\}^+$. The coordinated NMe_2Ph exhibits a singlet resonance at 2.49 ppm for the methyl groups (versus 2.65 ppm for free NMe_2Ph in $\text{C}_6\text{D}_5\text{Br}$). $\{[\text{CyNON}]\text{ZrMe}(\text{NMe}_2\text{Ph})\}^+$ is stable in solution at temperatures below $10\text{ }^\circ\text{C}$, but appears to decompose slowly at room temperature according to its ^1H NMR spectra.

Addition of 50 equivalents of 1-hexene to a $\text{C}_6\text{D}_5\text{Br}$ solution of $\{[\text{CyNON}]\text{ZrMe}(\text{NMe}_2\text{Ph})\}[\text{B}(\text{C}_6\text{F}_5)_4]$ at $0\text{ }^\circ\text{C}$ leads to a slow oligomerization of 1-hexene. New olefinic resonances are observed in the range of 5.42–5.34 ppm (Figure 1.4), a region that is consistent with their being internal olefinic protons, e.g., the product of β elimination or β transfer⁸⁶ from a 2,1-insertion product. The conversion of 1-hexene cannot be complete, even with an extended reaction time, presumably due to the less reactive and less stable 2,1-units.⁸⁷ The intensity suggests that approximately ten equivalents of 1-hexene were consumed for every two olefinic protons in an end group. Similar observation has also been reported in the polymerization of propylene catalyzed by *ansa*-zirconocene catalysts.⁸⁸ The end groups in the low

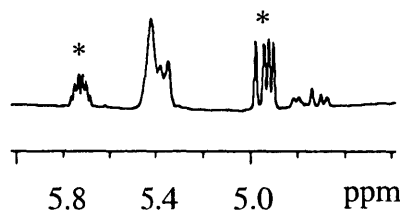


Figure 1.4. The olefin region of the ^1H NMR spectrum of the reaction between 1-hexene (50 equivalents) and $\{[\text{CyNON}]\text{ZrMe}(\text{NMe}_2\text{Ph})\}[\text{B}(\text{C}_6\text{F}_5)_4]$ at $0\text{ }^\circ\text{C}$. * denotes the olefinic signals for unreacted 1-hexene.

molecular weight polypropylene exhibit similar internal olefinic resonances for the β elimination products from the 2,1-units, e.g., compound **d** in Figure 1.5. Analogous reactions involving $[\text{HNMe}_2\text{Ph}][\text{B}(\text{C}_6\text{F}_5)_4]$ activated $[\text{MesNON}]\text{ZrMe}_2$ in $\text{C}_6\text{D}_5\text{Br}$ at $0\text{ }^\circ\text{C}$ leads to similar slow oligomerization.

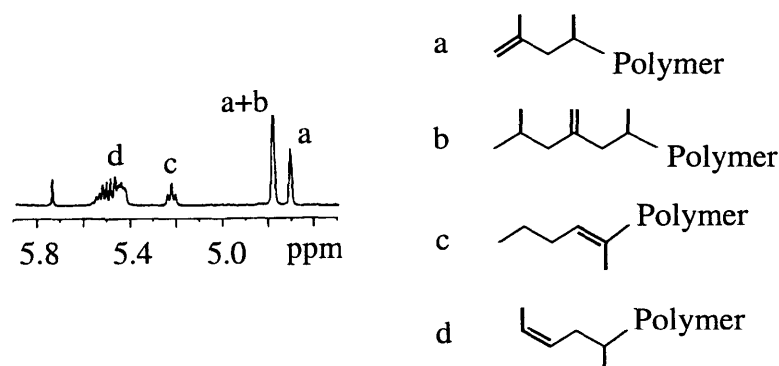


Figure 1.5. The olefin region of the ^1H NMR spectrum ($\text{C}_2\text{D}_2\text{Cl}_4$, $120\text{ }^\circ\text{C}$) of low molecular weight polypropylene prepared from MAO activated $\text{rac}[\text{ethylene}(1\text{-indenyl})_2]\text{ZrCl}_2$; see reference 88.

$[\text{RNON}]\text{ZrMe}_2$ ($\text{R} = \text{Cy}, \text{Mes}$) also reacts with $[\text{Ph}_3\text{C}][\text{B}(\text{C}_6\text{F}_5)_4]$ to yield active species for α -olefin polymerization. The ^1H NMR spectra suggest the activation is not as clean as that activated by $[\text{HNMe}_2\text{Ph}][\text{B}(\text{C}_6\text{F}_5)_4]$, presumably due to the lack of strongly coordinating bases for the former. However, they react with 1-hexene with higher catalytic activity. For instance, addition of 60 equivalents of 1-hexene to $[\text{Ph}_3\text{C}][\text{B}(\text{C}_6\text{F}_5)_4]$ activated $[\text{CyNON}]\text{ZrMe}_2$ or $[\text{MesNON}]\text{ZrMe}_2$ in $\text{C}_6\text{D}_5\text{Br}$ at $0\text{ }^\circ\text{C}$ leads to a complete conversion of 1-hexene in 10 minutes. The molecular weight of the poly(1-hexene) has not yet been determined. The cationic zirconium species which contain presumed 60 units of 1-hexene seem to slowly decompose by β elimination or β transfer to give new olefins. The new olefins exhibit both internal and terminal olefinic resonances in the ^1H NMR spectra, e.g., 5.46 and 4.84 ppm for $[\text{CyNON}]\text{ZrMe}_2$ initiator and 5.54 and 4.90 ppm for $[\text{MesNON}]\text{ZrMe}_2$ initiator (Figure 1.6). It seems likely that the rate of

propagation relative to β elimination or β transfer for the $[\text{Ph}_3\text{C}][\text{B}(\text{C}_6\text{F}_5)_4]$ activated $[\text{RNON}]\text{ZrMe}_2$ ($\text{R} = \text{Cy}, \text{Mes}$) is higher than that employing $[\text{HNMe}_2\text{Ph}][\text{B}(\text{C}_6\text{F}_5)_4]$.

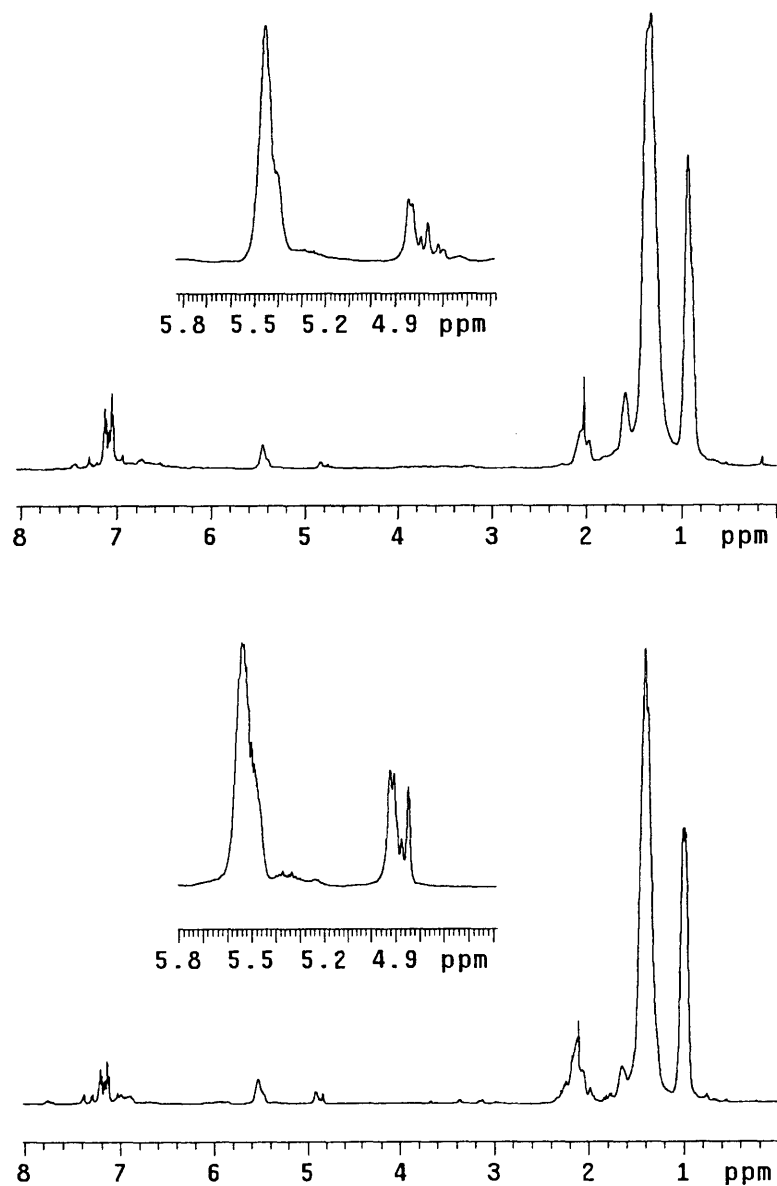


Figure 1.6. The ^1H NMR spectra (500 MHz) of the reactions between 1-hexene (60 equivalents) and $[\text{Ph}_3\text{C}][\text{B}(\text{C}_6\text{F}_5)_4]$ activated $[\text{CyNON}]\text{ZrMe}_2$ (top) or $[\text{MesNON}]\text{ZrMe}_2$ (bottom) in $\text{C}_6\text{D}_5\text{Br}$ at 0°C .

DISCUSSION

The results reported here suggest that complexes containing $[\text{RNON}]^{2-}$ ligands ($\text{R} = \text{Cy}$, Bde , Mes) are significantly less crowded than those containing $[\text{t-BuNON}]^{2-}$. Among the three ligands employed in this study, $[\text{MesNON}]^{2-}$ probably forms the most crowded complexes on the basis of difficult accessibility to synthesize its titanium dichloride complex, while $[\text{BdeNON}]^{2-}$ probably forms the least crowded complexes as evidenced by the requirement of an extra base for its zirconium complexes. $[\text{CyNON}]^{2-}$ is closely analogous to $[\text{i-PrNON}]^{2-}$,⁷³ so is their group 4 chemistry, at least that we have investigated. Therefore, the success of $[\text{t-BuNON}]\text{ZrMe}_2$ in polymerization is, at least in part, due to the steric crowding from the *t*-butyl groups.

It is likely that $[\text{CyNON}]^{2-}$ and $[\text{MesNON}]^{2-}$ complexes adopt a *mer* structure for these diamido/ether ligands in both solid state and solution. The NMR data of their group 4 dialkyl complexes are all consistent with species that contain two mirror planes on the NMR time scale, similar to those observed for $[\text{i-PrNON}]^{2-}$ and $[\text{t-BuNON}]^{2-}$, although the latter is caused by the fluxional process shown in equation 1.1.⁵² The mesityl rings in $[\text{MesNON}]\text{MX}_2$ complexes ($\text{M} = \text{Ti}$, Zr , Hf ; $\text{X} = \text{NMe}_2$, Cl , alkyl) exhibit only one resonance for *ortho* methyl groups. It should be noted that the *ortho* methyl groups are also equivalent on the NMR time scale in $[\text{ArN}_2\text{O}]\text{ZrMe}_2$ ⁷² and $[\text{MesN}_2\text{N}]\text{MMe}_2$ ($\text{M} = \text{Nb}$, Ta ; see Chapter 2), but inequivalent in $[\text{MesN}_2\text{NR}]\text{MMe}_2$ ($\text{M} = \text{Ti}$, Zr , Hf ; see Chapter 3). However, the NMR data of $[\text{MesNON}]\text{TiCl}(\text{NMe}_2)$ reveal inequivalent *ortho* mesityl methyl groups, indicating that rotation about the N-C_{ipso} bonds in $[\text{MesNON}]^{2-}$ is restricted for titanium complexes.

The NMR data of mononuclear $[\text{BdeNON}]^{2-}$ complexes suggest a *fac* structure for $[\text{BdeNON}]^{2-}$. The connection of the two "arms" associated with the tridentate feature of $[\text{BdeNON}]^{2-}$ successfully precludes the fluxional process shown in equation 1.1. $[\text{BdeNON}]^{2-}$ should be compared with its trimethylsilyl derived analogue, $[\text{TMSNON}]^{2-}$ ($\text{TMS} = \text{SiMe}_3$);⁷³ they are electronically essentially identical to one another. The NMR data of group 4 complexes containing $[\text{TMSNON}]^{2-}$ are all consistent with a five coordinate structure that contains two mirror planes on the NMR time scale. $[\text{BdeNON}]^{2-}$ is significantly less crowded than $[\text{TMSNON}]^{2-}$ since

zirconium complexes of the former require the coordination of an extra base or a second $[\text{BdeNON}]^{2-}$ to give a six coordinate structure, e.g., $[\text{BdeNON}]\text{ZrCl}_2(\text{py})$ and $\text{Zr}[\text{BdeNON}]_2$. A pseudo five coordinate $[\text{BdeNON}]^{2-}$ zirconium complex may be obtained by employing a sterically demanding ligand such as Cp^* .

The C-H bond activation of silicon-bound methyl groups is known for some time in several cases.⁸⁹⁻⁹¹ Early work by Andersen provides the direct evidence for the thermal decomposition of $[(\text{Me}_3\text{Si})_2\text{N}]_2\text{ZrR}_2$ ($\text{R} = \text{Me}, \text{Et}, \text{CH}_2\text{SiMe}_3$) to give a bimetallic $\{\text{cyclo-ZrCHSiMe}_2\text{NSiMe}_3[\text{N}(\text{SiMe}_3)_2]\}_2$.⁸⁴ The formation and high isolated yield of $[\text{BdeNON}][\text{BdeNON}']\text{Zr}_2(\text{CH}_2\text{SiMe}_3)_2$ suggest that C-H activation is the major decomposition pathway from the hypothetical $[\text{BdeNON}]\text{ZrR}_2$. It should be noted that the relatively weak N-Si bonds may also be involved in titanium chemistry although evidence is not clear in this study.

While hypothetical $[\text{BdeNON}]\text{MR}_2$ complexes ($\text{M} = \text{Ti}, \text{Zr}$) are not isolable, presumably due to their thermal instability, several dialkyl complexes containing $[\text{CyNON}]^{2-}$ and $[\text{MesNON}]^{2-}$ are synthesized and listed in equations 1.8 and 1.9 and Table 1.1. In general, these dialkyl complexes are thermally more stable when the alkyl ligands do not contain β hydrogens. For dialkyl complexes that contain β hydrogens, thermal stability increases when the employed metal goes down in the group 4 triad, presumably due to stronger M-C bonds.⁹² The thermal stability of β hydrogen containing dialkyl complexes is higher when the β hydrogens are sterically shielded, e.g., $[\text{CyNON}]\text{Zr}(\text{i-Bu})_2$ versus $[\text{CyNON}]\text{ZrEt}_2$. These phenomena are analogous to those observed in metallocene chemistry.^{93,94} $[\text{CyNON}]\text{MR}_2$ and $[\text{MesNON}]\text{MR}_2$ are much more stable than corresponding Cp_2MR_2 . For instance, $[\text{CyNON}]\text{TiNp}_2$ does not show decomposition in solution at room temperature over a period of several days, while Cp_2TiNp_2 can only be isolated below 0°C .⁹⁵ Cp_2ZrEt_2 is also not isolable,⁹³ while $[\text{CyNON}]\text{ZrEt}_2$ is.

This study also reveals that different conditions are required for the decomposition of $[\text{CyNON}]\text{ZrEt}_2$ and $[\text{CyNON}]\text{Zr}(\text{i-Bu})_2$ as the β hydrogens in the latter are much more sterically shielded. This is informative in terms of determining the potential β elimination or β transfer of the propagating chain in the polymerization of α -olefins. It should be noted that 1,2-insertion

produces a microstructure in the propagating chain which contains iso-butyl units, while 2,1-insertion produces sec-butyl-like microstructure, where β hydrogens are more easily accessible than the iso-butyl analogue. Therefore, 1,2-insertion product would discourage β elimination or β transfer, at least at a rate that is lower than that from 2,1-insertion product. The new internal olefinic resonances observed from the catalytic reactions between 1-hexene and activated $[\text{RNON}]\text{ZrMe}_2$ ($\text{R} = \text{Cy}, \text{Mes}$) are indicative of 2,1-insertion.

One of the main goals of this research was to attempt to determine the extent to which the t-butyl groups create a coordination sphere in $\{[\text{t-BuNON}]\text{ZrR}\}^+$ that leads to a living polymerization of 1-hexene. We now believe that the more crowded $[\text{t-BuNON}]^{2-}$ encourages 1,2-insertion of α -olefin to the Zr-C bond. In contrast, the more open coordination sphere in $\{[\text{RNON}]\text{ZrR}\}^+$ ($\text{R} = \text{Cy}, \text{Mes}$) allows for a significant degree of 2,1-insertion to give a less stable, perhaps also less reactive, insertion product. A similar proposition is given recently in the oligomerization or polymerization of propylene to give relatively low molecular weight polymer employing relatively well-defined metallocene based catalysts.^{87,96-99}

CONCLUSIONS

A series of tridentate diamido/ether ligands of the type $[\text{RNON}]^{2-}$ ($\text{R} = \text{Cy}, \text{Bde}, \text{Mes}$) have been designed and synthesized. A general entry into group 4 chemistry employing these ligands involves $\text{TiCl}_2(\text{NMe}_2)_2$ and $\text{M}(\text{NMe}_2)_4$ ($\text{M} = \text{Zr}, \text{Hf}$). The NMR study suggests a *fac* structure for $[\text{BdeNON}]^{2-}$, while a *mer* for $[\text{CyNON}]^{2-}$ and $[\text{MesNON}]^{2-}$. It is likely that the steric crowding of these ligands follows the order of $[\text{BdeNON}]^{2-} < [\text{CyNON}]^{2-} < [\text{MesNON}]^{2-}$, which seems less crowded than $[\text{t-BuNON}]^{2-}$. Dialkyl complexes containing $[\text{CyNON}]^{2-}$ and $[\text{MesNON}]^{2-}$ can be readily prepared, and activated by protonation or oxidative cleavage of the alkyl to yield cationic species. These cations are found to react with 1-hexene to give oligomer or polymer, while β elimination or β transfer appears to take place to a significant degree in these cases.

EXPERIMENTAL SECTION

General Procedures. Unless otherwise specified, all experiments were performed under nitrogen in a Vacuum Atmospheres glovebox (model HE-493) equipped with a regeneration/circulation device (Dri-Train) or by using standard Schlenk techniques. Oxygen level (< 2 ppm) were monitored with ZnEt_2 (1 M solution in hexane, Aldrich), and water levels (< 2 ppm) were monitored with TiCl_4 (neat, Strem). All solvents were reagent grade or better. Toluene was distilled from sodium/benzophenone ketyl. Diethyl ether was sparged with nitrogen and passed through two columns of activated alumina. Pentane was sparged with nitrogen, then passed through one column of activated alumina, and then through another of activated Q5.¹⁰⁰ Molecular sieves and Celite were activated *in vacuo* (10^{-3} Torr) for 24 hours at 175 and 125 °C, respectively. All NMR solvents were sparged with nitrogen and dried over activated 4 Å molecular sieves for days prior to use. All dry solvents were degassed with nitrogen before introduction into the glovebox, where they were stored over activated 4 Å molecular sieves.

Spectroscopic Analyses. The NMR spectra were recorded on Varian instruments (^1H , 500.2 or 300.0 MHz; ^{13}C , 125.8 or 75.4 MHz; ^{31}P , 121.5 MHz). Chemical shifts (δ) are listed as parts per million downfield from tetramethylsilane and coupling constants (J) are in hertz. ^1H NMR spectra are referenced using the residual solvent peak at δ 7.16 for C_6D_6 , δ 7.29 for $\text{C}_6\text{D}_5\text{Br}$ (the most upfield resonance), δ 7.27 for CDCl_3 , and δ 2.09 for toluene- d_8 (the most downfield resonance). ^{13}C NMR spectra are referenced using the residual solvent peak at δ 128.39 for C_6D_6 , δ 77.23 for CDCl_3 , and δ 137.86 for toluene- d_8 (the most downfield resonance). ^{31}P NMR spectra are externally referenced using a benzene solution of PPh_3 at δ -4.78. Routine coupling constants are not listed. All NMR spectra were recorded at room temperature unless noted otherwise. IR spectra were recorded as films in specified solvents between NaCl plates on a Perkin Elmer 1600 FTIR spectrometer. High resolution mass spectra were recorded on a Finnigan MAT 8200 Sector Mass Spectrometer at the MIT Department of Chemistry Instrumentation Facility. Elemental analyses were performed by H. Kolbe Mikroanalytisches Laboratorium, Mülheim an der Ruhr, Germany.

Starting materials. $O(o\text{-C}_6\text{H}_4\text{NH}_2)_2$,¹⁰¹ $\text{Ti}(\text{NMe}_2)_4$,¹⁰² $\text{TiCl}_2(\text{NMe}_2)_2$,⁷⁸ $\text{Zr}(\text{NMe}_2)_4$,⁷⁹ $\text{Zr}(\text{CH}_2\text{SiMe}_3)_4$,⁸² ZrBn_4 ,¹⁰³ ZrNp_4 ,¹⁰⁴ $\text{ZrCl}_2(\text{CH}_2\text{SiMe}_3)_2$,³⁸ $\text{Hf}(\text{NMe}_2)_4$,¹⁰⁵ NpLi ,¹⁰⁶ and NpMgCl ¹⁰⁷ were prepared according to the literature procedures. $\text{PhMe}_2\text{CCH}_2\text{MgCl}$ was prepared in a manner similar to the preparation of NpMgCl . Zinc dust (97.5%) was purchased from Strem and activated with 5% aqueous HCl prior to use.⁷⁴ HfCl_4 (99%, < 0.2% Zr) was purchased from Cerac; other metal halides were purchased from Strem. $[\text{HNMe}_2\text{Ph}][\text{B}(\text{C}_6\text{F}_5)_4]$ and $[\text{Ph}_3\text{C}][\text{B}(\text{C}_6\text{F}_5)_4]$ were provided by Exxon Chemical Corporation. All other chemicals were purchased from commercial suppliers. Pyridine and lutidines were sparged with nitrogen and dried over activated 4 Å molecular sieves prior to use. Mesityl bromide was sparged with nitrogen prior to use. 1-Hexene was refluxed over sodium for four days and distilled. All other chemicals were used as received.

E.1.1 $[\text{CyNON}]^{2-}$ ligand system.[@]

$\text{H}_2[\text{CyNON}]$. A 250 mL round-bottom one-necked flask was equipped with a condenser and charged with a Teflon-sealed stir bar, $O(o\text{-C}_6\text{H}_4\text{NH}_2)_2$ (5.03 g, 0.025 mol), cyclohexanone (4.93 g, 0.050 mol, 2 equiv.), zinc (16.42 g, 0.25 mol, 10 equiv.), and acetic acid (100 mL). The mixture was heated to 65 °C under nitrogen for 29 h. The gray-white suspension containing residual zinc was cooled to room temperature and MeOH (100 mL) was added. The white precipitate was removed by filtration using a glass frit and washed with MeOH (100 mL). The filtrate was concentrated on a rotary evaporator until the volume was ~10 mL and crushed ice (~100 g) and CH_2Cl_2 (100 mL) were added. Ammonium hydroxide was added until pH > 10. The organic layer was separated from the aqueous layer, which was further washed with CH_2Cl_2 (100 mL). The combined organic solutions were dried over MgSO_4 and the solvent was removed

[@] The compounds in this section have been published:

Baumann, R.; Stumpf, R.; Davis, W. M.; Liang, L.-C.; Schrock, R. R. *J. Am. Chem. Soc.* in press.

under reduced pressure to give a yellow oil, which was pure $\text{H}_2[\text{CyNON}]$ according to its ^1H NMR spectrum. The oil was directly used for subsequent organometallic chemistry without further purification; it occasionally crystallized at room temperature after several weeks; yield 8.03 g (88%): IR (Et_2O): $\text{NH}(\text{st.})$ 3412 cm^{-1} ; ^1H NMR (C_6D_6) δ 6.99 (t, 2, Aryl), 6.93 (d, 2, Aryl), 6.71 (d, 2, Aryl), 6.59 (t, 2, Aryl), 4.29 (s, 2, NH), 3.15 (m, 2, Cy), 1.88 (m, 4, Cy), 1.49 (m, 4, Cy), 1.39 (m, 2, Cy), 1.12 (m, 4, Cy), 0.95 (m, 6, Cy); ^1H NMR (CDCl_3) δ 6.99 (t, 2, Aryl), 6.76 (m, 4, Aryl), 6.59 (t, 2, Aryl), 4.19 (br s, 2, NH), 3.32 (m, 2, Cy), 2.08 (m, 4, Cy), 1.77-1.63 (m, 6, Cy), 1.44-1.16 (m, 10, Cy); ^{13}C NMR (CDCl_3) δ 143.98 (C, Aryl), 139.12 (C, Aryl), 124.33 (CH, Aryl), 118.02 (CH, Aryl), 116.27 (CH, Aryl), 11.92 (CH, Aryl), 51.54 (CH, Cy), 33.46 (CH_2 , Cy), 26.07 (CH_2 , Cy), 25.09 (CH_2 , Cy); HRMS (EI, 70 eV): m/z calcd. for $\text{C}_{24}\text{H}_{32}\text{N}_2\text{O}$ 364.251464, found 364.25132.

$[\text{CyNON}]\text{Ti}(\text{NMe}_2)_2$. $n\text{-BuLi}$ (1.15 mL, 2.5 M in hexane, 2.875 mmol, 2 equiv.) was added to a diethyl ether solution (10 mL) of $\text{H}_2[\text{CyNON}]$ (522 mg, 1.432 mmol) at $-30\text{ }^\circ\text{C}$. The mixture was stirred at room temperature for 1.5 h and cooled to $-30\text{ }^\circ\text{C}$. Solid $\text{TiCl}_2(\text{NMe}_2)_2$ (296 mg, 1.432 mmol) was added while the diethyl ether solution was stirred. The reaction mixture was stirred at room temperature overnight (~ 14 h). The dark red suspension was filtered through Celite and the insoluble materials were washed with diethyl ether (5 mL). The filtrate was concentrated *in vacuo* until the volume was ~ 2 mL. Pentane (1 mL) was layered on top and the solution was cooled to $-30\text{ }^\circ\text{C}$ to afford red crystals. The supernatant was decanted and the red crystals were dried *in vacuo*; yield 525 mg (74%): ^1H NMR (C_6D_6) δ 7.30 (d, 2, Aryl), 7.03 (t, 2, Aryl), 6.93 (d, 2, Aryl), 6.50 (t, 2, Aryl), 3.79 (m, 2, Cy), 3.13 (s, 12, TiNMe_2), 1.95 (m, 8, Cy), 1.79 (m, 4, Cy), 1.65 (m, 2, Cy), 1.36 (m, 4, Cy), 1.16 (m, 2, Cy); ^{13}C NMR (C_6D_6) δ 149.01 (C, Aryl), 146.00 (C, Aryl), 125.50 (CH, Aryl), 115.07 (CH, Aryl), 114.82 (CH, Aryl), 113.97 (CH, Aryl), 64.83 (CH, Cy), 47.09 (TiNMe_2), 33.57 (CH_2 , Cy), 27.56 (CH_2 , Cy), 27.07 (CH_2 , Cy). Anal. Calcd. for $\text{C}_{28}\text{H}_{42}\text{N}_4\text{OTi}$: C, 67.46; H, 8.49; N, 11.24. Found: C, 67.32; H, 8.55; N, 11.16.

[CyNON]TiCl₂. Neat Me₃SiCl (0.4 mL, 3.117 mmol, 3 equiv.) was added to a toluene solution (20 mL) of [CyNON]Ti(NMe₂)₂ (518 mg, 1.039 mmol) in a 100 mL Teflon-sealed Schlenk tube. The toluene solution was heated with stirring to 105 °C for 3 days. All volatile components were removed *in vacuo* at ~50 °C to yield a dark purple solid; yield 477 mg (95%): ¹H NMR (C₆D₆) δ 7.10 (d, 2, Aryl), 6.81 (t, 2, Aryl), 6.64 (d, 2, Aryl), 6.47 (t, 2, Aryl), 5.33 (tt, 2, Cy), 2.33 (m, 4, Cy), 2.02 (m, 4, Cy), 1.74 (m, 4, Cy), 1.52 (m, 2, Cy), 1.43 (m, 4, Cy), 1.02 (m, 2, Cy); ¹³C NMR (C₆D₆) δ 150.26 (C, Aryl), 145.65 (C, Aryl), 125.69 (CH, Aryl), 119.98 (CH, Aryl), 114.69 (CH, Aryl), 111.74 (CH, Aryl), 64.33 (CH, Cy), 28.97 (CH₂, Cy), 27.43 (CH₂, Cy), 26.43 (CH₂, Cy). Anal. Calcd. for C₂₄H₃₀Cl₂N₂OTi: C, 59.89; H, 6.28; N, 5.82. Found: C, 59.97; H, 6.31; N, 5.96.

[CyNON]TiMe₂. MeMgI (0.14 mL, 3 M in diethyl ether, 0.420 mmol, 2 equiv.) was added to a suspension of [CyNON]TiCl₂ (101 mg, 0.210 mmol) in diethyl ether (3 mL) at -30 °C. The reaction mixture was stirred at room temperature for 45 min. The solvent was removed *in vacuo* and the orange residue was extracted with pentane (10 mL). The pentane extract was filtered through Celite and the solvent was removed *in vacuo*. The solid residue was dissolved in diethyl ether (1 mL) and pentane (0.5 mL) was layered on top. The solution was cooled to -30 °C to give an orange crystalline solid. The supernatant was decanted and the orange solid dried *in vacuo*; yield 43 mg (47%): ¹H NMR (C₆D₆) δ 7.37 (d, 2, Aryl), 7.01 (d, 2, Aryl), 6.96 (t, 2, Aryl), 6.47 (t, 2, Aryl), 5.54 (m, 2, Cy), 2.39 (m, 4, Cy), 2.21 (m, 4, Cy), 1.86 (m, 4, Cy), 1.66 (m, 2, Cy), 1.48 (m, 4, Cy), 1.17 (m, 2, Cy), 1.02 (s, 6, TiMe); ¹³C NMR (C₆D₆) δ 148.67 (C, Aryl), 146.00 (C, Aryl), 125.09 (CH, Aryl), 116.21 (CH, Aryl), 113.75 (CH, Aryl), 112.27 (CH, Aryl), 59.47 (CH, Cy), 56.77 (TiMe), 29.88 (CH₂, Cy), 28.03 (CH₂, Cy), 26.79 (CH₂, Cy). Anal. Calcd. for C₂₆H₃₆N₂OTi: C, 70.90; H, 8.24; N, 6.36. Found: C, 71.15; H, 8.19; N, 6.32.

[CyNON]Ti(i-Bu)₂. i-BuMgCl (0.2 mL, 2 M in diethyl ether, 0.4 mmol, 2 equiv.) was added to a diethyl ether solution (3 mL) of [CyNON]TiCl₂ (96 mg, 0.199 mmol) at -30 °C. The reaction mixture was warmed to room temperature with stirring. After being stirred at room

temperature for 20 min, the solvent was removed *in vacuo*. The residue was extracted with pentane (10 mL) and the extract was filtered through Celite. The filtrate was concentrated *in vacuo* until the volume was ~1 mL. The solution was cooled to -30 °C to give an orange crystalline solid. The supernatant was decanted and the orange solid dried *in vacuo*; yield 75 mg (72%): ^1H NMR (C_6D_6) δ 7.40 (d, 2, Aryl), 7.11 (d, 2, Aryl), 6.98 (t, 2, Aryl), 6.47 (t, 2, Aryl), 5.66 (m, 2, Cy), 2.50 (m, 4, Cy), 2.35 (m, 4, Cy), 2.19 (m, 2, $\text{TiCH}_2\text{CHMe}_2$), 1.92 (m, 4, Cy), 1.74 (d, 4, $\text{TiCH}_2\text{CHMe}_2$), 1.68 (m, 2, Cy), 1.57 (m, 4, Cy), 1.24 (m, 2, Cy), 0.77 (d, 12, $\text{TiCH}_2\text{CHMe}_2$); ^{13}C NMR (C_6D_6) δ 147.68 (C, Aryl), 146.07 (C, Aryl), 125.30 (CH, Aryl), 115.68 (CH, Aryl), 113.59 (CH, Aryl), 112.94 (CH, Aryl), 94.44 ($\text{TiCH}_2\text{CHMe}_2$), 60.37 (CH, Cy), 32.60 ($\text{TiCH}_2\text{CHMe}_2$), 30.11 (CH_2 , Cy), 28.05 (CH_2 , Cy), 27.52 ($\text{TiCH}_2\text{CHMe}_2$), 26.90 (CH_2 , Cy). Anal. Calcd. for $\text{C}_{32}\text{H}_{48}\text{N}_2\text{OTi}$: C, 73.26; H, 9.22; N, 5.34. Found: C, 73.09; H, 9.20; N, 5.26.

[CyNON]TiNp₂. A diethyl ether solution (2 mL) of NpLi (33 mg, 0.423 mmol, 2 equiv.) at -30 °C was added to a diethyl ether solution (4 mL) of [CyNON]TiCl₂ (102 mg, 0.212 mmol) at -30 °C. The reaction mixture was stirred at room temperature for 50 min. The solvent was removed *in vacuo* and the solid residue was extract with pentane (10 mL). Insoluble materials were removed by filtration through Celite. The solvent was removed from the deep red filtrate to give a reddish purple solid; yield 94 mg (80%): ^1H NMR (C_6D_6) δ 7.28 (d, 2, Aryl), 7.10 (d, 2, Aryl), 7.00 (t, 2, Aryl), 6.44 (t, 2, Aryl), 5.31 (m, 2, Cy), 2.52 (m, 4, Cy), 2.45 (m, 4, Cy), 2.24 (s, 4, $\text{TiCH}_2\text{CMe}_3$), 1.89 (m, 4, Cy), 1.67 (m, 2, Cy), 1.53 (m, 4, Cy), 1.22 (m, 2, Cy), 0.86 (s, 18, $\text{TiCH}_2\text{CMe}_3$); ^{13}C NMR (C_6D_6) δ 146.60 (C, Aryl), 146.34 (C, Aryl), 125.64 (CH, Aryl), 115.66 (CH, Aryl), 113.81 (CH, Aryl), 113.75 (CH, Aryl), 104.90 ($\text{TiCH}_2\text{CMe}_3$), 62.25 (CH, Cy), 38.80 ($\text{TiCH}_2\text{CMe}_3$), 34.53 ($\text{TiCH}_2\text{CMe}_3$), 30.81 (CH_2 , Cy), 27.74 (CH_2 , Cy), 26.92 (CH_2 , Cy). Anal. Calcd. for $\text{C}_{34}\text{H}_{52}\text{N}_2\text{OTi}$: C, 73.89; H, 9.48; N, 5.07. Found: C, 73.38; H, 9.24; N, 5.28.

[CyNON]Zr(NMe₂)₂. Pentane (50 mL) was added to a solid mixture of H₂[CyNON] (2.681 g, 7.354 mmol) and Zr(NMe₂)₄ (1.966 g, 7.354 mmol) at room temperature. The mixture was shaken in order to dissolve the two starting materials. The pale yellow solution was stood at

room temperature overnight to allow for the crystallization of $[\text{CyNON}]\text{Zr}(\text{NMe}_2)_2$. Colorless crystals (1.25 g) were filtered off. The filtrate was concentrated *in vacuo* until the volume was ~20 mL to afford a second crop (1.41 g); yield 2.65 g (67%): ^1H NMR (C_6D_6) δ 7.29 (d, 2, Aryl), 7.05 (t, 2, Aryl), 6.85 (d, 2, Aryl), 6.46 (t, 2, Aryl), 3.46 (tt, 2, Cy), 2.82 (s, 12, ZrNMe_2), 2.03 (m, 4, Cy), 1.79 (m, 4, Cy), 1.65 (m, 2, Cy), 1.57 (m, 4, Cy), 1.33 (m, 4, Cy), 1.19 (m, 2, Cy); ^{13}C NMR (C_6D_6) δ 148.18 (C, Aryl), 144.59 (C, Aryl), 126.44 (CH, Aryl), 115.00 (CH, Aryl), 113.73 (CH, Aryl), 113.61 (CH, Aryl), 60.90 (CH, Cy), 42.54 (ZrNMe_2), 34.69 (CH_2 , Cy), 27.33 (CH_2 , Cy), 27.16 (CH_2 , Cy). Anal. Calcd. for $\text{C}_{28}\text{H}_{42}\text{N}_4\text{OZr}$: C, 62.06; H, 7.81; N, 10.34. Found: C, 62.04; H, 7.79; N, 10.33.

$[\text{CyNON}]\text{ZrCl}_2$. Neat Me_3SiCl (0.89 mL, 6.98 mmol, 3 equiv.) was added to a stirred solution of $[\text{CyNON}]\text{Zr}(\text{NMe}_2)_2$ (1.26 g, 2.33 mmol) in toluene (20 mL) at room temperature. Solid $[\text{CyNON}]\text{Zr}(\text{NMe}_2)_2$ completely dissolved in 30 min to give a homogeneous, clear yellow solution. After 7 h, pentane (~20 mL) was added to precipitate the yellow $[\text{CyNON}]\text{ZrCl}_2$, which was collected on a fritted funnel, washed with pentane (20 mL), and dried *in vacuo*; yield 0.985 g (81%). The product was recrystallized from toluene/pentane solution at $-30\text{ }^\circ\text{C}$ to give yellow crystals which contain 0.28 equiv. of toluene per zirconium according to its ^1H NMR spectrum: ^1H NMR (C_6D_6) δ 7.12 (d, 2, Aryl), 6.87 (t, 2, Aryl), 6.70 (d, 2, Aryl), 6.43 (t, 2, Aryl), 4.16 (m, 2, Cy), 2.19 (m, 8, Cy), 1.71 (m, 4, Cy), 1.50 (m, 2, Cy), 1.28 (m, 4, Cy), 1.09 (m, 2, Cy); ^{13}C NMR (C_6D_6) δ 148.19 (C, Aryl), 144.54 (C, Aryl), 126.23 (CH, Aryl), 117.74 (CH, Aryl), 115.47 (CH, Aryl), 113.89 (CH, Aryl), 59.29 (CH, Cy), 30.88 (CH_2 , Cy), 27.26 (CH_2 , Cy), 26.30 (CH_2 , Cy). Anal. Calcd. for $\text{C}_{24}\text{H}_{30}\text{Cl}_2\text{N}_2\text{OZr}(\text{toluene})_{0.28}$: C, 56.65; H, 5.90; N, 5.09. Found: C, 56.55; H, 6.01; N, 5.09.

$[\text{CyNON}]\text{Zr}(\text{CH}_2\text{SiMe}_3)_2$. Toluene (4 mL) was added to a solid mixture of $\text{H}_2[\text{CyNON}]$ (546 mg, 1.498 mmol) and $\text{Zr}(\text{CH}_2\text{SiMe}_3)_4$ (659 mg, 1.498 mmol) at room temperature. The reaction solution was shielded from light with aluminum foil and stirred at room temperature for 18 h. All volatile components were removed *in vacuo* to give a brown oil. Pentane (5 mL) was added to dissolve the oil. The solution was concentrated to ~3 mL and cooled

to -35 °C to afford a pale yellow crystalline solid. The supernatant was decanted and the solid dried *in vacuo*; yield 659 mg (70%): ^1H NMR (C_6D_6) δ 7.36 (d, 2, Aryl), 6.94 (m, 4, Aryl), 6.43 (t, 2, Aryl), 4.41 (m, 2, Cy), 2.27 (m, 8, Cy), 1.85 (m, 4, Cy), 1.64 (m, 2, Cy), 1.47 (m, 4, Cy), 1.20 (m, 2, Cy), 0.91 (s, 4, $\text{ZrCH}_2\text{SiMe}_3$), 0.06 (s, 18, $\text{ZrCH}_2\text{SiMe}_3$); ^1H NMR (toluene- d_8) δ 7.33 (d, 2, Aryl), 6.92 (m, 4, Aryl), 6.42 (t, 2, Aryl), 4.40 (m, 2, Cy), 2.26 (m, 8, Cy), 1.87 (m, 4, Cy), 1.67 (m, 2, Cy), 1.48 (m, 4, Cy), 1.22 (m, 2, Cy), 0.86 (s, 4, $\text{ZrCH}_2\text{SiMe}_3$), 0.02 (s, 18, $\text{ZrCH}_2\text{SiMe}_3$); ^{13}C NMR (C_6D_6) δ 146.68 (C, Aryl), 145.15 (C, Aryl), 125.79 (CH, Aryl), 115.45 (CH, Aryl), 114.38 (CH, Aryl), 113.77 (CH, Aryl), 58.33 ($\text{ZrCH}_2\text{SiMe}_3$), 56.51 (CH, Cy), 31.37 (CH_2 , Cy), 27.30 (CH_2 , Cy), 26.64 (CH_2 , Cy), 3.49 ($\text{ZrCH}_2\text{SiMe}_3$). Anal. Calcd. for $\text{C}_{32}\text{H}_{52}\text{N}_2\text{OSi}_2\text{Zr}$: C, 61.19; H, 8.34; N, 4.46. Found: C, 61.07; H, 8.59; N, 4.48.

[CyNON]ZrMe₂. MeMgI (0.1 mL, 3 M in diethyl ether, 0.3 mmol, 2 equiv.) was added to a yellow suspension of [CyNON]ZrCl₂ (79 mg, 0.150 mmol) in diethyl ether (1 mL) at -35 °C. The reaction mixture was stirred at room temperature for 45 min. All volatile components were removed *in vacuo* and the residue was extracted with pentane (10 mL). The extract was filtered through Celite and the solvent was removed *in vacuo* to give an off-white solid; yield 74 mg (100%): ^1H NMR (C_6D_6) δ 7.37 (d, 2, Aryl), 6.97 (t, 2, Aryl), 6.87 (d, 2, Aryl), 6.44 (t, 2, Aryl), 4.22 (m, 2, Cy), 2.21 (m, 8, Cy), 1.79 (m, 4, Cy), 1.60 (m, 2, Cy), 1.35 (m, 4, Cy), 1.15 (m, 2, Cy), 0.55 (s, 6, ZrMe); ^1H NMR (toluene- d_8) δ 7.28 (d, 2, Aryl), 6.93 (t, 2, Aryl), 6.83 (d, 2, Aryl), 6.40 (t, 2, Aryl), 4.18 (m, 2, Cy), 2.19 (m, 8, Cy), 1.82 (m, 4, Cy), 1.62 (m, 2, Cy), 1.37 (m, 4, Cy), 1.17 (m, 2, Cy), 0.49 (s, 6, ZrMe); ^1H NMR ($\text{C}_6\text{D}_5\text{Br}$) δ 7.39 (d, 2, Aryl), 6.99 (t, 2, Aryl), 6.87 (d, 2, Aryl), 6.49 (t, 2, Aryl), 4.18 (m, 2, Cy), 2.16 (m, 8, Cy), 1.86 (m, 4, Cy), 1.67 (m, 2, Cy), 1.40 (m, 4, Cy), 1.22 (m, 2, Cy), 0.45 (s, 6, ZrMe); ^{13}C NMR (C_6D_6) δ 147.23 (C, Aryl), 145.35 (C, Aryl), 125.71 (CH, Aryl), 115.24 (CH, Aryl), 114.30 (CH, Aryl), 112.92 (CH, Aryl), 56.40 (CH, Cy), 42.16 (ZrMe), 31.62 (CH_2 , Cy), 27.47 (CH_2 , Cy), 26.62 (CH_2 , Cy). Anal. Calcd. for $\text{C}_{26}\text{H}_{36}\text{N}_2\text{OZr}$: C, 64.55; H, 7.50; N, 5.79. Found: C, 64.50; H, 7.44; N, 5.69.

[CyNON]ZrEt₂. EtMgBr (0.1 mL, 3 M in diethyl ether, 0.3 mmol, 2 equiv.) was added to a yellow suspension of [CyNON]ZrCl₂ (79 mg, 0.150 mmol) in diethyl ether (1 mL) at -35 °C. After being stirred at room temperature for 15 min, the reaction was worked up as the procedures of [CyNON]ZrMe₂ and the product isolated as an orange solid; yield 47 mg (61%): ¹H NMR (C₆D₆) δ 7.35 (d, 2, Aryl), 6.98 (t, 2, Aryl), 6.89 (d, 2, Aryl), 6.43 (t, 2, Aryl), 4.18 (m, 2, Cy), 2.20 (m, 8, Cy), 1.81 (m, 4, Cy), 1.62 (m, 2, Cy), 1.37 (m, 8, containing ZrCH₂CH₃ (t, 6) and Cy (m, 2)), 1.18 (m, 4, Cy), 1.00 (q, 4, ZrCH₂CH₃); ¹³C NMR (C₆D₆) δ 146.89 (C, Aryl), 145.26 (C, Aryl), 125.76 (CH, Aryl), 115.04 (CH, Aryl), 114.32 (CH, Aryl), 113.11 (CH, Aryl), 56.57 (CH, Cy), 53.01 (ZrCH₂CH₃), 31.54 (CH₂, Cy), 27.55 (CH₂, Cy), 26.71 (CH₂, Cy), 11.04 (ZrCH₂CH₃).

[CyNON]Zr(i-Bu)₂. i-BuMgCl (0.2 mL, 2 M in diethyl ether, 0.400 mmol, 2 equiv.) was added to a yellow suspension of [CyNON]ZrCl₂ (105 mg, 0.200 mmol) in toluene (1 mL) at -35 °C. The reaction mixture was stirred at room temperature for 5 min. Pentane (8 mL) was added and the insoluble materials were removed by filtration with Celite. The filtrate was concentrated in vacuo until the volume was ~1 mL. The solution was cooled to -35 °C to give a colorless solid. The supernatant was decanted and the solid dried *in vacuo*; yield 80 mg (70%): ¹H NMR (C₆D₆) δ 7.31 (d, 2, Aryl), 6.95 (m, 4, Aryl), 6.42 (t, 2, Aryl), 4.36 (m, 2, Cy), 2.30 (m, 10, Cy), 1.85 (m, 4, Cy), 1.63 (m, 2, Cy), 1.42 (m, 4, Cy), 1.19 (m, 2, ZrCH₂CHMe₂), 1.11 (d, 4, ZrCH₂CHMe₂), 0.94 (d, 12, ZrCH₂CHMe₂); ¹³C NMR (C₆D₆) δ 146.68 (C, Aryl), 145.28 (C, Aryl), 125.84 (CH, Aryl), 115.11 (CH, Aryl), 114.30 (CH, Aryl), 113.51 (CH, Aryl), 76.63 (ZrCH₂CHMe₂), 56.91 (CH, Cy), 31.60 (CH₂, Cy), 30.31 (ZrCH₂CHMe₂), 28.70 (ZrCH₂CHMe₂), 27.51 (CH₂, Cy), 26.79 (CH₂, Cy). Anal. Calcd. for C₃₂H₄₈N₂OZr: C, 67.67; H, 8.52; N, 4.93. Found: C, 67.48; H, 8.46; N, 5.06.

[CyNON]ZrNp₂. A diethyl ether solution (5 mL) of NpLi (150 mg, 1.92 mmol, 2 equiv.) at -35 °C was added to a yellow suspension of [CyNON]ZrCl₂ (503 mg, 0.959 mmol) in diethyl ether (25 mL) at -35 °C. The reaction mixture was stirred at room temperature for 4 h. All volatile components were removed *in vacuo* and the residue was extracted with toluene (20 mL).

The extract was filtered through Celite and the solvent was removed *in vacuo*. The yellow solid residual was gently washed with pentane (5 mL x 2) to give an off-white solid which was dried *in vacuo*; yield 283 mg (50%): ^1H NMR (C_6D_6) δ 7.22 (d, 2, Aryl), 6.97 (m, 4, Aryl), 6.40 (t, 2, Aryl), 4.33 (m, 2, Cy), 2.46 (m, 4, Cy), 2.28 (m, 4, Cy), 1.84 (m, 4, Cy), 1.64 (m, 2, Cy), 1.43 (m, 4, Cy), 1.33 (s, 4, $\text{ZrCH}_2\text{CMe}_3$), 1.27 (m, 2, Cy), 1.02 (s, 18, $\text{ZrCH}_2\text{CMe}_3$); ^{13}C NMR (C_6D_6) δ 146.08 (C, Aryl), 145.37 (C, Aryl), 126.08 (CH, Aryl), 115.11 (CH, Aryl), 114.45 (CH, Aryl), 113.99 (CH, Aryl), 84.84 ($\text{ZrCH}_2\text{CMe}_3$), 58.07 (CH, Cy), 36.68 ($\text{ZrCH}_2\text{CMe}_3$), 35.49 ($\text{ZrCH}_2\text{CMe}_3$), 31.21 (CH_2 , Cy), 27.27 (CH_2 , Cy), 26.84 (CH_2 , Cy). Anal. Calcd. for $\text{C}_{34}\text{H}_{52}\text{N}_2\text{OZr}$: C, 68.52; H, 8.79; N, 4.70. Found: C, 68.32; H, 8.71; N, 4.62.

[CyNON]ZrBn₂. BnMgCl (0.41 mL, 1 M in diethyl ether, 0.412 mmol, 2 equiv.) was added to a yellow suspension of $[\text{CyNON}]\text{ZrCl}_2$ (108 mg, 0.206 mmol) in toluene (1 mL) at -35°C . The reaction mixture was stirred at room temperature for 15 min. All volatile components were removed *in vacuo* and the residue was extracted with toluene (5 mL). Insoluble materials were removed by filtration through Celite. The solvent was removed *in vacuo* to afford a yellow solid; yield 91 mg (70%): ^1H NMR (C_6D_6) δ 7.12 (d, 2, Aryl), 6.90 (m, 10, Aryl), 6.70 (m, 4, Aryl), 6.40 (t, 2, Aryl), 3.98 (m, 2, Cy), 2.53 (s, 4, ZrCH_2Ph), 2.14 (m, 8, Cy), 1.78 (m, 4, Cy), 1.64 (m, 2, Cy), 1.34 (m, 4, Cy), 1.19 (m, 2, Cy); ^{13}C NMR (C_6D_6) δ 146.64 (C, Aryl), 144.40 (C, Aryl), 143.35 (C, Aryl), 129.32 (CH, Aryl), 127.47 (CH, Aryl), 125.67 (CH, Aryl), 122.59 (CH, Aryl), 115.49 (CH, Aryl), 114.22 (CH, Aryl), 113.74 (CH, Aryl), 67.84 (ZrCH_2Ph), 56.75 (CH, Cy), 30.54 (CH_2 , Cy), 27.18 (CH_2 , Cy), 26.66 (CH_2 , Cy).

[CyNON]Zr($\text{CH}_2\text{CH}=\text{CH}_2$)₂. ($\text{CH}_2\text{CH}=\text{CH}_2$)MgBr (0.41 mL, 1 M in diethyl ether, 0.41 mmol, 2 equiv.) was added to a yellow suspension of $[\text{CyNON}]\text{ZrCl}_2$ (108 mg, 0.206 mmol) in diethyl ether (2 mL) at -35°C . The suspension color changed immediately from yellow to orange upon addition. The reaction mixture was stirred at room temperature for 15 min. All volatile components were removed *in vacuo* and the residue was extracted with toluene (10 mL). The extract was filtered through Celite and the solvent was removed *in vacuo*. The orange solid was gently washed with diethyl ether (1 mL) and dried *in vacuo*; yield 94 mg (85%): ^1H NMR

(C₆D₆) δ 7.35 (d, 2, Aryl), 6.91 (t, 2, Aryl), 6.62 (d, 2, Aryl), 6.47 (t, 2, Aryl), 6.24 (quintet, J = 12.5, 2, Cy), 3.64 (m, 8, Cy), 2.80 (m, 2, ZrCH₂CHCH₂), 1.72 (m, 4, ZrCH₂CHCH₂), 1.50 (m, 10, Cy), 1.02 (m, 4, ZrCH₂CHCH₂), 0.89 (m, 2, Cy); ¹H NMR (toluene-*d*₈) δ 7.30 (d, 2, Aryl), 6.86 (t, 2, Aryl), 6.56 (d, 2, Aryl), 6.43 (t, 2, Aryl), 6.22 (quintet, J = 12.5, 2, Cy), 3.58 (m, 8, Cy), 2.78 (m, 2, ZrCH₂CHCH₂), 1.69-1.43 (m, 14, containing 10H from Cy and 4H from ZrCH₂CHCH₂), 1.04 (m, 4, ZrCH₂CHCH₂), 0.90 (m, 2, Cy); ¹³C NMR (C₆D₆) δ 146.83 (C, Aryl), 145.55 (C, Aryl), 143.98 (ZrCH₂CHCH₂), 125.26 (CH, Aryl), 115.51 (CH, Aryl), 114.00 (CH, Aryl), 113.85 (ZrCH₂CHCH₂), 113.41 (CH, Aryl), 76.89 (ZrCH₂CHCH₂), 55.04 (CH, Cy), 30.45 (CH₂, Cy), 27.38 (CH₂, Cy), 26.49 (CH₂, Cy); ¹³C NMR (toluene-*d*₈) δ 146.86 (C, Aryl), 145.57 (C, Aryl), 144.00 (ZrCH₂CHCH₂), 125.28 (CH, Aryl), 115.52 (CH, Aryl), 113.90 (CH, Aryl), 113.78 (ZrCH₂CHCH₂), 113.42 (CH, Aryl), 76.86 (ZrCH₂CHCH₂), 55.17 (CH, Cy), 30.56 (CH₂, Cy), 27.49 (CH₂, Cy), 26.62 (CH₂, Cy). Anal. Calcd. for C₃₀H₄₀N₂OZr: C, 67.24; H, 7.52; N, 5.23. Found: C, 67.08; H, 7.46; N, 5.14.

[CyNON]Zr(η^2 -C₂H₄)(PMe₃)₂. A homogeneous, orange solution of [CyNON]ZrEt₂ (75 mg, 0.147 mmol) in neat PMe₃ (0.5 mL) was stirred at room temperature for 30 min. Pentane (5 mL) was added to precipitate the orange product, which was filtered off, washed with pentane (5 mL), and dried *in vacuo*; yield 65 mg (70%): ¹H NMR (C₆D₆) δ 7.43 (d, 2, Aryl), 6.91 (t, 2, Aryl), 6.57 (d, 2, Aryl), 6.44 (t, 2, Aryl), 2.65 (m, 2, Cy), 1.62 (m, 8, Cy), 1.36 (m, 2, Cy), 1.23 (s, 4, C₂H₄), 1.15 (m, 4, Cy), 0.92 (m, 18, containing 6H from Cy and 12H from PMe₃); ³¹P NMR (C₆D₆) δ -25.31, -60.86.

[CyNON]Zr(η^2 -C₂H₂Me₂)(PMe₃)₂. A solution of [CyNON]Zr(*i*-Bu)₂ (90 mg, 0.158 mmol) in neat PMe₃ (0.5 mL) was heated to 50 °C for 3 days in a Teflon-sealed Schlenk tube which was shielded from lightning by Aluminum foil. Pentane (10 mL) was added to precipitate the orange product, which was collected on a glass frit and washed with pentane (3 mL); yield 32 mg (31%): ¹H NMR (C₆D₆) δ 7.40 (d, 2, Aryl), 6.87 (t, 2, Aryl), 6.79 (d, 2, Aryl), 6.43 (t, 2, Aryl), 2.90 (m, 2, Cy), 2.21 (m, 2, Cy), 2.10 (m, 2, Cy), 1.98 (s, 6, C₂H₂Me₂), 1.69 (m, 4, Cy), 1.45 (m, 8, Cy), 1.26 (m, 4, Cy), 1.00 (br s, 11, containing 2H

from $C_2H_2Me_2$ and 9H from PMe_3), 0.86 (br s, 9, PMe_3); ^{13}C NMR (C_6D_6) δ 147.55, 146.02, 124.46, 116.26, 113.93, 113.61, 63.75, 53.84, 52.09, 34.38, 32.63, 32.25, 27.27, 26.53, 16.37, 15.77; ^{31}P NMR (C_6D_6) δ -26.50, -61.03.

Observation of $\{[CyNON]ZrMe(NMe_2Ph)\}\{B(C_6F_5)_4\}$. A C_6D_5Br solution (0.7 mL) of $[CyNON]ZrMe_2$ (10 mg, 0.021 mmol) at $-35\text{ }^\circ C$ was added to solid $[HNMe_2Ph][B(C_6F_5)_4]$ (17 mg, 0.021 mmol) at $-35\text{ }^\circ C$. Solution color changed immediately from colorless to yellow then yellowish orange in ~ 30 seconds. The solution was stirred at room temperature briefly and cooled to $-35\text{ }^\circ C$. The solution was transferred to a Teflon-sealed NMR tube and frozen with liquid nitrogen. The 1H NMR spectra showed the quantitative formation of $\{[CyNON]ZrMe(NMe_2Ph)\}\{B(C_6F_5)_4\}$. The spectra were recorded at temperatures between -30 and $50\text{ }^\circ C$ with an interval of temperature increase by $10\text{ }^\circ C$. Identical spectra were obtained between -30 and $10\text{ }^\circ C$. $\{[CyNON]ZrMe(NMe_2Ph)\}\{B(C_6F_5)_4\}$ was found to be briefly stable at room temperature; 1H NMR (C_6D_5Br , $0\text{ }^\circ C$) δ 7.24 (d, 2, Aryl), 7.19 (t, 2, Aryl), 7.00 (m, 3, Aryl), 6.75 (d, 2, Aryl), 6.68 (m, 4, Aryl), 3.37 (tt, 2, Cy), 2.49 (s, 6, NMe_2Ph), 1.85 (m, 4, Cy), 1.73 (m, 4, Cy), 1.58 (m, 4, Cy), 1.23 (m, 2, Cy), 1.07 (m, 6, Cy), 0.65 (s, 3, $ZrMe$).

Catalytic reaction between 1-hexene and $[HNMe_2Ph][B(C_6F_5)_4]$ activated $[CyNON]ZrMe_2$. A C_6D_5Br solution (0.3 mL) of $[CyNON]ZrMe_2$ (10 mg, 21 μmol) at $-30\text{ }^\circ C$ was added to a C_6D_5Br solution (0.4 mL) of $[HNMe_2Ph][B(C_6F_5)_4]$ (17 mg, 21 μmol) at $-30\text{ }^\circ C$. The solution color changed immediately from colorless to light yellow. The reaction mixture was briefly warmed to allow for the dissolution of the anilinium salt and kept at $0\text{ }^\circ C$. 1-Hexene (50 equiv.) was added to the above solution at $0\text{ }^\circ C$. The reactivity was monitored by 1H NMR spectroscopy which showed little or no conversion of 1-hexene in 10 min, but $\sim 50\%$ conversion in 6 h.

Catalytic reaction between 1-hexene and $[Ph_3C][B(C_6F_5)_4]$ activated $[CyNON]ZrMe_2$. A C_6D_5Br solution (0.3 mL) of $[CyNON]ZrMe_2$ (13 mg, 27 μmol) at $-30\text{ }^\circ C$ was added to a C_6D_5Br solution (0.4 mL) of $[Ph_3C][B(C_6F_5)_4]$ (24 mg, 26 μmol , 0.96 equiv.) at $-30\text{ }^\circ C$. The orange solution was kept at $0\text{ }^\circ C$ and 1-hexene (60 equiv.) was added. The reaction

was monitored by ^1H NMR spectroscopy which showed a complete conversion of 1-hexene to poly(1-hexene) in 10 min.

E.1.2 [BdeNON] $^{2-}$ ligand system.

$\text{H}_2[\text{BdeNON}]$. n-BuLi (20.0 mL, 2.5 M in hexane, 0.050 mol, 2 equiv.) was added dropwise to a THF solution (45 mL) of $\text{O}(o\text{-C}_6\text{H}_4\text{NH}_2)_2$ (4.975 g, 0.025 mol) at -78°C . The reaction mixture was stirred at room temperature for 3 h to give an orange suspension of $\text{O}(o\text{-C}_6\text{H}_4\text{NHLi})_2$. The suspension was transferred to a 120 mL additional funnel and extra THF was added until the volume reached 100 mL. A THF solution (100 mL) of $\text{ClMe}_2\text{SiCH}_2\text{CH}_2\text{SiMe}_2\text{Cl}$ (5.348 g, 0.025 mol) was prepared on the side and transferred to another 120 mL additional funnel. The two additional funnels were equipped on a 1 L two-necked flask which contained 500 mL THF and a magnetic stir bar. The $\text{O}(o\text{-C}_6\text{H}_4\text{NHLi})_2$ suspension and $\text{ClMe}_2\text{SiCH}_2\text{CH}_2\text{SiMe}_2\text{Cl}$ solution were simultaneously added at the same rate (~ 2 drops per second) to the THF with vigorous stirring. After the addition was finished, the reaction mixture was stirred at room temperature overnight. The solvent was removed on a rotary evaporator. The residue was extracted with pentane (300 mL) and LiCl was removed by filtration through Celite. The solvent was removed *in vacuo* to give a brown oil. The oil was directly used for the subsequent organometallic chemistry, or it might crystallize from a concentrated diethyl ether solution at -35°C to give colorless crystals; yield 5.885 g (69%); IR (Et_2O): $\text{NH}(\text{st.})$ 3393 cm^{-1} ; ^1H NMR (C_6D_6) δ 7.15 (d, 2, Aryl), 6.90 (m, 4, Aryl), 6.65 (m, 2, Aryl), 4.37 (br s, 2, NH), 0.70 (s, 4, CH_2), 0.03 (s, 12, SiMe); ^{13}C NMR (CDCl_3): δ 148.11 (C, Aryl), 139.47 (C, Aryl), 124.84 (CH, Aryl), 121.31 (CH, Aryl), 118.83 (CH, Aryl), 117.78 (CH, Aryl), 7.75 (CH_2), 0.60 (SiMe). HRMS (EI, 70 eV): m/z calcd. for $\text{C}_{18}\text{H}_{13}\text{N}_2\text{OSi}_2$ 342.15837, found 342.15842.

$[\text{BdeNON}]\text{Ti}(\text{NMe}_2)_2$. n-BuLi (1.17 mL, 2.5 M in hexane, 2.925 mmol, 2 equiv.) was added to a diethyl ether solution (20 mL) of $\text{H}_2[\text{BdeNON}]$ (500 mg, 1.459 mmol) at -35°C . The solution was stirred at room temperature for 3 h and cooled to -35°C . Solid $\text{TiCl}_2(\text{NMe}_2)_2$

(302 mg, 1.459 mmol) was added to this cold diethyl ether solution. The deep red suspension was stirred at room temperature overnight (~15 h). Insoluble materials were removed by filtration through Celite and washed with diethyl ether (5 mL). The filtrate was concentrated *in vacuo* until the volume was ~1 mL. Pentane (~1 mL) was layered on top and the solution was cooled to -35 °C (~3 h) to give a reddish purple crystalline solid. The supernatant was decanted and the solid was dried *in vacuo*; yield 373 mg (54%): ^1H NMR (C_6D_6) δ 7.42 (d, 2, Aryl), 6.94 (m, 4, Aryl), 6.77 (t, 2, Aryl), 3.26 (s, 6, TiNMe_2), 2.63 (s, 6, TiNMe_2), 1.21 (m, 2, SiCH_2), 0.94 (m, 2, SiCH_2), 0.46 (s, 6, SiMe_2), -0.07 (s, 6, SiMe_2); ^{13}C NMR (C_6D_6) δ 152.50 (C, Aryl), 146.86 (C, Aryl), 126.45 (CH, Aryl), 125.26 (CH, Aryl), 121.96 (CH, Aryl), 119.26 (CH, Aryl), 47.52 (TiNMe_2), 45.43 (TiNMe_2), 12.16 (SiCH_2), 3.83 (SiMe_2), -0.23 (SiMe_2). Anal. Calcd. for $\text{C}_{22}\text{H}_{24}\text{N}_4\text{OSi}_2\text{Ti}$: C, 56.89; H, 5.21; N, 12.06. Found: C, 57.06; H, 5.30; N, 11.94.

[BdeNON]TiCl₂. Neat Me_3SiCl (0.32 mL, 2.56 mmol, 4 equiv.) was added to a toluene solution (5 mL) of $[\text{BdeNON}]\text{Ti}(\text{NMe}_2)_2$ (305 mg, 0.64 mmol) at room temperature. The reaction mixture was stirred at room temperature for 21 h. All volatile materials were removed *in vacuo*. The dark residue was washed with diethyl ether (5 mL) to give a dark purple solid which was dried *in vacuo*; yield 230 mg (78%): ^1H NMR (C_6D_6) δ 7.15 (d, 2, Aryl), 6.86 (t, 2, Aryl), 6.66 (t, 2, Aryl), 6.46 (d, 2, Aryl), 1.62 (m, 2, SiCH_2), 0.80 (m, 2, SiCH_2), 0.66 (s, 6, SiMe_2), -0.11 (s, 6, SiMe_2); ^{13}C NMR (C_6D_6) δ 126.00 (CH, Aryl), 122.86 (CH, Aryl), 121.60 (CH, Aryl), 116.74 (CH, Aryl), 14.35 (SiCH_2), 0.49 (SiMe_2), -0.54 (SiMe_2), the ipso carbons were not found.

[BdeNON]Zr(NMe₂)₂(HNMe₂). A pentane solution (10 mL) of $\text{H}_2[\text{BdeNON}]$ (407 mg, 1.188 mmol) was added to a pentane solution (10 mL) of $\text{Zr}(\text{NMe}_2)_4$ (318 mg, 1.188 mmol) at room temperature. The homogeneous solution was shaken thoroughly and slowly poured to another flask to initiate the formation of crystals. The reaction solution was stood at room temperature overnight. Colorless crystals were filtered off and dried *in vacuo*. Reduction of the solvent from the mother liquor gave another crop; yield 603 mg (90%): ^1H NMR (C_6D_6) δ 7.33 (d, 2, Aryl), 7.00-6.96 (m, 4, Aryl), 6.59 (t, 2, Aryl), 2.86 (br s, 12, ZrNMe_2), 1.80 (d, 6,

HNMe₂), 1.43 (m, 2, SiCH₂), 1.18 (heptet, 1, HNMe₂), 0.98 (m, 2, SiCH₂), 0.49 (s, 6, SiMe₂), 0.15 (s, 6, SiMe₂); ¹³C NMR (C₆D₆) δ 153.73 (C, Aryl), 149.18 (C, Aryl), 126.07 (CH, Aryl), 123.74 (CH, Aryl), 120.02 (CH, Aryl), 117.49 (CH, Aryl), 44.04 (br s, ZrNMe₂), 40.11 (HNMe₂), 13.05 (SiCH₂), 5.07 (SiMe₂), 0.79 (SiMe₂). Anal. Calcd. for C₂₄H₄₃N₅OSi₂Zr: C, 51.02; H, 7.67; N, 12.39. Found: C, 50.88; H, 7.59; N, 12.32.

[BdeNON]Zr(NMe₂)₂(py). Neat pyridine (0.300 g, 3.793 mmol) was added to a diethyl ether solution (8 mL) of [BdeNON]Zr(NMe₂)₂(HNMe₂) (1.000 g, 1.770 mmol) at room temperature. Solution color changed immediately from colorless to yellow. The reaction mixture was stirred at room temperature for 4 h and a solution aliquot was analyzed by ¹H NMR spectroscopy which showed the complete formation of [BdeNON]Zr(NMe₂)₂(py). All volatile components were removed *in vacuo* to give a yellow crystalline solid; yield 1.050 g (99%): ¹H NMR (C₆D₆) δ 8.53 (d, 2, Aryl), 7.28 (d, 2, Aryl), 7.06 (d, 2, Aryl), 6.99 (t, 2, Aryl), 6.72 (t, 1, Aryl), 6.57 (t, 2, Aryl), 6.45 (t, 2, Aryl), 3.04 (br s, 6, ZrNMe₂), 2.76 (br s, 6, ZrNMe₂), 1.49 (m, 2, SiCH₂), 1.06 (m, 2, SiCH₂), 0.57 (s, 6, SiMe₂), 0.24 (s, 6, SiMe₂); ¹³C NMR (C₆D₆) δ 153.65 (C, Aryl), 150.78 (CH, Aryl), 149.25 (C, Aryl), 138.31 (CH, Aryl), 125.88 (CH, Aryl), 124.44 (CH, Aryl), 123.40 (CH, Aryl), 119.98 (CH, Aryl), 117.54 (CH, Aryl), 45.03 (ZrNMe₂), 44.22 (ZrNMe₂), 12.73 (SiCH₂), 4.90 (SiMe₂), 1.14 (SiMe₂). Anal. Calcd. for C₂₇H₄₁N₅OSi₂Zr: C, 54.14; H, 6.90; N, 11.69. Found: C, 53.94; H, 6.78; N, 11.56.

[BdeNON]Zr(NMe₂)₂(2,4-lutidine). Neat 2,4-lutidine (12 mg, 0.112 mmol) was added to a diethyl ether solution (1 mL) of [BdeNON]Zr(NMe₂)₂(HNMe₂) (12 mg, 0.021 mmol) at room temperature. The solution was stirred at room temperature for 6 h. All volatile materials were removed *in vacuo* to give a yellow crystalline solid; yield 13 mg (98%): ¹H NMR (C₆D₆) δ 8.48 (d, 1, H₂O, lutidine), 7.25 (d, 2, Aryl), 7.04 (d, 2, Aryl), 6.95 (t, 2, Aryl), 6.54 (t, 2, Aryl), 6.42 (m, 2, Aryl), 3.19 (br s, 6, ZrNMe₂), 2.71 (br s, 6, ZrNMe₂), 2.42 (s, 3, *Me*-lutidine), 1.73 (s, 3, *Me*-lutidine), 1.49 (m, 2, SiCH₂), 1.04 (m, 2, SiCH₂), 0.56 (s, 6, SiMe₂), 0.19 (s, 6, SiMe₂); ¹³C NMR (C₆D₆) δ 159.66 (C, Aryl), 153.39 (C, Aryl), 150.11 (CH, Aryl), 149.18 (C, Aryl), 148.34 (C, Aryl), 125.95 (CH, Aryl), 125.47 (CH, Aryl), 123.66 (CH, Aryl), 122.25

(CH, Aryl), 119.55 (CH, Aryl), 117.68 (CH, Aryl), 45.66 (br s, NMe), 44.13 (br s, NMe), 24.05 (Me, Lutidine), 20.76 (Me, Lutidine), 12.81 (SiCH₂), 4.87 (SiMe₂), 1.07 (SiMe₂). Anal. Calcd. for C₂₉H₄₅N₅OSi₂Zr: C, 55.54; H, 7.23; N, 11.17. Found: C, 55.39; H, 7.20; N, 11.12.

[BdeNON]ZrCl₂(py). Neat Me₃SiCl (1.4 mL, 10.764 mmol) was added to a solution of [BdeNON]Zr(NMe₂)₂(py) (496 mg, 0.828 mmol) in CH₂Cl₂ (10 mL) at room temperature. The reaction solution was stirred at room temperature overnight. The solvent was removed *in vacuo*. The yellow solid was washed with pentane (5 mL x 3) and dried *in vacuo*; yield 443 mg (92%): ¹H NMR (C₆D₆) δ 8.88 (d, 2, Aryl), 7.23 (d, 2, Aryl), 6.80 (m, 2, Aryl), 6.68-6.50 (m, 5, Aryl), 6.38 (t, 2, Aryl), 1.84 (m, 2, SiCH₂), 0.99 (m, 2, SiCH₂), 0.71 (s, 6, SiMe₂), 0.13 (s, 6, SiMe₂); ¹³C NMR (C₆D₆) δ 153.66 (C, Aryl), 150.58 (CH, Aryl), 145.28 (C, Aryl), 139.34 (CH, Aryl), 126.97 (CH, Aryl), 124.19 (CH, Aryl), 122.44 (CH, Aryl), 119.87 (CH, Aryl), 119.26 (CH, Aryl), 13.26 (SiCH₂), 2.32 (SiMe₂), 0.54 (SiMe₂). Anal. Calcd. for C₂₃H₂₉Cl₂N₃OSi₂Zr: C, 47.48; H, 5.02; N, 7.22. Found: C, 47.59; H, 5.10; N, 7.16.

[BdeNON][BdeNON']Zr₂(CH₂SiMe₃)₂. **Method A:** Me₃SiCH₂MgCl (0.344 mL, 1 M in diethyl ether, 0.344 mmol, 2 equiv.) was added to a diethyl ether solution (4 mL) of [BdeNON]ZrCl₂(py) (100 mg, 0.172 mmol) at -30 °C. The reaction mixture was stirred at room temperature for 20 min and the solvent was removed *in vacuo*. The residue was extracted with pentane (8 mL) and filtered through Celite. The filtrate was concentrated *in vacuo* until the volume was ~1 mL. The concentrated solution was cooled to -30 °C to give a pale yellow crystalline solid. The supernatant was decanted and the solid was dried *in vacuo*; yield 46 mg (52%). **Method B:** Li₂[BdeNON] was prepared by addition of 2 equiv. of n-BuLi to a pentane solution of H₂[BdeNON] at -30 °C and isolated as an off-white solid in quantitative yield. A diethyl ether solution of ZrCl₂(CH₂SiMe₃)₂ was prepared *in situ* as follows: under reduced lightning, a diethyl ether solution (3 mL) of LiCH₂SiMe₃ (90 mg, 0.961 mmol, 2 equiv.) at -30 °C was added to a diethyl ether suspension (3 mL) of ZrCl₄ (112 mg, 0.481 mmol) at -30 °C with vigorous stirring. The reaction mixture was stirred at room temperature for 30 min. Insoluble materials were

removed by filtration through Celite and the filtrate (containing $\text{ZrCl}_2(\text{CH}_2\text{SiMe}_3)_2(\text{Et}_2\text{O})_x$) was cooled to $-30\text{ }^\circ\text{C}$. Solid $\text{Li}_2[\text{BdeNON}]$ (170 mg, 0.481 mmol) was added to this diethyl ether solution of $\text{ZrCl}_2(\text{CH}_2\text{SiMe}_3)_2$. The reaction mixture was stirred at room temperature overnight. LiCl was removed by filtration through Celite and washed with diethyl ether (2 mL). The filtrate were concentrated *in vacuo* until the volume was $\sim 1\text{ mL}$. The concentrated solution was cooled to $-30\text{ }^\circ\text{C}$ to give a microcrystalline solid. The supernatant was decanted and the crystalline solid was dried *in vacuo*; yield 172 mg (69%). An X-ray quality crystal was obtained by recrystallization from a concentrated diethyl ether solution at $-30\text{ }^\circ\text{C}$: ^1H NMR (C_6D_6 ; the assignment was not completely certain) δ 7.24-6.36 (m, 16, Aryl), 5.42 (s, 1, ZrCHZr), 1.43-0.75 (m, 8, $\text{Si}(\text{CH}_2)_2\text{Si}$), 1.01 (s, 3, NSiMe_2), 0.53 (s, 9, $\text{ZrCH}_2\text{SiMe}_3$), 0.40 (s, 3, NSiMe_2), 0.39 (s, 3, NSiMe_2), 0.32 (s, 9, $\text{ZrCH}_2\text{SiMe}_3$), 0.24 (s, 3, NSiMe_2), 0.23 (s, 3, NSiMe_2), -0.02 (s, 3, NSiMe_2), -0.60 (s, 2, $\text{ZrCH}_2\text{SiMe}_3$), -0.91 (s, 2, $\text{ZrCH}_2\text{SiMe}_3$); ^{13}C NMR (C_6D_6) δ 163.59 (ZrCHZr , $^1J_{\text{CH}} = 103$), 157.55, 155.53, 152.23, 151.31, 147.92, 147.87, 146.65, 145.21, 144.66, 135.12, 134.80, 127.68, 127.21, 126.39, 126.30, 125.40, 124.26, 122.35, 120.95, 120.17, 118.75, 118.05, 117.20, 116.96, 71.29, 60.60, 34.79, 23.08, 15.79, 14.65, 9.38, 7.65, 5.04, 4.31, 4.15, 3.76, 0.39, -3.20, -5.13. Anal. Calcd. for $\text{C}_{44}\text{H}_{68}\text{N}_4\text{O}_2\text{Si}_6\text{Zr}_2$: C, 51.01; H, 6.62; N, 5.41. Found: C, 51.19; H, 6.53; N, 5.37.

$[\text{BdeNON}][\text{BdeNON}']\text{Zr}_2(\text{CH}_2\text{CMe}_2\text{Ph})_2$. $\text{PhMe}_2\text{CCH}_2\text{MgCl}$ (0.33 mL, 1.12 M in diethyl ether, 0.370 mmol, 2 equiv.) was added to a diethyl ether solution (4 mL) of $[\text{BdeNON}]\text{ZrCl}_2(\text{py})$ (106 mg, 0.182 mmol) at $-30\text{ }^\circ\text{C}$. The reaction mixture was stirred at room temperature for 2 h. The solvent was removed *in vacuo* and the solid residue was extracted with pentane (10 mL). Insoluble materials were removed by filtration through Celite and the filtrate was concentrated *in vacuo* until the volume was $\sim 1\text{ mL}$. The concentrated solution was cooled to $-30\text{ }^\circ\text{C}$ to give an orange crystalline solid. The supernatant was decanted and the solid was dried *in vacuo*; yield 33 mg (47%): Anal. Calcd. for $\text{C}_{56}\text{H}_{72}\text{N}_4\text{O}_2\text{Si}_4\text{Zr}_2$: C, 59.63; H, 6.43; N, 4.97. Found: C, 59.73; H, 6.56; N, 4.88.

[BdeNON]ZrCp*Cl. Solid Cp*Li (26 mg, 0.183 mmol) was added to a diethyl ether solution (3 mL) of [BdeNON]ZrCl₂(py) (104 mg, 0.179 mmol) at -30 °C. The reaction mixture was stirred at room temperature overnight. The solution was filtered through Celite and the insoluble materials were washed with diethyl ether (5 mL). The yellow filtrate was concentrated *in vacuo* until the volume was ~1 mL. The solution was cooled to -30 °C for 2 h to give yellow crystals. The supernatant was decanted and the crystals were dried *in vacuo*; yield 51 mg (47%): ¹H NMR (C₆D₆) δ 7.31 (d, 2, Aryl), 6.90 (d, 2, Aryl), 6.80 (m, 2, Aryl), 6.72 (t, 2, Aryl), 1.66 (s, 15, C₅Me₅), 1.61 (m, 2, SiCH₂), 0.72 (s, 6, SiMe₂), 0.67 (m, 2, SiCH₂), -0.02 (s, 6, SiMe₂); ¹³C NMR (C₆D₆) δ 151.67 (C, Aryl), 145.33 (C, Aryl), 127.39 (CH, Aryl), 124.55 (CH, Aryl), 124.31 (C₅Me₅), 120.23 (CH, Aryl), 116.26 (CH, Aryl), 15.08 (SiCH₂), 11.49 (C₅Me₅), 2.82 (SiMe₂), 2.11 (SiMe₂). Anal. Calcd. for C₂₈H₃₉ClN₂OSi₂Zr: C, 55.82; H, 6.52; N, 4.65. Found: C, 55.95; H, 6.44; N, 4.59.

Zr[BdeNON]₂. **Method A:** In the absence of lightning, a toluene solution (3 mL) of Zr(CH₂SiMe₃)₄ (56 mg, 0.127 mmol) and H₂[BdeNON] (87 mg, 0.255 mmol) was stirred at room temperature for 4 days. All volatile components were removed *in vacuo* to give an orange solid; yield 98 mg (99%). **Method B:** In the absence of lightning, a toluene solution (3 mL) of ZrBn₄ (27 mg, 0.059 mmol) and H₂[BdeNON] (40 mg, 0.059 mmol) was heated to 80 °C for 4 days. All volatile components were removed *in vacuo* to give an orange solid; yield 43 mg (94%): ¹H NMR (C₆D₆) δ 7.06 (dd, 4, Aryl), 6.97 (t, 2, Aryl), 6.88 (t, 4, Aryl), 6.57 (t, 4, Aryl), 6.45 (t, 4, Aryl), 1.64 (m, 4, SiCH₂), 1.05 (m, 4, SiCH₂), 0.46 (s, 6, SiMe₂), 0.09 (s, 6, SiMe₂), -0.03 (s, 6, SiMe₂), -0.04 (s, 6, SiMe₂); ¹³C NMR (C₆D₆) δ 153.84 (C, Aryl), 153.80 (C, Aryl), 140.82 (C, Aryl), 145.93 (C, Aryl), 127.05 (CH, Aryl), 126.44 (CH, Aryl), 122.72 (CH, Aryl), 121.08 (CH, Aryl), 120.54 (CH, Aryl), 119.69 (CH, Aryl), 119.22 (CH, Aryl), 118.03 (CH, Aryl), 12.28 (SiCH₂), 10.62 (SiCH₂), 5.30 (SiMe₂), 3.61 (SiMe₂), 1.76 (SiMe₂), 0.19 (SiMe₂). Anal. Calcd. for C₃₆H₄₈N₄O₂Si₄Zr: C, 55.98; H, 6.26; N, 7.25. Found: C, 56.09; H, 6.21; N, 7.20.

E.1.3 [MesNON]²⁻ ligand system.

H₂[MesNON]. A 250 mL Schlenk flask was charged with a magnetic stir bar, O(*o*-C₆H₄NH₂)₂ (5.00 g, 24.970 mmol), mesityl bromide (9.943 g, 49.940 mmol, 2 equiv.), tris(dibenzylideneacetone)dipalladium(0) (0.114 g, 0.125 mmol, 0.005 equiv.), rac-BINAP (0.233 g, 0.375 mmol, 0.015 equiv.), NaO-*t*-Bu (6.72 g, 69.916 mmol, 2.8 equiv.), and toluene (100 mL). The reaction mixture was stirred and heated to 95 °C for 6 days. All volatile components were removed *in vacuo* at ~40 °C. The dark brown solid residue thus obtained was dissolved in a mixture of diethyl ether (400 mL) and H₂O (300 mL). The two layers were separated. The diethyl ether solution was washed with H₂O (300 mL x 3), saturated aqueous NaCl solution (300 mL), and dried over MgSO₄. The MgSO₄ was removed by filtration and the solution was concentrated on a rotary evaporator until the volume was ~10 mL. The concentrated solution was loaded onto an alumina column (2.5 cm inner diameter x 27 cm height) and eluted with diethyl ether. The first 500 mL eluent was collected and the solvent was removed *in vacuo* to give a pale yellow solid; yield 7.19 g (66%): IR (CHCl₃): NH(st.) 3414 cm⁻¹; IR (Et₂O): NH(st.) 3389 cm⁻¹; ¹H NMR (C₆D₆) δ 7.04 (d, 2, Aryl), 6.83 (t, 2, Aryl), 6.80 (s, 4, Aryl), 6.62 (t, 2, Aryl), 6.41 (d, 2, Aryl), 5.69 (s, 2, NH), 2.17 (s, 6, Me_p), 2.09 (s, 12, Me_o); ¹H NMR (CDCl₃) δ 6.98 (d, 2, Aryl), 6.95 (s, 4, Aryl), 6.89 (t, 2, Aryl), 6.68 (t, 2, Aryl), 6.27 (d, 2, Aryl), 5.71 (s, 2, NH), 2.32 (s, 6, Me_p), 2.16 (s, 12, Me_o); ¹³C NMR (C₆D₆) δ 144.72 (C, Aryl), 139.05 (C, Aryl), 136.79 (C, Aryl), 136.03 (C, Aryl), 135.94 (C, Aryl), 130.01 (CH, Aryl), 125.28 (CH, Aryl), 119.25 (CH, Aryl), 118.36 (CH, Aryl), 112.99 (CH, Aryl), 21.42 (Me_p), 18.58 (Me_o). HRMS (EI, 70 eV): *m/z* calcd. for C₃₀H₃₂N₂O 436.251464, found 436.25091.

[MesNON]Ti(NMe₂)₂. *n*-BuLi (0.92 mL, 2.5 M in hexane, 2.3 mmol, 2 equiv.) was added to a diethyl ether solution (12 mL) of H₂[MesNON] (500 mg, 1.145 mmol) at -30 °C. The solution was stirred at room temperature for 1.5 h and cooled to -30 °C. Solid TiCl₂(NMe₂)₂ (237 mg, 1.145 mmol) was added to the cold diethyl ether solution. The reaction mixture was stirred at room temperature overnight (~14 h). Insoluble materials were removed by filtration through Celite

and washed with diethyl ether (5 mL). The filtrate was concentrated *in vacuo* until the volume was ~2 mL. Pentane (~1 mL) was layer on top and the solution was cooled to -30 °C to give a dark red needle-like crystalline solid. The supernatant was decanted and the solid was dried *in vacuo*; yield 475 mg (73%): ^1H NMR (C_6D_6) δ 7.63 (d, 2, Aryl), 6.87 (s, 4, Aryl), 6.86 (t, 2, Aryl), 6.60 (t, 2, Aryl), 6.22 (d, 2, Aryl), 2.77 (s, 12, TiNMe_2), 2.20 (s, 6, Me_p), 2.16 (s, 12, Me_o); ^{13}C NMR (C_6D_6) δ 148.61 (C, Aryl), 147.28 (C, Aryl), 147.14 (C, Aryl), 134.13 (C, Aryl), 133.63 (C, Aryl), 129.68 (CH, Aryl), 126.08 (CH, Aryl), 116.62 (CH, Aryl), 116.24 (CH, Aryl), 113.68 (CH, Aryl), 45.56 (TiNMe_2), 21.31 (Me_p), 19.67 (Me_o). Anal. Calcd. for $\text{C}_{34}\text{H}_{42}\text{N}_4\text{OTi}$: C, 71.57; H, 7.42; N, 9.82. Found: C, 71.69; H, 7.48; N, 9.71.

[MesNON]TiCl(NMe₂). **Method A:** A toluene solution (5 mL) of [MesNON]Ti(NMe₂)₂ (104 mg, 0.182 mmol) and Me₃SiCl (0.07 mL, 0.552 mmol, 3 equiv.) was heated to 105 °C for 6 days in a Teflon-sealed Schlenk tube. All volatile materials were removed *in vacuo* at ~40 °C to give a deep red solid which is pure [MesNON]TiCl(NMe₂) according to its ^1H NMR spectrum. The solid was recrystallized from a concentrated diethyl ether solution at -30 °C to give blood red crystals; yield 102 mg (100%). **Method B:** To a solid mixture of H₂[MesNON] (21 mg, 0.048 mmol) and TiCl₂(NMe₂)₂ (10 mg, 0.048 mmol) was added C₆D₆ (0.7 mL) at room temperature. All solid materials dissolved in 1 min. The solution was transferred to an NMR tube and kept at room temperature. The reaction was monitored by ^1H NMR spectroscopy which showed significant amount (~50%) of H₂[MesNON] after several days when TiCl₂(NMe₂)₂ signal disappeared. Red crystals were obtained in the solution after 6 days. The supernatant was decanted and the crystals were dried *in vacuo*; yield 13 mg (48%): ^1H NMR (C_6D_6) δ 7.53 (d, 2, Aryl), 6.83 (s, 2, Aryl), 6.79 (t, 2, Aryl), 6.76 (s, 2, Aryl), 6.56 (t, 2, Aryl), 6.02 (d, 2, Aryl), 2.58 (s, 6, TiNMe_2), 2.37 (s, 6, Me_p), 2.15 (s, 6, Me_o), 1.98 (s, 6, Me_o); ^{13}C NMR (C_6D_6) δ 149.15 (C, Aryl), 148.17 (C, Aryl), 146.67 (C, Aryl), 135.04 (C, Aryl), 134.70 (C, Aryl), 131.98 (C, Aryl), 130.10 (CH, Aryl), 129.66 (CH, Aryl), 126.23 (CH, Aryl), 118.37 (CH, Aryl), 117.09 (CH, Aryl), 112.30 (CH, Aryl), 46.09 (TiNMe_2), 21.24 (Me_p), 19.54 (Me_o),

18.81 (Me_o). Anal. Calcd. for C₃₂H₃₆ClN₃OTi: C, 68.39; H, 6.46; N, 7.48. Found: C, 68.48; H, 6.35; N, 7.39.

[MesNON]Zr(NMe₂)₂. Diethyl ether (10 mL) was added to a solid mixture of H₂[MesNON] (1.032 g, 2.364 mmol) and Zr(NMe₂)₄ (0.632 g, 2.364 mmol) at room temperature. The solution was stirred at room temperature overnight (~13 h). All volatile materials were removed *in vacuo* to give a pale yellow solid which was pure [MesNON]Zr(NMe₂)₂ according to the ¹H NMR spectrum. Colorless crystals were obtained from a concentrated diethyl ether solution at -30 °C. The crystals were collected by filtration and dried *in vacuo*; yield 1.429 g (98%): ¹H NMR (C₆D₆) δ 7.60 (d, 2, Aryl), 6.89 (s, 4, Aryl), 6.86 (t, 2, Aryl), 6.56 (t, 2, Aryl), 6.25 (d, 2, Aryl), 2.57 (s, 12, Me_o), 2.20 (s, 18, containing 6H from Me_p and 12H from ZrNMe₂); ¹H NMR (toluene-*d*₈) δ 7.56 (d, 2, Aryl), 6.85 (s, 4, Aryl), 6.79 (t, 2, Aryl), 6.52 (t, 2, Aryl), 6.17 (d, 2, Aryl), 2.54 (s, 12, Me_o), 2.17 (s, 6, Me_p), 2.16 (s, 12, ZrNMe₂); ¹³C NMR (C₆D₆) δ 147.56 (C, Aryl), 146.57 (C, Aryl), 143.40 (C, Aryl), 135.17 (C, Aryl), 134.08 (C, Aryl), 129.97 (CH, Aryl), 126.60 (CH, Aryl), 116.89 (CH, Aryl), 116.12 (CH, Aryl), 114.35 (CH, Aryl), 41.64 (ZrNMe₂), 21.36 (Me_p), 18.93 (Me_o). Anal. Calcd. for C₃₄H₄₂N₄OZr: C, 66.52; H, 6.90; N, 9.13. Found: C, 66.64; H, 6.82; N, 9.05.

[MesNON]ZrCl₂. Neat Me₃SiCl (0.64 mL, 5.068 mmol, 3 equiv.) was added to a toluene solution (20 mL) of [MesNON]Zr(NMe₂)₂ (1.037 g, 1.689 mmol) at room temperature. The reaction mixture was stirred at room temperature for 24 h. All volatile materials were removed *in vacuo* at ~40 °C to give a brown viscous oil. Diethyl ether was added dropwise to the oil to initiate crystallization. A crop of yellow crystalline solid (696 mg) was obtained from ~5 mL diethyl ether solution at room temperature. A second crop (225 mg) was obtained by cooling the mother liquor to -30 °C; yield 921 mg (91%). Diethyl ether (~0.67 equiv. per zirconium) was usually found in the solid [MesNON]ZrCl₂ according to the ¹H NMR spectrum; it might be removed by recrystallization from a toluene solution: ¹H NMR (C₆D₆) δ 7.34 (d, 2, Aryl), 6.81 (s, 4, Aryl), 6.75 (t, 2, Aryl), 6.52 (t, 2, Aryl), 6.06 (d, 2, Aryl), 2.30 (s, 12, Me_o), 2.10 (s, 6, Me_p); ¹³C NMR (C₆D₆) δ 148.29 (C, Aryl), 145.91 (C, Aryl), 139.50 (C, Aryl), 137.64 (C,

Aryl), 135.68 (C, Aryl), 130.91 (CH, Aryl), 127.22 (CH, Aryl), 119.50 (CH, Aryl), 116.69 (CH, Aryl), 114.12 (CH, Aryl), 21.37 (Me_p), 19.10 (Me_o). Anal. Calcd. for C₃₀H₃₀Cl₂N₂OZr(OEt₂)_{0.67}: C, 60.73; H, 5.72; N, 4.33. Found: C, 60.85; H, 5.86; N, 4.27.

[MesNON]ZrMe₂. MeMgI (0.1 mL, 3 M in diethyl ether, 0.3 mmol, 2 equiv.) was added to a diethyl ether solution (4 mL) of [MesNON]ZrCl₂ (98 mg, 0.15 mmol) at -30 °C. The reaction mixture was stirred at room temperature for 2.5 h. Solvent was removed *in vacuo*. The solid residue was triturated and extracted with pentane (10 mL). Insoluble materials were removed by filtration through Celite. The colorless filtrate was concentrated *in vacuo* until the volume was ~2 mL. The solution was cooled to -30 °C to give colorless crystals. The supernatant was decanted and the crystals were dried *in vacuo*; yield 71 mg (85%): ¹H NMR (C₆D₆) δ 7.53 (d, 2, Aryl), 6.92 (s, 4, Aryl), 6.82 (t, 2, Aryl), 6.52 (t, 2, Aryl), 6.20 (d, 2, Aryl), 2.27 (s, 12, Me_o), 2.16 (s, 6, Me_p), 0.58 (s, 6, ZrMe); ¹H NMR (toluene-*d*₈) δ 7.47 (d, 2, Aryl), 6.87 (s, 4, Aryl), 6.77 (t, 2, Aryl), 6.49 (t, 2, Aryl), 6.12 (d, 2, Aryl), 2.23 (s, 12, Me_o), 2.14 (s, 6, Me_p), 0.49 (s, 6, ZrMe); ¹H NMR (toluene-*d*₈, -80 °C) δ 7.33 (d, 2, Aryl), 6.73 (s, 4, Aryl), 6.70 (t, 2, Aryl), 6.38 (t, 2, Aryl), 6.11 (d, 2, Aryl), 2.20 (s, 12, Me_o), 2.00 (s, 6, Me_p), 0.58 (s, 6, ZrMe); ¹H NMR (toluene-*d*₈, 90 °C) δ 7.53 (d, 2, Aryl), 6.91 (s, 4, Aryl), 6.79 (t, 2, Aryl), 6.53 (t, 2, Aryl), 6.13 (d, 2, Aryl), 2.25 (s, 12, Me_o), 2.17 (s, 6, Me_p), 0.45 (s, 6, ZrMe); ¹³C NMR (C₆D₆) δ 147.03 (C, Aryl), 146.19 (C, Aryl), 138.43 (C, Aryl), 136.87 (C, Aryl), 136.65 (C, Aryl), 130.75 (CH, Aryl), 126.43 (CH, Aryl), 117.31 (CH, Aryl), 115.18 (CH, Aryl), 113.80 (CH, Aryl), 49.85 (ZrMe), 21.42 (Me_p), 19.00 (Me_o). Anal. Calcd. for C₃₂H₃₆N₂OZr: C, 69.14; H, 6.53; N, 5.04. Found: C, 69.26; H, 6.37; N, 5.11.

[MesNON]ZrNp₂. A diethyl ether solution (2 mL) of NpLi (28 mg, 0.359 mmol, 2 equiv.) at -30 °C was added to a diethyl ether suspension (4 mL) of [MesNON]ZrCl₂ (116 mg, 0.179 mmol) at -30 °C. The reaction mixture was stirred at room temperature for 70 min. Solvent was removed *in vacuo*. The solid residue was extracted with pentane (10 mL). Insoluble materials were removed by filtration with Celite. The solvent was removed from the filtrate *in vacuo* to give a pale yellow solid; yield 100 mg (83%): ¹H NMR (C₆D₆) δ 7.60 (d, 2, Aryl), 6.91 (s, 4, Aryl),

6.81 (t, 2, Aryl), 6.55 (t, 2, Aryl), 6.23 (d, 2, Aryl), 2.37 (s, 12, Me_o), 2.17 (s, 6, Me_p), 1.29 (s, 4, ZrCH₂CMe₃), 0.90 (s, 18, ZrCH₂CMe₃); ¹³C NMR (C₆D₆) δ 147.24 (C, Aryl), 147.11 (C, Aryl), 141.90 (C, Aryl), 136.37 (C, Aryl), 135.99 (C, Aryl), 130.80 (CH, Aryl), 126.47 (CH, Aryl), 117.58 (CH, Aryl), 116.30 (CH, Aryl), 114.43 (CH, Aryl), 96.57 (ZrCH₂CMe₃), 36.99 (ZrCH₂CMe₃), 34.52 (ZrCH₂CMe₃), 21.32 (Me_p), 19.64 (Me_o). Anal. Calcd. for C₄₀H₅₂N₂OZr: C, 71.91; H, 7.85; N, 4.19. Found: C, 73.08; H, 7.74; N, 4.18.

[MesNON]ZrPh₂. PhMgBr (0.1 mL, 3 M in diethyl ether, 0.3 mmol, 2 equiv.) was added to a diethyl ether suspension (4 mL) of [MesNON]ZrCl₂(OEt₂)_{0.67} (97 mg, 0.150 mmol) at -30 °C. The color of the suspension changed immediately from green to yellow. The reaction mixture was stirred at room temperature for 90 min and 1,4-dioxane (5 drops) was added. Insoluble materials were removed by filtration through Celite and the filtrate was concentrated *in vacuo* until the volume was ~1 mL. The concentrated solution was cooled to -30 °C overnight to give a yellow crystalline solid. The supernatant was decanted and the product was dried *in vacuo*; yield 94 mg (92%): ¹H NMR (C₆D₆) δ 7.62 (d, 2, Aryl), 7.52 (m, 4, Aryl), 7.00 (m, 6, Aryl), 6.80 (t, 2, Aryl), 6.75 (s, 4, Aryl), 6.61 (t, 2, Aryl), 6.19 (d, 2, Aryl), 2.15 (s, 6, Me_p), 2.05 (s, 12, Me_o); ¹³C NMR (C₆D₆) δ 191.70 (ZrC_{ipso}), 147.29 (C, Aryl), 147.08 (C, Aryl), 139.72 (C, Aryl), 136.76 (C, Aryl), 136.67 (C, Aryl), 133.94 (CH, Aryl), 130.59 (CH, Aryl), 129.68 (CH, Aryl), 127.37 (CH, Aryl), 126.62 (CH, Aryl), 118.15 (CH, Aryl), 116.17 (CH, Aryl), 114.04 (CH, Aryl), 21.31 (Me_p), 19.17 (Me_o). Anal. Calcd. for C₄₂H₄₀N₂OZr: C, 74.18; H, 5.93; N, 4.12. Found: C, 74.08; H, 6.05; N, 4.18.

[MesNON]Hf(NMe₂)₂ and [MesNON]HfCl₂. Diethyl ether (20 mL) was added to a solid mixture of H₂[MesNON] (1.301 g, 2.980 mmol) and Hf(NMe₂)₄ (1.057 g, 2.981 mmol) at room temperature. The solution was stirred at room temperature and monitored by ¹H NMR spectroscopy which showed [MesNON]Hf(NMe₂)₂ was formed quantitatively in 6 h. All volatile components were removed *in vacuo* to give an off-white solid; yield 2.09 g (100%): ¹H NMR (C₆D₆) δ 7.57 (d, 2, Aryl), 6.90 (s, 4, Aryl), 6.85 (t, 2, Aryl), 6.55 (t, 2, Aryl), 6.26 (d, 2, Aryl), 2.62 (s, 12, HfNMe₂), 2.22 (s, 12, Me_o), 2.19 (s, 6, Me_p). Neat Me₃SiCl (1.4 mL,

11.924 mmol, 4 equiv.) was added to a toluene solution (5 mL) of [MesNON]Hf(NMe₂)₂ at room temperature. The solution was stirred at room temperature for 22 h. All volatile components were removed *in vacuo* at ~45 °C. The off-white solid was washed with pentane (~20 mL) and dried *in vacuo*; yield 1.447 g (71%): ¹H NMR (C₆D₆) δ 7.28 (d, 2, Aryl), 6.82 (s, 4, Aryl), 6.77 (t, 2, Aryl), 6.47 (t, 2, Aryl), 6.11 (d, 2, Aryl), 2.13 (s, 12, Me_O), 2.11 (s, 6, Me_p); ¹³C NMR (C₆D₆) δ 148.05 (C, Aryl), 145.98 (C, Aryl), 140.41 (C, Aryl), 137.06 (C, Aryl), 135.68 (C, Aryl), 130.82 (CH, Aryl), 127.61 (CH, Aryl), 119.09 (CH, Aryl), 117.05 (CH, Aryl), 115.14 (CH, Aryl), 21.32 (Me_p), 19.01 (Me_O). Anal. Calcd. for C₃₀H₃₀Cl₂HfN₂O: C, 52.68; H, 4.42; N, 4.10. Found: C, 52.83; H, 4.50; N, 4.29.

[MesNON]HfMe₂. MeMgI (0.1 mL, 3 M in diethyl ether, 0.3 mmol, 2 equiv.) was added to a diethyl ether suspension (8 mL) of [MesNON]HfCl₂ (102 mg, 0.149 mmol) at -30 °C. The reaction mixture was stirred at room temperature for 40 min and 1,4-dioxane (5 drops) was added. Insoluble materials were removed by filtration through Celite. The filtrate was concentrated *in vacuo* until the volume was ~0.5 mL. The concentrated solution was kept at -30 °C overnight to give a colorless crystalline solid. The supernatant was decanted and the solid was washed with pentane (1 mL) and dried *in vacuo*; yield 84 mg (88%): ¹H NMR (C₆D₆) δ 7.50 (d, 2, Aryl), 6.91 (s, 4, Aryl), 6.81 (t, 2, Aryl), 6.50 (t, 2, Aryl), 6.21 (d, 2, Aryl), 2.28 (s, 12, Me_O), 2.16 (s, 6, Me_p), 0.40 (s, 6, HfMe); ¹³C NMR (C₆D₆) δ 147.24 (C, Aryl), 146.73 (C, Aryl), 138.86 (C, Aryl), 136.74 (C, Aryl), 136.34 (C, Aryl), 130.73 (CH, Aryl), 126.74 (CH, Aryl), 117.26 (CH, Aryl), 115.66 (CH, Aryl), 114.67 (CH, Aryl), 60.18 (HfMe), 21.40 (Me_p), 18.97 (Me_O). Anal. Calcd. for C₃₂H₃₆HfN₂O: C, 59.76; H, 5.64; N, 4.36. Found: C, 59.86; H, 5.73; N, 4.26.

[MesNON]HfEt₂. EtMgBr (0.1 mL, 3 M in diethyl ether, 0.3 mmol, 2 equiv.) was added to a diethyl ether suspension (3 mL) of [MesNON]HfCl₂ (103 mg, 0.151 mmol) at -30 °C. The reaction mixture was stirred at room temperature for 1 h and 1,4-dioxane (5 drops) was added. Insoluble materials were removed by filtration through Celite. The pale yellow filtrate was concentrated *in vacuo* until the volume was ~1 mL to give a colorless crystalline solid. The

solution was cooled to $-30\text{ }^{\circ}\text{C}$ for several hours to allow for the completion of crystallization. The supernatant was decanted and the crystals were dried *in vacuo*; yield 89 mg (88%): ^1H NMR (C_6D_6) δ 7.50 (d, 2, Aryl), 6.91 (s, 4, Aryl), 6.84 (t, 2, Aryl), 6.51 (t, 2, Aryl), 6.23 (d, 2, Aryl), 2.30 (s, 12, Me_o), 2.17 (s, 6, Me_p), 1.28 (t, 6, HfCH_2CH_3), 0.77 (q, 4, HfCH_2CH_3); ^{13}C NMR (C_6D_6) δ 147.15 (C, Aryl), 147.04 (C, Aryl), 139.06 (C, Aryl), 136.71 (C, Aryl), 136.18 (C, Aryl), 130.66 (CH, Aryl), 126.67 (CH, Aryl), 117.34 (CH, Aryl), 116.13 (CH, Aryl), 114.81 (CH, Aryl), 73.34 (HfCH_2CH_3), 21.36 (Me_p), 18.94 (Me_o), 12.05 (HfCH_2CH_3). Anal. Calcd. for $\text{C}_{34}\text{H}_{40}\text{HfN}_2\text{O}$: C, 60.84; H, 6.01; N, 4.17. Found: C, 60.69; H, 5.92; N, 4.21.

[MesNON]Hf(i-Bu)₂. i-BuMgBr (0.15 mL, 2 M in diethyl ether, 0.3 mmol, 2 equiv.) was added to a diethyl ether suspension (3 mL) of [MesNON]HfCl₂ (103 mg, 0.151 mmol) at $-30\text{ }^{\circ}\text{C}$. The reaction mixture was stirred at room temperature for 30 min. The solvent was removed *in vacuo* and the solid residue was extracted with pentane (8 mL). The extract was filtered through Celite and pentane was removed *in vacuo* to give a colorless oil. The oil was cooled to $-30\text{ }^{\circ}\text{C}$ overnight to give a colorless, wet waxy solid. The solid was washed with pentane (0.5 mL) and dried *in vacuo*; yield 86 mg (79%): ^1H NMR (C_6D_6) δ 7.55 (d, 2, Aryl), 6.92 (s, 4, Aryl), 6.83 (t, 2, Aryl), 6.52 (t, 2, Aryl), 6.22 (d, 2, Aryl), 2.34 (s, 12, Me_o), 2.17 (s, 6, Me_p), 2.02 (septet, 2, $\text{HfCH}_2\text{CHMe}_2$), 0.82 (d, 4, $\text{HfCH}_2\text{CHMe}_2$), 0.81 (d, 12, $\text{HfCH}_2\text{CHMe}_2$); ^{13}C NMR (C_6D_6) δ 147.32 (C, Aryl), 147.15 (C, Aryl), 139.95 (C, Aryl), 136.47 (C, Aryl), 136.22 (C, Aryl), 130.72 (CH, Aryl), 126.75 (CH, Aryl), 117.45 (CH, Aryl), 116.16 (CH, Aryl), 114.98 (CH, Aryl), 94.96 ($\text{HfCH}_2\text{CHMe}_2$), 30.22 ($\text{HfCH}_2\text{CHMe}_2$), 29.03 ($\text{HfCH}_2\text{CHMe}_2$), 21.32 (Me_p), 19.17 (Me_o). Anal. Calcd. for $\text{C}_{38}\text{H}_{48}\text{HfN}_2\text{O}$: C, 62.75; H, 6.65; N, 3.85. Found: C, 62.84; H, 6.53; N, 3.77.

[MesNON]HfNp₂. A diethyl ether solution (2 mL) of NpLi (23 mg, 0.295 mmol) at $-30\text{ }^{\circ}\text{C}$ was added to a diethyl ether suspension (4 mL) of [MesNON]HfCl₂ (100 mg, 0.146 mmol) at $-30\text{ }^{\circ}\text{C}$. The reaction mixture was stirred at room temperature for 80 min. Insoluble solid was removed by filtration through Celite. The solvent was removed *in vacuo* to give an off-white solid product; yield 103 mg (93%): ^1H NMR (C_6D_6) δ 7.56 (d, 2, Aryl), 6.92 (s, 4, Aryl), 6.81 (t, 2,

Aryl), 6.50 (t, 2, Aryl), 6.22 (d, 2, Aryl), 2.37 (s, 12, Me_o), 2.17 (s, 6, Me_p), 0.96 (s, 4, HfCH₂CMe₃), 0.93 (s, 18, HfCH₂CMe₃); ¹³C NMR (C₆D₆) δ 147.43 (C, Aryl), 147.24 (C, Aryl), 142.39 (C, Aryl), 136.19 (C, Aryl), 136.12 (C, Aryl), 130.77 (CH, Aryl), 126.82 (CH, Aryl), 117.47 (CH, Aryl), 116.40 (CH, Aryl), 115.29 (CH, Aryl), 104.97 (HfCH₂CMe₃), 37.09 (HfCH₂CMe₃), 35.26 (HfCH₂CMe₃), 21.31 (Me_p), 19.61 (Me_o). Anal. Calcd. for C₄₀H₅₂HfN₂O: C, 63.60; H, 6.94; N, 3.71. Found: C, 63.46; H, 6.84; N, 3.78.

[MesNON]HfPh₂. PhMgBr (0.1 mL, 3 M in diethyl ether, 0.3 mmol, 2 equiv.) was added to a diethyl ether suspension (4 mL) of [MesNON]HfCl₂ (103 mg, 0.151 mmol) at -30 °C. The reaction mixture was stirred at room temperature for 1 h and 1,4-dioxane (5 drops) was added. Insoluble materials were removed by filtration through Celite. The yellow filtrate was concentrated *in vacuo* until the volume was ~1 mL. The solution was cooled to -30 °C overnight to give a pale yellow crystalline solid. The supernatant was decanted and the solid was dried *in vacuo*; yield 110 mg (95%): ¹H NMR (C₆D₆) δ 7.58 (d, 2, Aryl), 7.52 (d, 4, Aryl), 7.10 (t, 4, Aryl), 6.99 (t, 2, Aryl), 6.81 (t, 2, Aryl), 6.76 (s, 4, Aryl), 6.55 (t, 2, Aryl), 6.20 (d, 2, Aryl), 2.15 (s, 6, Me_p), 2.09 (s, 12, Me_o); ¹³C NMR (C₆D₆) δ 205.28 (HfC_{ipso}), 147.47 (C, Aryl), 147.35 (C, Aryl), 139.75 (C, Aryl), 137.00 (C, Aryl), 136.52 (C, Aryl), 136.48 (CH, Aryl), 130.57 (CH, Aryl), 129.61 (CH, Aryl), 127.76 (CH, Aryl), 126.95 (CH, Aryl), 118.08 (CH, Aryl), 116.45 (CH, Aryl), 115.07 (CH, Aryl), 21.29 (Me_p), 19.14 (Me_o). Anal. Calcd. for C₄₂H₄₀HfN₂O: C, 65.75; H, 5.25; N, 3.65. Found: C, 65.55; H, 5.20; N, 3.59.

Catalytic reaction between 1-hexene and [HNMe₂Ph][B(C₆F₅)₄] activated [MesNON]ZrMe₂. A C₆D₅Br solution (0.3 mL) of [MesNON]ZrMe₂ (5 mg, 9 μmol) at -30 °C was added to a C₆D₅Br solution (0.4 mL) of [HNMe₂Ph][B(C₆F₅)₄] (7 mg, 8.7 μmol, 0.97 equiv.) at -30 °C. The solution color changed immediately from colorless to light yellow. The reaction mixture was briefly warmed to allow for the dissolution of the anilinium salt and kept at 0 °C. 1-Hexene (60 equiv.) was added to the above solution at 0 °C. The reactivity was monitored by ¹H NMR spectroscopy which showed little or no conversion of 1-hexene in 10 min, but ~50% conversion in 4 h.

Catalytic reaction between 1-hexene and $[\text{Ph}_3\text{C}][\text{B}(\text{C}_6\text{F}_5)_4]$ activated $[\text{MesNON}]\text{ZrMe}_2$. A $\text{C}_6\text{D}_5\text{Br}$ solution (0.3 mL) of $[\text{MesNON}]\text{ZrMe}_2$ (10 mg, 18 μmol) at $-30\text{ }^\circ\text{C}$ was added to a $\text{C}_6\text{D}_5\text{Br}$ solution (0.4 mL) of $[\text{Ph}_3\text{C}][\text{B}(\text{C}_6\text{F}_5)_4]$ (16 mg, 17 μmol , 0.96 equiv.) at $-30\text{ }^\circ\text{C}$. The orange solution was kept at $0\text{ }^\circ\text{C}$. 1-Hexene (60 equiv.) was added to the above solution at $0\text{ }^\circ\text{C}$. The reaction was monitored by ^1H NMR spectroscopy which showed a complete conversion of 1-hexene to poly(1-hexene) in 10 min.

Chapter 2

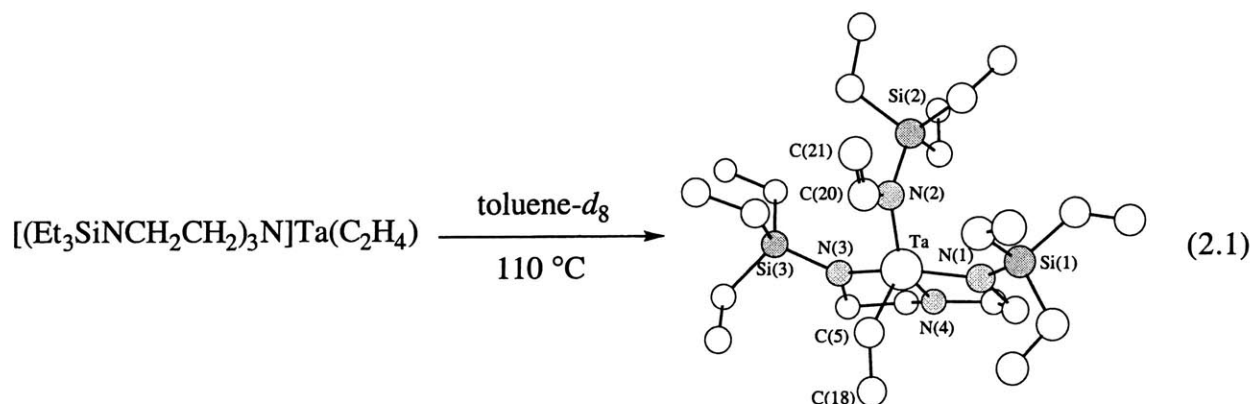
Synthesis of Group 5 Complexes Containing Tridentate Amido Ligands

INTRODUCTION

Efforts have been made to search for group 5 complexes as catalysts for the polymerization of α -olefins. Attention seems to focus on employing six-electron dianionic ligands such as dicarbollide,^{108,109} butadiene,¹¹⁰ borollide,¹¹¹⁻¹¹³ trimethylenemethane,¹¹⁴⁻¹¹⁶ and their derivatives to replace one of cyclopentadienyl rings in a metallocene, particularly for tantalum chemistry. It is interesting to note that tantalum-butadiene complexes have catalyzed the living polymerization of ethylene.¹¹⁷ Recent work by Kempe reveals that niobium complexes containing monoanionic pyridylamido ligands can also be catalysts for olefin polymerization.¹¹⁸ In general, the catalytic activity of group 5 complexes is not as high as that of their group 4 relatives.

Tetradentate triamidoamine complexes have been intensively investigated in our laboratory.²⁴ Certain tantalum complexes that contain the triamidoamine ligand $[(R_3SiNCH_2CH_2)_3N]^{3-}$; R = Me or Et) decompose to yield trigonal bipyramidal tantalum complexes containing a planar tridentate triamido ligand, $[(R_3SiNCH_2CH_2)_2N]^{3-}$ (equation 2.1, where R = Et).^{119,120} In the reaction shown in equation 2.1, a β hydride has moved from C(20) to the ethylene ligand to give an ethyl ligand (C(5)-C(18)) and the N(4)-C(21) bond has been cleaved, leaving a vinyl-substituted amido ligand (N(2)) in the equatorial position of the trigonal bipyramidal complex. The resulting planar triamido ligand (N(1), N(3), N(4)) spans the two axial

positions and one equatorial position. Planar triamido ligands are related to planar, substituted pyridine ligands of the type $[2,6-(\text{ArylNCH}_2)_2\text{C}_5\text{H}_3\text{N}]^{2-}$ that have been employed to prepare trigonal bipyramidal complexes of Ti,^{121,122} Zr,¹²³⁻¹²⁵ Ta,^{126,127} and W.¹²⁸



As a part of our research interest in transition-metal-amido chemistry, we set out to prepare group 5 complexes that contain the tridentate triamido ligands. While the research program was under way, we found out that a proton may be kept on the central nitrogen in a metal complex thus giving a complex containing a diamidoamine ligand, which is electronically analogous to the pyridine derived diamido $[2,6-(\text{ArylNCH}_2)_2\text{C}_5\text{H}_3\text{N}]^{2-}$. The diamidoamine ligands are also isoelectronic with their diamido/ether analogues.^{52,71,72} This chapter covers group 5 chemistry based on these three types of ligands with a variation on the central donor atom/group, i.e., triamide, diamidoamine, and diamido/ether. A portion of this work has been published previously.¹²⁹

SPECIFIC GOALS

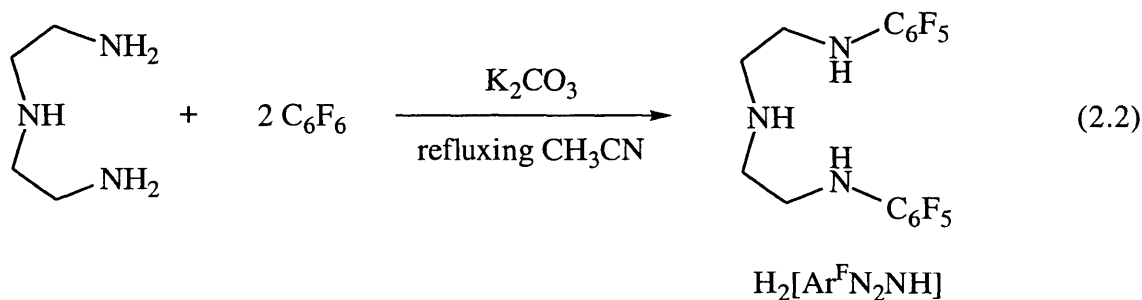
The research objective was the synthesis of group 5 complexes containing the tridentate amido ligands mentioned above. Since the ligand design thus far had only involved alkyl-aryl and aryl-aryl substituents on the amido nitrogen (Chapter 1), a new set of alkyl-alkyl amido ligands

was desired so as to compare and realize the nature of these ligands. Reactivity and thermal stability of their group 5 complexes were compared. Another goal was the isolation of cationic group 5 complexes since these cations are isoelectronic with the neutral group 4 relatives discussed in Chapters 1 and 3. The polymerization activity of these group 5 complexes with 1-hexene was examined. A comparison between group 4 and 5 chemistry based on tridentate amido ligands was attempted.

RESULTS

2.1 Design and synthesis of triamines.

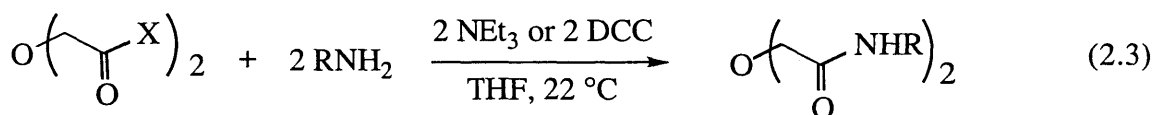
Two triamines are designed and used in this study. $(\text{MesNHCH}_2\text{CH}_2)_2\text{NH}$ ($\text{H}_2[\text{MesN}_2\text{NH}]$) and $(\text{C}_6\text{F}_5\text{NHCH}_2\text{CH}_2)_2\text{NH}$ ($\text{H}_2[\text{Ar}^{\text{F}}\text{N}_2\text{NH}]$) contain the same ethylene backbone but with different amido substituents. The mesityl groups in $[\text{MesN}_2\text{N}]^{3-}$ or $[\text{MesN}_2\text{NH}]^{2-}$ complexes feature more crowded but less electrophilic metal centers as compared to the C_6F_5 groups in $[\text{Ar}^{\text{F}}\text{N}_2\text{N}]^{3-}$ or $[\text{Ar}^{\text{F}}\text{N}_2\text{NH}]^{2-}$. The synthesis of $\text{H}_2[\text{MesN}_2\text{NH}]$ involves a palladium catalyzed C-N bond-forming reaction and is described in Chapter 3, where it is more extensively used. $\text{H}_2[\text{Ar}^{\text{F}}\text{N}_2\text{NH}]$ was synthesized by the reaction of diethylenetriamine with hexafluorobenzene in the presence of potassium carbonate (equation 2.2).¹²⁹ Acetonitrile is a more convenient solvent than dimethylsulfoxide, the preferred solvent for the synthesis of $\text{N}(\text{CH}_2\text{CH}_2\text{NHC}_6\text{F}_5)_3$.⁶²



2.2 Synthesis of diamine/ether ligands, $H_2[RN_2O]$ ($R = t\text{-Bu, Ad, i-Pr, Ph, 2-t-BuC}_6\text{H}_4$).

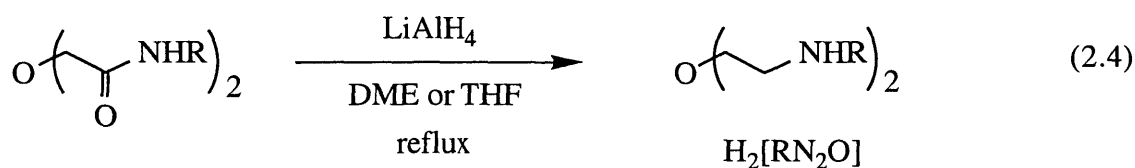
It has been shown that $H_2[\text{ArylN}_2\text{O}]$ can be synthesized by bimolecular nucleophilic substitution reactions of $\text{O}(\text{CH}_2\text{CH}_2\text{OTs})_2$ with LiNHAryl .^{71,72} An undesirable ring-closing reaction may be competitive or even predominant if the anilide does not contain sterically bulky substituents on *both ortho* positions. For example, reaction between $\text{O}(\text{CH}_2\text{CH}_2\text{OTs})_2$ and LiNHAr led to $(\text{ArNHCH}_2\text{CH}_2)_2\text{O}$ ($H_2[\text{ArN}_2\text{O}]$; $\text{Ar} = 2,6\text{-C}_6\text{H}_3\text{Me}_2$) in moderate yield. When anilide LiNHPh or $\text{LiNH}(2\text{-t-BuC}_6\text{H}_4)$ was employed, the reaction was primarily directed toward the formation of N-substituted morpholines. Therefore, a protection group on the anilide nitrogen such as trimethylsilyl was necessary for the synthesis of these compounds.

Equations 2.3 and 2.4 show another general route to the synthesis of the diamine/ether ligands. The advantage of this methodology is that the amine substituents do not have to be sterically protected. The reactions between primary amines and diglycolyl chloride or diglycolic acid produce $\text{O}[\text{CH}_2\text{C}(\text{O})\text{NHR}]_2$ in essentially quantitative yields. Subsequent reduction of the carbonyl function groups with lithium aluminum hydride yields $H_2[RN_2O]$ in moderate yields. The substituents on the amine nitrogens can be aromatic or aliphatic depending on the primary amine employed.



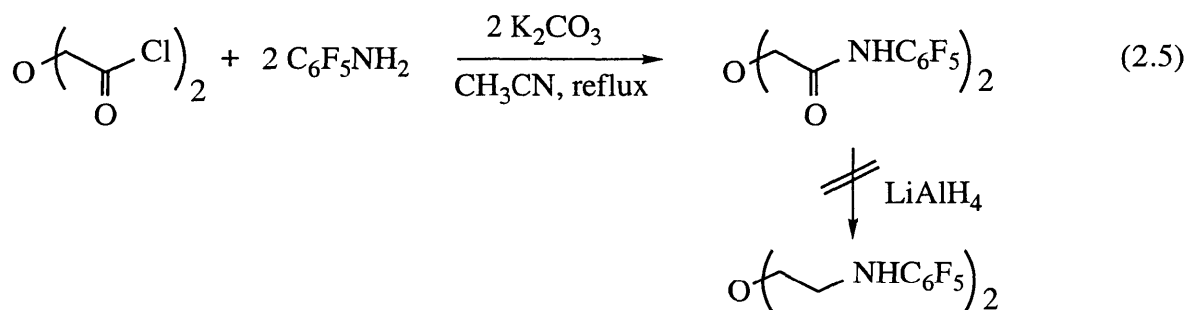
$\text{X} = \text{Cl, OH}$

$\text{R} = t\text{-Bu, Ad, i-Pr, Ph, 2-t-BuC}_6\text{H}_4, 3,5\text{-C}_6\text{H}_3(\text{CF}_3)_2$



$\text{R} = t\text{-Bu, Ad, i-Pr, Ph, 2-t-BuC}_6\text{H}_4$

The synthesis of $\text{O}[\text{CH}_2\text{C}(\text{O})\text{NHC}_6\text{F}_5]_2$ (equation 2.5) requires potassium carbonate as the base since $\text{C}_6\text{F}_5\text{NH}_2$ is less nucleophilic to react with the diglycolyl chloride as compared to triethylamine which is used in equation 2.3. Subsequent reduction of $\text{O}[\text{CH}_2\text{C}(\text{O})\text{NHC}_6\text{F}_5]_2$ with lithium aluminum hydride does not lead to the desired product, presumably because it is too reducing for either the amide carbonyl groups or the C_6F_5 rings.

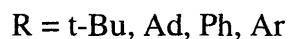
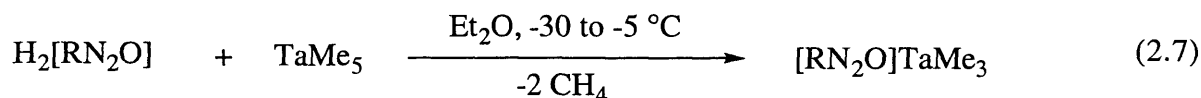
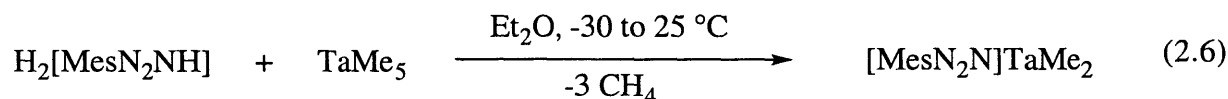


The NMR data of these amines are all characteristic of C_{2v} symmetric structures. $\text{H}_2[\text{t-BuN}_2\text{O}]$ and $\text{H}_2[\text{AdN}_2\text{O}]$ are moisture sensitive and tend to form hydrogen bonds with water. The hydrogen-bonded water can be removed by calcium hydride in refluxing toluene over a period of several days. $\text{H}_2[\text{t-BuN}_2\text{O}]$ is an oil at room temperature and may solidify slowly at 0°C . Sublimation of $\text{H}_2[\text{t-BuN}_2\text{O}]$ gives colorless needle-like crystals which can be stored at temperatures $< -20^\circ\text{C}$.

2.3 Reactions between TaMe_5 and $\text{H}_2[\text{MesN}_2\text{NH}]$ or $\text{H}_2[\text{RN}_2\text{O}]$ ($\text{R} = \text{t-Bu, Ad, Ph, Ar}$).

Attempts to synthesize tantalum complexes containing the amido ligands mentioned above by salt metathesis between TaCl_5 and lithium amides do not give any desirable tantalum products in reasonable isolated yields. Reactions involving $\text{Ta}(\text{NMe}_2)_5$ ¹³⁰ produce a mixture from which compound separation is difficult. The most convenient entry into the tantalum chemistry employs TaMe_5 .^{131,132} TaMe_5 can be prepared readily in diethyl ether from TaMe_3Cl_2 ^{133,134} and MeLi . It has rarely been used as a starting material to make tantalum methyl complexes, perhaps in part

because it begins to decompose in diethyl ether above $-0\text{ }^{\circ}\text{C}$. As a result, reactions involving TaMe_5 must compete effectively with its decomposition. Addition of $\text{H}_2[\text{MesN}_2\text{NH}]$ to a diethyl ether solution of TaMe_5 at $-30\text{ }^{\circ}\text{C}$ followed by slow warming of the solution to room temperature produces orange crystalline dimethyl complex, $[\text{MesN}_2\text{N}]\text{TaMe}_2$, in $\sim 90\%$ yield (equation 2.6). It seems likely that a diamine adduct of TaMe_5 analogous to $(\text{dmpe})\text{TaMe}_5$ ¹³¹ forms first and stabilizes TaMe_5 toward intermolecular loss of methane. In contrast, the coordination of the oxygen atom in the diamine/ether type of ligands $\text{H}_2[\text{RN}_2\text{O}]$ ($\text{R} = \text{t-Bu, Ad, Ph, Ar}$) to TaMe_5 does not effectively prevent the intermolecular decomposition of TaMe_5 , due to its being less basic than a nitrogen donor. Therefore, the synthesis of trimethyl $[\text{RN}_2\text{O}]\text{TaMe}_3$ generally requires longer reaction times at a temperature where TaMe_5 does not decompose in order for the yield of $[\text{RN}_2\text{O}]\text{TaMe}_3$ to be high (equation 2.7).



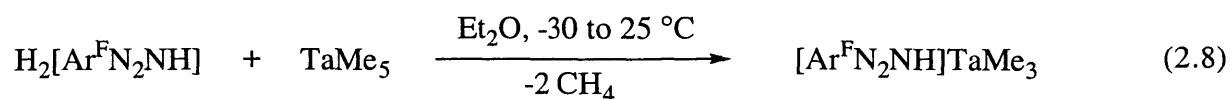
Arylated dimethyl $[\text{MesN}_2\text{N}]\text{TaMe}_2$ and trimethyl $[\text{RN}_2\text{O}]\text{TaMe}_3$ ($\text{R} = \text{Ph, Ar}$) are all thermally stable at room temperature as solids or solutions, but alkyl substituted $[\text{t-BuN}_2\text{O}]\text{TaMe}_3$ and $[\text{AdN}_2\text{O}]\text{TaMe}_3$ complexes tend to decompose to give dark brown unidentified materials. The NMR data of $[\text{MesN}_2\text{N}]\text{TaMe}_2$ are characteristic of a molecule that has C_{2v} symmetry. The methyl ligands are observed as a singlet resonance at 0.63 ppm in the ^1H NMR spectrum and at 66.18 ppm in the $^{13}\text{C}\{^1\text{H}\}$ NMR spectrum. The *ortho* mesityl methyl groups are observed as a singlet resonance at 2.35 ppm in the ^1H NMR spectrum, which is in contrast to the inequivalent *ortho* methyl groups observed for the five coordinate group 4 complexes containing a diamidoamine

ligand, [MesN₂NH]MMe₂ (M = Ti, Zr, Hf; see Chapter 3), presumably due to a higher symmetry (C_{2v}) for the former.

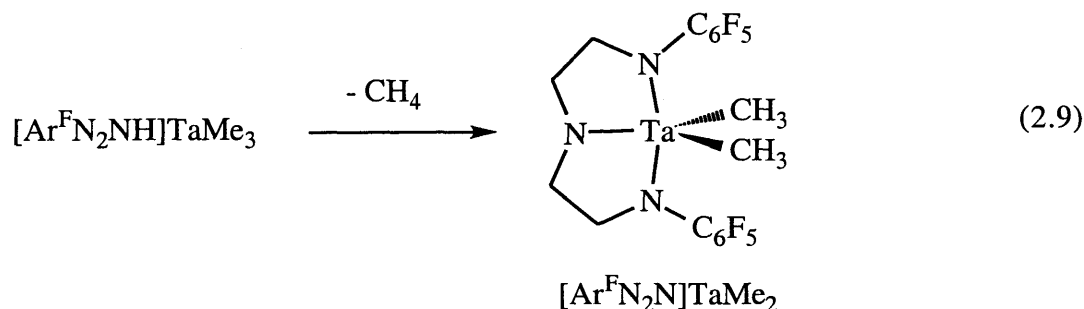
The NMR spectra of six coordinate trimethyl complexes [RN₂O]TaMe₃ (R = t-Bu, Ad, Ph, Ar) reveal only one singlet resonance for the methyl ligands, suggesting a fluxional exchange process. It should be noted that the diamido/ether ligands adopt different structures in group 4 chemistry, e.g., *fac* or *mer* or any variation in between.⁷² It is not yet possible to conclusively assign the geometry of the diamido/ether ligands in [RN₂O]TaMe₃ with the NMR data alone. The mechanism of methyl group equilibration could consist of either the dissociation of the oxygen donor to give a fluxional *five* coordinate species, or a "turn-stile" rotation of the three methyl groups with respect to the three donor atoms if [RN₂O]²⁻ is *fac*. More exotic mechanisms involving reversible migration of a methyl group to an amido nitrogen or to the oxygen donor cannot be discounted, but seem considerably less likely to take place at a rate of the order of the NMR time scale.

2.4 Reaction between TaMe₅ and H₂[Ar^FN₂NH].

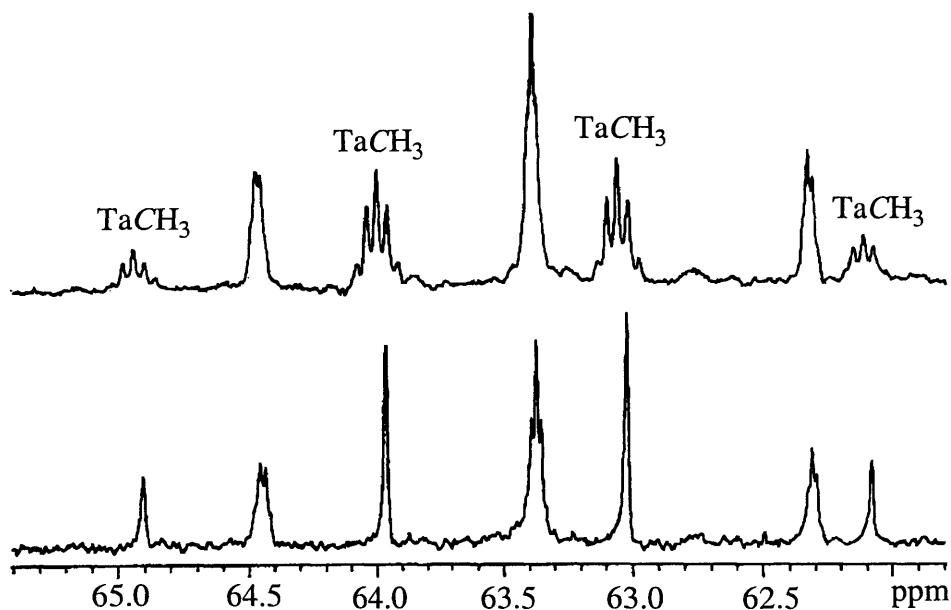
Addition of H₂[Ar^FN₂NH] to TaMe₅ yields a trimethyl complex in which a proton remains on the central nitrogen atom (equation 2.8).¹²⁹ The coordination core of [Ar^FN₂NH]TaMe₃ is isoelectronic with that of [RN₂O]TaMe₃. The ¹H NMR spectrum at room temperature reveals that the methyl groups are equivalent (0.96 ppm) and the NH resonance is observed as a broad singlet at 2.43 ppm. The methyl ligand exchange is slower at low temperatures. Below -80 °C in toluene-*d*₈ the methyl resonance divides into two broad resonances in a ratio of 2:1. The mechanism of methyl group exchange in [Ar^FN₂NH]TaMe₃ is presumably the same as that proposed for [RN₂O]TaMe₃.



$[\text{Ar}^{\text{F}}\text{N}_2\text{NH}]\text{TaMe}_3$ is relatively unstable, even in the solid state. It evolves one equivalent of methane to give $[\text{Ar}^{\text{F}}\text{N}_2\text{N}]\text{TaMe}_2$ (equation 2.9). The ^1H and ^{13}C NMR spectra of



$[\text{Ar}^{\text{F}}\text{N}_2\text{N}]\text{TaMe}_2$ are somewhat unusual. They both are characteristic of a molecule with C_{2v} symmetry, but the methyl resonance in each is a quintet (0.63 ppm in the ^1H NMR spectrum with $J = 3.6$ Hz; 63.49 ppm in the ^{13}C NMR spectrum with $J = 5.0$ Hz). The proton-coupled, fluorine-decoupled ^{13}C NMR spectrum (Scheme 2.1) shows no coupling beyond that attributable

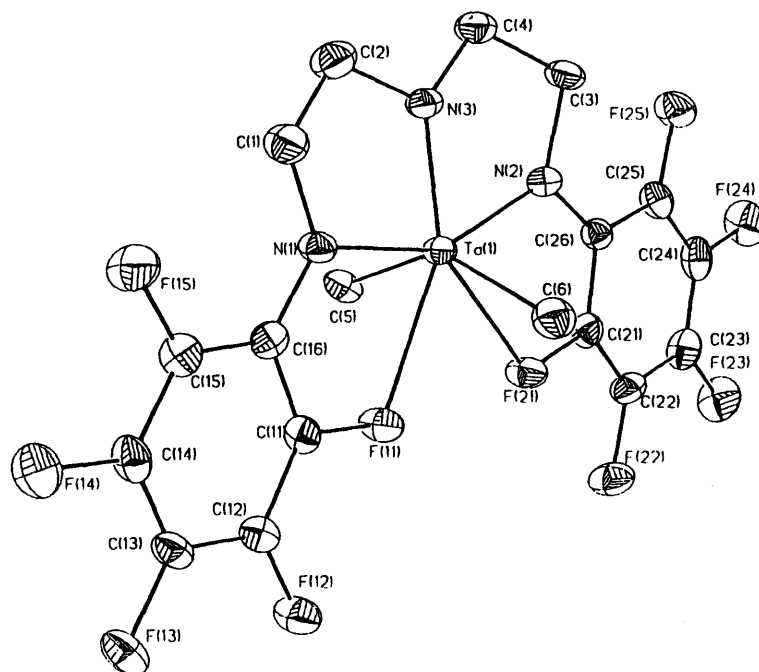


Scheme 2.1. A portion of the ^{13}C NMR spectra of $[\text{Ar}^{\text{F}}\text{N}_2\text{N}]\text{TaMe}_2$ (22 °C, CD_2Cl_2); only the TaMe and one CH_2 resonances are shown. Top: proton-coupled fluorine-coupled ^{13}C NMR spectrum ($J_{\text{CF}} = 5.0$ Hz). Bottom: proton-coupled fluorine-decoupled ^{13}C NMR spectrum.

to C-H coupling. Therefore we propose that the quintet arises from coupling to four fluorines, presumably the four *ortho* fluorines in the C₆F₅ rings. Similar observation is reported for the NMR spectra of [(C₆F₅NCH₂CH₂)₃N]TiMe, ¹³⁵ in which the H-F and C-F couplings are smaller ($J = 1.5$ and 1.9 Hz, respectively), presumably due to the smaller size of Ti(IV) than Ta(V). ¹³⁶

2.5 X-ray structure of [Ar^FN₂N]TaMe₂.

An X-ray study of [Ar^FN₂N]TaMe₂ reveals a molecule that has an trigonal bipyramidal structure (Figure 2.1) analogous to that of [(Et₃SiNCH₂CH₂)₂N]TaEt[N(CH=CH₂)(SiEt₃)] ¹²⁰ shown in equation 2.1. The triamido ligands in both complexes adopt a *mer* geometry. The core structure of [Ar^FN₂N]TaMe₂ is also closely analogous to that of [(Me₃SiN-o-C₆H₄)₂N]TaMe₂ ¹²⁹ (Table 2.1), but in [Ar^FN₂N]TaMe₂ two *ortho* fluorine atoms are within a weakly bonding distance of the metal. An interaction of this general type is also found in [(C₆F₅NCH₂CH₂)₃N]V, ⁶⁰ although the V...F distance (average 2.652 Å) is much longer than the Ta...F distance in [Ar^FN₂N]TaMe₂ (average 2.432 Å), a difference that is even more remarkable when one considers the smaller size of V(III) relative to Ta(V). ¹³⁶ The Ta...F distance is much longer than a typical Ta-F covalent bond, e.g., ~1.90 Å in [Ta₂F₁₀O]²⁻ or [Cp*₂TaF₄]₂. ^{137,138} Since the C₆F₅ rings are freely rotating on the ¹⁹F NMR time scale, even at -80 °C, the strength of the Ta...F interaction cannot be more than ~10 Kcal mol⁻¹. This interaction is presumably the origin of the two-bond (CF) or three-bond (HF) coupling, which are averages of coupling to a fluorine that is bound to tantalum and one that is unbound. Simultaneous averaging of couplings has also been reported for the N-methyl groups in N,N-dimethylformamide. ⁸¹ As a consequence of the interaction between Ta and F(11) and F(21), the entire ligand system forms an approximately planar pentagonal arrangement around the metal with the internal angles (starting with F-Ta-F and proceeding clockwise in Figure 2.1) being 65°, 72°, 76°, 76°, and 72°, for a total of ~360°. The C(5)-Ta-C(6) angle is therefore forced "open" to 142.9(2)°. The Ta-C bond



Bond Lengths

Ta(1)-N(1)	2.087(4)
Ta(1)-N(2)	2.078(5)
Ta(1)-N(3)	1.967(4)
Ta(1)-C(5)	2.191(6)
Ta(1)-C(6)	2.199(6)
Ta(1)-F(11)	2.452(3)
Ta(1)-F(21)	2.413(3)

Bond Angles

C(5)-Ta(1)-C(6)	142.9(2)
N(1)-Ta(1)-N(2)	152.0(2)
Ta(1)-N(1)-C(16)	121.3(4)
Ta(1)-N(2)-C(26)	122.3(4)
F(11)-Ta(1)-F(21)	64.53(11)
C(2)-N(3)-C(4)	112.4(5)

Dihedral Angles^a

N(1)/N(3)-Ta(1)-N(2)	179.0	N(3)/C(5)-Ta(1)-C(6)	175.0
Ta(1)-N(1)-C(16)-C(11)	4.3	Ta(1)-N(2)-C(26)-C(21)	3.9
C(4)/Ta(1)-N(3)-C(2)	157.5		

Figure 2.1. An ORTEP drawing (35% probability level) of the structure of $[\text{Ar}^{\text{F}}\text{N}_2\text{N}]\text{TaMe}_2$, with selected bond lengths (Å), bond angles (deg), and dihedral angles (deg). ^a Obtained from a Chem 3D model.

lengths, however, are virtually the same as in $[(\text{Me}_3\text{SiN-o-C}_6\text{H}_4)_2\text{N}]\text{TaMe}_2$, as is the $\text{N}_{\text{ax}}\text{-Ta-N}_{\text{ax}}$ angle. The Ta-N_{eq} distance in $[\text{Ar}^{\text{F}}\text{N}_2\text{N}]\text{TaMe}_2$ is ~ 0.1 Å shorter than that in $[(\text{Me}_3\text{SiN-o-C}_6\text{H}_4)_2\text{N}]\text{TaMe}_2$, while the Ta-N_{ax} distances are ~ 0.07 Å longer (Table 2.1).

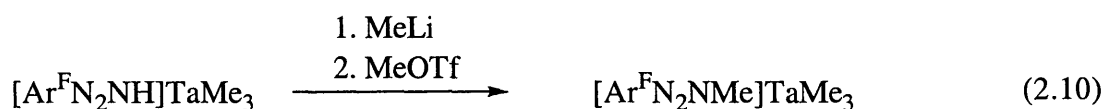
Table 2.1. A comparison of core bond lengths (Å) and angles (deg) in five coordinate Ta and Zr complexes containing tridentate amido ligands having a *mer* structure.

	M-N _{eq}	M-N _{ax}	N _{ax} -M-N _{ax}	M-C _α	C _α -M-C _α
$[\text{Ar}^{\text{F}}\text{N}_2\text{N}]\text{TaMe}_2$	1.967(4)	2.087(4)	152.0(2)	2.191(6)	142.9(2)
		2.078(5)		2.199(6)	
$[\text{TESN}_2\text{N}]\text{TaEt}[\text{N}(\text{CH}=\text{CH}_2)(\text{TES})]^{\text{a}}$	1.996(8)	2.025(7)	152.2(3)	2.17(1)	111.2 ^b
		2.035(8)		2.009(7) ^c	
$[(\text{Me}_3\text{SiN-o-C}_6\text{H}_4)_2\text{N}]\text{TaMe}_2^{\text{d}}$	2.077(4)	2.010(4)	149.8(2)	2.191(5)	130.6(2)
		2.007(4)		2.164(5)	
$\{[\text{Ar}^{\text{F}}\text{N}_2\text{NH}]\text{TaMe}_2\}^{+\text{e}}$	2.280(15)	1.981(12)	142.6(5)	2.09(2)	102.0(6)
		1.965(13)		2.11(2)	
$[(\text{Me}_3\text{SiNCH}_2\text{CH}_2)_2\text{NAlMe}_3]\text{TaMe}_2^{\text{d}}$	2.22(2)	1.985(9)	148.9(6)	2.14(3)	106.6(12)
		1.985(9)		2.20(3)	
$[\text{MesN}_2\text{NH}]\text{ZrMe}_2^{\text{f}}$	2.392(7)	2.097(6)	140.0(3)	2.249(9)	102.3(3)
		2.097(6)		2.260(9)	
$[2,6\text{-(ArylNCH}_2)_2\text{C}_5\text{H}_3\text{N}]\text{ZrMe}_2^{\text{g}}$	2.325(4)	2.101(4)	139.6(2)	2.243(6)	102.4(3)
		2.104(5)		2.248(7)	

^a $\text{TESN}_2\text{N} = (\text{Et}_3\text{SiNCH}_2\text{CH}_2)_2\text{N}$; see reference 120. ^b Angle of N(2)-Ta-C(5) in the structure shown in equation 2.1. ^c Distance between Ta and the nitrogen in $\text{N}(\text{CH}=\text{CH}_2)(\text{TES})$ ligand. ^d See reference 129. ^e Anion = $\{\text{MeB}(\text{C}_6\text{F}_5)_3\}^-$; see Section 2.10. ^f See Chapter 3. ^g Aryl = 2,6-Et₂C₆H₃; see reference 123.

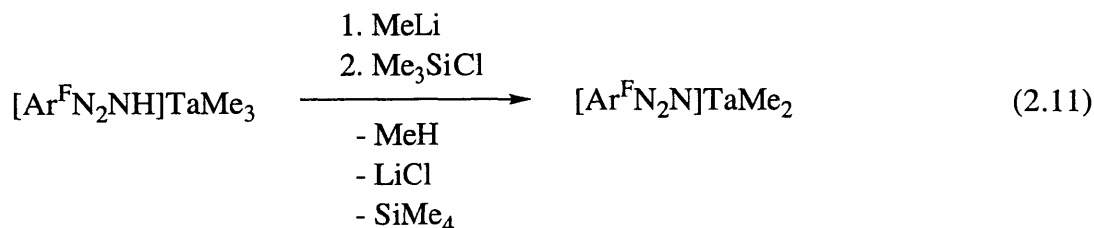
2.6 Deprotonation-alkylation of $[\text{Ar}^{\text{F}}\text{N}_2\text{NH}]\text{TaMe}_3$.

The NH proton in $[\text{Ar}^{\text{F}}\text{N}_2\text{NH}]\text{TaMe}_3$ is relatively acidic as evidenced by the methane elimination from the trimethyl complex to give $[\text{Ar}^{\text{F}}\text{N}_2\text{N}]\text{TaMe}_2$. Addition of MeLi to $[\text{Ar}^{\text{F}}\text{N}_2\text{NH}]\text{TaMe}_3$ leads to deprotonation of the amino nitrogen according to the ^1H NMR spectrum. Subsequent addition of MeOTf produces yellow crystalline $[\text{Ar}^{\text{F}}\text{N}_2\text{NMe}]\text{TaMe}_3$ (equation 2.10). At room temperature, the ^1H NMR spectrum of $[\text{Ar}^{\text{F}}\text{N}_2\text{NMe}]\text{TaMe}_3$ reveals a singlet resonance at 2.14 ppm for NMe and a singlet resonance at 1.07 ppm for TaMe. The equivalent methyl ligands are all distinguishable at low temperatures. At $-80\text{ }^\circ\text{C}$ in toluene- d_8 , three singlet resonances are found at 1.47, 1.15, and 0.89 ppm, two of which coalesce at $-60\text{ }^\circ\text{C}$ to give two signals at 1.22 and 0.86 ppm in a ratio of 2:1. Therefore, we propose that the static structure of $[\text{Ar}^{\text{F}}\text{N}_2\text{NMe}]\text{TaMe}_3$ is *mer*. The *mer* structure is also found for the mesitylated diamidoamine ligand in five coordinate group 4 complexes such as $[\text{MesN}_2\text{NMe}]\text{ZrMe}_2$ (see Chapter 3). The mechanism of the methyl ligand exchange in $[\text{Ar}^{\text{F}}\text{N}_2\text{NMe}]\text{TaMe}_3$ is presumably the same as that proposed for $[\text{RN}_2\text{O}]\text{TaMe}_3$ and $[\text{Ar}^{\text{F}}\text{N}_2\text{NH}]\text{TaMe}_3$. It is possible that the activation energy for the fluxional process in $[\text{Ar}^{\text{F}}\text{N}_2\text{NMe}]\text{TaMe}_3$ is higher than that in $[\text{Ar}^{\text{F}}\text{N}_2\text{NH}]\text{TaMe}_3$. The propensity of this fluxional exchange process in $[\text{Ar}^{\text{F}}\text{N}_2\text{NR}]\text{TaMe}_3$ ($\text{R} = \text{H}, \text{Me}$) is consistent with the difference in coordination strength between NH and NMe, assuming that dissociation of the amino nitrogen plays an important role in this process. It should be noted that a fluxional exchange process is also observed for five coordinate $[(\text{Me}_3\text{SiNCH}_2\text{CH}_2)_2\text{NSiMe}_3]\text{MR}_2$ ($\text{M} = \text{Ti}, \text{R} = \text{Me}; \text{M} = \text{Zr}, \text{R} = \text{Bn}$) due to the weak coordination of the central amino nitrogen.^{139,140}



In contrast to the formation of $[\text{Ar}^{\text{F}}\text{N}_2\text{NMe}]\text{TaMe}_3$ with MeOTf, deprotonation of $[\text{Ar}^{\text{F}}\text{N}_2\text{NH}]\text{TaMe}_3$ followed by addition of Me_3SiCl produces orange crystalline $[\text{Ar}^{\text{F}}\text{N}_2\text{N}]\text{TaMe}_2$ (equation 2.11). The formation of $[\text{Ar}^{\text{F}}\text{N}_2\text{N}]\text{TaMe}_2$ is unexpected and the mechanism is not clear

at this point. It is likely that the reaction proceeds *via* a presumed trimethyl intermediate, $[\text{Ar}^{\text{F}}\text{N}_2\text{NSiMe}_3]\text{TaMe}_3$, which eliminates tetramethylsilane to give $[\text{Ar}^{\text{F}}\text{N}_2\text{N}]\text{TaMe}_2$ as the thermodynamic product.

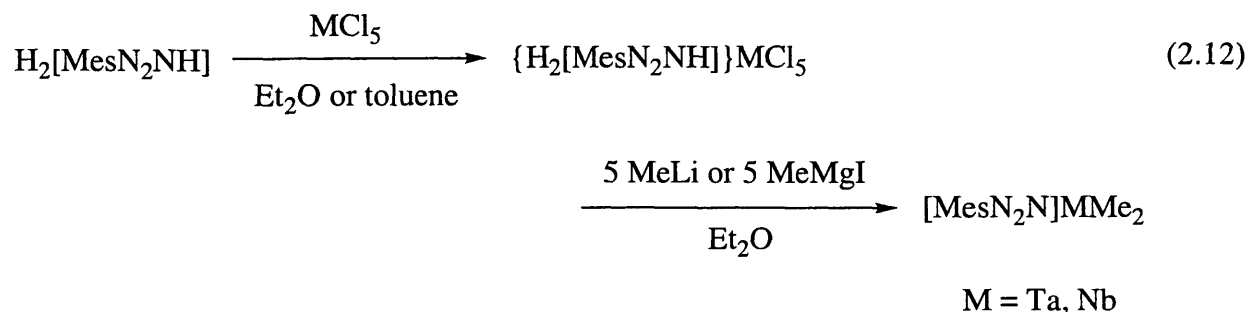


2.7 Direct synthesis of dialkyl tantalum and niobium complexes containing $[\text{MesN}_2\text{N}]^{3-}$.

A synthetic methodology that takes advantage of the coordination chemistry of electrophilic early transition metal halides with Lewis bases has been developed. Molybdenum triamidoamine methyl complexes can be synthesized by addition of four equivalents of MeLi to a THF suspension containing $\text{MoCl}_4(\text{THF})_2$ and $\text{N}(\text{CH}_2\text{CH}_2\text{NHAr})_3$.⁵⁸ It is likely that three equivalents of MeLi are used to deprotonate the metal-ligand adduct and that the remaining one equivalent alkylates the metal center. This methodology can be applied to group 4 and 5 chemistry providing a simple and practical synthesis of some otherwise inaccessible complexes. The chemistry involving group 4 metals and $\text{H}_2[\text{MesN}_2\text{NH}]$ is described in Chapter 3.

Stirring a suspension of $\text{H}_2[\text{MesN}_2\text{NH}]$ and TaCl_5 in diethyl ether or toluene results in a thick slurry which presumably contains the $\{\text{H}_2[\text{MesN}_2\text{NH}]\}\text{TaCl}_5$ adduct. The insolubility of this adduct in regular solvents precludes its characterization by solution NMR spectroscopy. Attempts to observe the NH absorption by IR spectroscopy did not prove successful. Nevertheless, the adduct can be either used *in situ* or isolated as a yellow solid. The isolated form is preferred to allow for a higher yield in the subsequent reaction. Addition of five equivalents of MeLi or MeMgI to $\{\text{H}_2[\text{MesN}_2\text{NH}]\}\text{TaCl}_5$ in diethyl ether produces $[\text{MesN}_2\text{N}]\text{TaMe}_2$ (39% yield

from the *in situ* prepared $\{H_2[MesN_2NH]\}TaCl_5$ and 92% yield from the isolated $\{H_2[MesN_2NH]\}TaCl_5$; equation 2.12).

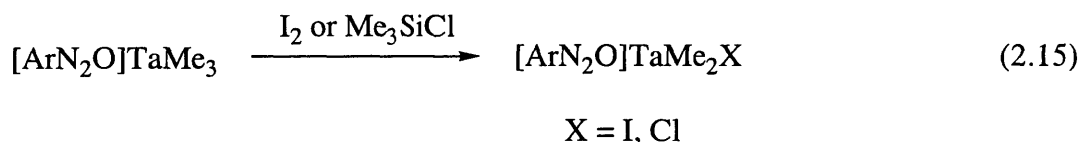
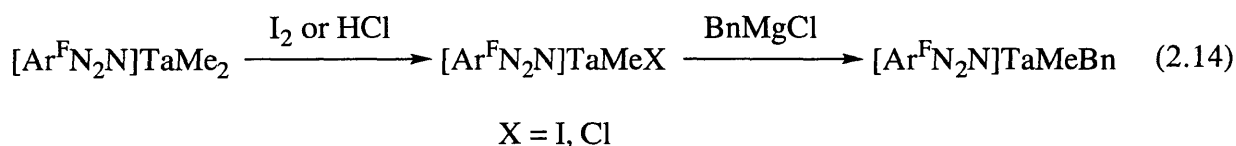


The analogous niobium complex can be obtained in a similar manner. Addition of five equivalents of MeMgI to adduct $\{H_2[MesN_2NH]\}NbCl_5$ produces $[MesN_2N]NbMe_2$ as blood red crystals in moderate yield (equation 2.12). The NMR data of $[MesN_2N]NbMe_2$ are all similar to those of $[MesN_2N]TaMe_2$. The 1H NMR spectrum of $[MesN_2N]NbMe_2$ reveals a singlet resonance at 0.81 ppm for NbMe and a singlet at 2.33 ppm for the *ortho* mesityl methyl groups, thus indicating C_{2v} symmetry. Attempts were also made to synthesize $[MesN_2NH]NbMe_2$, which is presumably structurally analogous to $[MesN_2NH]ZrMe_2$ (see Chapter 3) and has the formal oxidation state of Nb(IV). Interestingly, the reaction between $NbCl_4(THF)_2$ ¹⁴¹ and $H_2[MesN_2NH]$ followed by addition of four equivalents of MeMgI leads to a low yield of $[MesN_2N]NbMe_2$ as the only isolable product (equation 2.13). It is obvious that an undesired redox process occurs on the niobium center as the reaction proceeds.



2.8 Synthesis of mixed-alkyl complexes.

Mixed-alkyl complexes can be prepared *via* alkyl halide intermediates. Addition of one equivalent of element iodine to $[\text{Ar}^{\text{F}}\text{N}_2\text{N}]\text{TaMe}_2$ or $[\text{ArN}_2\text{O}]\text{TaMe}_3$ produces $[\text{Ar}^{\text{F}}\text{N}_2\text{N}]\text{TaMeI}$ and $[\text{ArN}_2\text{O}]\text{TaMe}_2\text{I}$, respectively (equations 2.14-2.15). Analogous chloride complexes $[\text{Ar}^{\text{F}}\text{N}_2\text{N}]\text{TaMeCl}$ and $[\text{ArN}_2\text{O}]\text{TaMe}_2\text{Cl}$ can also be prepared by employing ethereal HCl or Me_3SiCl . Alternatively, the iodide complex $[\text{Ar}^{\text{F}}\text{N}_2\text{N}]\text{TaMeI}$ can be obtained by the treatment of $[\text{Ar}^{\text{F}}\text{N}_2\text{N}]\text{TaMeCl}$ with Me_3SiI . Attempts to synthesize di- or trihalide complexes in a similar manner were not successful.



Subsequent alkylation of the methyl halide complexes produces the mixed-alkyl complexes. For instance, the reaction between $[\text{Ar}^{\text{F}}\text{N}_2\text{N}]\text{TaMeCl}$ and BnMgCl yields orange crystalline $[\text{Ar}^{\text{F}}\text{N}_2\text{N}]\text{TaMeBn}$ in moderate yield. Similar to the methyl resonance observed for $[\text{Ar}^{\text{F}}\text{N}_2\text{N}]\text{TaMe}_2$, the ^1H NMR spectrum of $[\text{Ar}^{\text{F}}\text{N}_2\text{N}]\text{TaMeBn}$ also reveals a quintet resonance at 0.15 ppm ($J = 6.8$ Hz) for the methyl protons and a quintet resonance at 1.88 ppm ($J = 5.3$ Hz) for the benzylic protons. The core structure of $[\text{Ar}^{\text{F}}\text{N}_2\text{N}]\text{TaMeBn}$ is presumably analogous to that of $[\text{Ar}^{\text{F}}\text{N}_2\text{N}]\text{TaMe}_2$.

2.9 Observation and isolation of cationic tantalum complexes.

Cationic tantalum complexes can be obtained by protonation of the central amido nitrogen in the dimethyl complexes containing the triamido ligands, or by abstraction of a methyl ligand

from the trimethyl complexes containing the diamido/donor ligands (equation 2.16; Table 2.2). The first method can be regarded as a retrosynthesis from $[\text{ArylN}_2\text{NH}]^{2-}$ to $[\text{ArylN}_2\text{N}]^{3-}$ shown in

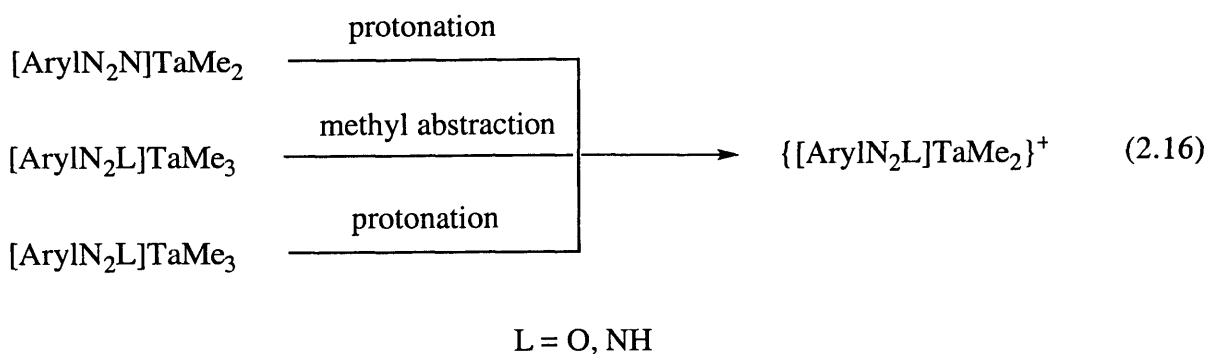


Table 2.2. Synthesis of cationic tantalum dimethyl complexes according to equation 2.16.^a

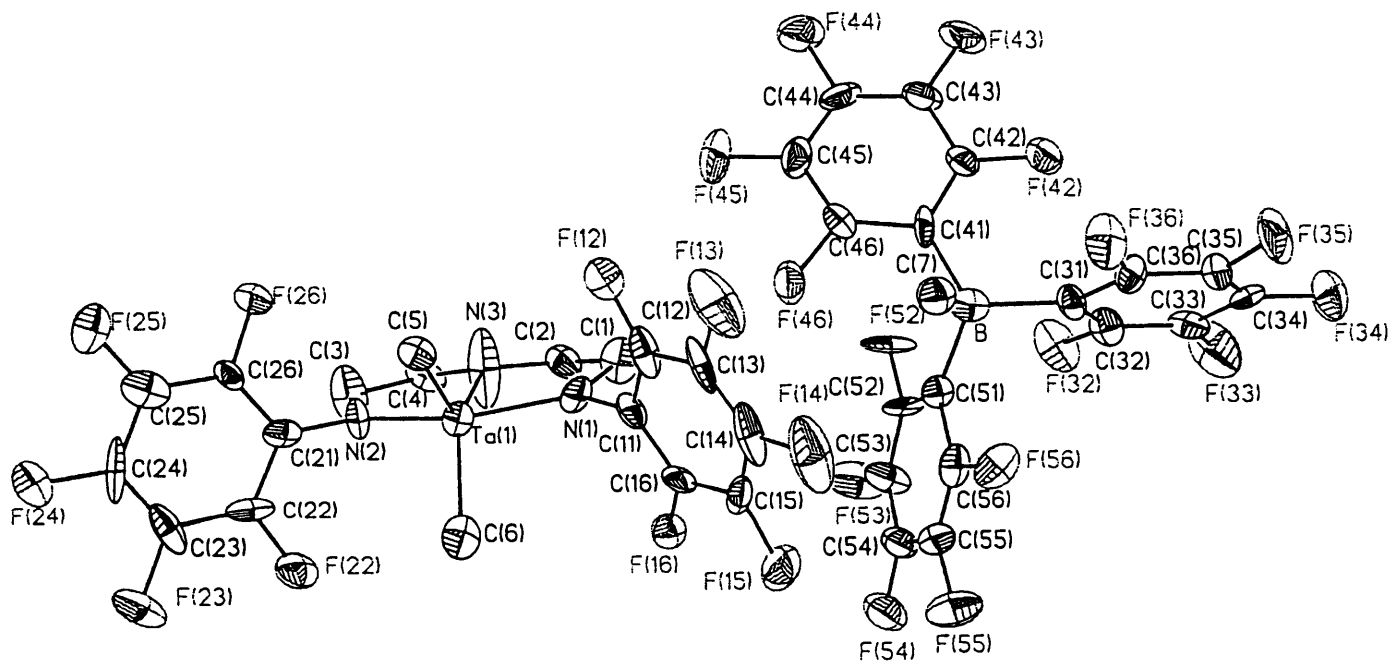
Ta complex	reagent	solvent	cation	anion
$[\text{Ar}^{\text{F}}\text{N}_2\text{N}]\text{TaMe}_2$	$[\text{PhMe}_2\text{NH}][\text{B}(\text{C}_6\text{F}_5)_4]$	CD_2Cl_2	$[\text{Ar}^{\text{F}}\text{N}_2\text{NH}]\text{TaMe}_2$	$\text{B}(\text{C}_6\text{F}_5)_4$
$[\text{Ar}^{\text{F}}\text{N}_2\text{NH}]\text{TaMe}_3$	$[\text{PhMe}_2\text{NH}][\text{B}(\text{C}_6\text{F}_5)_4]$	CD_2Cl_2	$[\text{Ar}^{\text{F}}\text{N}_2\text{NH}]\text{TaMe}_2$	$\text{B}(\text{C}_6\text{F}_5)_4$
$[\text{Ar}^{\text{F}}\text{N}_2\text{NH}]\text{TaMe}_3$	$\text{B}(\text{C}_6\text{F}_5)_3$	PhCH_3	$[\text{Ar}^{\text{F}}\text{N}_2\text{NH}]\text{TaMe}_2$	$\text{MeB}(\text{C}_6\text{F}_5)_3$
$[\text{PhN}_2\text{O}]\text{TaMe}_3$	$\text{B}(\text{C}_6\text{F}_5)_3$	CH_2Cl_2	$[\text{PhN}_2\text{O}]\text{TaMe}_2$	$\text{MeB}(\text{C}_6\text{F}_5)_3$
$[\text{PhN}_2\text{O}]\text{TaMe}_3$	$[\text{Ph}_3\text{C}][\text{B}(\text{C}_6\text{F}_5)_4]$	$\text{C}_6\text{D}_5\text{Br}$	$[\text{PhN}_2\text{O}]\text{TaMe}_2$	$\text{B}(\text{C}_6\text{F}_5)_4$
$[\text{ArN}_2\text{O}]\text{TaMe}_3$	$\text{B}(\text{C}_6\text{F}_5)_3$	CD_2Cl_2	$[\text{ArN}_2\text{O}]\text{TaMe}_2$	$\text{MeB}(\text{C}_6\text{F}_5)_3$
$[\text{ArN}_2\text{O}]\text{TaMe}_3$	$[\text{Ph}_3\text{C}][\text{B}(\text{C}_6\text{F}_5)_4]$	CH_2Cl_2	$[\text{ArN}_2\text{O}]\text{TaMe}_2$	$\text{B}(\text{C}_6\text{F}_5)_4$
$[\text{ArN}_2\text{O}]\text{TaMe}_3$	$[\text{Ph}_3\text{C}][\text{BF}_4]$	CD_2Cl_2	$[\text{ArN}_2\text{O}]\text{TaMe}_2$	BF_4
$[\text{ArN}_2\text{O}]\text{TaMe}_3$	$[\text{Ph}_3\text{C}][\text{PF}_6]$	CH_2Cl_2	$[\text{ArN}_2\text{O}]\text{TaMe}_2$	PF_6

^a The ^1H NMR spectra of each reaction aliquot reveal quantitative formation of each product.

equations 2.9 and 2.11. Protonation of a methyl ligand in the trimethyl complexes also leads to a cationic species. For instance, the ^1H NMR spectrum of a mixture of $[\text{PhMe}_2\text{NH}][\text{B}(\text{C}_6\text{F}_5)_4]$ and $[\text{Ar}^{\text{F}}\text{N}_2\text{N}]\text{TaMe}_2$ or $[\text{Ar}^{\text{F}}\text{N}_2\text{NH}]\text{TaMe}_3$ in CD_2Cl_2 suggests that $\{[\text{Ar}^{\text{F}}\text{N}_2\text{NH}]\text{TaMe}_2\}\{\text{B}(\text{C}_6\text{F}_5)_4\}$ and free Me_2NPh are formed. The NH proton is found at 4.50 ppm as a broad singlet resonance. Methyl abstraction of $[\text{Ar}^{\text{F}}\text{N}_2\text{NH}]\text{TaMe}_3$ by $\text{B}(\text{C}_6\text{F}_5)_3$ in toluene produces an ion pair $\{[\text{Ar}^{\text{F}}\text{N}_2\text{NH}]\text{TaMe}_2\}\{\text{MeB}(\text{C}_6\text{F}_5)_3\}$, which can be isolated as a toluene solvate in quantitative yield. Similarly, the reactions of $[\text{RN}_2\text{O}]\text{TaMe}_3$ ($\text{R} = \text{Ph}, \text{Ar}$) with $\text{B}(\text{C}_6\text{F}_5)_3$ or $[\text{Ph}_3\text{C}]^+$ also give corresponding cationic tantalum dimethyl complexes in high isolated yields. These five coordinate cationic tantalum complexes containing the diamido/donor (donor = O, NH) ligands are isoelectronic with the corresponding neutral group 4 complexes. In general, these cations are stable in the solid state at $-30\text{ }^\circ\text{C}$, although their ultimate thermal stability has yet to be determined. No reaction was found between 1-hexene and these cationic tantalum complexes under conditions similar to those employed for the group 4 chemistry discussed in Chapters 1 and 3.

2.10 X-ray structure of $\{[\text{Ar}^{\text{F}}\text{N}_2\text{NH}]\text{TaMe}_2\}\{\text{MeB}(\text{C}_6\text{F}_5)_3\}$.

A single crystal of $\{[\text{Ar}^{\text{F}}\text{N}_2\text{NH}]\text{TaMe}_2\}\{\text{MeB}(\text{C}_6\text{F}_5)_3\}$ was grown from a concentrated dichloromethane solution at $-30\text{ }^\circ\text{C}$. An X-ray structure (Figure 2.2) shows that the anion is separated from the cation, with no contacts less than 3 \AA . The cation (Figure 2.3, Table 2.1) has a core structure that is analogous to that of zwitterionic $[(\text{Me}_3\text{SiNCH}_2\text{CH}_2)_2\text{NAlMe}_3]\text{TaMe}_2$, which is obtained by attaching AlMe_3 to the central amido nitrogen in $[(\text{Me}_3\text{SiNCH}_2\text{CH}_2)_2\text{N}]\text{TaMe}_2$.¹²⁹ It is interesting to note that the central amino nitrogen in $\{[\text{Ar}^{\text{F}}\text{N}_2\text{NH}]\text{TaMe}_2\}^+$ is only modestly distorted from planarity with $\text{C-N}_{\text{eq}}\text{-C} = 123.1^\circ$ and $\text{Ta-N}_{\text{eq}}\text{-C}$ angles of 116.4° and 115.6° (sum = 355.1°). For comparison, the analogous angles in $[(\text{Et}_3\text{SiNCH}_2\text{CH}_2)_2\text{N}]\text{TaEt}[\text{N}(\text{CH}=\text{CH}_2)(\text{SiEt}_3)]$ are 110.2° , 120.9° , and 122.8° (sum = 353.9°),¹²⁰ while the analogous sum of angles in $[(\text{Me}_3\text{SiNCH}_2\text{CH}_2)_2\text{NAlMe}_3]\text{TaMe}_2$ is



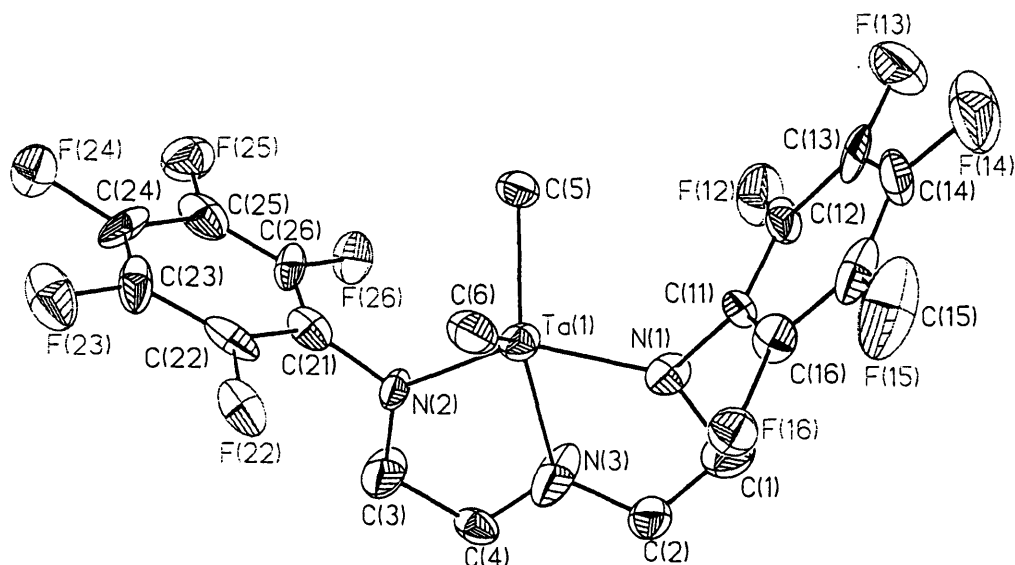
Bond Lengths

B-C(7)	1.65(3)
B-C(31)	1.66(3)

Bond Angle

C(7)-B-C(51)	109(2)
--------------	--------

Figure 2.2. An ORTEP drawing (35% probability level) of the structure of $\{[\text{Ar}^{\text{F}}\text{N}_2\text{NH}]\text{TaMe}_2\}\{\text{MeB}(\text{C}_6\text{F}_5)_3\}$, with selected bond lengths (Å) and bond angle (deg) in the anion.



Bond Lengths

Ta(1)-N(1)	1.965(13)
Ta(1)-N(2)	1.981(12)
Ta(1)-N(3)	2.280(15)
Ta(1)-C(5)	2.11(2)
Ta(1)-C(6)	2.09(2)

Bond Angles

C(5)-Ta(1)-C(6)	102.0(6)
N(1)-Ta(1)-N(2)	142.6(5)
Ta(1)-N(1)-C(11)	118.6(10)
Ta(1)-N(2)-C(21)	118.7(10)
C(2)-N(3)-C(4)	123(2)

Dihedral Angles^a

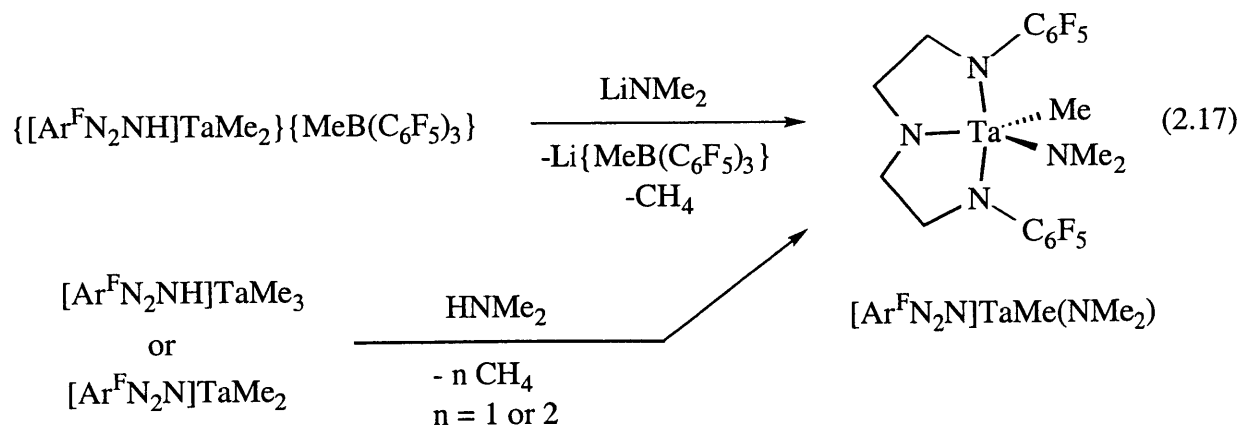
N(1)/N(3)-Ta(1)-N(2)	177.5	N(3)/C(5)-Ta(1)-C(6)	178.2
Ta(1)-N(1)-C(11)-C(12)	87.8	Ta(1)-N(2)-C(21)-C(22)	91.5

Figure 2.3. An ORTEP drawing (35% probability level) of the structure of cationic $\{[\text{Ar}^{\text{F}}\text{N}_2\text{NH}]\text{TaMe}_2\}^+$, with selected bond lengths (Å), bond angles (deg), and dihedral angles (deg). ^a Obtained from a Chem 3D model.

326.5°. ¹²⁹ The C-Ta-C angle in {[Ar^FN₂NH]TaMe₂}⁺ is 102.0(6)°, which is ~41° smaller than that found in [Ar^FN₂N]TaMe₂ but close to that found in [(Me₃SiNCH₂CH₂)₂NaI Me₃]TaMe₂ (106.6(12)°). We propose that the *ortho* fluorines on the C₆F₅ rings in {[Ar^FN₂NH]TaMe₂}⁺ have no room to interact with the metal, as they do in [Ar^FN₂N]TaMe₂ (Figure 2.1), and that the rings are consequently turned approximately perpendicular to the TaN₃ "pseudo-plane". The more spherically symmetric (versus almost planar) cation may also result from more efficient packing in the crystal.

2.11 Reaction between LiNMe₂ and cationic {[Ar^FN₂NH]TaMe₂}⁺.

Stable group 5 methyldiene complexes are rare. ^{142,143} It has been shown that methyldiene complexes can be obtained by deprotonation of a methyl group in cationic [Cp*₂TaMe₂]⁺. Attempts to synthesize a tantalum methyldiene complex bearing tridentate diamido/donor ligands using a similar methodology have not been successful. Addition of LiNMe₂ to {[Ar^FN₂NH]TaMe₂} {MeB(C₆F₅)₃} produces [Ar^FN₂N]TaMe(NMe₂) as a yellow crystalline solid in moderate yield (equation 2.17). It is likely that the formation of [Ar^FN₂N]TaMe(NMe₂) is accompanied by methane elimination from a presumed six coordinate intermediate [Ar^FN₂NH]TaMe₂(NMe₂). The methane elimination is analogous to that observed for the formation of [Ar^FN₂N]TaMe₂ from [Ar^FN₂NH]TaMe₃.

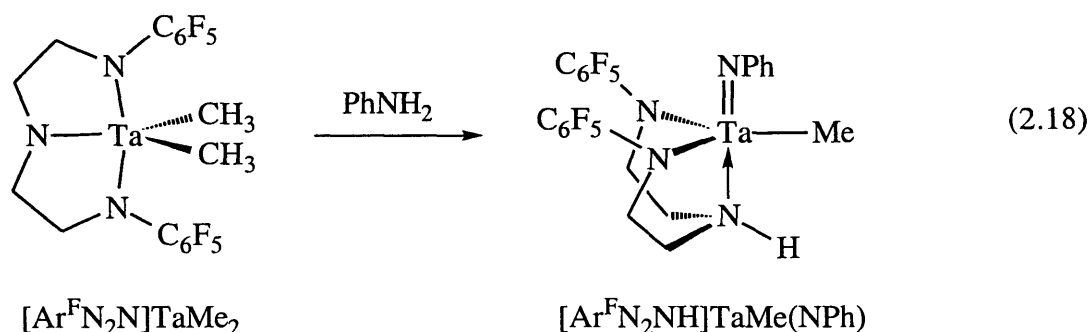


The composition of $[\text{Ar}^{\text{F}}\text{N}_2\text{N}]\text{TaMe}(\text{NMe}_2)$ has been authenticated by combustion analysis and by another synthetic approach involving the reactions of HNMe_2 with $[\text{Ar}^{\text{F}}\text{N}_2\text{NH}]\text{TaMe}_3$ or $[\text{Ar}^{\text{F}}\text{N}_2\text{N}]\text{TaMe}_2$ (equation 2.17). The ^1H NMR spectrum of $[\text{Ar}^{\text{F}}\text{N}_2\text{N}]\text{TaMe}(\text{NMe}_2)$ reveals two broad singlet resonances for the NMe_2 ligand, suggesting that the Ta-NMe_2 bond does not rotate readily and that the C-N-C plane in the NMe_2 ligand is not perpendicular to the equatorial plane of the tantalum complex, presumably as a consequence of either the steric interaction between NMe_2 and the C_6F_5 rings or the p_π orientation of the dimethylamide nitrogen. The ^{19}F NMR spectrum of $[\text{Ar}^{\text{F}}\text{N}_2\text{N}]\text{TaMe}(\text{NMe}_2)$, however, indicates a free rotation of the C_6F_5 rings at room temperature on the NMR time scale. Therefore, the inequivalent methyl groups in NMe_2 is presumably due to the $\text{p}_\pi\text{-d}_\pi$ interaction between the dimethylamide nitrogen and the metal center. It is likely that the orientation of NMe_2 in $[\text{Ar}^{\text{F}}\text{N}_2\text{N}]\text{TaMe}(\text{NMe}_2)$ is analogous to that of the $\text{N}(\text{CH}=\text{CH}_2)(\text{SiEt}_3)$ ligand in $[(\text{Et}_3\text{SiNCH}_2\text{CH}_2)_2\text{N}]\text{TaEt}[\text{N}(\text{CH}=\text{CH}_2)(\text{SiEt}_3)]$ (a structure shown in equation 2.1), in which $\text{C}(20)$ and $\text{Si}(2)$ lie on the equatorial plane with dihedral angles of $\text{N}(4)\text{-Ta-N}(2)\text{-C}(20)$ and $\text{N}(4)\text{-Ta-N}(2)\text{-Si}(2)$ being $\sim 0^\circ$,¹²⁰ presumably due to the amide nitrogen p_π interaction with the tantalum center ($\text{Ta-N}(2) = 2.009(7) \text{ \AA}$). As it has been shown that $[(\text{Et}_3\text{SiNCH}_2\text{CH}_2)_2\text{N}]\text{TaEt}[\text{N}(\text{CH}=\text{CH}_2)(\text{SiEt}_3)]$ is obtained by thermolysis of a triamidoamine olefin complex $[(\text{Et}_3\text{SiNCH}_2\text{CH}_2)_3\text{N}]\text{Ta}(\text{C}_2\text{H}_4)$ at 110°C , it is likely that the formation of $[\text{Ar}^{\text{F}}\text{N}_2\text{N}]\text{TaMe}(\text{NMe}_2)$ instead of methyldiene $[\text{Ar}^{\text{F}}\text{N}_2\text{NH}]\text{TaMe}(\text{CH}_2)$ is for the thermodynamic reason.

2.12 Reaction between PhNH_2 and $[\text{Ar}^{\text{F}}\text{N}_2\text{N}]\text{TaMe}_2$.

Addition of PhNH_2 to $[\text{Ar}^{\text{F}}\text{N}_2\text{N}]\text{TaMe}_2$ produces a yellow crystalline compound for which the combustion analysis and NMR data are consistent with a composition of tautomeric $[\text{Ar}^{\text{F}}\text{N}_2\text{N}]\text{TaMe}(\text{NHPh})$ or $[\text{Ar}^{\text{F}}\text{N}_2\text{NH}]\text{TaMe}(\text{NPh})$. The NH proton is observed at 1.62 ppm as a broad singlet resonance. The ^{19}F NMR data suggest a high rotational barrier for the C_6F_5 rings.

Between -80 and 15 °C, five distinct fluorine resonances with equal intensity are observed. Two fluorine signals coalesce at ~25 °C and another two at ~60 °C. The C₆F₅ rings can rotate readily only at temperatures > 80 °C. The ¹H NMR spectrum indicates a free rotation of the phenyl ring at room temperature, suggesting that the hindered rotation of the C₆F₅ rings does not arise from steric interactions with the phenyl group. It should be noted that in the *mer* structures of [Ar^FN₂N]TaMe₂ (-80 °C) and [Ar^FN₂N]TaMeX (X = Cl, I, Bn; 25 °C) the C₆F₅ rings rotate readily on the NMR time scale. The pπ-dπ interaction observed between NMe₂ and Ta in [Ar^FN₂N]TaMe(NMe₂) seems not to affect the rotation of its C₆F₅ rings. Therefore, it is likely that the product from the reaction between PhNH₂ and [Ar^FN₂N]TaMe₂ is [Ar^FN₂NH]TaMe(NPh), which contains a diamidoamine ligand with a *fac* geometry (equation 2.18). [Ar^FN₂NH]TaMe(NPh) can be regarded as an analogue of the triamidoamine-based imido complex, [(Me₃SiNCH₂CH₂)₃N]Ta=NPh,¹¹⁹ except that one of the arms in the triamidoamine ligand has been disconnected.



The *fac* structure of [Ar^FN₂NH]TaMe(NPh) is analogous to that observed in rhenium^{144,145} and vanadium⁶⁰ complexes containing similar C₆F₅-substituted diamidoamine ligands. The phenyl substituted imido group presumably occupies an axial position, similar to that observed for the oxygen atom in [(C₆F₅NCH₂CH₂)₂NCH₂CH₂NHC₆F₅]ReCl(O). This reaction should also be compared with that of [(Me₃SiNCH₂CH₂)₂N]TaMe₂ with t-BuNH₂, from which a *fac* [(Me₃SiNCH₂CH₂)₂NH]TaMe(N-t-Bu) containing an imido ligand trans (N_{imide}-Ta-N_{amine} =

174.0°) to the NH donor is isolated.¹⁴⁶ The TaN₄C core of [Ar^FN₂NH]TaMe(NPh) is presumably analogous to that of [(Me₃SiNCH₂CH₂)₂NH]TaMe(N-t-Bu).

DISCUSSION

We have shown that several tantalum complexes can be synthesized by employing a series of tridentate amido ligands, in which the central donor functionality can be amide, amine, or ether. Ligand design involves the incorporation of ethylene backbone and either aryl or alkyl substituents on the amido nitrogens. It is obvious that aryl-alkyl amides are better ancillaries than alkyl-alkyl amides due to their higher thermal stability and thereby more abundant chemistry. The alkyl substituted amides [t-BuN₂O]²⁻ and [AdN₂O]²⁻ are probably too reducing, and therefore their tantalum trimethyl complexes are only briefly stable at room temperature, in contrast to the tantalum trimethyl complexes obtained from aryl substituted amides, [PhN₂O]²⁻ and [ArN₂O]²⁻. Decomposition involving t-butyl radicals has been proposed in systems which contain [(t-BuNSiMe₂CH₂)₂PPh]²⁻¹⁴⁷ or [t-BuNON]²⁻.⁵² However, adamantyl derived [AdN₂O]TaMe₃ does not show higher stability than the t-butyl analogue, although the formation of adamantyl radicals is usually much slower due to its strained bicyclic rings.^{148,149} It should be noted that attempts to synthesize group 4 complexes containing [t-BuN₂O]²⁻ and [AdN₂O]²⁻ ligands do not lead to any identifiable compounds, in contrast to the recent reports of titanium complexes containing monodentate alkyl-alkyl amides such as [N(i-Pr)₂]⁻ and [NCy₂]⁻.^{150,151}

Several ligands employed in this study contain an aryl substituent on the amido nitrogen. Aryl ring rotation can be used as a convenient tool for understanding steric crowding in the complexes. Hindered rotation of mesityl rings is observed for five coordinate group 4 diamidoamine complexes of the type [MesN₂NR]MMe₂ (M = Ti, Zr, Hf; R = H, Me, Bn, Bn^F; see Chapter 3), while free rotation of C₆F₅ rings is usually observed for five coordinate group 5 complexes, including neutral [Ar^FN₂N]TaMeX (X = Me, Bn, NMe₂, Cl, I) and cationic

$\{[\text{Ar}^{\text{F}}\text{N}_2\text{NH}]\text{TaMe}_2\}^+$. Steric interaction between equatorial ligands and mesityl groups is more significant than that arising from C_6F_5 rings, due to the different sizes of these aromatic rings. *Fac* $[\text{Ar}^{\text{F}}\text{N}_2\text{NH}]\text{TaMe}(\text{NPh})$ is the only compound in this study with significant hindered rotation for the C_6F_5 rings, but the steric hindrance is probably between the two C_6F_5 rings.

An important issue in amido complexes is the degree of π bonding between the amido nitrogen and the metal. In general, the orientation of aromatic substituents in the amido complexes can be indicative of this interaction. In $[\text{Ar}^{\text{F}}\text{N}_2\text{N}]\text{TaMe}_2$, the C_6F_5 rings are aligned on the TaN_3 plane such that the C_6F_5 aromatic system is probably in conjugation with the lone pairs of the axial nitrogens, while in $\{[\text{Ar}^{\text{F}}\text{N}_2\text{NH}]\text{TaMe}_2\}^+$ the rings are turned 90° such that the lone pair is likely primarily involved in π bonding to the metal. Therefore, the π bonding for the former is expected to be less significant than the latter. X-ray structural data show that the average Ta-N_{ax} bond lengths in $[\text{Ar}^{\text{F}}\text{N}_2\text{N}]\text{TaMe}_2$ is $\sim 0.11 \text{ \AA}$ longer than that in $\{[\text{Ar}^{\text{F}}\text{N}_2\text{NH}]\text{TaMe}_2\}^+$.

Several five coordinate tantalum dialkyl complexes have been synthesized. Trigonal bipyramidal geometry is probably a general structure for all of the dimethyl complexes reported here, including neutral $[\text{ArylN}_2\text{N}]\text{TaMe}_2$ ($\text{Aryl} = \text{Ar}^{\text{F}}, \text{Mes}$) and cationic $\{[\text{ArylN}_2\text{L}]\text{TaMe}_2\}^+$ ($\text{Aryl} = \text{Ar}^{\text{F}}, \text{Ph}, \text{Ar}; \text{L} = \text{O}, \text{NH}$). The π bonding in the trigonal bipyramidal complexes discussed here can be evaluated qualitatively using the coordinate system shown in Figure 2.4.

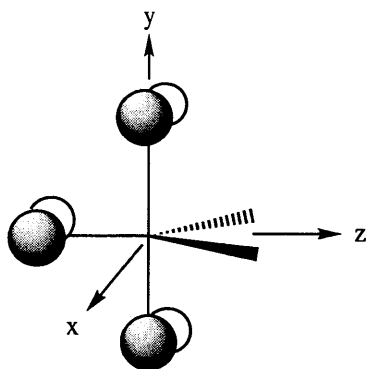


Figure 2.4. The coordinate system for trigonal bipyramidal complexes. The three p orbitals parallel to the x axis correspond to the three p orbitals on the nitrogen atoms.

The two d orbitals that are likely to be most important for π bonding are the d_{xy} (A_2 symmetry in C_{2v} , overlapping with the unsymmetric combination of the p orbitals on the axial nitrogens) and d_{xz} (B_1 symmetry in C_{2v} , overlapping with the p orbital on the equatorial nitrogen). The X-ray structural data suggest that in $[\text{Ar}^{\text{F}}\text{N}_2\text{N}]\text{TaMe}_2$ there is a considerable degree of π bonding between tantalum and both axial and equatorial nitrogens. A representation of the equatorial σ bonds transforms as $2A_1$ (p_z , $d_{x^2-y^2}$, or d_{z^2}) + B_1 (p_x or d_{xz}). Therefore, in the presence of d_{xz} π bonding to N_{eq} in $[\text{Ar}^{\text{F}}\text{N}_2\text{N}]\text{TaMe}_2$, only p_x is available to form two σ hybrids to the two methyl groups in the equatorial positions and the C-Ta-C angle is consequently relatively large. In the absence of significant π bonding between the metal and N_{eq} , as in $\{[\text{Ar}^{\text{F}}\text{N}_2\text{NH}]\text{TaMe}_2\}^+$, d_{xz} also may be used to form the bonds to the methyl groups, and the C-Ta-C angle can be much smaller. It should be noted, however, that the Ta- N_{eq} bond length in $[(\text{Et}_3\text{SiNCH}_2\text{CH}_2)_2\text{N}]\text{TaEt}[\text{N}(\text{CH}=\text{CH}_2)(\text{SiEt}_3)]$ (1.966(8) Å) suggests that π bonding (using the d_{xz} orbital) is significant,¹²⁰ yet the N_{eq} -Ta- C_{eq} angle in $[(\text{Et}_3\text{SiNCH}_2\text{CH}_2)_2\text{N}]\text{TaEt}[\text{N}(\text{CH}=\text{CH}_2)(\text{SiEt}_3)]$ (111.2°) is closer to the "small" C-Ta-C angle found in $\{[\text{Ar}^{\text{F}}\text{N}_2\text{NH}]\text{TaMe}_2\}^+$.

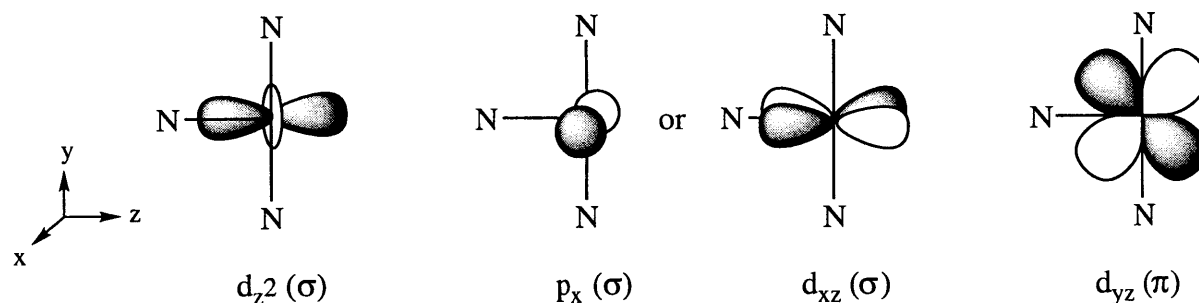
The structure of $\{[\text{Ar}^{\text{F}}\text{N}_2\text{NH}]\text{TaMe}_2\}^+$ is remarkably similar to that of $[\text{MesN}_2\text{NH}]\text{ZrMe}_2$ and $[2,6-(\text{ArylNCH}_2)_2\text{C}_5\text{H}_3\text{N}]\text{ZrMe}_2$ (Aryl = 2,6- $\text{Et}_2\text{C}_6\text{H}_3$). Several structural data for these species are listed in Table 2.1. The Ta- N_{ax} , Ta- N_{eq} , and Ta- C_{α} distances are all approximately 0.1 Å shorter than the corresponding distances in the zirconium complexes, presumably as a consequence of the larger size of Zr(IV) compared to Ta(V).¹³⁶ However, the N_{ax} -M- N_{ax} and C_{α} -M- C_{α} angles in these complexes are closely similar, consistent with relatively poor or no π bonding between the pyridyl nitrogen and the zirconium center in $[2,6-(\text{ArylNCH}_2)_2\text{C}_5\text{H}_3\text{N}]\text{ZrMe}_2$. It was concluded on the basis of extended Hückel molecular orbital studies that $[2,6-(\text{ArylNCH}_2)_2\text{C}_5\text{H}_3\text{N}]^{2-}$ is an eight electron ligand, and that the frontier orbitals in the $[2,6-(\text{ArylNCH}_2)_2\text{C}_5\text{H}_3\text{N}]\text{Zr}$ fragment consist of two a_1 orbitals and one b_2 orbital,¹²³ although their energies are significantly different than the a_1 and b_2 orbital energies in the analogous Cp_2Zr fragment. Therefore it is perhaps not circumstantial that the C_{α} -M- C_{α} angles

in $[\text{MesN}_2\text{NH}]\text{ZrMe}_2$, $[2,6-(\text{ArNCH}_2)_2\text{C}_5\text{H}_3\text{N}]\text{ZrMe}_2$, and $\{[\text{Ar}^{\text{F}}\text{N}_2\text{NH}]\text{TaMe}_2\}^+$ are all similar to each other and not much different than in a typical zirconocene dialkyl complex (e.g., $95.6(12)^\circ$ in Cp_2ZrMe_2).¹⁵²

The cationic dimethyl complexes $\{[\text{ArylN}_2\text{L}]\text{TaMe}_2\}^+$ ($\text{Aryl} = \text{Ar}^{\text{F}}, \text{Ph}, \text{Ar}; \text{L} = \text{O}, \text{NH}$) are especially interesting in view of the rarity of cationic tantalum(V) complexes¹⁵³ which do not contain cyclopentadienyl derived ligands. $[\text{Cp}_2\text{TaMe}_2][\text{BF}_4]$ and related species are prepared by treating trimethyl complexes with $[\text{Ph}_3\text{C}][\text{BF}_4]$ in dichloromethane.^{142,143} $[(\eta^5\text{-C}_5\text{H}_4\text{Me})_2\text{TaMe}_2][\text{BF}_4]$ and $[\text{Cp}(\eta^5\text{-C}_5\text{H}_4\text{Me})\text{TaMe}_2][\text{BF}_4]$ are prepared by similar methods. $[(\eta^5\text{-C}_5\text{H}_4\text{Me})_2\text{TaMeBr}]^+$ salts are also prepared, although they have not been thoroughly characterized. Niobium and tantalum complexes of the type $[\text{Cp}_2\text{M}(\text{CH}_2\text{SiMe}_3)_2]^+$ are prepared by oxidation of the $\text{Cp}_2\text{M}(\text{CH}_2\text{SiMe}_3)_2$ complexes with AgBF_4 or AgSbF_6 .¹⁵⁴ Two biscyclopentadienyl complexes have been structurally characterized, $[\text{Cp}^*_2\text{TaMe}(\text{OH})][\text{B}(\text{OH})(\text{C}_6\text{F}_5)_3]^{155}$ and $[\text{CpCp}^*\text{TaMe}_2][\text{OTf}]$.¹⁵⁶ In each case, a pseudotetrahedral cation is observed. In the latter compound, the triflate ion is interacting weakly with the cation through contacts that vary between 3.3 Å and 3.5 Å. The Cp-Ta-Cp^* angle is typical (136°), as are the Me-Ta-Me angle (96°) and Ta-Me distances (2.168(12) Å and 2.174(12) Å). These values should be compared with the $\text{N}_{\text{ax}}\text{-Ta-N}_{\text{ax}}$ angle (143°), Me-Ta-Me angle (102°) and Ta-Me distances (2.09(2) Å and 2.11(2) Å) in $\{[\text{Ar}^{\text{F}}\text{N}_2\text{NH}]\text{TaMe}_2\}^+$. We could find no other examples of Ta(V) alkyl cations in the literature in which the tantalum is the cationic center. (In a complex such as $[\text{Cp}^*(\text{i-Pr}_2\text{HNBC}_4\text{H}_4)\text{TaMe}_2]^+$, the positive charge is localized on the nitrogen center.¹¹¹) Relatively weakly coordinating anions such as $[\text{MeB}(\text{C}_6\text{F}_5)_3]^{-157,158}$ and $[\text{B}(\text{C}_6\text{F}_5)_4]^{-159,160}$ are most likely to be compatible with cationic tantalum centers, unless the coordination sphere is extremely crowded, as in 16 electron biscyclopentadienyl complexes such as $[(\eta^5\text{-C}_5\text{H}_4\text{Me})_2\text{TaMe}_2][\text{BF}_4]$. Even in $[(\text{Me}_3\text{SiNCH}_2\text{CH}_2)_3\text{N}]\text{TaMe}(\text{OTf})$, the triflate ion binds to the metal ($\text{Ta-O} = 2.243$ Å) at the expense of amine nitrogen donor binding ($\text{Ta-N} = 2.536$ Å).¹⁶¹

Attempts to synthesize a methyldiene complex by deprotonation of cationic $\{[\text{Ar}^{\text{F}}\text{N}_2\text{NH}]\text{TaMe}_2\}^+$ were not successful, presumably because the methyl protons are less acidic

than those in the tantalocene complexes.¹⁴³ However, the synthesis of diamido/donor tantalum complexes that contain a metal–ligand double bond should be possible. We have shown that in $[\text{Ar}^{\text{F}}\text{N}_2\text{N}]\text{TaMe}(\text{NMe}_2)$ the dimethylamide ligand binds to the tantalum center with a bond order presumably greater than one. According to NMR data, the π orbital on this nitrogen does not lie on the TaN_2C equatorial plane. The structural data of $[(\text{Et}_3\text{SiNCH}_2\text{CH}_2)_2\text{N}]\text{TaEt}[\text{N}(\text{CH}=\text{CH}_2)(\text{SiEt}_3)]$ ¹²⁰ reveals that the nitrogen p_π orbital is probably perpendicular to the two σ frontier orbitals for the TaN_3 fragment. A set of proposed frontier orbitals is shown in Scheme 2.3, in which the σ bonding can involve either $d_{z^2} + p_x$ or $d_{z^2} + d_{xz}$ depending on whether the d_{xz} is used for π bonding to the N_{eq} in the tridentate amido ligand. In either case, the π orbital (d_{yz}) is perpendicular to the plane that contains the two σ orbitals, i.e., $p_x(\sigma)$ or $d_{xz}(\sigma)$. The difference with metallocene chemistry thus becomes significant. The three frontier orbitals in bent metallocenes lie on the same plane that bisects the Cp_2M wedge.¹⁶²



Scheme 2.3. Proposed frontier orbitals for $[\text{RN}_2\text{N}]\text{Ta}$ and $[\text{RN}_2\text{NH}]\text{Ta}^+$ fragment in trigonal bipyramidal complexes.

Catalytic polymerization may be understood by electron count of the cationic species. The stability of $\{[\text{ArylN}_2\text{L}]\text{TaMe}_2\}^+$ ($\text{Aryl} = \text{Ar}^{\text{F}}, \text{Ph}, \text{Ar}; \text{L} = \text{O}, \text{NH}$) species perhaps accounts for their being inactive for α -olefin polymerization. $\{[\text{ArylN}_2\text{L}]\text{TaMe}_2\}^+$ is a twelve electron species if only one significant π bond is invoked from the diamido/donor ligand. They are isoelectronic with all neutral dialkyl or cationic monoalkyl monosolvate group 4 complexes that contain diamido/donor ligands. It has been shown that twelve electron monoalkyl group 4 cations must

lose a base to yield a ten electron active species for α -olefin polymerization.⁷² Therefore, it may not be surprising that the cationic tantalum complexes reported here are not active catalysts since there are no potentially labile ligands present. In addition, the coordination of α -olefins to the cationic metal center is presumably weak as a consequence of the steric crowding of six coordinate olefin adducts and the frontier orbital orientation from the $[\text{ArylN}_2\text{L}]\text{Ta}^+$ fragment ($\text{L} = \text{O}, \text{NH}$).

CONCLUSIONS

A series of tantalum complexes that contain a tridentate amido ligand have been synthesized in both neutral and cationic forms. The ligand family includes trianionic triamido and dianionic diamido/donor (donor = O, NR) ligands. TaMe_5 proved to be a general and convenient starting material for this study. Direct synthesis involving metal halides, neutral ligands, and alkyl Grignard/lithium is another important entry into group 5 chemistry, particularly for niobium.

The nature of the ancillary ligands is proven to be vital in this study. Non-aromatic derivatives such as $[\text{t-BuN}_2\text{O}]^{2-}$ and $[\text{AdN}_2\text{O}]^{2-}$ do not afford significant chemistry as compared to their aromatic counterparts such as $[\text{PhN}_2\text{O}]^{2-}$ and $[\text{ArN}_2\text{O}]^{2-}$. Trimethyl $[\text{t-BuN}_2\text{O}]\text{TaMe}_3$ and $[\text{AdN}_2\text{O}]\text{TaMe}_3$ are far less stable than their arylated analogues. In spite of essentially the same steric bulk between $[\text{t-BuN}_2\text{O}]^{2-}$ and $[\text{t-BuNON}]^{2-}$,^{52,53} the electronic property of the former significantly limits the synthesis of its group 4 and 5 complexes.

Trigonal bipyramid is a general type of structure for all neutral or cationic dialkyl tantalum complexes. The π bonding in these trigonal bipyramidal complexes is briefly discussed by employing structural and NMR data. The frontier orbitals for the TaN_3 fragment are different from those in bent metallocenes,¹⁶² particularly in the orientation of the π orbitals. The stable cationic tantalum complexes reported here constitute a new group of tantalum(V) cations which is outside the cyclopentadienyl class. In view of the search for non-cyclopentadienyl ligand systems related to metallocene chemistry, the diamido/donor ligands are beneficial at this standpoint.

EXPERIMENTAL SECTION

General Procedures. Unless otherwise specified, all experiments were performed under nitrogen in a Vacuum Atmospheres glovebox (model HE-493) equipped with a regeneration/circulation device (Dri-Train) or by using standard Schlenk techniques. Oxygen level (< 2 ppm) were monitored with ZnEt_2 (1 M solution in hexane, Aldrich), and water levels (< 2 ppm) were monitored with TiCl_4 (neat, Strem). All solvents were reagent grade or better. Toluene and 1,2-dimethoxyethane were distilled from sodium/benzophenone ketyl. Diethyl ether and tetrahydrofuran were sparged with nitrogen and passed through two columns of activated alumina. Pentane was sparged with nitrogen, and passed through one column of activated alumina followed by another column of activated Q5.¹⁰⁰ Dichloromethane was distilled from CaH_2 under nitrogen. Molecular sieves and Celite were activated *in vacuo* (10^{-3} Torr) for 24 hours at 175 and 125 °C, respectively. All dry solvents were degassed with nitrogen before introduction into the glovebox, where they were stored over activated 4 Å molecular sieves. All NMR solvents were sparged with nitrogen and dried over activated 4 Å molecular sieves for days prior to use.

Spectroscopic Analyses. The NMR spectra were recorded on Varian instruments (^1H , 500.2 or 300.0 MHz; ^{19}F , 470.6 or 282.1 MHz; ^{13}C , 125.8 or 75.4 MHz; ^{31}P , 121.5 MHz). Chemical shifts (δ) are listed as parts per million downfield from tetramethylsilane and coupling constants (J) are in hertz. ^1H NMR spectra are referenced using the residual solvent peak at δ 7.16 for C_6D_6 , δ 7.27 for CDCl_3 , δ 7.29 for $\text{C}_6\text{D}_5\text{Br}$ (the most upfield resonance), δ 5.32 for CD_2Cl_2 , δ 2.09 for toluene- d_8 (the most downfield resonance), and δ 2.05 for CD_3COCD_3 . ^{13}C NMR spectra are referenced using the residual solvent peak at δ 128.39 for C_6D_6 , δ 77.23 for CDCl_3 , δ 54.00 for CD_2Cl_2 , δ 137.86 for toluene- d_8 (the most downfield resonance), and δ 29.92 for CD_3COCD_3 (the upfield resonance). ^{19}F NMR spectra are externally referenced using a chloroform solution of CFCl_3 at δ 0. ^{31}P NMR spectra are externally referenced using a benzene solution of PPh_3 at δ -4.78. Routine coupling constants are not listed. All NMR spectra were recorded at room temperature unless noted otherwise. IR spectra were recorded as films in specified solvents between NaCl plates on Perkin Elmer 1600 FTIR spectrometer. High resolution

mass spectra were recorded on a Finnigan MAT 8200 Sector Mass Spectrometer at the MIT Department of Chemistry Instrumentation Facility. Elemental analyses were performed in our laboratory on a Perkin Elmer 2400 CHN analyzer or by H. Kolbe Mikroanalytisches Laboratorium, Mülheim an der Ruhr, Germany.

Starting materials. $\text{H}_2[\text{ArN}_2\text{O}]$,^{71,72} $\text{NbCl}_4(\text{THF})_2$,¹⁴¹ TaMe_3Cl_2 ,^{133,134} and TaMe_5 ^{131,132} were prepared according to the literature procedures. The synthesis procedure for $\text{H}_2[\text{MesN}_2\text{NH}]$ was described in Chapter 3. $[\text{HNMe}_2\text{Ph}][\text{B}(\text{C}_6\text{F}_5)_4]$ and $[\text{Ph}_3\text{C}][\text{B}(\text{C}_6\text{F}_5)_4]$ were provided by Exxon Chemical Corporation. All other chemicals were purchased from commercial suppliers. MeLi was titrated with *i*-PrOH by employing 1,10-phenanthroline as an indicator. Aniline, 1,4-dioxane, and triethylamine were sparged with nitrogen and dried over activated 4 Å molecular sieves for days prior to use. All other chemicals were used as received.

E.2.1 $[\text{MesN}_2\text{N}]^{3-}$ ligand system.

$[\text{MesN}_2\text{N}]\text{TaMe}_2$. Method A: A diethyl ether solution of TaMe_5 was prepared *in situ* as follows: MeLi (0.29 mL, 2.12 M in diethyl ether, 0.615 mmol, 2 equiv.) was added to a diethyl ether solution (3 mL) of TaMe_3Cl_2 (91 mg, 0.306 mmol) at -30 °C. The formation of TaMe_5 was judged by the observation of LiCl precipitation from the diethyl ether solution. The temperature of TaMe_5 solution was carefully maintained below 0 °C to avoid rapid decomposition. (A dark solution with black precipitates was typically observed if TaMe_5 decomposed in diethyl ether.) To the TaMe_5 solution at -30 °C was added a diethyl ether solution (4 mL) of $\text{H}_2[\text{MesN}_2\text{NH}]$ (104 mg, 0.306 mmol) at -30 °C. The reaction solution was stirred at room temperature overnight (~19 h) and filtered through Celite to remove LiCl. The filtrate was concentrated *in vacuo* until the volume was ~1 mL. Pentane (~1 mL) was layered on top and the solution was cooled to -30 °C to give an orange crystalline solid. The supernatant was decanted and the orange solid was dried *in vacuo*; yield 147 mg (88%). **Method B:** Cold diethyl ether (3 mL, -30 °C) was added to a solid mixture of TaCl_5 (106 mg, 0.296 mmol) and $\text{H}_2[\text{MesN}_2\text{NH}]$ (100 mg, 0.295 mmol) at -30 °C.

The reaction mixture was stirred at room temperature for 1 h to give an off-white thick slurry. The slurry was cooled to $-30\text{ }^{\circ}\text{C}$ and MeLi (1.08 mL, 1.4 M in diethyl ether, 1.512 mmol, 5.1 equiv.) or MeMgI (0.71 mL, 2.12 M in diethyl ether, 1.505 mmol, 5.1 equiv.) was added. Gas evolution was observed. The reaction mixture was stirred at room temperature overnight (~ 21 h). Insoluble materials were removed by filtration with Celite and washed with diethyl ether (2 mL). The filtrate was concentrated *in vacuo* to give an orange crystalline solid; yield 63 mg (39%). **Method C:** Analogous to Method B except the adduct $\{\text{H}_2[\text{MesN}_2\text{NH}]\}\text{TaCl}_5$ was prepared and isolated from a mixture of TaCl_5 (106 mg, 0.296 mmol) and $\text{H}_2[\text{MesN}_2\text{NH}]$ (100 mg, 0.295 mmol) in toluene (10 mL) at $80\text{ }^{\circ}\text{C}$ for 12 h. MeLi was added to a diethyl ether suspension of $\{\text{H}_2[\text{MesN}_2\text{NH}]\}\text{TaCl}_5$; yield 149 mg (92%): ^1H NMR (C_6D_6) δ 6.83 (s, 4, Aryl), 4.14 (t, 4, NCH_2), 4.02 (t, 4, NCH_2), 2.35 (s, 12, Me_o), 2.10 (s, 6, Me_p), 0.63 (s, 6, TaMe); ^{13}C NMR (C_6D_6) δ 145.80 (C, Aryl), 136.11 (C, Aryl), 135.57 (C, Aryl), 130.43 (CH, Aryl), 66.18 (TaMe), 63.52 (NCH_2), 62.45 (NCH_2), 21.29 (Me_p), 18.95 (Me_o). Anal. Calcd. for $\text{C}_{24}\text{H}_{36}\text{N}_3\text{Ta}$: C, 52.65; H, 6.63; N, 7.67. Found: C, 52.49; H, 6.57; N, 7.53.

[MesN₂N]NbMe₂. Method A: Cold diethyl ether (3 mL, $-30\text{ }^{\circ}\text{C}$) was added to a solid mixture of $\text{H}_2[\text{MesN}_2\text{NH}]$ (99 mg, 0.292 mmol) and NbCl_5 (79 mg, 0.292 mmol) at $-30\text{ }^{\circ}\text{C}$ to give a homogeneous dark brown solution. The solution was stirred at room temperature and dark solid precipitated after 10 min. After being stirred for 2 h, the reaction mixture was cooled to $-30\text{ }^{\circ}\text{C}$ and MeMgI (0.49 mL, 3 M in diethyl ether, 1.470 mmol, 5 equiv.) was added. The reaction mixture was stirred at room temperature for 4 h and 1,4-dioxane (5 drops) was added. Insoluble materials were removed by filtration through Celite. The filtrate was concentrated *in vacuo* until the volume was ~ 1 mL. The concentrated solution was cooled to $-30\text{ }^{\circ}\text{C}$ to give blood red crystals. The supernatant was decanted and the crystals were dried *in vacuo*; yield 60 mg (45%). **Method B:** A mixture of diethyl ether (3 mL) and THF (1 mL) at $-30\text{ }^{\circ}\text{C}$ was added to a solid mixture of $\text{H}_2[\text{MesN}_2\text{NH}]$ (99 mg, 0.292 mmol) and $\text{NbCl}_4(\text{THF})_2$ (110 mg, 0.290 mmol) at $-30\text{ }^{\circ}\text{C}$. The brown solution was stirred at room temperature for 1.5 h and cooled to $-30\text{ }^{\circ}\text{C}$. MeMgI (0.39 mL, 3 M in diethyl ether, 1.17 mmol, 4 equiv.) was added to this cold solution.

Gas evolution was observed and the solution immediately turned deep red along with solid precipitation. The reaction mixture was stirred at room temperature for 3 h. All volatile components were removed *in vacuo*. The residue was treated with diethyl ether (5 mL) and 1,4-dioxane (5 drops). Insoluble materials were removed by filtration through Celite. The filtrate was concentrated *in vacuo* until the volume was ~1 mL and cooled to -30 °C overnight to give blood red crystals; yield 14 mg (10%): ^1H NMR (C_6D_6) δ 6.81 (s, 4, Aryl), 3.98 (s, 8, NCH_2), 2.33 (s, 12, Me_O), 2.08 (s, 6, Me_P), 0.81 (s, 6, NbMe); ^{13}C NMR (C_6D_6) δ 146.14 (C, Aryl), 136.09 (C, Aryl), 135.74 (C, Aryl), 130.43 (CH, Aryl), 65.06 (NCH_2), 62.86 (NCH_2), 21.30 (Me_P), 19.05 (Me_O), NbMe not found. Anal. Calcd. for $\text{C}_{24}\text{H}_{36}\text{N}_3\text{Nb}$: C, 62.74; H, 7.90; N, 9.15. Found: C, 62.59; H, 7.78; N, 9.06.

E.2.2 $[\text{RN}_2\text{O}]^{2-}$ ligand system (R = alkyl, aryl).

$\text{O}[\text{CH}_2\text{C}(\text{O})\text{NH}(\text{t-Bu})]_2$. A 500 mL one-neck round-bottom flask was charged with a THF solution (150 mL) of $\text{O}[\text{CH}_2\text{C}(\text{O})\text{Cl}]_2$ (16.977 g, 0.099 mol). The solution was cooled to 0 °C. A mixture of NEt_3 (20.095 g, 0.199 mol, 2 equiv.) and t-BuNH_2 (14.524 g, 0.199 mol, 2 equiv.) in THF (30 mL) was transferred to the diglycolyl chloride solution *via* a cannula. An exothermic reaction occurred and a large amount of white solid formed immediately. After the heat subsided, the reaction mixture was stirred at room temperature for an additional 12 h. The white solid was removed by filtration using a coarse frit and washed with THF (25 mL x 2). The filtrate was evaporated on a rotary evaporator and dried *in vacuo* to give a light yellow oil which solidified at room temperature upon standing; yield 24.26 g (100%): ^1H NMR (CDCl_3) δ 6.27 (br s, 2, NH), 3.86 (s, 4, OCH_2), 1.33 (s, 18, NCMe_3); ^{13}C NMR (CDCl_3) δ 167.72 (CO), 71.53 (OCH_2), 51.28 (NCMe_3), 28.86 (NCMe_3).

$\text{H}_2[\text{t-BuN}_2\text{O}]$. To a suspension of LiAlH_4 (19.471 g, 0.513 mol, 5.23 equiv.) in DME (200 mL) at 0 °C was added a solution of $\text{O}[\text{CH}_2\text{C}(\text{O})\text{NH}(\text{t-Bu})]_2$ (23.880 g, 0.098 mol) in DME (50 mL) at a rate such that gas evolution was under control. After heat and gas evolution subsided,

the ice bath was removed and the solution was heated to refluxing for 25 h under nitrogen. The reaction mixture was cooled to room temperature and poured into an empty 1 L beaker. The mixture was quenched by sequential addition of deionized water (20 mL), 15% aqueous NaOH solution (20 mL), and deionized water (60 mL) at a rate such that gas evolution was under control. The gray solid thus generated was removed by filtration and washed with CHCl_3 (40 mL x 2). The filtrate was dried over MgSO_4 and filtered. All volatile components were removed from the filtrate on a rotary evaporator and the residue was dried over CaH_2 in refluxing toluene. All insoluble components were removed by filtration. Colorless crystals were obtained by sublimation of the toluene filtrate ($23^\circ\text{C}/80\text{ mTorr}$) on a cold surface (temperature $< -15^\circ\text{C}$). Yield varied (23-30%) depending on the effectiveness of sublimation: IR (THF): NH(st) 3463 cm^{-1} ; ^1H NMR (CDCl_3) δ 3.53 (t, 4, OCH_2), 2.59 (t, 4, NCH_2), 1.01 (s, 18, NCMe_3), NH not found; ^1H NMR (toluene- d_8) δ 3.48 (t, 4, OCH_2), 2.43 (t, 4, NCH_2), 0.93 (s, 18, NCMe_3), NH not found; ^1H NMR (C_6D_6) δ 3.48 (t, 4, OCH_2), 2.41 (t, 4, NCH_2), 0.99 (s, 18, NCMe_3), NH not found; ^{13}C NMR (CDCl_3) δ 61.48 (OCH_2), 50.24 (NCMe_3), 44.17 (NCH_2), 29.02 (NCMe_3).

$\text{O}[\text{CH}_2\text{C}(\text{O})\text{NHAd}]_2$. A 300 mL one-neck round-bottom flask was charged with a THF solution (100 mL) of $\text{O}[\text{CH}_2\text{C}(\text{O})\text{Cl}]_2$ (6.132 g, 35.864 mmol). The solution was cooled to 0°C . A mixture of NEt_3 (7.258 g, 71.728 mmol, 2 equiv.) and 1-adamantanamine (10.849 g, 71.728 mmol, 2 equiv.) in THF (60 mL) was transferred to the diglycolyl chloride solution *via* a cannula. An exothermic reaction occurred immediately and a large amount of white solid formed. After the heat subsided, the reaction mixture was stirred at room temperature for an additional 12 h. The white solid was removed by filtration using a coarse frit and washed with THF (15 mL x 2). The solvent was removed *in vacuo*. The product was obtained as a light yellow oil which solidified at room temperature upon standing; yield 14.35 g (99%): ^1H NMR (CDCl_3): 6.06 (br s, 2, NH), 3.91 (s, 4, OCH_2), 2.11 (br s, 6, Ad), 2.03 (br s, 12, Ad), 1.70 (br s, 12, Ad); ^{13}C NMR (CDCl_3): 167.37 (CO), 71.24 (OCH_2), 51.86 (C, Ad), 41.55 (CH_2 , Ad), 36.21 (CH_2 , Ad), 28.35 (CH, Ad). HRMS (EI, 70 eV): m/z calcd. for $\text{C}_{14}\text{H}_{21}\text{N}_2\text{O}_3$ 400.272593, found 400.27246.

H₂[AdN₂O]. To a suspension of LiAlH₄ (7.100 g, 0.187 mol, 5.2 equiv.) in DME (100 mL) at 0 °C was added solid O[CH₂C(O)NHAd]₂ (14.36 g, 0.036 mol) at a rate such that gas evolution was under control. After heat and gas evolution subsided, the ice bath was removed and the solution was heated to refluxing for 24 h under nitrogen. The reaction mixture was cooled to room temperature and poured into an empty 1 L beaker. The reaction was quenched by sequential addition of deionized water (7.1 mL), 15% aqueous NaOH solution (7.1 mL), and deionized water (21.3 mL) at a rate such that gas evolution was under control. The gray solid thus obtained was removed by filtration and washed with CHCl₃ (20 mL x 2). The CHCl₃ solution was dried over MgSO₄ and filtered. All volatile components were evaporated and the resulting residue was dried over CaH₂ in refluxing toluene. All insoluble components were removed by filtration and the solvent was removed *in vacuo* until the volume was ~10 mL. Pentane (50 mL) was added to precipitate a white solid which was collected by filtration and washed with pentane; yield 4.12 g (31%): IR (THF): NH(st) 3503 cm⁻¹; ¹H NMR (C₆D₆) δ 3.43 (t, 4, OCH₂), 2.43 (t, 4, NCH₂), 1.92 (br s, 6, Ad), 1.58-1.41 (m, 24, Ad), NH not found; ¹H NMR (toluene-*d*₈) δ 3.40 (t, 4, CH₂), 2.42 (t, 4, CH₂), 1.90-1.39 (m, 30, Ad), NH not found; ¹H NMR (CDCl₃) δ 3.56 (t, 4, OCH₂), 2.68 (t, 4, NCH₂), 2.02 (br s, 6, Ad), 1.64-1.46 (m, 24, Ad), NH not found; ¹H NMR (CD₂Cl₂) δ 3.47 (t, 4, OCH₂), 2.70 (t, 4, NCH₂), 2.04 (br s, 6, Ad), 1.68-1.60 (m, 24, Ad), NH not found; ¹³C NMR (CDCl₃) δ 61.94 (OCH₂), 41.99 (NCH₂), 50.40 (NC, Ad), 43.11 (CH₂, Ad), 36.91 (CH₂, Ad), 29.77 (CH, Ad).

O[CH₂C(O)NH(i-Pr)]₂. To a THF solution (60 mL) of O[CH₂C(O)Cl]₂ (4.012 g, 23.465 mmol) at -35 °C was added a cold mixture of NEt₃ (4.749 g, 46.929 mmol, 2 equiv.) and i-PrNH₂ (2.774 g, 46.929 mmol, 2 equiv.) in THF (10 mL) at -35 °C. The reaction mixture was stirred at room temperature for an additional 4 h. White solid was removed by filtration using a coarse frit and washed with THF (25 mL x 3). The solvent was evaporated from the filtrate to give an off-white solid; yield 5.06 g (100%): ¹H NMR (CDCl₃) δ 6.41 (br s, 2, NH), 4.12 (septet, 2, CHMe₂), 3.99 (s, 4, OCH₂), 1.17 (d, 12, CHMe₂).

H₂[i-PrN₂O]. This compound was prepared from O[CH₂C(O)NH(i-Pr)]₂ and LiAlH₄ in a manner similar to that of H₂[t-BuN₂O] or H₂[AdN₂O] except in refluxing THF for 26 h; yield 28%: ¹H NMR (CDCl₃) δ 3.56 (t, 4, OCH₂), 2.80 (septet, 2, CHMe₂), 2.77 (t, 4, NCH₂), 1.06 (d, 12, CHMe₂), NH not found.

O[CH₂C(O)NHPh]₂. To a THF solution (20 mL) of O[CH₂C(O)Cl]₂ (512 mg, 3.817 mmol) was sequentially added a THF solution (15 mL) of N,N'-dicyclohexylcarbodiimide (1.575 g, 7.633 mmol, 2 equiv.) and a THF solution (10 mL) of aniline (711 mg, 7.633 mmol, 2 equiv.) with stirring at room temperature. An exothermic reaction occurred during addition of aniline. After being stirred at room temperature for 18 h, the reaction mixture was filtered with a fritted funnel. The filtrate was concentrated on a rotary evaporator and the solvent was completely removed *in vacuo* to give an off-white solid; yield 1.07 g (98 %): ¹H NMR (CD₃COCD₃) δ 9.64 (br s, 2, NH), 7.75 (d, 4, H_O), 7.33 (t, 4, H_m), 7.10 (t, 2, H_p), 4.32 (s, 4, OCH₂).

H₂[PhN₂O]. LiAlH₄ (763 mg, 20.119 mmol, 5.2 equiv.) was slowly added to a stirred diethyl ether solution (40 mL) of O[CH₂C(O)NHPh]₂ (1.10 g, 3.869 mmol) at 0 °C. The addition was controlled at a rate such that gas evolution was mild. The reaction mixture was stirred at room temperature for 18 h and quenched by addition of saturated aqueous NaHCO₃ solution (200 mL) in the presence of crushed ice (~100 mL). The mixture was filtered and the filtrate was extracted with diethyl ether (200 mL). The extract was dried over MgSO₄ and filtered. The solvent was removed *in vacuo* to give a yellow oil; yield 630 mg (63%): ¹H NMR (CD₃COCD₃) δ 7.09 (t, 4, H_m), 6.64 (d, 4, H_O), 6.58 (t, 2, H_p), 4.86 (br s, 2, NH), 3.67 (t, 4, OCH₂), 3.28 (q, 4, NCH₂); ¹H NMR (CDCl₃) δ 7.19 (t, 4, H_m), 6.73 (t, 2, H_p), 6.64 (d, 4, H_O), 3.94 (br s, 2, NH), 3.71 (t, 4, OCH₂), 3.33 (t, 4H, NCH₂); ¹³C NMR (C₆D₆) δ 149.0 (C_{ipso}), 129.9 (C_m), 118.2 (C_p), 113.7 (C_O), 69.9 (OCH₂), 44.0 (NCH₂). HRMS (EI, 70 eV): *m/z* calcd. for C₁₆H₂₀N₂O 256.157563, found 256.15765.

O[CH₂C(O)NH(2-t-Bu-C₆H₄)]₂. To a THF solution (40 mL) of O[CH₂C(O)Cl]₂ (3.016 g, 17.639 mmol) at -35 °C was added a mixture of NEt₃ (3.570 g, 35.279 mmol, 2 equiv.) and 2-tert-butylaniline (5.265 g, 35.279 mmol, 2 equiv.) in THF (10 mL). The reaction mixture

was stirred at room temperature for an additional 30 min. White solid was removed by filtration using a coarse frit and washed with THF (25 mL x 3). The solvent was evaporated from the filtrate to give a light-yellow oil which solidified at room temperature upon standing; yield 6.95 g (99%): ^1H NMR (CDCl_3) δ 8.64 (br s, 2, NH), 7.99 (d, 2, Aryl), 7.70 (d, 2, Aryl), 7.55 (t, 2, Aryl), 7.48 (t, 2, Aryl), 4.66 (s, 4, OCH_2), 1.70 (s, 18, CMe_3); ^{13}C NMR (CDCl_3) δ 166.53 (CO), 142.46 (C_{ipso}), 134.19 (C-t-Bu, Aryl), 127.22 (CH, Aryl), 127.01 (CH, Aryl), 126.81 (CH, Aryl), 126.57 (CH, Aryl), 71.99 (OCH_2), 34.63 (CMe_3), 30.75 (CMe_3).

$\text{H}_2[(2\text{-t-Bu-C}_6\text{H}_4)\text{N}_2\text{O}]$. This compound was prepared from $\text{O}[\text{CH}_2\text{C}(\text{O})\text{NH}(2\text{-t-Bu-C}_6\text{H}_4)]_2$ (6.71 g, 0.017 mol) and LiAlH_4 (3.40 g, 0.090 mol, 5.3 equiv.) in a manner similar to that of $\text{H}_2[\text{t-BuN}_2\text{O}]$ or $\text{H}_2[\text{AdN}_2\text{O}]$ except in refluxing THF (100 mL) for 20 h. After work-up the oily residue was purified by vacuum distillation. The product was obtained as a red viscous oil (180 °C/140 mTorr); yield 2.48 g (40%): ^1H NMR (CD_3COCD_3) δ 7.17 (d, 2, Aryl), 7.05 (t, 2, Aryl), 6.69 (d, 2, Aryl), 6.61 (t, 2, Aryl), 4.47 (br s, 2, NH), 3.84 (t, 4, OCH_2), 3.38 (t, 4, NCH_2), 1.38 (s, 18, CMe_3); ^{13}C NMR (CD_3COCD_3) δ 147.39 (C_{ipso}), 134.08 (C^tBu , Aryl), 127.80 (CH, Aryl), 126.75 (CH, Aryl), 117.80 (CH, Aryl), 112.71 (CH, Aryl), 69.94 (OCH_2), 44.68 (NCH_2), 34.68 (CMe_3), 30.13 (CMe_3). HRMS (EI, 70eV): m/z calcd. for $\text{C}_{24}\text{H}_{36}\text{N}_2\text{O}$ 368.282764, found 368.28290.

$\text{O}\{\text{CH}_2\text{C}(\text{O})\text{NH}[3,5\text{-C}_6\text{H}_3(\text{CF}_3)_2]\}_2$. A 250 mL one-neck round-bottom flask was charged with a THF solution (40 mL) of $\text{O}[\text{CH}_2\text{C}(\text{O})\text{Cl}]_2$ (8.205 g, 0.048 mol) and cooled to 0 °C. A mixture of NEt_3 (9.712 g, 0.096 mol, 2 equiv.) and 3,5-bis(trifluoromethyl)aniline (21.991 g, 0.096 mol, 2 equiv.) in THF (40 mL) was transferred to the diglycolyl chloride solution *via* a cannula. An exothermic reaction occurred and a large amount of white solid formed immediately. After the heat subsided, the reaction mixture was stirred at room temperature for an additional 12 h. White solid was removed by filtration using a coarse frit and washed with THF (30 mL x 2). The solvent was removed *in vacuo*. The off-white solid thus obtained was washed with diethyl ether (25 mL x 2) to give a snow-white solid; yield 16.12 g (60%): ^1H NMR (CD_3COCD_3) δ 10.44 (br s, 2, NH), 8.50 (s, 4, H_O), 7.76 (s, 2, H_p), 4.47 (s, 4, OCH_2); ^{13}C

NMR (CDCl_3) δ 169.13 (CO), 139.85 (C_{ipso}), 131.84 (CCF_3 , Aryl, $^2J_{\text{CF}} = 31$), 123.40 (CF_3 , $^1J_{\text{CF}} = 272$), 120.24 (CH, Aryl), 117.35 (CH, Aryl), 72.50 (OCH_2). HRMS (EI, 70 eV): m/z calcd. for $\text{C}_{20}\text{H}_{12}\text{F}_{12}\text{N}_2\text{O}_3$ 556.065631, found 556.0650.

$\text{O}[\text{CH}_2\text{C}(\text{O})\text{NHAr}^{\text{F}}]_2$. A 250 mL one-necked round-bottom flask was sequentially charged with $\text{O}[\text{CH}_2\text{C}(\text{O})\text{Cl}]_2$ (3.450 g, 20.180 mmol), acetonitrile (100 mL), pentafluoroaniline (7.389 g, 40.359 mmol, 2 equiv.), and K_2CO_3 (5.578 g, 40.359 mmol, 2 equiv.). The flask was equipped with a condenser and the solution was heated to refluxing for 45 min. The reaction mixture was cooled to room temperature and deionized water (200 mL) was added. Organic compounds were extracted with diethyl ether (150 mL), washed with saturated aqueous NaCl solution (~50 mL), and dried over MgSO_4 . The MgSO_4 was removed by filtration and the solvent was evaporated. The residue was washed with diethyl ether (10 mL x 2) to give an off-white solid which was dried *in vacuo*; yield 5.795 g (62%): ^1H NMR (CD_3COCD_3) δ 9.43 (br s, 2, NH), 4.51 (s, 4, OCH_2); ^{19}F NMR (CD_3COCD_3) δ -147.69 (d, 4, F_O), -160.62 (t, 2, F_p), -166.70 (t, 4, F_m); ^{13}C NMR (CD_3COCD_3) δ 168.95 (CO), 144.17 (C_O , $^1J_{\text{CF}} = 248$), 140.74 (C_p , $^1J_{\text{CF}} = 250$), 138.51 (C_m , $^1J_{\text{CF}} = 247$), 112.95 (C_{ipso}), 71.58 (OCH_2). HRMS (EI, 70 eV): m/z calcd. for $\text{C}_{16}\text{H}_6\text{F}_{10}\text{N}_2\text{O}_3$ 464.021875, found 464.02184.

$[\text{t-BuN}_2\text{O}]\text{TaMe}_3$. A diethyl ether solution of TaMe_5 was prepared *in situ* as follows: MeLi (0.85 mL, 1.4 M in diethyl ether, 1.185 mmol, 2 equiv.) was added to a diethyl ether solution (3 mL) of TaMe_3Cl_2 (176 mg, 0.593 mmol) at $-35\text{ }^\circ\text{C}$. The formation of TaMe_5 was judged by the observation of LiCl precipitation from the diethyl ether solution. The temperature of TaMe_5 solution was carefully maintained below $0\text{ }^\circ\text{C}$ to avoid rapid decomposition. (A dark solution with black precipitates was typically observed if TaMe_5 decomposed in diethyl ether.) To the TaMe_5 solution at $-35\text{ }^\circ\text{C}$ was added a diethyl ether solution (3 mL) of $\text{H}_2[\text{t-BuN}_2\text{O}]$ (128 mg, 0.593 mmol) at $-35\text{ }^\circ\text{C}$. The reaction solution was transferred to an air-free Teflon-sealed Schlenk tube and kept in an isothermal bath at $-15\text{ }^\circ\text{C}$ for 14 h; at this moment an aliquot was checked by ^1H NMR spectroscopy which showed quantitative formation of the product. LiCl was removed by filtration through Celite at $\sim 0\text{ }^\circ\text{C}$ to give yellow filtrate. (**Note:** The product decomposes at room

temperature.) All volatile components were removed *in vacuo* and the product was obtained as a yellowish brown oil; yield 192 mg (74%): ^1H NMR (C_6D_6) δ 4.56 (t, 4, OCH_2), 2.79 (dt, 4, NCH_2), 1.06 (s, 18, NCMe_3), 0.47 (s, 9, TaMe); ^{13}C NMR (C_6D_6) δ 73.76 (OCH_2), 52.34 (NCMe_3), 50.36 (NCMe_3), 45.72 (NCH_2), 29.75 (TaMe).

[AdN₂O]TaMe₃. A diethyl ether solution of TaMe_5 was prepared *in situ* (as described above in the preparation of $[\text{t-BuN}_2\text{O}]\text{TaMe}_3$) from a diethyl ether solution (3 mL) of TaMe_3Cl_2 (90 mg, 0.303 mmol) and MeLi (0.44 mL, 1.4 M in diethyl ether, 0.616 mmol, 2.03 equiv.) at $-35\text{ }^\circ\text{C}$. Solid $\text{H}_2[\text{AdN}_2\text{O}]$ (113 mg, 0.303 mmol) was added to the TaMe_5 solution at $-35\text{ }^\circ\text{C}$. The reaction mixture was transferred to an air-free Teflon-sealed Schlenk tube and kept in an isothermal bath at $-5\text{ }^\circ\text{C}$ for 12 h; at this moment an aliquot was analyzed by ^1H NMR spectroscopy which showed quantitative formation of $[\text{AdN}_2\text{O}]\text{TaMe}_3$. The reaction solution was filtered through Celite at $\sim 0\text{ }^\circ\text{C}$ to give colorless filtrate. (**Note:** The product slowly decomposes at room temperature.) The solvent was removed *in vacuo* to give a colorless oil which was pure $[\text{AdN}_2\text{O}]\text{TaMe}_3$ according to its ^1H NMR spectrum; yield 169 mg (94%): ^1H NMR (C_6D_6) δ 4.61 (t, 4, OCH_2), 2.88 (dt, 4, NCH_2), 0.54 (s, 9, TaMe), 1.98 (br s, 6, Ad), 1.65 - 1.58 (m, 24, Ad); ^{13}C NMR (C_6D_6) δ 74.00 (OCH_2), 52.50 (TaMe), 50.56 (NC, Ad), 43.86 (CH_2 , Ad), 43.75 (NCH_2), 37.54 (CH_2 , Ad), 30.48 (CH, Ad).

[PhN₂O]TaMe₃. A diethyl ether solution of TaMe_5 was prepared *in situ* (as described above in the preparation of $[\text{t-BuN}_2\text{O}]\text{TaMe}_3$) from a diethyl ether solution (3 mL) of TaMe_3Cl_2 (297 mg, 1.000 mmol) and MeLi (1.43 mL, 1.4 M in diethyl ether, 2.000 mmol, 2 equiv.) at $-35\text{ }^\circ\text{C}$. To this TaMe_5 solution at $-35\text{ }^\circ\text{C}$ was added a diethyl ether solution (2 mL) of $\text{H}_2[\text{PhN}_2\text{O}]$ (256 mg, 1.000 mmol) at $-35\text{ }^\circ\text{C}$. Insoluble LiCl was removed from the reaction mixture by filtration at $-10\text{ }^\circ\text{C}$. The clear reaction solution was kept at $-35\text{ }^\circ\text{C}$ for several hours to give bright yellow crystals. The supernatant was decanted and the product was dried *in vacuo*. The bright yellow crystals darkened at room temperature after several hours to become yellowish brown surfaced crystals, but no decomposition was observed according to the ^1H NMR spectrum; yield 206 mg (43%): ^1H NMR (C_6D_6) δ 7.17 (t, 4, H_m), 7.10 (d, 4, H_o), 6.92 (t, 2, H_p), 3.64 (t, 4,

OCH₂), 3.33 (t, 4, NCH₂), 1.21 (s, 9, TaMe); ¹³C NMR (C₆D₆) δ 151.08 (C_{ipso}), 129.68 (C_m), 124.60 (C_p), 124.42 (C_o), 73.53 (OCH₂), 62.19 (TaMe), 60.73 (NCH₂). Anal. Calcd. for C₁₉H₂₇N₂OTa: C, 47.51; H, 5.67; N, 5.83. Found: C, 47.38; H, 5.58; N, 5.77.

[ArN₂O]TaMe₃. A diethyl ether solution (10 mL) of H₂[ArN₂O] (1.591 g, 5.092 mmol) at -35 °C was added to a diethyl ether solution of TaMe₅ at -35 °C which was prepared *in situ* (as described above in the preparation of [t-BuN₂O]TaMe₃) from a diethyl ether solution (40 mL) of TaMe₃Cl₂ (1.512 g, 5.092 mmol) and MeLi (7.3 mL, 1.4 M in diethyl ether, 10.183 mmol, 2 equiv.) at -35 °C. The reaction mixture was transferred to an air-free Teflon-sealed reaction tube and kept in an isothermal bath at -5 °C for 41 h. The reaction mixture was filtered through Celite to give yellowish green filtrate. The filtrate was concentrated *in vacuo* until emerald crystalline solid appeared. The concentrated solution (~10 mL) was cooled to -35 °C for several hours to complete the crystallization. The supernatant was decanted and the emerald crystals dried *in vacuo*; yield 2.02 g (74%): ¹H NMR (C₆D₆) δ 7.01 (d, 4, H_m), 6.93 (t, 2, H_p), 3.32 (s, 8, CH₂), 2.31 (s, 12, Me_o), 1.03 (br s, 9, TaMe); ¹H NMR (toluene-*d*₈) δ 6.96 (d, 4, H_m), 6.87 (t, 2, H_p), 3.41 (t, 4, OCH₂), 3.32 (t, 4, NCH₂), 2.29 (s, 12, Me_o), 0.92 (br s, 9, TaMe); ¹³C NMR (toluene-*d*₈) δ 152.11 (C_{ipso}), 134.83 (C_m), 129.47 (C_o), 125.69 (C_p), 73.50 (OCH₂), 67.89 (Me_o), 58.84 (NCH₂), 19.59 (TaMe). Anal. Calcd. for C₂₃H₃₅N₂OTa: C, 51.49; H, 6.58; N, 5.22. Found: C, 51.34; H, 6.46; N, 5.17.

[ArN₂O]TaMe₂I. A diethyl ether solution (2 mL) of element iodine (45 mg, 0.177 mmol) at -35 °C was added to a diethyl ether solution (2 mL) of [ArN₂O]TaMe₃ (97 mg, 0.181 mmol) at -35 °C. The iodine purple color faded immediately and the solution turned cloudy at the end of addition; at this moment yellow precipitate was observed from the reaction solution. The reaction mixture was stirred at room temperature for 20 h. The solvent was removed *in vacuo*. The solid residue was washed with pentane (5 mL) and dried *in vacuo* to give a yellow solid; yield 115 mg (98%): ¹H NMR (C₆D₆) δ 6.96-6.89 (m, 6, Aryl), 3.76 (s, 8, CH₂), 2.54 (br s, 12, Me_o), 1.28 (br s, 6, TaMe); ¹H NMR (CD₂Cl₂) δ 7.13-7.06 (m, 6, Aryl), 4.59 (t, 4, OCH₂), 4.36 (t, 4, NCH₂), 2.52 (s, 12, Me_o), 0.83 (s, 6, TaMe); ¹³C NMR (CD₂Cl₂) δ 147.35 (C_{ipso}),

136.24 (C_o), 129.66 (C_m), 127.17 (C_p), 74.34 (TaMe), 74.01 (OCH_2), 60.67 (NCH_2), 20.92 (Me_o). Anal. Calcd. for $C_{22}H_{32}IN_2OTa$: C, 40.76; H, 4.97; N, 4.32. Found: C, 40.66; H, 5.05; N, 4.22.

[ArN₂O]TaMe₂Cl. An ethereal HCl solution (0.14 mL, 1 M in diethyl ether, 0.14 mmol) was added to a solution of [ArN₂O]TaMe₃ (78 mg, 0.145 mmol) in diethyl ether (4 mL) at -35 °C. The solution turned cloudy and white precipitate was observed within 5 min. The reaction mixture was stirred at room temperature for 20 h and concentrated *in vacuo* until the volume was ~1 mL and a large quantity of white precipitate was formed. The supernatant was decanted. The off-white solid was washed with cold diethyl ether (~2 mL) and dried *in vacuo*; yield 41 mg (51%): ¹H NMR (CD_2Cl_2) δ 7.04 (m, 6, Aryl), 4.63 (m, 2, OCH_2), 4.44 (m, 2, OCH_2), 4.24 (m, 2, NCH_2), 4.02 (m, 2, NCH_2), 2.53 (s, 6, Me_o), 2.29 (s, 6, Me_o), 0.82 (s, 3, TaMe), 0.50 (s, 3, TaMe); ¹H NMR (C_6D_6 with 5 drops of CH_2Cl_2) δ 7.16 (m, 6, Aryl), 4.68 (m, 2, OCH_2), 4.48 (m, 2, OCH_2), 4.23 (m, 2, NCH_2), 4.08 (m, 2, NCH_2), 2.66 (s, 6, Me_o), 2.40 (s, 6, Me_o), 0.99 (s, 3, TaMe), 0.65 (s, 3, TaMe); ¹³C NMR (CD_2Cl_2) δ 146.97 (C, Aryl), 137.87 (C, Aryl), 135.04 (C, Aryl), 129.50 (C_m), 126.93 (C_p), 74.18 (TaMe), 73.46 (OCH_2), 68.26 (TaMe), 60.09 (NCH_2), 20.50 (Me_o), 19.03 (Me_o). Anal. Calcd. for $C_{22}H_{32}ClN_2OTa$: C, 47.45; H, 5.79; N, 5.03. Found: C, 47.53; H, 5.68; N, 4.88.

Observation of {[PhN₂O]TaMe₂}{B(C₆F₅)₄}. A solution of [Ph₃C][B(C₆F₅)₄] (35 mg, 0.0375 mmol) in C_6D_5Br (0.4 mL) at -35 °C was added to a solution of [PhN₂O]TaMe₃ (18 mg, 0.0375 mmol) in C_6D_5Br (0.3 mL) at -35 °C. The mixture was transferred to an NMR tube and analyzed by ¹H NMR spectroscopy within 10 min. The ¹H NMR spectrum showed quantitative formation of the product and Ph₃CMe: ¹H NMR (C_6D_5Br) δ 7.29-7.03 (m, 25, Ph), 4.02 (t, 4, OCH_2), 3.89 (t, 4, NCH_2), 2.01 (s, 3, Ph₃CMe), 0.81 (s, 6, TaMe).

{[PhN₂O]TaMe₂}{MeB(C₆F₅)₃}. A solution of B(C₆F₅)₃ (111 mg, 0.216 mmol) in CH_2Cl_2 (1 mL) at -35 °C was added to a solution of [PhN₂O]TaMe₃ (104 mg, 0.216 mmol) in CH_2Cl_2 (1 mL) at -35 °C. The reaction solution was stirred at room temperature for 10 min. The solvent was removed *in vacuo* to give a brown oil which solidified slow at -35 °C after several

days; yield 209 mg (97%): ^1H NMR (C_6D_6) δ 7.13 (t, 4, H_m), 7.00 (d, 4, H_o), 6.96 (t, 2, H_p), 3.64 (t, 4, OCH_2), 3.40 (t, 4, NCH_2), 1.28 (br s, 3, Me_B), 0.62 (s, 6, TaMe); ^{19}F NMR (C_6D_6) δ -133.32 (d, 6, F_o), -165.11 (t, 3, F_p), -167.84 (t, 6, F_m); ^{19}F NMR (CD_2Cl_2) δ -133.38 (d, 6, F_o), -164.18 (t, 3, F_p), -166.90 (t, 6, F_m). Anal. Calcd. for $\text{C}_{37}\text{H}_{27}\text{BF}_{15}\text{N}_2\text{OTa}$: C, 44.78; H, 2.74; N, 2.82. Found: C, 44.86; H, 2.64; N, 2.90.

Observation of $\{[\text{ArN}_2\text{O}]\text{TaMe}_2\}\{\text{MeB}(\text{C}_6\text{F}_5)_3\}$. A solution of $\text{B}(\text{C}_6\text{F}_5)_3$ (15 mg, 0.0293 mmol) in CD_2Cl_2 (0.4 mL) at -35°C was added to a solution of $[\text{ArN}_2\text{O}]\text{TaMe}_3$ (16 mg, 0.0298 mmol) in CD_2Cl_2 (0.3 mL) at -35°C . The yellowish emerald color faded immediately to give a colorless solution. The reaction solution was transferred to an NMR tube and analyzed by ^1H NMR spectroscopy within 10 min. The ^1H NMR spectrum showed quantitative formation of $\{[\text{ArN}_2\text{O}]\text{TaMe}_2\}\{\text{MeB}(\text{C}_6\text{F}_5)_3\}$. ^1H NMR (CD_2Cl_2) δ 7.30 (s, 6, Aryl), 4.66 (t, 4, OCH_2), 4.49 (t, 4, NCH_2), 2.37 (s, 12, Me_o), 1.08 (s, 6, TaMe), 0.50 (br s, 3, Me_B).

$\{[\text{ArN}_2\text{O}]\text{TaMe}_2\}\{\text{B}(\text{C}_6\text{F}_5)_4\}$. A solution of $[\text{Ph}_3\text{C}][\text{B}(\text{C}_6\text{F}_5)_4]$ (180 mg, 0.196 mmol) in CH_2Cl_2 (2 mL) at -35°C was added to a solution of $[\text{ArN}_2\text{O}]\text{TaMe}_3$ (105 mg, 0.196 mmol) in CH_2Cl_2 (2 mL) at -35°C . The reaction mixture was stirred at room temperature for 10 min; at this moment a reaction aliquot was analyzed by ^1H NMR spectroscopy which showed quantitative formation of product. Solvent was removed *in vacuo*. The greenish solid thus obtained was washed with pentane (5 mL) and dried *in vacuo*; yield 210 mg (89%). Colorless crystalline Ph_3CMe (46 mg, 95%) was obtained from the pentane solution: ^1H NMR (CD_2Cl_2) δ 7.31-7.11 (m, 6, Aryl), 4.66 (t, 4, OCH_2), 4.50 (t, 4, NCH_2), 2.38 (s, 12, Me_o), 1.10 (s, 6, TaMe); ^1H NMR (3 drops of CH_2Cl_2 in 0.7 mL C_6D_6) δ 6.95 (m, 2, Aryl), 6.90 (m, 4, Aryl), 3.54 (s, 8, CH_2), 1.90 (s, 12, Me_o), 0.56 (s, 6, TaMe); ^{19}F NMR (3 drops of CH_2Cl_2 in 0.7 mL C_6D_6) δ -132.70 (d, 8, F_o), -163.03 (t, 4, F_p), -167.08 (t, 8, F_m); ^{13}C NMR (3 drops of CH_2Cl_2 in 0.7 mL C_6D_6) δ 149.32 (C_o , $^1J_{\text{CF}} = 242$, C_6F_5), 139.24 (C_m , $^1J_{\text{CF}} = 240$, C_6F_5), 137.33 (C_p , $^1J_{\text{CF}} = 240$, C_6F_5), 140.34 (NC_{ipso}), 136.81 (C_o , NAryl), 130.68 (C_m , NAryl), 129.45 (C_p , NAryl), 78.93 (OCH_2), 77.34 (NCH_2), 59.53 (TaMe), 18.33 (Me_o), BC_{ipso} not found.

Observation of $\{[\text{ArN}_2\text{O}]\text{TaMe}_2\}\{\text{BF}_4\}$. A solution of $[\text{Ph}_3\text{C}][\text{BF}_4]$ (12 mg, 0.035 mmol) in CD_2Cl_2 (0.4 mL) at $-35\text{ }^\circ\text{C}$ was added to a solution of $[\text{ArN}_2\text{O}]\text{TaMe}_3$ (19 mg, 0.035 mmol) in CD_2Cl_2 (0.3 mL) at $-35\text{ }^\circ\text{C}$. The orange reaction mixture was transferred to an NMR tube and kept at room temperature. The orange color faded within 5 min to become light brown. A room temperature ^1H NMR spectrum was obtained 10 min after the reaction was initiated. The ^1H NMR spectrum showed quantitative formation of $\{[\text{ArN}_2\text{O}]\text{TaMe}_2\}\{\text{BF}_4\}$ and Ph_3CMe : ^1H NMR (CD_2Cl_2) δ 7.30-7.06 (m, 21, Aryl), 4.58 (m, 2, OCH_2), 4.46 (m, 2, OCH_2), 4.33 (m, 2, NCH_2), 4.14 (m, 2, NCH_2), 2.40 (s, 6, Me_O), 2.37 (s, 6, Me_O), 2.18 (s, 6, TaMe), 0.79 (s, 3, Ph_3CMe).

$\{[\text{ArN}_2\text{O}]\text{TaMe}_2\}\{\text{PF}_6\}$. A solution of $[\text{Ph}_3\text{C}][\text{PF}_6]$ (72 mg, 0.185 mmol) in CH_2Cl_2 (4 mL) at $-35\text{ }^\circ\text{C}$ was added to a solution of $[\text{ArN}_2\text{O}]\text{TaMe}_3$ (99 mg, 0.185 mmol) in CH_2Cl_2 (2 mL) at $-35\text{ }^\circ\text{C}$. The reaction mixture was stirred at room temperature for 10 min; at this moment an aliquot was analyzed by ^1H NMR spectroscopy which showed quantitative formation of $\{[\text{ArN}_2\text{O}]\text{TaMe}_2\}\{\text{PF}_6\}$. The solvent was removed *in vacuo* and the solid residue was washed with pentane (2 mL x 3) until it became colorless. The pentane-insoluble material was dried *in vacuo* to give an off-white solid; yield 110 mg (89%). Ph_3CMe (46 mg, 96%) was obtained as a white solid from the pentane solution: ^1H NMR (CD_2Cl_2) δ 7.24 (br s, 6, Aryl), 4.74 (t, 4, OCH_2), 4.46 (t, 4, NCH_2), 2.38 (s, 12, Me_O), 0.99 (s, 6, TaMe); ^{19}F NMR (CD_2Cl_2) δ -73.30 (d, $J_{\text{FP}} = 713.4$); ^{13}C NMR (CD_2Cl_2) δ 141.75 (C_{ipso}), 137.45 (C_O), 130.41 (C_m), 129.10 (C_p), 78.88 (OCH_2), 77.85 (NCH_2), 60.22 (TaMe), 18.78 (Me_O); ^{31}P NMR (CD_2Cl_2) δ -143.90 (septet, $J_{\text{FP}} = 713.4$). Anal. Calcd. for $\text{C}_{22}\text{H}_{32}\text{F}_6\text{N}_2\text{OPTa}$: C, 39.65; H, 4.84; N, 4.20. Found: C, 39.78; H, 4.88; N, 4.11.

E.2.3 $[\text{Ar}^{\text{F}}\text{N}_2\text{NH}]^{2-}$ or $[\text{Ar}^{\text{F}}\text{N}_2\text{N}]^{3-}$ ligand system.[#]

* **$\text{H}_2[\text{Ar}^{\text{F}}\text{N}_2\text{NH}]$.** Hexafluorobenzene (43.7 g, 234 mmol) was added to a mixture of diethylenetriamine (7.34 g, 71.2 mmol) and K_2CO_3 (21.6 g, 156 mmol) in CH_3CN (60 mL). The mixture was heated to refluxing for 20 h under nitrogen. The reaction mixture was cooled to room temperature and water (450 mL) was added. The organic components were extracted with CHCl_3 (3 x 200 mL). The pale yellow extract was dried over MgSO_4 and filtered. The solution was concentrated *in vacuo* to give a yellow oil. The oil was loaded onto an alumina column (5 cm inner diameter x 20 cm height) and eluted with diethyl ether. The first 400 mL of eluent was collected and the diethyl ether was removed *in vacuo*. The thick yellow oil thus obtained was pure product according to the ^1H NMR spectrum. The oil solidified overnight at $-35\text{ }^\circ\text{C}$ to give a waxy solid; yield 13.01 g (42 %): IR (THF): $\text{NH}(\text{st})$ 3371 cm^{-1} (br); ^1H NMR (CDCl_3) δ 4.15 (s, 2, ArylNH), 3.41 (t, 4, CH_2), 2.89 (t, 4, CH_2), 1.07 (s, 1, CH_2NHCH_2); ^1H NMR (C_6D_6) δ 3.84 (s, 2, ArylNH), 2.87 (t, 4, CH_2), 2.15 (t, 4, CH_2), 0.01 (s, 1, CH_2NHCH_2); ^{19}F NMR (CDCl_3) δ -160.45 (d, 4, F_o), -165.21 (t, 4, F_m), -172.40 (t, 2, F_p); ^{13}C NMR (C_6D_6) δ 138.96 (C_o), 138.64 (C_m), 133.72 (C_p), 124.90 (C_{ipso}), 48.79 (CH_2), 45.87 (CH_2). HRMS (EI, 70 eV): m/z calcd. for $\text{C}_{16}\text{H}_{11}\text{F}_{10}\text{N}_3$ 435.079330, found 435.0788.

* **$[\text{Ar}^{\text{F}}\text{N}_2\text{NH}]\text{TaMe}_3$.** A diethyl ether solution of TaMe_5 was prepared *in situ* as follows: MeLi (1.10 mL, 1.4 M in Et_2O , 1.54 mmol, 2 equiv.) was added to a diethyl ether solution (6 mL) of TaMe_3Cl_2 (229 mg, 0.771 mmol) at $-35\text{ }^\circ\text{C}$. The formation of TaMe_5 was judged by the observation of LiCl precipitation from the diethyl ether solution. The temperature of TaMe_5 solution was carefully maintained below $0\text{ }^\circ\text{C}$ to avoid rapid decomposition. (A dark solution with black precipitates was typically observed if TaMe_5 decomposed in diethyl ether.) To the TaMe_5 solution at $-35\text{ }^\circ\text{C}$ was added a diethyl ether solution (2 mL) of $\text{H}_2[\text{Ar}^{\text{F}}\text{N}_2\text{NH}]$ (336 mg, 0.771 mmol) at $-35\text{ }^\circ\text{C}$. The reaction mixture was then stirred at room temperature for 10 min; at this moment an aliquot was analyzed by ^1H and ^{19}F NMR spectroscopy which indicated a quantitative

[#] The compounds denoted with * in this section have been published in print:

Schrock, R. R.; Lee, J.; Liang, L.-C.; Davis, W. M. *Inorg. Chim. Acta* **1998**, 270, 353.

formation of the product. The mixture was filtered through Celite to remove LiCl and the solvent was evaporated to afford a pale yellow crystalline solid; yield 504 mg (99%): ^1H NMR (C_6D_6) δ 3.40 (m, 2, CH_2), 3.04 (m, 2, CH_2), 2.43 (br s, 1, NH), 2.15 (m, 4, CH_2), 0.96 (s, 9, TaMe); ^{19}F NMR (C_6D_6) δ -149.86 (d, 4, F_O), -162.15 (t, 2, F_P), -165.39 (t, 4, F_M); ^{13}C NMR (CD_2Cl_2) δ 144.41 (C_O , $^1J_{\text{CF}} = 244$), 138.76 (C_M , $^1J_{\text{CF}} = 253$), 138.40 (C_P , $^1J_{\text{CF}} = 244$), 130.00 (C_ipso), 69.30 (CH_2), 60.29 (CH_2), 49.20 (TaMe). Anal. Calcd. for $\text{C}_{19}\text{H}_{18}\text{N}_3\text{F}_{10}\text{Ta}$: C, 34.61; H, 2.75; N, 6.37. Found: C, 34.56; H, 2.63; N, 6.38.

* **$[\text{Ar}^{\text{F}}\text{N}_2\text{N}]\text{TaMe}_2$. Method A:** A 100 mL air-free Teflon-sealed reaction vessel was charged with a yellow solution of $[\text{Ar}^{\text{F}}\text{N}_2\text{NH}]\text{TaMe}_3$ (975 mg, 1.479 mmol) in toluene (15 mL). The toluene solution was heated to 65 °C. The solution color gradually changed from yellow to orange. After being heated for 9 h, the orange solution was evaporated to give an orange crystalline solid; yield 886 mg (93%). **Method B:** MeLi (0.07 mL, 1.4 M in diethyl ether, 0.098 mmol, 1.15 equiv.) was added to a diethyl ether solution (3 mL) of $[\text{Ar}^{\text{F}}\text{N}_2\text{NH}]\text{TaMe}_3$ (56 mg, 0.085 mmol) at -30 °C. The solution was stirred at room temperature overnight (~12 h) and Me_3SiCl (0.1 mL, 0.788 mmol, 9.3 equiv.) was added at room temperature with stirring. The reaction mixture turned cloudy within 10 min and LiCl precipitated. After being stirred for 4 h, the reaction mixture was evaporated. The residue was extracted with pentane (5 mL) and the extract was filtered through Celite. The orange filtrate was concentrated *in vacuo* until the volume was ~0.5 mL. The concentrated solution was cooled to -30 °C overnight to give an orange crystalline solid; yield 41 mg (75%). A single crystal of $[\text{Ar}^{\text{F}}\text{N}_2\text{N}]\text{TaMe}_2$ was grown from a mixture of diethyl ether and toluene solution at -35 °C: ^1H NMR (C_6D_6) δ 3.99 (t, 4, CH_2), 3.71 (t, 4, CH_2), 0.63 (quintet, 6, TaMe, $J_{\text{HF}} = 3.6$); ^{19}F NMR (toluene- d_8) δ -150.93 (d, 4, F_O), -164.25 (t, 4, F_M), -164.63 (t, 2, F_P); ^{13}C NMR (CD_2Cl_2) δ 143.33 (C_O , $^1J_{\text{CF}} = 248$), 139.17 (C_M , $^1J_{\text{CF}} = 254$), 138.14 (C_P , $^1J_{\text{CF}} = 255$), 127.44 (C_ipso), 63.75 (TaMe), 63.44 (CH_2), 60.31 (CH_2). Anal. Calcd. for $\text{C}_{18}\text{H}_{14}\text{N}_3\text{F}_{10}\text{Ta}$: C, 33.61; H, 2.19; N, 6.53. Found: C, 33.31; H, 1.97; N, 6.43.

[Ar^FN₂NMe]TaMe₃. MeLi (0.25 mL, 1.4 M in diethyl ether, 0.35 mmol) was added to a diethyl ether solution (10 mL) of [ArN₂NH]TaMe₃ (203 mg, 0.308 mmol) at -35 °C. The reaction mixture was stirred at room temperature overnight. The reddish orange solution was cooled to -35 °C and MeOTf (0.35 mL, 3.093 mmol, 10 equiv.) was added. After being stirred at room temperature for 4 h, the reaction mixture was filtered through Celite. The orange filtrate was concentrated *in vacuo* until the volume was ~1 mL. The concentrated solution was cooled to -35 °C to give a yellow crystalline solid. The supernatant was decanted and the solid was dried *in vacuo*; yield 130 mg (63%): ¹H NMR (C₆D₆) δ 3.50 (m, 2, CH₂), 3.03 (m, 2, CH₂), 2.34 (m, 2, CH₂), 2.14 (s, 3, NMe), 1.99 (m, 2, CH₂), 1.07 (s, 9, TaMe); ¹H NMR (CD₂Cl₂) δ 4.19 (m, 2, CH₂), 3.82 (m, 2, CH₂), 3.47 (m, 2, CH₂), 3.15 (m, 2, CH₂), 3.00 (s, 3, NMe), 0.67 (s, 9, TaMe); ¹⁹F NMR (C₆D₆) δ -149.25 (d, 4, F_O), -161.58 (t, 2, F_p), -164.24 (t, 4, F_m). Anal. Calcd. for C₂₀H₂₀F₁₀N₃Ta: C, 35.68; H, 2.99; N, 6.24. Found: C, 35.78; H, 2.92; N, 6.17.

[Ar^FN₂N]TaMeCl. Method A: A solution of ethereal HCl (3.5 mL, 1 M, 3.5 mmol, 0.96 equiv.) was added to a diethyl ether solution (35 mL) of [Ar^FN₂NH]TaMe₃ (2.397 g, 3.637 mmol) at room temperature. The reaction mixture was stirred for 20 h to afford an orange solution; an aliquot was analyzed by ¹H and ¹⁹F NMR spectroscopy which showed the quantitative formation of [Ar^FN₂N]TaMeCl. The orange solution was filtered through Celite and the filtrate was concentrated *in vacuo* to give an orange crystalline solid. The concentrated solution was cooled to -35 °C for 2 h to facilitate crystallization. The orange crystalline solid was collected by filtration and dried *in vacuo*; yield 1.977 g (85%). **Method B:** Neat Me₃SiCl (0.5 mL, 3.94 mmol, 36.8 equiv.) was added to a diethyl ether solution (2 mL) of [Ar^FN₂N]TaMe₂ (69 mg, 0.107 mmol) at -35 °C. The reaction mixture was stirred at room temperature for 3 days. The solution was concentrated *in vacuo* until the volume was ~1 mL and the concentrated solution was cooled to -35 °C to give an orange crystalline solid. The supernatant was decanted and the orange solid was dried *in vacuo*; yield 57 mg (80%): ¹H NMR (C₆D₆) δ 3.89 (m, 4, CH₂), 3.66 (m, 2, CH₂), 3.32 (m, 2, CH₂), 1.23 (s, 3, TaMe); ¹⁹F NMR (C₆D₆) δ -146.86 (d, 4, F_O), -159.31 (t, 2, F_p), -164.95 (td, 4, F_m); ¹³C NMR (CD₂Cl₂) δ 144.35 (C_O, ¹J_{CF} = 244), 139.85 (C_p, ¹J_{CF} =

238), 138.77 (C_m , $^1J_{CF} = 248$), 127.06 (C_{ipso}), 62.79 (CH_2), 62.32 (CH_2), 47.77 (TaMe). Anal. Calcd. for $C_{17}H_{11}ClF_{10}N_3Ta$: C, 30.77; H, 1.67; N, 6.33. Found: C, 30.56; H, 1.61; N, 6.22.

[Ar^FN₂N]TaMeI. Method A: A diethyl ether solution (2 mL) of element iodine (51 mg, 0.201 mmol) was added dropwise to a diethyl ether solution (4 mL) of [Ar^FN₂N]TaMe₂ (129 mg, 0.201 mmol) at -35 °C with stirring. Upon addition of iodine solution, the orange solution of [Ar^FN₂N]TaMe₂ turned red immediately. The reaction solution was stirred at room temperature and monitored by ¹H and ¹⁹F NMR spectroscopy which showed no [Ar^FN₂N]TaMe₂ signals after 6 h. The solution was concentrated *in vacuo* until the volume was ~2 mL. The concentrated solution was cooled to -35 °C to give a red crystalline solid (123 mg). Recrystallization from a mixture of diethyl ether and toluene afforded analytically pure product; yield 102 mg (67%). **Method B:** A diethyl ether solution (1 mL) of Me₃SiI (48 mg, 0.240 mmol) at -35 °C was added to a diethyl ether solution (6 mL) of [Ar^FN₂N]TaMeCl (159 mg, 0.240 mmol) at -35 °C. The reaction mixture was stirred at room temperature for 20 h. The solution was concentrated *in vacuo* until the volume was ~2 mL. The concentrated solution was cooled to -35 °C to give a red crystalline solid. The supernatant was decanted and the red solid was dried *in vacuo*; yield 110 mg (61%): ¹H NMR (CD₂Cl₂) δ 4.68 (m, 2, CH₂), 4.44 (m, 2, CH₂), 4.33 (m, 2, CH₂), 3.99 (m, 2, CH₂), 0.95 (s, 3, TaMe); ¹H NMR (C₆D₆) δ 3.85 (s, 6, CH₂), 3.19 (m, 2, CH₂), 1.05 (s, 3, TaMe); ¹⁹F NMR (CD₂Cl₂) δ -147.66 (d, 4, F_O), -162.97 (t, 2, F_P), -164.91 (t, 4, F_M); ¹⁹F NMR (C₆D₆) δ -148.07 (d, 4, F_O), -161.84 (t, 2, F_P), -163.76 (t, 4, F_M). Anal. Calcd. for $C_{17}H_{11}N_3F_{10}TaI$: C, 27.04; H, 1.47; N, 5.56. Found: C, 27.35; H, 1.66; N, 5.38.

[Ar^FN₂N]TaMeBn. PhCH₂MgCl (0.45 mL, 1 M in diethyl ether, 0.45 mmol) was added to a diethyl ether solution (5 mL) of [Ar^FN₂N]TaMeCl (301 mg, 0.454 mmol) at -35 °C. The reaction mixture was stirred at room temperature for 16 h. Insoluble materials were removed by filtration through Celite. The reddish orange filtrate was concentrated *in vacuo* until the volume was ~1 mL. The concentrated solution was cooled to -35 °C for 3 h to afford orange microcrystals. The supernatant was decanted and the orange crystalline solid was washed with

cold pentane (1 mL) and dried *in vacuo*; yield 158 mg (49 %): ^1H NMR (CD_2Cl_2) δ 7.16 (t, 2, H_m), 6.69 (t, 1, H_p), 6.60 (d, 2, H_o), 4.44 (m, 4, CH_2), 3.94 (m, 2, CH_2), 3.40 (m, 2, CH_2), 1.88 (quintet, 2, TaCH_2Ph , $J_{\text{HF}} = 5.3$), 0.15 (quintet, 3, TaMe , $J_{\text{HF}} = 6.8$); ^{19}F NMR (C_6D_6) δ -157.6 (br s, 4, F_o), -163.8 (m, 4, F_m), -171.4 (t, 2, F_p); ^{13}C NMR (CD_2Cl_2) δ 143.46 (C_o , $^1J_{\text{CF}} = 259$), 139.63 (C_m , $^1J_{\text{CF}} = 256$), 133.82 (C_p , $^1J_{\text{CF}} = 248$), 129.92, 127.95, 127.70, 127.41, 122.72, 79.93 (CH_2Ph), 64.16 (CH_2), 54.98 (CH_2), 54.18 (TaMe).

* **Observation of $\{[\text{Ar}^{\text{F}}\text{N}_2\text{NH}]\text{TaMe}_2\}\{\text{B}(\text{C}_6\text{F}_5)_4\}$. Method A:** A CD_2Cl_2 solution (0.4 mL) of $[\text{PhMe}_2\text{NH}][\text{B}(\text{C}_6\text{F}_5)_4]$ (24 mg, 0.0300 mmol) at 22 °C was added to a CD_2Cl_2 solution (0.3 mL) of $[\text{Ar}^{\text{F}}\text{N}_2\text{N}]\text{TaMe}_2$ (19 mg, 0.0303 mmol) at -35 °C. The reaction solution was stirred at room temperature briefly and transferred to an NMR tube. The ^1H and ^{19}F NMR spectra indicated a mixture of $\{[\text{Ar}^{\text{F}}\text{N}_2\text{NH}]\text{TaMe}_2\}\{\text{B}(\text{C}_6\text{F}_5)_4\}$ and free Me_2NPh . **Method B:** The procedures were identical to those in Method A except using $[\text{Ar}^{\text{F}}\text{N}_2\text{NH}]\text{TaMe}_3$ (20 mg, 0.0303 mmol) and $[\text{PhMe}_2\text{NH}][\text{B}(\text{C}_6\text{F}_5)_4]$ (24 mg, 0.0300 mmol): ^1H NMR (CD_2Cl_2) δ 4.65 (td, 2, CH_2), 4.50 (br s, 1, NH), 4.17 (dd, 2, CH_2), 3.90 (dt, 2, CH_2), 3.44 (m, 2, CH_2), 1.30 (br s, 6, TaMe); ^{19}F NMR (CD_2Cl_2) δ -134.51 (br s, 8), -143.63 (d, 4), -151.60 (t, 2), -160.32 (t, 4), -164.81 (t, 4), -168.80 (t, 8). Resonances for Me_2NPh were observed at 7.29 (t, 2, Ph), 6.85-6.81 (m, 3, Ph), and 2.99 (s, 6, NMe) in the ^1H NMR spectrum.

* **$\{[\text{Ar}^{\text{F}}\text{N}_2\text{NH}]\text{TaMe}_2\}\{\text{MeB}(\text{C}_6\text{F}_5)_3\}(\text{toluene})$.** A colorless toluene solution (4 mL) of $\text{B}(\text{C}_6\text{F}_5)_3$ (154 mg, 0.301 mmol) was added to a toluene solution (2 mL) of $[\text{Ar}^{\text{F}}\text{N}_2\text{NH}]\text{TaMe}_3$ (198 mg, 0.301 mmol) at -35 °C with stirring. The reaction mixture was warmed to room temperature. Pale yellow solid precipitated from the solution within 20 min. The supernatant was decanted and the solid was dried *in vacuo*; yield 335 mg (95%). Colorless single crystals were obtained from a concentrated dichloromethane solution at -35 °C: ^1H NMR (CD_2Cl_2) δ 4.72 (td, 2, CH_2), 4.19 (dd, 2, CH_2), 4.01 (dt, 2, CH_2), 3.49 (m, 2, CH_2), 1.38 (s, 3, Me), 1.27 (s, 3, Me), 0.47 (s, 3, Me), the NH resonance was found as a shoulder on the resonance at 4.72 ppm, one equiv. of toluene was found according to integration and the resonance was not reported; ^{19}F NMR (CD_2Cl_2) δ -134.72 (d, 6), -143.38 (d, 4), -151.20 (t, 2), -160.06 (t, 4),

-166.27 (t, 3), -169.04 (t, 6). Anal. Calcd. for $C_{44}H_{26}N_3F_{25}BTa$: C, 41.83; H, 2.07; N, 3.33. Found: C, 41.51; H, 1.84; N, 3.18.

[Ar^FN₂N]TaMe(NMe₂). **Method A:** LiNMe₂ (5 mg, 0.104 mmol) was added as a solid to a pale yellow solution of {[Ar^FN₂NH]TaMe₂}{MeB(C₆F₅)₃}(toluene) (131 mg, 0.104 mmol) in diethyl ether (3 mL) at -35 °C with stirring. A bright yellow solution was generated after several minutes. After being stirred at room temperature for 2.5 h, the solvent was removed *in vacuo*. The solid residue thus obtained was extracted with pentane. The extract was filtered through Celite and yellow filtrate was concentrated *in vacuo* to give a yellow crystalline solid; yield 27 mg (39%). **Method B:** A solution of HNMe₂ (0.084 mL, 2.0 M in THF, 0.168 mmol) was added to a diethyl ether solution (2 mL) of [Ar^FN₂N]TaMe₂ (108 mg, 0.168 mmol) at -35 °C. The solution was stirred at room temperature for 21 h; an aliquot was analyzed by ¹H and ¹⁹F NMR spectroscopy which showed quantitative formation of product. The solution was filtered through Celite and the filtrate was concentrated *in vacuo* until the volume was ~1 mL. The concentrated solution was cooled at -35 °C for 1 h to give yellow crystals; yield 74 mg (66%). **Method C:** The conditions for this method are analogous to Method B except using [Ar^FN₂NH]TaMe₃ instead of [Ar^FN₂N]TaMe₂ and reaction time being 45 h; yield 70%: ¹H NMR (C₆D₆) δ 4.15 (m, 2, CH₂), 3.79 (m, 2, CH₂), 3.70 (m, 2, CH₂), 3.48 (m, 2, CH₂), 2.43 (br s, 3, NMe), 1.96 (br s, 3, NMe), 1.20 (s, 3, TaMe); ¹⁹F NMR (C₆D₆) δ -152.40 (d, 4, F_O), -166.24 (m, 6, containing F_m and F_p); ¹³C NMR (C₆D₆) δ 143.23 (C_O, ¹J_{CF} = 241), 138.16 (C_m, ¹J_{CF} = 256), 137.04 (C_p, ¹J_{CF} = 252), 131.58 (C_{ipso}), 62.71 (CH₂), 58.68 (CH₂), 48.35 (TaMe), 37.43 (NMe). Anal. Calcd. for C₁₉H₁₇N₄F₁₀Ta: C, 33.94; H, 2.55; N, 8.33. Found: C, 33.77; H, 2.25; N, 8.11.

[Ar^FN₂NH]TaMe(NPh). A diethyl ether solution (2 mL) of aniline (27 mg, 0.294 mmol) was added to a diethyl ether solution (5 mL) of [Ar^FN₂N]TaMe₂ (189 mg, 0.294 mmol) at -35 °C with stirring. The reaction mixture was stirred at room temperature for 14 h. The solution was filtered through Celite. The filtrate was concentrated *in vacuo* until the volume was ~1 mL and the concentrated solution was cooled to -35 °C to give yellow crystals. The supernatant was decanted and the crystals were dried *in vacuo*; yield 163 mg (77%): ¹H NMR (C₆D₆) δ 6.88 (t, 2,

Aryl), 6.51 (m, 3, Aryl), 3.23 (m, 2, CH₂), 3.10 (m, 2, CH₂), 2.18 (m, 4, CH₂), 1.62 (br s, 1, NH), 0.61 (s, 3, TaMe); ¹⁹F NMR (C₆D₆) δ -151.64 (br s, 2, F_O), -152.90 (br s, 2, F_O), -165.09 (t, 2, F_p), -165.99 (br s, 4, F_m); ¹³C NMR (C₆D₆) δ 155.99 (C_{ipso}, Ph), 143.15 (br, C_O, C₆F₅, ¹J_{CF} = 243), 138.25 (containing C_m and C_p of C₆F₅, ¹J_{CF} = 262), 132.20 (C_{ipso}, C₆F₅), 128.29 (C_O, Ph), 126.03 (C_m, Ph), 123.16 (C_p, Ph), 56.70 (CH₂), 47.60 (CH₂), 35.27 (TaMe). Anal. Calcd. for C₂₃H₁₇N₄F₁₀Ta: C, 38.35; H, 2.38; N, 7.78. Found: C, 38.07; H, 2.45; N, 7.60.

Chapter 3

Synthesis of Group 4 Complexes Containing Diamidoamine Ligands and the Polymerization of 1-Hexene by Activated Zirconium Dimethyl Complexes

INTRODUCTION

Several types of diamido/donor ligands and their group 4 complexes have been synthesized in the last several years, often with the intent of preparing new olefin polymerization catalysts.^{44,52,53,71,72,121,123,139,140,163-166} Five coordinate group 4 complexes that contain the diamido/ether ligands such as $[\text{t-BuNON}]^{2-}$ and $[\text{ArN}_2\text{O}]^{2-}$ ($\text{Ar} = 2,6\text{-C}_6\text{H}_3\text{Me}_2$) are active catalysts for polymerization of α -olefins when activated with $[\text{Ph}_3\text{C}][\text{B}(\text{C}_6\text{F}_5)_4]$ or $[\text{HNMe}_2\text{Ph}][\text{B}(\text{C}_6\text{F}_5)_4]$.^{52,71,72} In the first case, the polymerization of 1-hexene was found to take place primarily *via* 1,2-insertion of the olefin into the cationic monoalkyl zirconium complexes in a living manner up to a 500mer at 0 °C.^{52,53} The diamido/donor ligands can adopt different geometries. Trigonal bipyramidal structures including both *fac* and *mer* geometries have been observed in the five-coordinate diamido/ether complexes, as well as the square pyramidal structure, an approximately half-way intermediate between *fac* and *mer*.^{71,72} An X-ray study of $[\text{t-BuNON}]\text{ZrMe}_2$ shows it to have a *fac* structure, but NMR data suggest a relatively fast fluxional exchange between the axial and equatorial methyl ligands,⁵² presumably due to the ability of the oxygen donor to adopt a trigonal planar configuration. The success of $[\text{t-BuNON}]\text{ZrMe}_2$ in

polymerization has been ascribed to the steric crowding of the *t*-butyl substituents on the [t-BuNON]²⁻ ligand as discussed in Chapter 1.

SPECIFIC GOALS

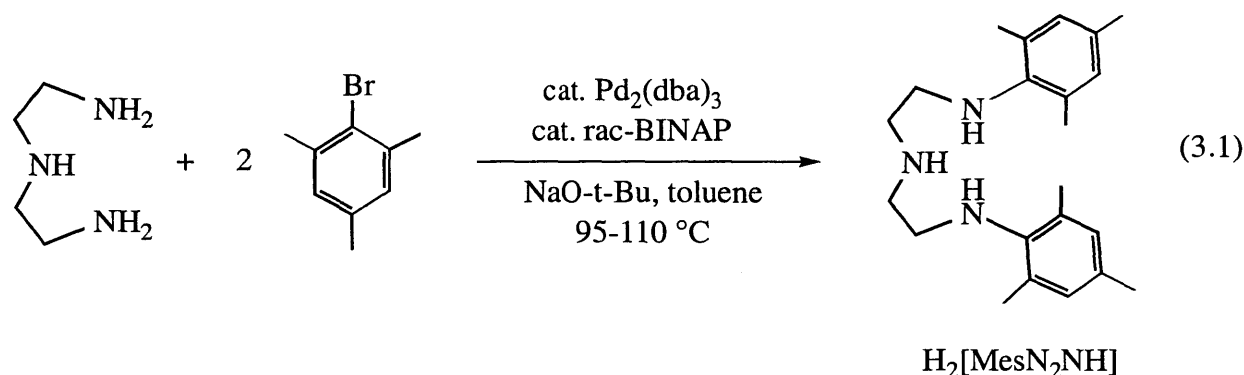
We were interested in preparing the diamido/donor ligands which cannot readily achieve the planar geometry, thereby preventing the fluxional exchange process. One way to achieve this goal is to utilize an amine or a phosphine as the donor. Also, since the thermal stability of the zirconium catalysts containing [t-BuNON]²⁻ is not high,⁵² the development of more thermally stable catalysts was also attempted. This chapter covers the synthesis of group 4 complexes containing the mesitylated diamidoamine ligands, [(MesNCH₂CH₂)₂NR]²⁻ ([MesN₂NR]²⁻; Mes = 2,4,6-C₆H₂Me₃; R = H, alkyl), and the polymerization of 1-hexene by activated zirconium dimethyl complexes. The thermal stability of cationic propagating intermediates was also investigated.

RESULTS

3.1 Synthesis of H₂[MesN₂NH].

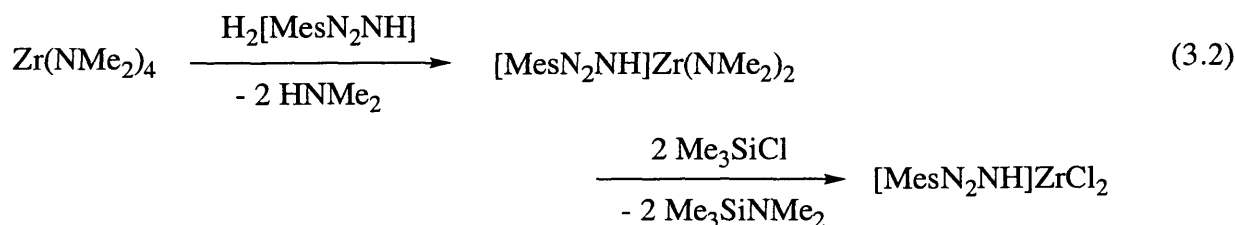
The arylation of amines catalyzed by palladium is recently well-documented.^{77,167} We have found that double arylation can be readily conducted between diethylenetriamine and mesityl bromide to give H₂[MesN₂NH] (equation 3.1) under a condition similar to those reported by Buchwald and co-workers.⁷⁶ The choice of mesityl bromide instead of 2,6-C₆H₃Me₂Br simply reflects their cost from commercial suppliers. The coupling reaction was monitored by ¹H NMR spectroscopy which showed no sign of the formation of monoarylated intermediate. The *ortho* and *para* methyl resonances in the mesityl bromide were directly replaced by those in the double arylated product. In general, the reaction is complete in hours to days depending on the concentration, scale, and temperature. The yield of H₂[MesN₂NH] is virtually quantitative and the

reaction has been carried out without complications to give a 100 g of product. After standard workup $\text{H}_2[\text{MesN}_2\text{NH}]$ can be isolated as a red needle-like crystalline solid and used directly for the subsequent organometallic reactions, or it can be recrystallized from hexane to give pale yellow rocks. Synthesis of analogous *o*-tolyl-substituted diethylenetriamine using similar methods has been reported recently,¹⁶⁸ as has arylation of triethylenetetramine.⁵⁸ Arylation of the central nitrogen in $\text{H}_2[\text{MesN}_2\text{NH}]$ seems difficult, presumably for steric reasons. Attempts to phenylate $\text{H}_2[\text{MesN}_2\text{NH}]$ in the presence of a catalytic amount of various palladium and phosphine reagents were not successful. It has been documented that palladium catalyzed C-N bond formation between acyclic secondary aliphatic amines and aryl halides are more difficult.⁷⁷



3.2 Synthesis of $[\text{MesN}_2\text{NH}]\text{ZrCl}_2$.

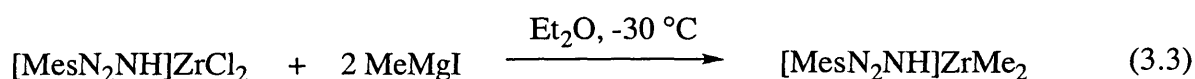
Zirconium complexes containing the $[\text{MesN}_2\text{NH}]^{2-}$ ligand can be prepared from $\text{Zr}(\text{NMe}_2)_4$ as shown in equation 3.2. The dichloride $[\text{MesN}_2\text{NH}]\text{ZrCl}_2$ was obtained in two steps in ~60% overall yield. Both $[\text{MesN}_2\text{NH}]\text{Zr}(\text{NMe}_2)_2$ and $[\text{MesN}_2\text{NH}]\text{ZrCl}_2$ have mirror symmetry according to ^1H and ^{13}C NMR data. In $[\text{MesN}_2\text{NH}]\text{Zr}(\text{NMe}_2)_2$, the two dimethylamido groups are inequivalent at room temperature on the NMR time scale, consistent with no rapid inversion of configuration at the central nitrogen donor, presumably as a consequence of it being strongly bonded to the metal. This observation is in contrast to the ready inversion at oxygen observed in



[t-BuNON]²⁻ complexes (presumably while the oxygen binds to the metal)⁵² and to the fluxional process observed in [(Me₃SiNCH₂CH₂)₂NSiMe₃]²⁻ complexes (presumably while the central nitrogen dissociates from the metal).^{140,163} The NH resonances in [MesN₂NH]Zr(NMe₂)₂ and [MesN₂NH]ZrCl₂ are found as broadened singlets at 1.80 and 2.20 ppm, respectively. The mesityl rings do not rotate rapidly about the N-C_{ipso} bonds on the NMR time scale in either [MesN₂NH]Zr(NMe₂)₂ or [MesN₂NH]ZrCl₂. For example, three mesityl methyl groups are observed in the ¹H NMR spectrum of [MesN₂NH]ZrCl₂ at 2.50, 2.40, and 2.13 ppm, along with two *meta* mesityl aryl proton resonances at 6.88 and 6.83 ppm. Slow rotation of 2,6-disubstituted aryl rings has also been observed in a pseudo-tetrahedral dialkyl complex that contains a chelating arylated diamido ligand that lacks a central donor.¹⁶⁹ These data are consistent with *either* a *fac* or a *mer* arrangement for the [MesN₂NH]²⁻ ligand in a trigonal bipyramidal structure. However, a dimeric [MesN₂NH]ZrCl₂ containing two bridging chlorides in the solid state is also possible.

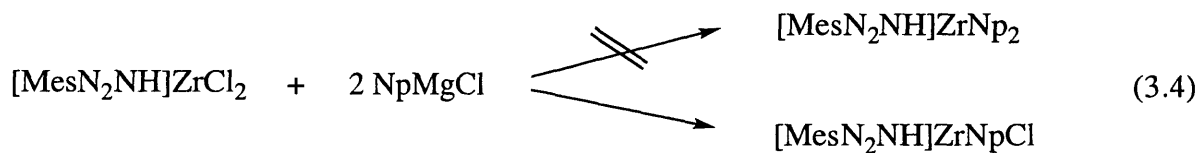
3.3 Alkylation of [MesN₂NH]ZrCl₂.

Treatment of [MesN₂NH]ZrCl₂ with two (or more) equivalents of MeMgI in diethyl ether produces white crystalline [MesN₂NH]ZrMe₂ in high yield (equation 3.3). After standard workup, [MesN₂NH]ZrMe₂ can be recrystallized by addition of pentane to a saturated diethyl ether solution to give pure product according to ¹H NMR spectrum. The inequivalent ZrMe resonances are found at 0.24 and 0.07 ppm in the ¹H NMR spectrum, and the NH proton resonance is found



at 1.16 ppm. The two methyl ligands do not exchange at temperatures between 20 and 80 °C in toluene-*d*₈ (~15 mM), suggesting that the NH group is tightly bound to zirconium. However, the mesityl rings begin to rotate at 60 °C to give one singlet resonance for *ortho* mesityl methyl groups in the ¹H NMR spectrum. [MesN₂NH]ZrMe₂ is relatively stable in solution at room temperature, although it slowly decomposes over a period of several days. When a colorless toluene-*d*₈ solution (~15 mM) of [MesN₂NH]ZrMe₂ is heated to 80 °C in a sealed tube, the solution becomes orange and a methane resonance is observed.

In contrast, the treatment of [MesN₂NH]ZrCl₂ with two equivalents of NpMgCl affords [MesN₂NH]ZrNpCl instead of [MesN₂NH]ZrNp₂ in moderate yield (equation 3.4). Alternatively, [MesN₂NH]ZrNpCl can be obtained in high yield by addition of one equivalent of NpMgCl to [MesN₂NH]ZrCl₂. This result along with the slow rotation of the mesityl rings about the N-C_{ipso} bonds in all of the [MesN₂NH]²⁻ complexes in solution suggests that the introduction of two neopentyl ligands is precluded due to steric reasons. A similar phenomenon is also found in the [t-BuNON]²⁻ system.⁷³

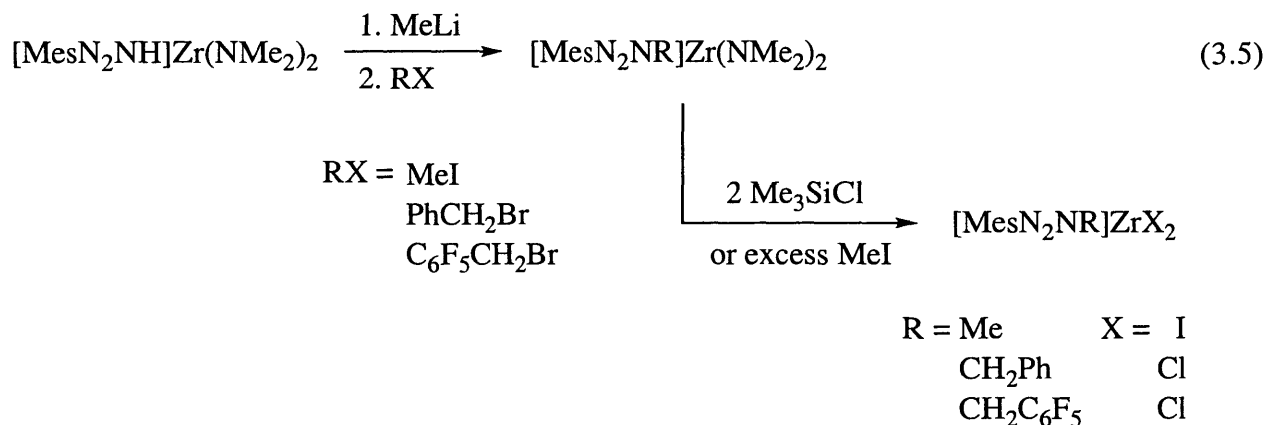


3.4 Synthesis of zirconium dialkyl complexes involving deprotonation-alkylation sequence.

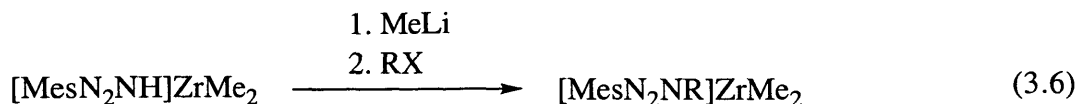
It is interesting to note that MeMgI does not deprotonate the central NH proton in [MesN₂NH]ZrX₂ (X = Cl, Me) in diethyl ether at room temperature, while MeLi does. Both [MesN₂NH]Zr(NMe₂)₂ and [MesN₂NH]ZrMe₂ can be deprotonated cleanly by MeLi in diethyl ether to give what we formulate as [MesN₂NLi]Zr(NMe₂)₂(OEt₂) and [MesN₂NLi]ZrMe₂(OEt₂), respectively, according to their ¹H NMR data. In contrast, addition of MeLi (1 to 3 equivalents) to [MesN₂NH]ZrCl₂ results in a mixture, presumably due to the formation of

$[\text{MesN}_2\text{NLi}]\text{ZrCl}_2(\text{OEt}_2)_x$ in which the NLi further reacts with ZrCl either intermolecularly or intramolecularly.

Several alkyl groups can be attached to the central nitrogen. The reactions between $[\text{MesN}_2\text{NLi}]\text{Zr}(\text{NMe}_2)_2(\text{OEt}_2)$ and alkyl halides such as MeI, PhCH_2Br , and $\text{C}_6\text{F}_5\text{CH}_2\text{Br}$ produce exclusively the corresponding bis(dimethylamide) complexes $[\text{MesN}_2\text{NR}]\text{Zr}(\text{NMe}_2)_2$ ($\text{R} = \text{Me}$, Bn , Bn^{F}). These compounds can be readily converted to the corresponding dihalide complexes (equation 3.5). These deprotonation-alkylation-halogenation reactions can be performed in one pot starting from $[\text{MesN}_2\text{NH}]\text{Zr}(\text{NMe}_2)_2$, and the dihalide complexes can be isolated in high overall



yields. A diiodo complex $[\text{MesN}_2\text{NMe}]\text{ZrI}_2$ is prepared by addition of excess MeI to $[\text{MesN}_2\text{NLi}]\text{Zr}(\text{NMe}_2)_2(\text{OEt}_2)$. The ligand transformation from $\text{Zr}(\text{NMe}_2)_2$ to ZrI_2 is relatively slow. The slow conversion of NMe_2 to I is also reported by Cummins and co-workers.¹⁷⁰ Dialkyl complexes can then be synthesized from these dihalide complexes. For instance, addition of two equivalents of MeMgI to $[\text{MesN}_2\text{NMe}]\text{ZrI}_2$ produces $[\text{MesN}_2\text{NMe}]\text{ZrMe}_2$ in high yield. Alternatively, the deprotonation-alkylation sequence can also be used to synthesize dimethyl $[\text{MesN}_2\text{NR}]\text{ZrMe}_2$ ($\text{R} = \text{Me}$, Bn , Bn^{F}). These complexes are isolated from the reactions between MeLi and $[\text{MesN}_2\text{NH}]\text{ZrMe}_2$ followed by addition of the corresponding alkyl halides as shown in equation 3.6.



The ^1H and ^{13}C NMR data for $[\text{MesN}_2\text{NR}]\text{ZrMe}_2$ ($\text{R} = \text{Me}, \text{Bn}, \text{Bn}^{\text{F}}$) are similar to those of their protio analogue, i.e., inequivalent ZrMe signals, mirror symmetry, and slow rotation of mesityl rings about the N-C_{ipso} bonds. For instance, the ^1H NMR spectra of $[\text{MesN}_2\text{NMe}]\text{ZrMe}_2$ (0.015 M, toluene- d_8) between 25 to 80 °C exhibit two singlet resonances for the *ortho* mesityl methyl groups and two singlet resonances for the *meta* aromatic protons. The methyl ligands in $[\text{MesN}_2\text{NMe}]\text{ZrMe}_2$ do not exchange readily on the NMR time scale, even at 80 °C, suggesting the coordination of amino nitrogen to zirconium is strong. The benzylic protons of $[\text{MesN}_2\text{NBn}]\text{ZrMe}_2$ are observed as a singlet resonance at 3.96 ppm, and those of $[\text{MesN}_2\text{NBn}^{\text{F}}]\text{ZrMe}_2$ are observed at 3.85 ppm. The ^{19}F NMR spectrum of $[\text{MesN}_2\text{NBn}^{\text{F}}]\text{ZrMe}_2$ shows three resonances at room temperature in C_6D_6 , suggesting free rotation of the C_6F_5 ring on the NMR time scale. From these data a *fac* or a *mer* structure for these diamidoamine ligands can not be determined.

3.5 Comparison of the thermal stability of dimethyl $[\text{MesN}_2\text{NR}]\text{ZrMe}_2$ ($\text{R} = \text{H}, \text{Me}, \text{Bn}, \text{Bn}^{\text{F}}$).

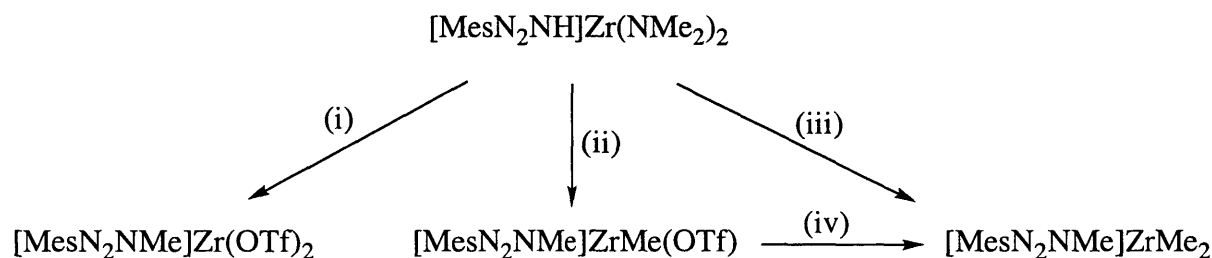
These dimethyl complexes exhibit different thermal stability. For instance, a solution of $[\text{MesN}_2\text{NMe}]\text{ZrMe}_2$ (0.015 M) and $[\text{MesN}_2\text{NBn}^{\text{F}}]\text{ZrMe}_2$ (0.015 M) in C_6D_6 showed no detectable decomposition at room temperature for several days according to their ^1H NMR spectra. However, $[\text{MesN}_2\text{NH}]\text{ZrMe}_2$ (0.015 M in C_6D_6) and $[\text{MesN}_2\text{NBn}]\text{ZrMe}_2$ (0.015 M in C_6D_6) decompose over a period of 3 days at room temperature. The decomposition of $[\text{MesN}_2\text{NH}]\text{ZrMe}_2$ and $[\text{MesN}_2\text{NBn}]\text{ZrMe}_2$ seems to be accelerated by coordinating solvents such as diethyl ether and THF. The decomposition products of $[\text{MesN}_2\text{NH}]\text{ZrMe}_2$ and

$[\text{MesN}_2\text{NBn}]\text{ZrMe}_2$ have not been identified so far. Apparently $[\text{MesN}_2\text{NBn}]\text{ZrMe}_2$ is less stable than its pentafluorinated analogue $[\text{MesN}_2\text{NBn}^{\text{F}}]\text{ZrMe}_2$. We suspect that the stability of $[\text{MesN}_2\text{NBn}]\text{ZrMe}_2$ is decreased due to partial coordination of the phenyl moiety to the metal center. The ^{19}F NMR spectrum of $[\text{MesN}_2\text{NBn}^{\text{F}}]\text{ZrMe}_2$ suggests that the C_6F_5 ring rotates readily at room temperature on the NMR time scale. It is likely that the electron-withdrawing ability of C_6F_5 and the greater C-F bond strength (as compared to C-H bonds)⁹² increase the thermal stability of $[\text{MesN}_2\text{NBn}^{\text{F}}]\text{ZrMe}_2$.

In addition to the thermal instability, $[\text{MesN}_2\text{NBn}]\text{ZrMe}_2$ exhibits quite unusual solubility as compared to the other three zirconium dimethyl complexes reported here. The dimethyl complexes $[\text{MesN}_2\text{NR}]\text{ZrMe}_2$ ($\text{R} = \text{H}, \text{Me}, \text{Bn}^{\text{F}}$) are readily soluble in benzene and toluene, while the poor solubility of $[\text{MesN}_2\text{NBn}]\text{ZrMe}_2$ in toluene leads to only ~10% isolated yield. A better workup solvent for $[\text{MesN}_2\text{NBn}]\text{ZrMe}_2$ is dichloromethane.

3.6 Synthesis of zirconium dialkyl complexes involving triflate intermediates.

Triflate complexes that contain $[\text{MesN}_2\text{NMe}]^{2-}$ can also be isolated by the deprotonation-alkylation methodology. As shown in Scheme 3.1, depending on the stoichiometric amount of

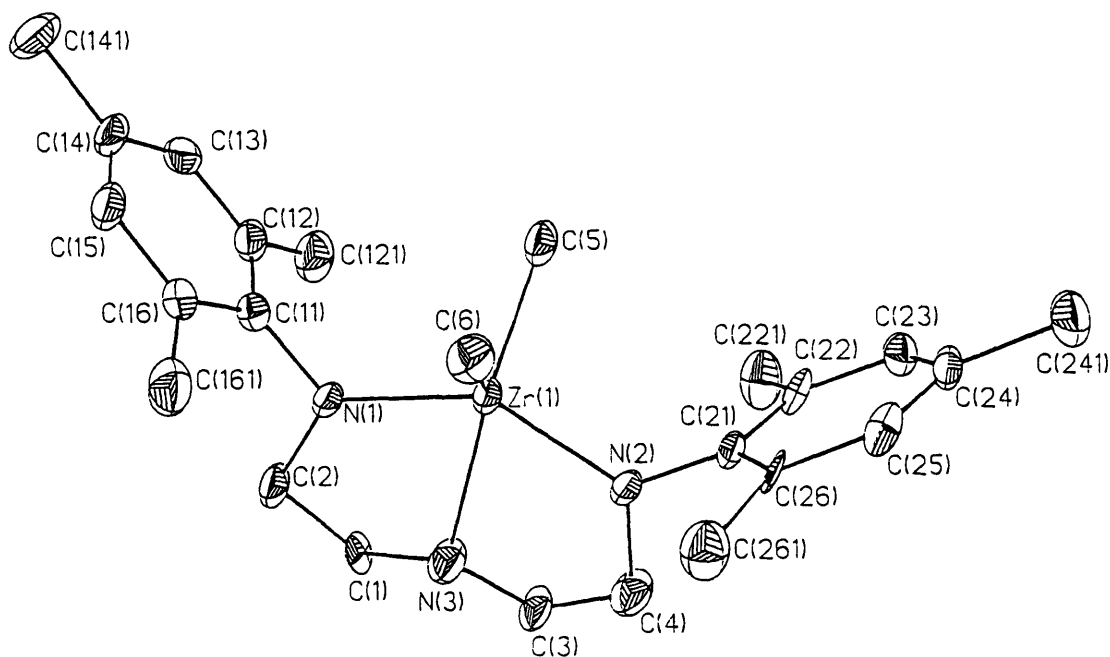


Scheme 3.1. Synthesis of $[\text{MesN}_2\text{NMe}]\text{ZrMe}_2$ *via* triflate intermediates. Conditions: (i) MeLi, -30 to 25 °C, 2 h; 3 equiv. MeOTf, -30 to 25 °C, 15 min. (ii) 2 equiv. MeLi, -30 to 25 °C, 2 h; 3 equiv. MeOTf, -30 to 25 °C, 15 min. (iii) 3 equiv. MeLi, -30 to 25 °C, 2 h; 3 equiv. MeOTf, -30 to 25 °C, 15 min. (iv) MeLi, -30 to 25 °C, 1 h.

MeLi employed, $[\text{MesN}_2\text{NMe}]\text{Zr}(\text{OTf})_2$, $[\text{MesN}_2\text{NMe}]\text{ZrMe}(\text{OTf})$, and $[\text{MesN}_2\text{NMe}]\text{ZrMe}_2$ can be independently isolated. For instance, addition of *two* equivalents of MeLi to $[\text{MesN}_2\text{NH}]\text{Zr}(\text{NMe}_2)_2$ followed by addition of three equivalents of MeOTf produces $[\text{MesN}_2\text{NMe}]\text{ZrMe}(\text{OTf})$ as a pale yellow crystalline solid in ~60% yield. The reactions presumably proceed *via* the $[\text{MesN}_2\text{NMe}]\text{Zr}(\text{OTf})_2$ intermediate, in which the OTf ligands can be replaced with the remaining second and/or third equivalent of MeLi in reaction solution. Since the reactions are all performed in one pot, it is likely that MeOTf does not react with MeLi for kinetic reasons. It is surprising that MeOTf shows such selective reactivity as it is an extremely powerful methylation reagent.¹⁷¹ Alternatively, the dimethyl $[\text{MesN}_2\text{NMe}]\text{ZrMe}_2$ may be obtained by addition of MeLi to $[\text{MesN}_2\text{NMe}]\text{ZrMe}(\text{OTf})$. The conversion of $\text{Zr}(\text{NMe}_2)$ to $\text{Zr}(\text{OTf})$ is analogous to that of $\text{Zr}(\text{NMe}_2)$ to ZrI , but the latter is much slower.

3.7 X-ray structures of $[\text{MesN}_2\text{NH}]\text{ZrMe}_2$ and $[\text{MesN}_2\text{NMe}]\text{ZrMe}_2$.

The complexes $[\text{MesN}_2\text{NH}]\text{ZrMe}_2$ and $[\text{MesN}_2\text{NMe}]\text{ZrMe}_2$ have been structurally characterized by X-ray crystallography. A single crystal of $[\text{MesN}_2\text{NH}]\text{ZrMe}_2$ was grown from a saturated solution of diethyl ether, toluene, and hexamethyldisiloxane at -30 °C, and that of $[\text{MesN}_2\text{NMe}]\text{ZrMe}_2$ was grown from diethyl ether and pentane. The ORTEP diagrams and selected bond lengths, bond angles, and dihedral angles are given in Figures 3.1 and 3.2. The structures of $[\text{MesN}_2\text{NH}]\text{ZrMe}_2$ and $[\text{MesN}_2\text{NMe}]\text{ZrMe}_2$ are similar. Table 3.1 summarizes the core bond lengths and angles of these complexes for comparison. The Zr-N_{amine} bond distance in $[\text{MesN}_2\text{NMe}]\text{ZrMe}_2$ (2.373(5) Å) is ~0.02 Å shorter than that in $[\text{MesN}_2\text{NH}]\text{ZrMe}_2$ (2.392(7) Å). The dihedral angle of Zr(1)/C(3)-N(3)-C(1) in $[\text{MesN}_2\text{NH}]\text{ZrMe}_2$ is 131.4° and the corresponding angle in $[\text{MesN}_2\text{NMe}]\text{ZrMe}_2$ is 124.2°. The ~7.2° difference of the dihedral angles apparently reflects the steric difference between Me and H in $[\text{MesN}_2\text{NMe}]\text{ZrMe}_2$ and $[\text{MesN}_2\text{NH}]\text{ZrMe}_2$, respectively. These dihedral angles should be compared to the corresponding angles in the



Bond Lengths

Zr(1)-N(1)	2.097(6)
Zr(1)-N(2)	2.097(6)
Zr(1)-N(3)	2.392(7)
Zr(1)-C(5)	2.249(9)
Zr(1)-C(6)	2.260(9)

Bond Angles

C(5)-Zr(1)-C(6)	102.3(3)
N(1)-Zr(1)-N(2)	140.0(3)
Zr(1)-N(1)-C(11)	121.8(5)
Zr(1)-N(2)-C(21)	120.4(5)
C(1)-N(3)-C(3)	116.5(7)

Dihedral Angles^a

N(2)/N(3)-Zr(1)-N(1)	174.0	C(5)/N(3)-Zr(1)-C(6)	179.6
Zr(1)-N(1)-C(11)-C(12)	91.5	Zr(1)-N(2)-C(21)-C(26)	88.2
Zr(1)/C(3)-N(3)-C(1)	131.4		

Figure 3.1. An ORTEP drawing (35% probability level) of the structure of [MesN₂NH]ZrMe₂, with selected bond lengths (Å), bond angles (deg), and dihedral angles (deg). ^a Obtained from a Chem 3D model.

Bond Lengths		Bond Angles	
Zr(1)-N(1)	2.095(4)	C(1)-Zr(1)-C(2)	103.2(3)
Zr(1)-N(1A)	2.095(4)	N(1)-Zr(1)-N(1A)	140.5(2)
Zr(1)-N(2)	2.373(5)	Zr(1)-N(1)-C(11)	118.8(3)
Zr(1)-C(1)	2.240(7)	C(3)-N(2)-C(4)	109.3(4)
Zr(1)-C(2)	2.265(7)	C(3)-N(2)-C(4A)	109.3(4)
		C(4)-N(2)-C(4A)	112.2(6)
Dihedral Angles ^a			
N(1)/N(2)-Zr(1)-N(1A)	177.7	C(2)/N(2)-Zr(1)-C(1)	180.0
Zr(1)-N(1)-C(11)-C(16)	89.9	C(3)-N(2)-Zr(1)-N(1)	91.2
Zr(1)/C(4)-N(2)-C(4A)	124.2		

Table 3.1. A comparison of some bond lengths (Å) and angles (deg) in the five-coordinate diamido/ N_{donor} complexes with a *mer* geometry.

	M-N _{eq}	M-N _{ax}	N _{ax} -M-N _{ax}	M-C _α	C _α -M-C _α
[MesN ₂ NH]ZrMe ₂	2.392(7)	2.097(6)	140.0(3)	2.249(9)	102.3(3)
		2.097(6)		2.260(9)	
[MesN ₂ NMe]ZrMe ₂	2.373(5)	2.095(4)	140.5(2)	2.240(7)	103.2(3)
		2.095(4)		2.265(7)	
[2,6-(ArylNCH ₂) ₂ C ₅ H ₃ N]ZrMe ₂ ^a	2.325(4)	2.101(4)	139.6(2)	2.243(6)	102.4(3)
		2.104(5)		2.248(7)	
{[Ar ^F N ₂ NH]TaMe ₂ } ^{+b}	2.280(15)	1.981(12)	142.6(5)	2.09(2)	102.0(6)
		1.965(13)		2.11(2)	

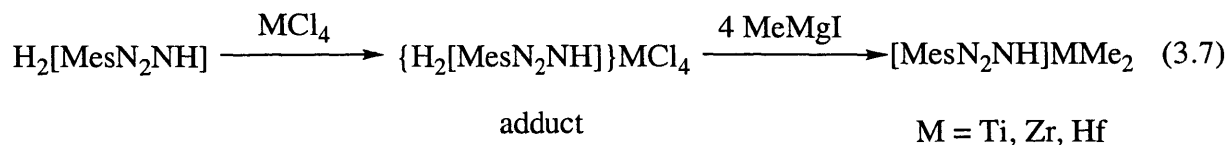
^a Aryl = 2,6-Et₂C₆H₃; see reference 123. ^b Anion = {MeB(C₆F₅)₃}⁻; see Chapter 2.

triamidoamine complexes such as [(C₆F₅NCH₂CH₂)₃N]MoCl (average 120°),⁶² which contain an amino donor with sp³ configuration. Both [MesN₂NH]ZrMe₂ and [MesN₂NMe]ZrMe₂ occupy a distorted trigonal bipyramidal structure in which the [MesN₂NR]²⁻ (R = H, Me) ligands adopt a *mer* geometry rather than a *fac*. The equatorial plane can be well-defined by C_α/N_{amine}-Zr-C_α with little distortion (dihedral angle of 0.4° in [MesN₂NH]ZrMe₂ and 0° in [MesN₂NMe]ZrMe₂). The two amido nitrogen atoms in [MesN₂NH]ZrMe₂ and [MesN₂NMe]ZrMe₂ occupy two axial positions with N_{amide}/N_{amine}-Zr-N_{amide} dihedral angles of 6.0° and 2.3°, respectively. Similar dihedral angles are observed for [ArN₂O]²⁻ systems, e.g., 0° for both axial and equatorial planes of [ArN₂O]ZrMe₂.^{71,72} The two amido nitrogens in [MesN₂NMe]ZrMe₂ are bent only slightly away from the side of the molecule that contains C(3) (Figure 3.2), as judged by the C(3)-N(2)-Zr-N(1)

dihedral angle of 91.2° . The donor amine nitrogen in $[\text{MesN}_2\text{NMe}]\text{ZrMe}_2$ nevertheless is virtually tetrahedral with C-N-C angles of 109° , 109° , and 112° . The Zr-N_{amine} bond length, Zr-N_{amide} bond lengths, Zr-C $_{\alpha}$ bond lengths, and C $_{\alpha}$ -Zr-C $_{\alpha}$, N-Zr-N, and Zr-N-C $_{\alpha}$ angles are all typical of diamido/N_{donor} complexes having a *mer* geometry, e.g., $[\text{2,6-(2,6-Et}_2\text{C}_6\text{H}_3\text{NCH}_2)_2\text{C}_5\text{H}_3\text{N}]\text{ZrMe}_2$.¹²³ It is also interesting to compare the structure of $[\text{MesN}_2\text{NH}]\text{ZrMe}_2$ with that of its isoelectronic cationic relative $\{[\text{Ar}^{\text{F}}\text{N}_2\text{NH}]\text{TaMe}_2\}^+$ (see Chapter 2). The corresponding distances and angles are listed in Table 3.1 for comparison.

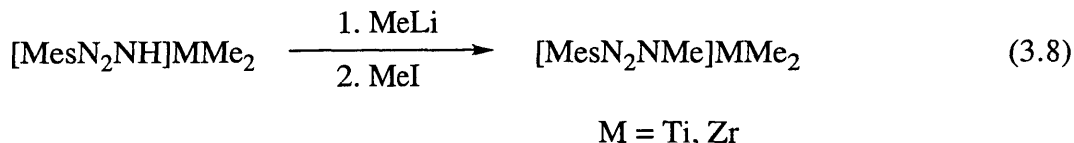
3.8 Direct synthesis of group 4 dialkyl complexes containing $[\text{MesN}_2\text{NR}]^{2-}$ (R = H, alkyl).

The apparent stability and ease of formation of $[\text{MesN}_2\text{NH}]\text{ZrMe}_2$ led us to attempt to form it directly from ZrCl_4 , $\text{H}_2[\text{MesN}_2\text{NH}]$, and MeMgI . Addition of ZrCl_4 to $\text{H}_2[\text{MesN}_2\text{NH}]$ in diethyl ether results in the formation of a precipitate in which we assume the ligand has been at least partially attached to the metal to form an adduct complex. The adduct can also be prepared from a toluene suspension of ZrCl_4 and $\text{H}_2[\text{MesN}_2\text{NH}]$ at 80°C , a condition in which the complexation seems more complete. The adduct may be used *in situ* or isolated as an off-white solid which can be stored under nitrogen. The solubility of the adduct in regular solvents is so poor that the characterization by solution NMR spectroscopy is prohibited. Nevertheless addition of four equivalents of MeMgI to $\{\text{H}_2[\text{MesN}_2\text{NH}]\}\text{ZrCl}_4$ in diethyl ether followed by standard workup yields $[\text{MesN}_2\text{NH}]\text{ZrMe}_2$ in ~40% yield (equation 3.7). A similar "direct" approach in

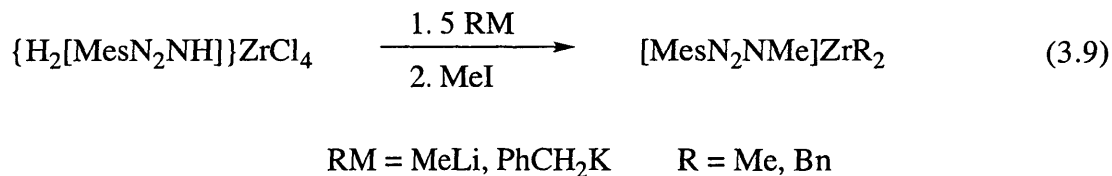


diethyl ether also gives red $[\text{MesN}_2\text{NH}]\text{TiMe}_2$ in ~35% yield and white $[\text{MesN}_2\text{NH}]\text{HfMe}_2$ in ~35% yield. NMR data for the Ti and Hf species are similar to those for $[\text{MesN}_2\text{NH}]\text{ZrMe}_2$. If the reaction is performed in toluene, $[\text{MesN}_2\text{NH}]\text{ZrMe}_2$ can be synthesized in 86% yield on a 60 g

scale.¹⁷² The direct synthetic approach to the dimethyl complexes is an attractive method in that potential polymerization initiators can be prepared quickly in one step from free ligand and metal tetrachlorides. Similar methodology is also applicable to the group 5 chemistry as described in Chapter 2. Sequential deprotonation-alkylation reactions then give yellow $[\text{MesN}_2\text{NMe}]\text{TiMe}_2$ and white $[\text{MesN}_2\text{NMe}]\text{ZrMe}_2$ (equation 3.8).



Perhaps the most convenient way to synthesize dialkyl complexes containing $[\text{MesN}_2\text{NR}]^2-$ in which R is not H is the one-pot method involving the removal of the *three* NH protons in $\{\text{H}_2[\text{MesN}_2\text{NH}]\}\text{MCl}_4$ at once. Addition of *five* equivalents of MeLi followed by one equivalent of MeI to $\{\text{H}_2[\text{MesN}_2\text{NH}]\}\text{ZrCl}_4$ in diethyl ether produces $[\text{MesN}_2\text{NMe}]\text{ZrMe}_2$ in 95% yield on a 8 g scale.¹⁷² Analogous yellow dibenzyl $[\text{MesN}_2\text{NMe}]\text{ZrBn}_2$ can also be synthesized in a similar manner with five equivalents of PhCH_2K (equation 3.9). The ^1H and ^{13}C NMR data of $[\text{MesN}_2\text{NMe}]\text{ZrBn}_2$ are similar to those of $[\text{MesN}_2\text{NMe}]\text{ZrMe}_2$. Two inequivalent benzylic resonances are observed, in contrast to that for $[(\text{Me}_3\text{SiNCH}_2\text{CH}_2)_2\text{NSiMe}_3]\text{ZrBn}_2$ in which the two benzyl groups undergo fluxional exchange at 25 °C *via* a dissociation of the amine nitrogen followed by inversion at the nitrogen and recoordination.¹⁴⁰



3.9 Polymerization of 1-hexene by activated $[\text{MesN}_2\text{NR}]\text{ZrMe}_2$ ($\text{R} = \text{H}, \text{Me}, \text{CH}_2\text{Ph}, \text{CH}_2\text{C}_6\text{F}_5$).

Preliminary information obtained from NMR experiments.

NMR experiments indicate that the titanium complex $[\text{MesN}_2\text{NH}]\text{TiMe}_2$ is not an active catalyst precursor for the polymerization of 1-hexene presumably due to the instability of the cationic intermediate, while activated zirconium dimethyl complexes $[\text{MesN}_2\text{NR}]\text{ZrMe}_2$ ($\text{R} = \text{H}, \text{Me}, \text{Bn}, \text{Bn}^{\text{F}}$) are all capable of polymerizing 1-hexene under similar conditions. When treated with $[\text{Ph}_3\text{C}][\text{B}(\text{C}_6\text{F}_5)_4]$ (0.016 M in $\text{C}_6\text{D}_5\text{Br}$), all $[\text{MesN}_2\text{NR}]\text{ZrMe}_2$ solutions (0.015 M in $\text{C}_6\text{D}_5\text{Br}$) turned yellow except $[\text{MesN}_2\text{NBn}]\text{ZrMe}_2$ which became red. Subsequent addition of 1-hexene (50 equivalents) to these yellow or red solutions resulted in the complete formation of poly(1-hexene) within several minutes according to ^1H NMR spectroscopy. No olefinic signal was observed in these polymer containing solutions, suggesting no significant β elimination, which is in contrast to those observed in $[\text{RNON}]^{2-}$ systems ($\text{R} = \text{Cy}, \text{Mes}$; see Chapter 1). The polymerization rate is highly dependent on the cocatalysts which follow the reactivity order of $[\text{Ph}_3\text{C}][\text{B}(\text{C}_6\text{F}_5)_4] > [\text{HNMe}_2\text{Ph}][\text{B}(\text{C}_6\text{F}_5)_4] \gg \text{B}(\text{C}_6\text{F}_5)_3$. For instance, in the case of $[\text{MesN}_2\text{NMe}]\text{ZrMe}_2$ (0.015 M in toluene) the polymerization of 1-hexene (50 equivalents) with $[\text{Ph}_3\text{C}][\text{B}(\text{C}_6\text{F}_5)_4]$ is fast (100% conversion, < 10 minutes), while those with $[\text{HNMe}_2\text{Ph}][\text{B}(\text{C}_6\text{F}_5)_4]$ (100% conversion, ~17 hours) and $\text{B}(\text{C}_6\text{F}_5)_3$ (< 50% conversion, > 4 days) are much slower. The catalyst activity seems very sensitive to coordinating solvents. Addition of diethyl ether (2 drops) to the trityl activated $[\text{MesN}_2\text{NMe}]\text{ZrMe}_2$ (0.015 M in $\text{C}_6\text{D}_5\text{Br}$) does not give significant catalytic polymerization of 1-hexene (50 equivalents, < 5% conversion, ~17 hours) under the similar conditions.

3.10 Bulk polymerization of 1-hexene by trityl activated $[\text{MesN}_2\text{NR}]\text{ZrMe}_2$ ($\text{R} = \text{H}, \text{Me}$).

Table 3.2 shows the data of poly(1-hexene) prepared with trityl activated $[\text{MesN}_2\text{NR}]\text{ZrMe}_2$ ($\text{R} = \text{H}, \text{Me}$) catalysts. The choice of $[\text{Ph}_3\text{C}][\text{B}(\text{C}_6\text{F}_5)_4]$ is based on its rapid catalytic activity compared with $[\text{HNMe}_2\text{Ph}][\text{B}(\text{C}_6\text{F}_5)_4]$ and $\text{B}(\text{C}_6\text{F}_5)_3$. Addition of

Table 3.2. Characterization of the poly(1-hexene) prepared with [MesN₂NR]ZrMe₂ initiators.^a

#	R	equiv	10 ⁻³ M _n (calcd.)	10 ⁻³ M _n (found)	10 ⁻³ M _w	M _w /M _n
1	H	134	11.3	12.5 ^b	16.2 ^b	1.3
2	H	313	26.3	17.0 ^c	20.9 ^c	1.2
3	H	313	26.3	17.2 ^b	22.5 ^b	1.3
4	H	626	52.7	12.7 ^c	17.2 ^c	1.4
5	H	626	52.7	15.3 ^b	19.4 ^b	1.2
6	Me	139	11.7	23.9 ^b	30.7 ^b	1.3
7	Me	139	11.7	23.7	26.2	1.1
8	Me	139	11.7	16.7 ^b	19.2 ^b	1.1
9 ^d	Me	278	23.4	32.1	40.0	1.2
10	Me	325	27.4	28.7 ^b	39.6 ^b	1.4
11 ^d	Me	325	27.4	25.8 ^c	39.8 ^c	1.5
12 ^d	Me	325	27.4	27.3 ^c	40.6 ^c	1.5
13	Me	649	54.6	29.1 ^b	45.0 ^b	1.5
14	Me	649	54.6	24.9 ^b	36.3 ^b	1.5

^a The catalysts were prepared as described in the text. Reaction temperature was controlled at 0 °C in an isothermal bath except runs 9, 11, 12. Quantitative yields were obtained in each experiment.

^b Average of three determinations with GPC. ^c Average of two determinations with GPC.

^d Reaction run at 20 °C without temperature control.

[Ph₃C][B(C₆F₅)₄] to [MesN₂NH]ZrMe₂ or [MesN₂NMe]ZrMe₂ in chlorobenzene at 0 °C led to the formation of a yellow solution. A stoichiometric amount of 1-hexene was added to these solutions. The reactions were performed at 0 °C except runs 9,11,12, in which the polymerization

was initiated at 20 °C and temperature increased in seconds to ~30 °C. The exotherm then recessed slowly over a period of several minutes. In each case, the still yellow reaction solution was quenched in 1 hour with ethereal HCl and the poly(1-hexene) isolated and analyzed by GPC. Poly(1-hexene) was obtained as extremely viscous gel in quantitative yield in all reactions. Molecular weight distribution (M_w/M_n) is found in the range of ~1.1-1.5, which is lower than that of polyolefins produced from well-defined "single-site" catalysts such as activated metallocenes (typical $M_w/M_n = 2-2.5$).³³ The number average molecular weight of the poly(1-hexene) obtained was usually lower than the molecular weight of a polymer containing the stated number of equivalents of monomer, consistent with some chain transfer, presumably *via* β elimination. For $[\text{MesN}_2\text{NH}]\text{ZrMe}_2$ as the initiator the molecular weight appears to maximize at ~17000, consistent with one β elimination every ~200 insertions on the average (runs 1-5), while for $[\text{MesN}_2\text{NMe}]\text{ZrMe}_2$ as the initiator the molecular weight appears to maximize at ~28000, consistent with one β elimination every ~330 insertions on the average (runs 6-14). Therefore, $[\text{MesN}_2\text{NMe}]\text{ZrMe}_2$ outperforms $[\text{MesN}_2\text{NH}]\text{ZrMe}_2$ as an initiator in terms of having a lower rate of β elimination relative to propagation. The initiation temperature of the polymerization (0 °C versus 20 °C) and the inherent exotherm generated in runs 9, 11,12 appear to have little influence on the polymerization results (run 10 versus 11 and 12). It is interesting to note that the number average molecular weight of the obtained poly(1-hexene) in run 9 is about twice as much as that obtained in run 8 although these two experiments were performed at different temperatures.

3.11 Thermal stability investigation of the propagating species.

We were interested in understanding the thermal stability of the propagating intermediate in the catalytic cycles. Several controlled polymerization experiments were performed. Table 3.3 summarizes the data of poly(1-hexene) prepared with $[\text{Ph}_3\text{C}][\text{B}(\text{C}_6\text{F}_5)_4]$ activated $[\text{MesN}_2\text{NMe}]\text{ZrMe}_2$ under controlled conditions involving different reaction times and

Table 3.3. Poly(1-hexene) prepared with trityl-activated [MesN₂NMe]ZrMe₂^a under controlled conditions.

#	equiv ^b	T/°C(time/min)	GPC observation ^c	10 ⁻³ M _n (calcd.)	10 ⁻³ M _n (found)	10 ⁻³ M _w	M _w /M _n	Yield(%)
1	278	20(60)	monomodal	23.4	32.1	40.0	1.2	100
2	19 259	20(30) 20(60)	monomodal	23.4	26.5	43.5	1.6	100
3	46 232	20(30) 20(60)	monomodal	23.4	20.7 ^d	38.2	1.8	100
4	93 185	20(30) 20(60)	monomodal	23.4	15.3 ^d	32.1	2.1	100
5	139 139	20(30) 20(60)	trimodal	23.4	N/A	N/A	N/A	100
6	139 139	20(90) 20(60)	bimodal	23.4	16.3	22.7	1.4	62
7	139 139	20(60), 65(10) 20(60)	bimodal	23.4	17.4	21.3	1.2	65
8	139 139	20(10), 65(10) 20(60)	trimodal	23.4	N/A	N/A	N/A	68
9	139 139	20(10), 65(10) 20(1500)	bimodal	23.4	15.7	30.7	2.0	61

^a [MesN₂NMe]ZrMe₂ was activated with [Ph₃C][B(C₆F₅)₄] in chlorobenzene at 0 °C and the solution was warmed to 20 °C before the first addition of 1-hexene. ^b 1-Hexene was added in one or two portions at 20 °C. ^c For multi-modal signals, only well-resolved peaks were analyzed and the highest molecular weight data were given. ^d Average of two determinations with GPC.

temperatures. The total amount of monomer was arbitrarily controlled to be the same in all experiments for comparison. Catalysts were prepared at 0 °C in chlorobenzene and warmed to 20 °C before the addition of monomer. Poly(1-hexene) was isolated and analyzed by GPC as described previously. 1-Hexene was added in two portions except in run 1 in which 1-hexene was added in one shot. Multi-modal GPC signals (runs 5-8) suggest more than one active species. Yields vary depending on the condition employed (runs 1-5: ~100%; runs 6-9: ~60%).

Addition of 19 equivalents of 1-hexene followed by a 30-minute pause at 20 °C (run 2 in Table 3.3) affords a still yellow solution. A second portion of monomer (259 equivalents) was added to this solution at 20 °C to result in an immediate exotherm; the temperature increased to 30 °C. The yield is quantitative, suggesting that after a pause, the zirconium species is still active and can convert additional monomers to polymeric material. Monomodal signal was observed from the GPC analysis. The number average molecular weight obtained is about the same as what we would expect, but is smaller than that obtained from run 1. This is consistent with a higher M_w/M_n of the polymer obtained in run 2 than that obtained in run 1.

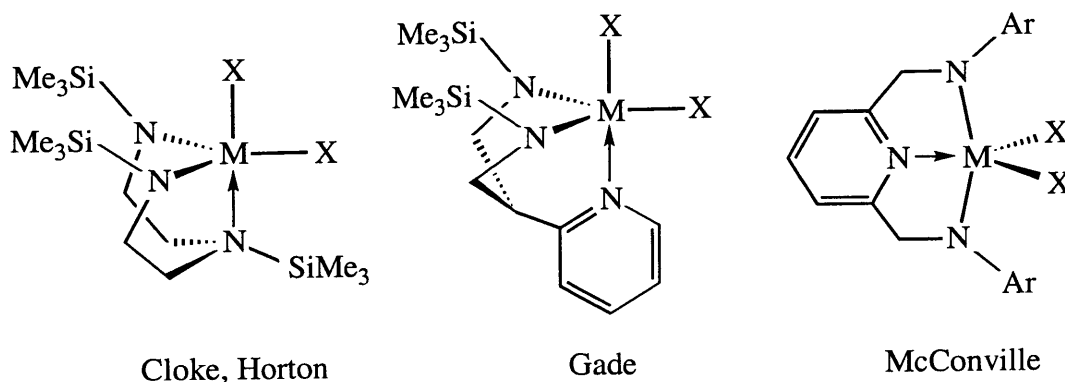
Interestingly, when the stoichiometric amount of 1-hexene employed in the first addition gradually increases (runs 2-5), the molecular weight distribution increases and eventually multi-modal signal can be observed (run 5). This result suggests that the thermal stability of the cationic zirconium species is, at least in part, related to the chain lengths of the polymer attached to the zirconium. Run 5 reveals that significant β elimination occurs during the 30-minute pause at 20 °C to give a trimodal GPC signal. This indicates that (at least) three active species are generated during this pause. The quantitative yield obtained in run 5 suggests that each of the presumed β elimination products is relatively stable and can initiate a second chain to complete the conversion of the monomer. This may also explain why the $[\text{MesN}_2\text{NR}]^{2-}$ initiators give a polymer whose molecular weight maximizes at a certain number (Table 3.2), although quantitative yields were obtained. In agreement with this observation, the quantitative yield obtained in run 5 drops to ~60% when the pause is extended to 1.5 hours at 20 °C (run 6) or 10 minutes at 65 °C (runs 7-9). Multi-modal GPC results were obtained in these experiments (runs 6-9). The molecular weight of

the more abundant signal in runs 6, 7, 9 is approximately half as much as that obtained in run 1, and the same as that obtained in Table 3.2 run 8, suggesting that the polymerization of first 139 equivalents of monomer is complete, but β elimination during the pause is significantly irreversible to give species that are inactive for polymerization.

DISCUSSION

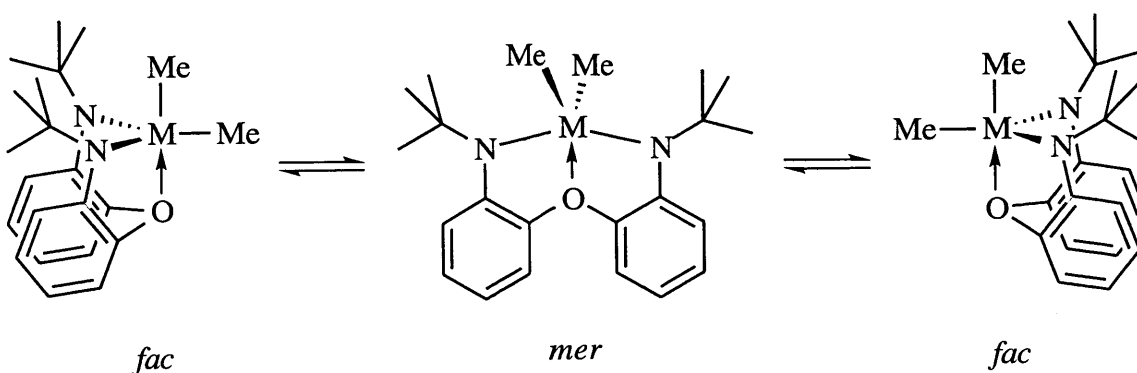
The arylation of primary amines has provided an important entry into the ligand design of amido transition metal chemistry. The steric and electronic properties of the amido ligands can be easily fine-tuned by changing the aromatic or aliphatic substituents. It has been documented that sterically demanding amido ligands containing aryl alkyl substituents exhibit significantly important reactivity in early transition metal chemistry.^{65,66} The tridentate diamidoamine ligands $[\text{MesN}_2\text{NR}]^{2-}$ were designed on this basis.

Group 4 diamidoamine complexes have been shown in the literature for some time, primarily aiming at the development of new Ziegler-Natta polymerization catalysts, but no significant result has been reported so far. Cloke and Horton independently reported the synthesis of trimethylsilyl derived diamidoamine complexes $[(\text{Me}_3\text{SiNCH}_2\text{CH}_2)_2\text{NSiMe}_3]\text{MX}_2$ ($\text{M} = \text{Ti}, \text{Zr}$; $\text{X} = \text{halide or alkyl}$; Scheme 3.2).^{139,140,163,164} Gade reported pyridine derived diamido complexes containing trimethylsilyl groups on the amido nitrogen.^{166,173} These complexes exhibit a *fac* structure for the diamido/ N_{donor} ligands. The low polymerization activity is presumably due to the instability of the N-Si bonds. McConville reported the synthesis of planar pyridine diamido complexes^{121,123} which contain potentially more stable N-aryl bonds, but the rigidity of the planar pyridine backbone presumably cannot provide significant steric shielding for the metal center against β elimination (see discussion below).



Scheme 3.2. Representative literature examples of five coordinate group 4 complexes containing the diamido/ N_{donor} ligands.

It has been documented that *fac* and *mer* structures are relatively close in energy in five coordinate group 4 diamido/ether complexes.⁷² In the solid state, the diamido/ether ligand adopts a *fac* structure in $[\text{t-BuNON}]\text{MMe}_2$ ($\text{M} = \text{Ti}, \text{Zr}$) where the two methyl ligands occupy one axial and one equatorial position in a trigonal bipyramidal geometry. In solution, however, the ^1H NMR spectra reveal a fast interconversion between these two methyl ligands, presumably *via* a *mer* intermediate structure for the diamido/ether ligand as shown in Scheme 3.3.^{52,73} By reducing the steric size of the amido substituent from t-Bu to i-Pr, only a *mer* structure is found for all



Scheme 3.3. The proposed fluxional process in $[\text{t-BuNON}]\text{MMe}_2$ ($\text{M} = \text{Ti}, \text{Zr}$); see references 52,73.

$[\text{i-PrNON}]^{2-}$ complexes according to X-ray structural studies.⁷³ The *mer* structure of $[\text{MesN}_2\text{NR}]\text{ZrMe}_2$ ($\text{R} = \text{H}, \text{Me}$) contrasts with the *fac* structures found for $[(\text{Me}_3\text{SiNCH}_2\text{CH}_2)_2\text{NSiMe}_3]\text{ZrX}_2$ ($\text{X} = \text{halide or alkyl}$) complexes.^{140,163} We propose that *mer* structures for $[(\text{Me}_3\text{SiNCH}_2\text{CH}_2)_2\text{NSiMe}_3]\text{ZrX}_2$ complexes are disfavored as a consequence of steric interaction between the amido SiMe_3 groups and the X groups. Although a *mer* structure is found for $[\text{MesN}_2\text{NR}]\text{ZrMe}_2$ ($\text{R} = \text{H}, \text{Me}$), the steric interaction between the mesityl groups and methyl ligands is presumably the minimum for a *mer* structure as evidenced by the hindered rotation of the mesityl rings.

The central nitrogen donor in the $[\text{MesN}_2\text{NR}]^{2-}$ complexes seems to bind tightly to all group 4 metals. The bond distance between the sp^3 -hybridized nitrogen donor and the metal center in $[\text{MesN}_2\text{NR}]\text{ZrMe}_2$ ($\text{R} = \text{H}, \text{Me}$) is $\sim 0.3\text{--}0.4$ Å shorter than those in $[(\text{Me}_3\text{SiNCH}_2\text{CH}_2)_2\text{NSiMe}_3]\text{TiMe}_2$ ($2.732(2)$ Å)¹³⁹ and $[(\text{Me}_3\text{SiNCH}_2\text{CH}_2)_2\text{NSiMe}_3]\text{ZrCl}[\text{CH}(\text{SiMe}_3)_2]$ ($2.770(5)$ Å).¹⁶³ It should be noted that the difference between $\text{M-N}_{\text{amine}}$ bond distances in these compounds should partially reflect the inherent difference between a *fac* and a *mer* geometry; however, we believe that it is not predominant in this case. It has been shown that the Zr-O bond distance in the *mer* $[\text{i-PrNON}]\text{ZrMe}_2$ ($2.309(2)$ Å) is ~ 0.109 Å shorter than that in the *fac* $[\text{t-BuNON}]\text{ZrMe}_2$ ($2.418(3)$ Å).^{52,73} The ^1H NMR spectra of $[\text{MesN}_2\text{NR}]\text{MMe}_2$ ($\text{M} = \text{Ti}, \text{Zr}, \text{Hf}; \text{R} = \text{H}, \text{Me}, \text{Bn}, \text{Bn}^{\text{F}}$) and $[(\text{Me}_3\text{SiNCH}_2\text{CH}_2)_2\text{NSiMe}_3]\text{MMe}_2$ ($\text{M} = \text{Ti}, \text{Zr}$) also suggest different $\text{M-N}_{\text{amine}}$ bond strength. For instance, $[\text{MesN}_2\text{NMe}]\text{TiMe}_2$ displays two singlet resonances at 0.96 and 0.58 ppm at room temperature for the two methyl ligands, while $[(\text{Me}_3\text{SiNCH}_2\text{CH}_2)_2\text{NSiMe}_3]\text{TiMe}_2$ exhibits only one resonance at 0.79 ppm, as a consequence of facile amino nitrogen dissociation for the latter complex.¹³⁹ The strong coordination of the sp^3 nitrogen donor in the diamidoamine $[\text{MesN}_2\text{NR}]^{2-}$ complexes successfully prevent the facile fluxional exchange process that is observed for the diamido/ether system shown in Scheme 3.3.

Although $[\text{MesN}_2\text{NR}]\text{ZrMe}_2$ ($\text{R} = \text{H}, \text{Me}$) and $[2,6\text{-(ArylNCH}_2)_2\text{C}_5\text{H}_3\text{N}]\text{ZrMe}_2$ ($\text{Aryl} = 2,6\text{-Et}_2\text{C}_6\text{H}_3$) are all trigonal bipyramid with the diamidoamine or diamidopyridine ligand having a

mer geometry, the central nitrogen donors in these complexes adopt different configurations. A tetrahedral sp^3 configuration is found for the donor nitrogen in $[\text{MesN}_2\text{NR}]\text{ZrMe}_2$, while the coordinated pyridine nitrogen in $[2,6-(\text{ArylNCH}_2)_2\text{C}_5\text{H}_3\text{N}]\text{ZrMe}_2$ ($\text{Aryl} = 2,6\text{-C}_6\text{H}_3\text{R}_2$; $\text{R} = \text{Me}, \text{Et}, i\text{-Pr}$)¹²³ is planar sp^2 hybridization. The bond distance between the donor nitrogen and zirconium for $[2,6-(\text{ArylNCH}_2)_2\text{C}_5\text{H}_3\text{N}]\text{ZrMe}_2$ ($\text{Aryl} = 2,6\text{-C}_6\text{H}_3\text{Et}_2$) is $\sim 0.052 \text{ \AA}$ shorter than that for $[\text{MesN}_2\text{NMe}]\text{ZrMe}_2$, presumably due to some (presumably poor) π interaction for the former. Nevertheless, the ^1H NMR data of $[\text{MesN}_2\text{NR}]^{2-}$ complexes ($\text{R} = \text{H}, \text{Me}, \text{Bn}, \text{Bn}^{\text{F}}$) suggest that they are all sterically demanding ligands for five coordinate group 4 complexes as evidenced by hindered rotation about the N-aryl bonds.

The steric pressure in the five coordinate $[\text{MesN}_2\text{NR}]^{2-}$ complexes should be released upon activation to form the presumed four coordinate cationic species. The *mer* structure of $[\text{MesN}_2\text{NR}]^{2-}$ ligands in the dialkyl complexes presumably becomes a *fac* structure in the pseudo-tetrahedral monoalkyl cationic complexes as a consequence of minimizing the inter-ligand steric interaction. It should be noted that a prerequisite for this structural transformation is that the diamido/donor ligand backbone must not be rigid. Planar pyridine diamido complexes probably cannot efficiently form the pseudo-tetrahedral cationic intermediate due to the rigid pyridine fragment;^{121,123} therefore, the cationic metal center is not sterically well-shielded and some decompositions such as β elimination may be easily accessible. We propose that the *fac* or *mer* structure in the five coordinate dialkyl complexes is probably not the key to the development of active polymerization catalysts which contain the diamido/donor ligands, but the propensity to form the *fac* structure in the pseudo-tetrahedral cationic intermediate.

The bond strength of the donor atom coordination in the diamido/donor complexes is presumably stronger for cationic species than for the neutral precursors. Bond distance contraction ($\sim 0.162 \text{ \AA}$) is observed for the Zr-O bond when $[\text{t-BuNON}]\text{ZrMe}_2$ is activated to become zwitterionic $\{[\text{t-BuNON}]\text{ZrMe}\}\{\text{MeB}(\text{C}_6\text{F}_5)_3\}$.^{52,73} It is likely that an analogous bond distance contraction also takes place for the sp^3 nitrogen coordination in the $[\text{MesN}_2\text{NR}]^{2-}$ system, therefore increasing the tendency to form a pseudo-tetrahedral monoalkyl cationic complex.

The polymerization activity in this study depends on the cocatalyst employed following the reactivity order of $[\text{Ph}_3\text{C}][\text{B}(\text{C}_6\text{F}_5)_4] > [\text{HNMe}_2\text{Ph}][\text{B}(\text{C}_6\text{F}_5)_4] \gg \text{B}(\text{C}_6\text{F}_5)_3$. The presence of coordinating solvents such as diethyl ether dramatically decreases the polymerization activity. This phenomenon is consistent with the coordination nature of anions or potentially available bases to the cationic metal center. It has been shown that the cationic intermediates can be stabilized by an external base and the polymerization activity largely relies on the lability of this base. Early work by Jordan reveals that the cationic monomethyl zirconocene complex can be isolated as a THF adduct, which can only lead to low polymerization activity presumably due to strong coordination of the THF oxygen.^{174,175} Partial alkyl abstraction activated by $\text{B}(\text{C}_6\text{F}_5)_3$ has been reported in several cases to result in a zwitterionic structure^{52,118,157,158,176-179} in which the zwitter-anionic $[\text{RB}(\text{C}_6\text{F}_5)_3]^-$ moiety may be labile and replaced by incoming olefins. If $[\text{HNMe}_2\text{Ph}][\text{B}(\text{C}_6\text{F}_5)_4]$ is used as the cocatalyst, one of the coordination sites in the cation may be occupied by the liberated NMe_2Ph thus increasing the cation stability. Depending on the steric bulk of ligands in the cation, the coordinated NMe_2Ph may be labile.⁵² The solvent used for polymerization reactions may also act as the coordinating base; however, the lability of the solvent molecules usually lead to a less stable cation.⁵¹

The polymerization results described here should be compared to those found for the zirconium systems employing $[\text{t-BuNON}]\text{ZrMe}_2$ as an initiator, which yields poly(1-hexene) *via* primarily a 1,2-insertion process with little β elimination during synthesis of up to a 500mer.^{52,53} The reason that this system is successful is in part as a consequence of the significant steric crowding imposed by t-butyl substituents and the subsequent formation of relatively crowded pseudo-tetrahedral monoalkyl cations. It should be noted that a 2,1-insertion process may also be possible if the steric crowding of the cation is not significant. The 2,1-insertion product would have a different reactivity (presumably lower) and a different stability (presumably also lower) than a 1,2-insertion product, as has been proposed in propylene polymerization systems.^{87,96-99} Therefore we hypothesize that $[\text{MesN}_2\text{NR}]^{2-}$ is not as significantly crowded as $[\text{t-BuNON}]^{2-}$ and that 2,1 "mistake" insertion occurs in the former system. We also hypothesize that

$\{[\text{MesN}_2\text{NR}]\text{Zr}(\text{polymer})\}^+$ intermediates become more stable toward β elimination when R is a methyl group, in part because of a lower percentage of sterically more difficult 2,1-insertions.

These results should also be compared with those from the systems employing $[\text{ArN}_2\text{O}]\text{ZrMe}_2$ and $[\text{ArN}_2\text{S}]\text{ZrMe}_2$ initiators,^{71,72} in which the ligands are all comprised of essentially the same components as those in $[\text{MesN}_2\text{NR}]\text{ZrMe}_2$, i.e., ethylene backbone and arylated amides. The major difference between these ligands is the central donor atom (O, S, N) which may or may not contain a substituent. The *para* mesityl methyl groups in $[\text{MesN}_2\text{NR}]\text{ZrMe}_2$ are believed to have little influence on the polymerization. All of these systems show the tendency for chain termination during polymerization to give a polymer whose molecular weight seems to maximize at a certain number. These numbers are summarized in Table 3.4. The difference between these polymerization data presumably arises from the inherent property of O, S, and NR. Thus NR (R = H, Me) is superior to O and S as a donor as a consequence of having less

Table 3.4. Comparison of the poly(1-hexene) data obtained with $[\text{ArN}_2\text{O}]\text{ZrMe}_2$, $[\text{ArN}_2\text{S}]\text{ZrMe}_2$, and $[\text{MesN}_2\text{NR}]\text{ZrMe}_2$ (R = H, Me) initiators.^a

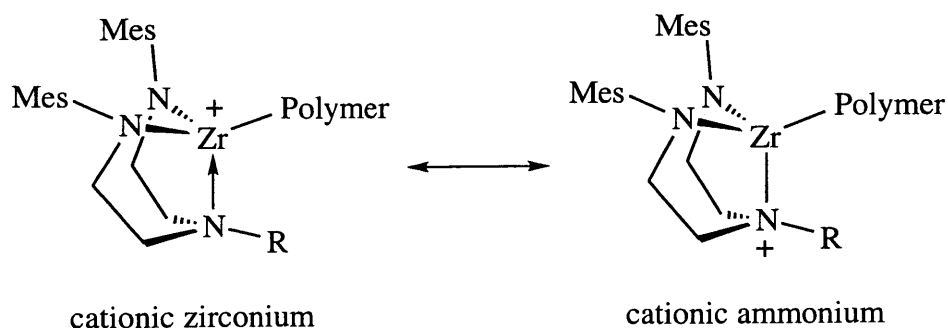
Initiator	Geometry	Donor	$10^{-3}M_n^b$	M_w/M_n	Yield(%)
$[\text{ArN}_2\text{O}]\text{ZrMe}_2^c$	<i>mer</i>	O	11.7	1.6	100
$[\text{ArN}_2\text{S}]\text{ZrMe}_2^c$	<i>fac</i>	S	16.0	1.2	86 ^d
$[\text{MesN}_2\text{NH}]\text{ZrMe}_2$	<i>mer</i>	NH	17.0	1.2	100
$[\text{MesN}_2\text{NMe}]\text{ZrMe}_2$	<i>mer</i>	NMe	28.7	1.4	100

^a Data were selected from the cited references with same condition: $[\text{Ph}_3\text{C}][\text{B}(\text{C}_6\text{F}_5)_4]$, 0 °C, 1 hour, chlorobenzene. ^b M_n indicates the maximal value of number average molecular weight.

^c See reference 72. ^d Quantitative yield may be obtained if the reaction time is 3 hours. Essentially identical M_n and M_w/M_n are listed in the cited reference.

percentage of chain termination, presumably due to the propensity of sp^3 nitrogen to assist the formation of pseudo-tetrahedral cations. The substituent on the amino nitrogen seems to sterically discourage mistake 2,1-insertions, even when the substituent is an H. In addition, the donor NR is also better than S in terms of having higher catalytic activity to complete the polymerization.⁷² We presume that this is due to the higher electronegativity of N (3.0) as compared to S (2.5),^{180,181} which would encourage the electrophilicity of the cation.

The stability of the active species in the diamido/donor systems is in contrast to that found for the chelating diamido system which lacks the central donor. Titanium complexes containing a propylene-linked diamido ligand can polymerize α -olefins in a living manner *only* in the presence of enormously excess monomer. After the monomer is nearly depleted, an irreversible decomposition terminates the polymerization.⁵¹ Zirconium complexes containing the diamido/ether ligand comprise another living system for the olefin polymerization in which the active species is stable (at 0 °C) in the absence of monomer.^{52,53} It is obvious that the coordination of the central donor atom in the diamido/donor ligands effectively increases the stability of the active species. Therefore, the cation stability presumably can be fine-tuned by changing the nature of the donor. Replacement of O by NMe as the donor seems to higher the thermal stability of the cation (up to 30 °C). Although some decompositions are found in the $[\text{MesN}_2\text{NR}]^{2-}$ system (Table 3.2), presumably due to the steric unsaturation of the ligand, controlled experiments (Table 3.3) reveal that the presumed decomposition products are still active even in the absence of monomer and able to initiate another polymer chain. This is also in contrast to that found for the propylene-linked diamido system which lacks a central donor atom.⁵¹ We propose that the thermal stability of cationic $\{[\text{MesN}_2\text{NR}]\text{Zr}(\text{polymer})\}^+$ is elevated by its cationic nature which can be stabilized by an ammonium resonance form shown in Scheme 3.4. It is also possible to form an oxonium resonance for the diamido/ether system, but an oxonium is not as energetically favorable as an ammonium.



Scheme 3.4. Proposed resonance contributors of the presumed cationic monoalkyl zirconium complex containing the diamidoamine ligands.

We have reasoned that steric crowding provided by the donor substituent in the diamido/donor ligands plays an important role on encouraging 1,2-insertion for chain propagation, as shown in the $[\text{MesN}_2\text{NMe}]^{2-}$ and $[\text{MesN}_2\text{NH}]^{2-}$ systems. The diamidoamine ligand system holds the promise to be sterically manipulated much easier than the diamido/ether system, in which no substituent can be attached to the central donor atom. Direct synthesis of the dialkyl complexes provides a fast means to screen the ligand system for catalytic polymerization purpose. The deprotonation-alkylation of a coordinated NH allows for the synthesis of a new ligand *on* the metal. This methodology is unique since the synthesis of the ligand itself may not be necessary. Electronically, $[\text{MesN}_2\text{NMe}]^{2-}$ is also different from $[\text{MesN}_2\text{NH}]^{2-}$, but we believe that the electronic effect is not as significant as the steric effect in this case. Two benzyl derivatives are designed for this purpose, but the nature of the electronic effect is not clear at this moment, although preliminary results reveal that they are both active species for α -olefin polymerization. It is also not clear that by which N-N-C face(s) the olefin approaches the metal center of the four coordinate cation, e.g., $\text{N}_{\text{amide}}\text{-N}_{\text{amide}}\text{-C}$ face versus two $\text{N}_{\text{amide}}\text{-N}_{\text{amine}}\text{-C}$ faces. A low (perhaps C_1) symmetric diamidoamine ligand system may provide a better insight for this unsolved but important question.

CONCLUSIONS

Group 4 dialkyl complexes containing the diamidoamine ligands of the type $[\text{MesN}_2\text{NR}]^{2-}$ have been synthesized from several different approaches. Among them, the direct synthesis provides an efficient way to make the catalyst precursors in virtually one step. Several alkyl groups can be attached to the amino nitrogen by a deprotonation-alkylation sequence. The amino nitrogen in $[\text{MesN}_2\text{NR}]\text{MMe}_2$ ($\text{M} = \text{Ti}, \text{Zr}, \text{Hf}$; $\text{R} = \text{H}, \text{Me}, \text{Bn}, \text{Bn}^{\text{F}}$) is found to tightly bind to all group 4 metals. Pseudo-tetrahedral geometry is found for the amino nitrogen. Consequently, no fluxional exchange between the two methyl ligands can be observed for $[\text{MesN}_2\text{NR}]\text{MMe}_2$.

Zirconium complexes of the type $[\text{MesN}_2\text{NR}]\text{ZrMe}_2$ ($\text{R} = \text{H}, \text{Me}, \text{Bn}, \text{Bn}^{\text{F}}$) are all active catalysts for the polymerization of 1-hexene when activated with boron derived Lewis acids. The polymerization rate depends on the cocatalysts employed following the reactivity order of $\text{B}(\text{C}_6\text{F}_5)_3 < [\text{HNMe}_2\text{Ph}][\text{B}(\text{C}_6\text{F}_5)_4] < [\text{Ph}_3\text{C}][\text{B}(\text{C}_6\text{F}_5)_4]$. No polymerization activity is observed when an oxygen donor such as diethyl ether is bound to zirconium. In terms of having less tendency towards β elimination, $[\text{MesN}_2\text{NMe}]\text{ZrMe}_2$ is superior to $[\text{MesN}_2\text{NH}]\text{ZrMe}_2$, which is better than the analogous compounds with O or S donor. Although the living polymerization activity for the diamidoamine system is currently not as high as that found for $[\text{t-BuNON}]\text{ZrMe}_2$, the enhanced thermal stability provided by the pseudo-tetrahedral amino donor promises the opportunity to design a catalyst with greater thermal stability and higher activity if the cation is sterically more crowded than that in the $[\text{MesN}_2\text{NMe}]^{2-}$ system.

EXPERIMENTAL SECTION^{\$}

General Procedures. Unless otherwise specified, all experiments were performed under nitrogen in a Vacuum Atmospheres glovebox (model HE-493) equipped with a regeneration/circulation device (Dri-Train) or by using standard Schlenk techniques. Oxygen level (< 2 ppm) were monitored with ZnEt₂ (1 M solution in hexane, Aldrich), and water levels (< 2 ppm) were monitored with TiCl₄ (neat, Strem). All solvents were reagent grade or better. Toluene was distilled from sodium/benzophenone ketyl. Diethyl ether and tetrahydrofuran were sparged with nitrogen and passed through two columns of activated alumina. Pentane was sparged with nitrogen, then passed through one column of activated alumina, and then through another of activated Q5.¹⁰⁰ Dichloromethane and chlorobenzene (Aldrich HPLC Grade, 99.9%) was distilled from CaH₂ under nitrogen. Molecular sieves and Celite were activated *in vacuo* (10⁻³ Torr) for 24 hours at 175 and 125 °C, respectively. All NMR solvents were sparged with nitrogen and dried over activated 4 Å molecular sieves for days prior to use. All dry solvents were degassed with nitrogen before introduction into the glovebox, where they were stored over activated 4 Å molecular sieves.

Spectroscopic Analyses. The NMR spectra were recorded on Varian instruments (¹H, 500.2 or 300.0 MHz; ¹⁹F, 470.6 or 282.1 MHz; ¹³C, 125.8 or 75.4 MHz). Chemical shifts (δ) are listed as parts per million downfield from tetramethylsilane and coupling constants (*J*) are in hertz. ¹H NMR spectra are referenced using the residual solvent peak at δ 7.16 for C₆D₆, δ 7.27 for CDCl₃, δ 7.29 for C₆D₅Br (the most upfield resonance), and δ 2.09 for toluene-*d*₈ (the most downfield resonance). ¹³C NMR spectra are referenced using the residual solvent peak at δ 128.39 for C₆D₆, and δ 137.86 for toluene-*d*₈ (the most downfield resonance). ¹⁹F NMR spectra are externally referenced using a chloroform solution of CFC₃ at δ 0. Routine coupling constants are not listed. All NMR spectra were recorded at room temperature unless otherwise noted. IR

^{\$} The compounds denoted with * in this section have been published in print:

Liang, L.-C.; Schrock, R. R.; Davis, W. M.; McConville, D. H. *J. Am. Chem. Soc.* **1999**, *121*, 5797.

spectra were recorded as films in specified solvents between NaCl plates on Perkin Elmer 1600 FTIR spectrometer. High resolution mass spectra were recorded on a Finnigan MAT 8200 Sector Mass Spectrometer at the MIT Department of Chemistry Instrumentation Facility. Elemental analyses were performed by H. Kolbe Mikroanalytisches Laboratorium, Mülheim an der Ruhr, Germany.

Polymer analyses. Gel permeation chromatography (GPC) analyses were carried out on a system equipped with two Jordi-Gel DVB Mixed Bed columns (250 mm length x 10 mm inner diameter) in series. HPLC grade CH_2Cl_2 was continuously dried and distilled from CaH_2 . Solvent was supplied at a flow rate of 1.0 mL/min with a Knauer 64 HPLC pump. A Wyatt Technology mini Dawn light scattering detector coupled to a Knauer differential-refractometer was employed. Solutions of samples dissolved in CH_2Cl_2 were filtered through a Millex-SR 0.5 μm filter. All GPC data were analyzed using Astrette 1.2 (Wyatt Technology). Values of the differential refractive index increment (dn/dc) were obtained under the assumption that all of the sample eluted from the column, and were averaged for various runs.⁵² The low value of dn/dc for poly(1-hexene) limited the accuracy of the data obtained *via* light scattering.

Starting materials. $\text{Zr}(\text{NMe}_2)_4$,⁷⁹ $\text{TiCl}_4(\text{THF})_2$,¹⁴¹ PhCH_2K ,¹⁸² and NpMgCl ¹⁰⁷ were prepared according to the literature procedures. $[\text{HNMe}_2\text{Ph}][\text{B}(\text{C}_6\text{F}_5)_4]$ and $[\text{Ph}_3\text{C}][\text{B}(\text{C}_6\text{F}_5)_4]$ were provided by Exxon Chemical Corporation. All other chemicals were purchased from commercial suppliers. Diethylenetriamine and mesityl bromide were sparged with nitrogen prior to use. MeLi was titrated with *i*-PrOH by employing 1,10-phenanthroline as an indicator. MeI and PhCH_2Br were dried over activated 4 Å molecular sieves for days prior to use. 1-Hexene was refluxed over sodium for four days and distilled. All other chemicals were used as received.

* **$\text{H}_2[\text{MesN}_2\text{NH}]$.** A 2 L one-armed Schlenk flask was charged with a magnetic stir bar, diethylenetriamine (23.450 g, 0.227 mol), mesityl bromide (90.51 g, 0.455 mol, 2 equiv.), tris(dibenzylideneacetone)dipalladium(0) (1.041 g, 1.14 mmol, 0.005 equiv.), rac-BINAP (2.123 g, 3.41 mmol, 0.015 equiv.), NaO-*t*-Bu (65.535 g, 0.682 mol, 3 equiv.), and toluene (800 mL).

The reaction mixture was heated to 95 °C with stirring and the reaction was monitored by ^1H NMR spectroscopy. After 4 days the reaction was complete with $\text{H}_2[\text{MesN}_2\text{NH}]$ being the only significant product. The solvent was removed *in vacuo* at ~50 °C to leave a dark brown solid residue. Diethyl ether (1 L) and water (1 L) were added to dissolve the solid residue and the aqueous portion was removed. The diethyl ether solution was washed with water (1 L x 3), saturated aqueous NaCl solution (0.5 L), and dried over MgSO_4 . The MgSO_4 was removed by filtration and the solvent was evaporated *in vacuo* to yield a red oil which was further heated at 70 °C overnight (~12 h) at 40 mTorr. The red oil crystallized upon cooling to room temperature under nitrogen to give red needle-like crystals; yield 71.10 g (92%). The red crystals were pure according to ^1H NMR spectrum and was used in subsequent organometallic reactions. Recrystallization from pentane or hexane gave yellow crystals; yield 65.45 g (85%). This reaction can be scaled up to give ~100 g of product: IR (CHCl_3): NH(st) 3357 cm^{-1} ; IR (Et_2O): NH(st) 3355 cm^{-1} ; ^1H NMR (C_6D_6) δ 6.83 (s, 4, H_m), 3.39 (br s, 2, ArylNH), 2.86 (t, 4, CH_2), 2.49 (t, 4, CH_2), 2.27 (s, 12, Me_o), 2.21 (s, 6, Me_p), 0.68 (br s, 1, CH_2NHCH_2); ^1H NMR (CDCl_3) δ 6.83 (s, 4, H_m), 3.08 (t, 4, CH_2), 2.89 (t, 4, CH_2), 2.29 (s, 12, Me_o), 2.24 (s, 6, Me_p), NH not found; ^{13}C NMR (C_6D_6) δ 143.74 (C, Aryl), 131.35 (C, Aryl), 129.83 (C, Aryl), 129.55 (CH, Aryl), 50.17 (CH_2), 48.56 (CH_2), 20.70 (Me_p), 18.51 (Me_o); HRMS (EI, 70 eV): m/z calcd. for $\text{C}_{22}\text{H}_{33}\text{N}_3$ 339.267448, found 339.26732. Anal. Calcd. for $\text{C}_{22}\text{H}_{33}\text{N}_3$: C, 77.83; H, 9.80; N, 12.38. Found: C, 77.85; H, 9.72; N, 12.31.

* **$[\text{MesN}_2\text{NH}]\text{Zr}(\text{NMe}_2)_2$.** Diethyl ether (15 mL) was added to a solid mixture of $\text{H}_2[\text{MesN}_2\text{NH}]$ (1.018 g, 3.00 mmol) and $\text{Zr}(\text{NMe}_2)_4$ (0.802 g, 3.00 mmol) at room temperature. The reaction mixture was stirred at room temperature overnight (~13 h). Insoluble materials were removed by filtration and washed with pentane (5 mL). The filtrate was concentrated *in vacuo* until the volume was ~5 mL. Pentane (~1 mL) was layered on top and the mixture was cooled to -30 °C to yield pale orange crystals. The crystals were collected on a glass frit, washed with pentane (~1 mL), and dried *in vacuo*; yield 990 mg (64%): ^1H NMR (C_6D_6) δ 6.96 (s, 2, H_m), 6.95 (s, 2, H_m), 3.36 (m, 2, CH_2), 3.05 (s, 6, Me), 3.01 (m, 2, CH_2), 2.61 (m, 4, CH_2), 2.47

(s, 6, Me), 2.45 (s, 6, Me), 2.28 (s, 6, Me), 2.21 (s, 6, Me), 1.80 (br s, 1, NH); ^{13}C NMR (C_6D_6) δ 150.48 (C, Aryl), 134.49 (C, Aryl), 132.06 (C, Aryl), 129.61 (C_m), 55.59 (CH_2), 49.26 (CH_2), 44.62 (ZrNMe), 41.27 (ZrNMe), 21.31 (Me_p), 19.52 (Me_o). Anal. Calcd. for $\text{C}_{26}\text{H}_{43}\text{N}_5\text{Zr}$: C, 60.42; H, 8.39; N, 13.55. Found: C, 60.31; H, 8.29; N, 13.39.

* **[MesN₂NH]ZrCl₂.** Neat Me_3SiCl (0.56 mL, 4.41 mmol, 3 equiv.) was added to a toluene solution (20 mL) of $[\text{MesN}_2\text{NH}]\text{Zr}(\text{NMe}_2)_2$ (755 mg, 1.461 mmol) at room temperature. The solution was stirred at room temperature overnight (~16 h). All volatile components were removed *in vacuo* until the volume reached ~5 mL. Pentane (7 mL) was added to the concentrated solution to precipitate the pale brown solid product, which was collected on a fritted funnel, washed with pentane (7 mL), and dried *in vacuo*; yield 635 mg (87%): ^1H NMR (C_6D_6) δ 6.88 (s, 2, H_m), 6.83 (s, 2, H_m), 3.32 (m, 2, CH_2), 2.86 (m, 2, CH_2), 2.50 (s, 6, *Me*-Aryl), 2.45 (m, 4, CH_2), 2.40 (s, 6, *Me*-Aryl), 2.20 (br s, 1, NH), 2.13 (s, 6, *Me*-Aryl); ^{13}C NMR (C_6D_6) δ 146.28 (C, Aryl), 135.52 (C, Aryl), 134.48 (C, Aryl), 134.14 (C, Aryl), 130.48 (C_m), 130.28 (C_m), 57.13 (CH_2), 49.43 (CH_2), 21.33 (Me, Aryl), 19.49 (Me, Aryl), 19.41 (Me, Aryl). Anal. Calcd. for $\text{C}_{22}\text{H}_{31}\text{Cl}_2\text{N}_3\text{Zr}$: C, 52.89; H, 6.25; N, 8.41. Found: C, 52.76; H, 6.35; N, 8.48.

* **[MesN₂NH]ZrMe₂. Method A:** MeMgI (0.1 mL, 3 M in diethyl ether, 0.3 mmol, 2 equiv.) was added to a diethyl ether solution (5 mL) of $[\text{MesN}_2\text{NH}]\text{ZrCl}_2$ (75 mg, 0.150 mmol) at $-30\text{ }^\circ\text{C}$. The reaction mixture was stirred at room temperature for 10 min; at this moment an aliquot was analyzed by ^1H NMR spectroscopy which showed quantitative formation of $[\text{MesN}_2\text{NH}]\text{ZrMe}_2$. 1,4-Dioxane (5 drops) was added and the precipitate was removed by filtration through Celite. The filtrate was concentrated *in vacuo* until the volume was ~1 mL. Pentane (2 mL) was added to the concentrated diethyl ether solution to precipitate the white solid product; yield 69 mg (76%). **Method B:** Solid ZrCl_4 (0.709 g, 3.043 mmol) was added in portions to a diethyl ether solution (20 mL) of $\text{H}_2[\text{MesN}_2\text{NH}]$ (1.033 g, 3.043 mmol) at $-30\text{ }^\circ\text{C}$ with vigorous stirring. The suspension was warmed to room temperature. Pale yellow solid precipitated gradually over a period of 1 h. The yellow suspension was cooled to $-30\text{ }^\circ\text{C}$ and MeMgI (4.1 mL, 3 M in diethyl ether, 12.3 mmol, 4.1 equiv.) was added. Gas evolved and the

solution turned white and cloudy immediately. The solution was stirred at room temperature for 10 min and 1,4-dioxane (1.2 g, 4.5 equiv.) was added. The reaction mixture was filtered through Celite, which was washed with diethyl ether (10 mL x 2). The yellow filtrate was concentrated *in vacuo* until the volume was ~20 mL. The concentrated solution was cooled to -30 °C for 1 h to give colorless crystals. The crystals were collected by filtration on a glass frit and dried *in vacuo*; yield 0.571g (41%). **Method C:** The procedures were analogous to those of Method B except that the adduct $\{H_2[MesN_2NH]\}ZrCl_4$ was formed from a suspension of $H_2[MesN_2NH]$ and $ZrCl_4$ in toluene at 80 °C overnight and that $MeMgBr$ was added to a toluene suspension of $\{H_2[MesN_2NH]\}ZrCl_4$. This condition produced 60 g of $[MesN_2NH]ZrMe_2$; yield 86%.¹⁷² X-ray quality crystals of $[MesN_2NH]ZrMe_2$ were grown from a mixture of diethyl ether, toluene, and hexamethyldisiloxane at -30 °C: 1H NMR (C_6D_6) δ 6.99 (s, 2, H_m), 6.97 (s, 2, H_m), 3.31 (m, 2, CH_2), 3.13 (m, 2, CH_2), 2.53 (s, 6, *Me*-Aryl), 2.43 (s, 6, *Me*-Aryl), 2.36 (m, 4, CH_2), 2.21 (s, 6, *Me*-Aryl), 1.16 (br s, 1, NH), 0.24 (s, 3, ZrMe), 0.07 (s, 3, ZrMe); 1H NMR (toluene-*d*₈) δ 6.89 (s, 2, H_m), 6.88 (s, 2, H_m), 3.26 (m, 2, CH_2), 3.11 (m, 2, CH_2), 2.47 (s, 6, *Me*-Aryl), 2.42 (m, 4, CH_2), 2.36 (s, 6, *Me*-Aryl), 2.16 (s, 6, *Me*-Aryl), 1.20 (br s, 1, NH), 0.13 (s, 3, ZrMe), -0.09 (s, 3, ZrMe); 1H NMR (toluene-*d*₈, 50 °C) δ 6.88 (s, 2, H_m), 6.87 (s, 2, H_m), 3.27 (m, 2, CH_2), 3.18 (m, 2, CH_2), 2.51 (m, 4, CH_2), 2.47 (s, 6, *Me*-Aryl), 2.35 (s, 6, *Me*-Aryl), 2.15 (s, 6, *Me*-Aryl), 1.42 (br s, 1, NH), 0.12 (s, 3, ZrMe), -0.16 (s, 3, ZrMe); ^{13}C NMR (C_6D_6) δ 146.56 (C, Aryl), 136.07 (C, Aryl), 135.55 (C, Aryl), 134.23 (C, Aryl), 130.29 (C_m), 129.98 (C_m), 57.46 (CH_2), 51.27 (CH_2), 42.45 (ZrMe), 39.63 (ZrMe), 21.44 (Me, Aryl), 19.39 (Me, Aryl), 19.28 (Me, Aryl). Anal. Calcd. for $C_{24}H_{37}N_3Zr$: C, 62.83; H, 8.13; N, 9.16. Found: C, 62.91; H, 8.02; N, 9.04.

$[MesN_2NH]ZrNpCl$. Method A: $NpMgCl$ (0.05 mL, 2.27 M in diethyl ether, 0.113 mmol) was added to a diethyl ether solution (10 mL) of $[MesN_2NH]ZrCl_2$ (53 mg, 0.106 mmol) at -30 °C. The reaction mixture was stirred at room temperature for 20 min and 1,4-dioxane (10 drops) was added. Insoluble materials were removed by filtration through Celite. The pale yellow filtrate was concentrated *in vacuo* until the volume was ~1 mL. Pentane (1 mL) was layered on top

and the solution was cooled to $-30\text{ }^{\circ}\text{C}$ to give a pale yellow crystalline solid. The supernatant was decanted and the solid was dried *in vacuo*; yield 49 mg (86%). **Method B:** The procedures were analogous to those of Method A except using two equiv. of NpMgCl . A reaction between $[\text{MesN}_2\text{NH}]\text{ZrCl}_2$ (150 mg, 0.300 mmol) and NpMgCl (0.27 mL, 2.27 M in diethyl ether, 0.613 mmol, 2 equiv.) produced crystalline $[\text{MesN}_2\text{NH}]\text{ZrNpCl}$; yield 48 mg (30%): ^1H NMR (C_6D_6) δ 6.95 (s, 2, H_m), 6.91 (s, 2, H_m), 3.23 (m, 2, CH_2), 3.04 (m, 2, CH_2), 2.54 (s, 6, *Me*-Aryl), 2.44 (s, 6, *Me*-Aryl), 2.42 (m, 4, CH_2), 2.16 (s, 6, *Me*-Aryl), 1.77 (br s, 1, NH), 1.26 (s, 9, $\text{ZrCH}_2\text{CMe}_3$), 1.05 (s, 2, $\text{ZrCH}_2\text{CMe}_3$); ^{13}C NMR (C_6D_6) δ 147.33 (C, Aryl), 134.80 (C, Aryl), 134.71 (C, Aryl), 134.68 (C, Aryl), 130.32 (C_m), 130.08 (C_m), 74.21 ($\text{ZrCH}_2\text{CMe}_3$), 66.26 ($\text{ZrCH}_2\text{CMe}_3$), 56.34 ($\text{NCH}_2\text{CH}_2\text{N}$), 49.01 ($\text{NCH}_2\text{CH}_2\text{N}$), 35.35 ($\text{ZrCH}_2\text{CMe}_3$), 21.36 (Me, Aryl), 20.07 (Me, Aryl), 19.84 (Me, Aryl). Anal. Calcd. for $\text{C}_{27}\text{H}_{42}\text{ClN}_3\text{Zr}$: C, 60.58; H, 7.91; N, 7.85. Found: C, 60.65; H, 8.03; N, 7.75.

$[\text{MesN}_2\text{NMe}]\text{ZrI}_2$. MeLi (1.9 mL, 1.4 M in diethyl ether, 2.66 mmol) was added to a diethyl ether solution (50 mL) of $[\text{MesN}_2\text{NH}]\text{Zr}(\text{NMe}_2)_2$ (1.347 g, 2.61 mmol) at $-30\text{ }^{\circ}\text{C}$. The mixture was stirred at room temperature for 2 h and cooled to $-30\text{ }^{\circ}\text{C}$. MeI (3.9 mL, 62.65 mmol, 24 equiv.) was added to the cold solution and the reaction was monitored by ^1H NMR spectroscopy which showed quantitative formation of $[\text{MesN}_2\text{NMe}]\text{ZrI}_2$ in 3 days. The solvent was removed *in vacuo*. The product was extracted with CH_2Cl_2 (50 mL) and the extract was filtered through Celite to remove LiI. The filtrate was concentrated *in vacuo* until the volume was $\sim 1\text{ mL}$ to give a pale yellow crystalline solid. The supernatant was decanted and the solid was dried *in vacuo*; yield 1.717 g (94%): ^1H NMR (C_6D_6) δ 6.88 (s, 2, H_m), 6.83 (s, 2, H_m), 3.31 (m, 2, CH_2), 2.90 (m, 2, CH_2), 2.68 (s, 6, *Me*-Aryl), 2.57 (m, 2, CH_2), 2.38 (s, 6, *Me*-Aryl), 2.30 (s, 3, NMe), 2.21 (m, 2, CH_2), 2.11 (s, 6, *Me*-Aryl); ^{13}C NMR (C_6D_6) δ 146.27 (C, Aryl), 136.30 (C, Aryl), 134.11 (C, Aryl), 133.82 (C, Aryl), 130.95 (C_m), 130.53 (C_m), 57.73 (CH_2), 56.62 (CH_2), 48.62 (NMe), 21.36 (Me_o), 20.40 (Me_p). Anal. Calcd. for $\text{C}_{23}\text{H}_{33}\text{I}_2\text{N}_3\text{Zr}$: C, 39.66; H, 4.78; N, 6.03. Found: C, 39.48; H, 4.86; N, 5.93.

[MesN₂NMe]Zr(OTf)₂. MeLi (0.1 mL, 2.12 M in diethyl ether, 2.12 mmol) was added to a solution of [MesN₂NH]Zr(NMe₂)₂ (108 mg, 0.209 mmol) in diethyl ether (3 mL) at -30 °C. The solution was stirred at room temperature for 2 h and a reaction aliquot was analyzed by ¹H NMR spectroscopy which showed the quantitative formation of [MesN₂NLi]Zr(NMe₂)₂(OEt₂): ¹H NMR (C₆D₆) δ 7.00 (s, 4, Aryl), 3.93 (m, 2, CH₂), 3.52 (br s, 6), 3.10 (q, 4, OCH₂CH₃), 2.86 (br s, 6), 2.58 (br s, 6), 2.47 (br s, 6), 2.26 (s, 12, NMe), 0.95 (t, 6, OCH₂CH₃). The diethyl ether suspension of [MesN₂NLi]Zr(NMe₂)₂(OEt₂) was cooled to -30 °C and MeOTf (0.09 mL, 0.820 mol, 3.9 equiv.) was added. The solution color immediately changed from orange to yellow upon addition of MeOTf. The reaction mixture was stirred at room temperature for 15 min and filtered through Celite. The filtrate was concentrated *in vacuo* until the volume was ~1 mL and pentane (~2 mL) was added to precipitate the crude product which was recrystallized from concentrated diethyl ether solution at -30 °C to give colorless crystals; yield 88 mg (57%): ¹H NMR (C₆D₆) δ 6.83 (s, 2, H_m), 6.75 (s, 2, H_m), 3.31 (m, 2, CH₂), 2.88 (m, 2, CH₂), 2.72 (m, 2, CH₂), 2.57 (s, 3, NMe), 2.46 (m, 2, CH₂), 2.35 (s, 6, *Me*-Aryl), 2.20 (s, 6, *Me*-Aryl), 2.10 (s, 6, *Me*-Aryl); ¹⁹F NMR (C₆D₆) δ -77.34 (s, 3, OTf), -77.49 (s, 3, OTf). Anal. Calcd. for C₂₅H₃₃F₆N₃O₆S₂Zr: C, 40.53; H, 4.49; N, 5.67. Found: C, 40.68; H, 4.38; N, 5.59.

[MesN₂NMe]ZrMe(OTf). MeLi (0.16 mL, 2.8 M in diethyl ether, 0.448 mmol, 2.3 equiv.) was added to a diethyl ether solution (4 mL) of [MesN₂NH]Zr(NMe₂)₂ (102 mg, 0.197 mmol) at -30 °C. The clear solution turned cloudy immediately. The reaction mixture was stirred at room temperature for 2 h and cooled to -30 °C. MeOTf (0.07 mL, 0.638 mmol, 3.2 equiv.) was added to this cold orange suspension. The suspension turned pale yellow immediately. The reaction mixture was stirred at room temperature for 15 min. Insoluble materials were removed by filtration through Celite and washed with pentane (2 mL). The filtrate was concentrated until the volume was ~1 mL and cooled to -30 °C to give a pale yellow crystalline solid. The supernatant was decanted and the product was dried *in vacuo*; yield 70 mg (58%). The crystals of the product contain one equiv. of diethyl ether according to ¹H NMR and elemental analysis: ¹H NMR (C₆D₆)

δ 6.94 (s, 2, H_m), 6.92 (s, 2, H_m), 3.36 (m, 2, CH₂), 3.05 (m, 2, CH₂), 2.67 (m, 2, CH₂), 2.45 (s, 6, *Me*-Aryl), 2.30 (s, 6, *Me*-Aryl), 2.25 (s, 3, NMe), 2.18 (s, 6, *Me*-Aryl), 2.13 (m, 2, CH₂), 0.51 (s, 3, ZrMe); ¹³C NMR (C₆D₆) δ 145.29 (C, Aryl), 135.36 (C, Aryl), 134.96 (C, Aryl), 134.42 (C, Aryl), 130.43 (C_m), 130.19 (C_m), 58.12 (CH₂), 56.53 (OTf, ¹J_{CF} = 167), 54.78 (CH₂), 46.25 (Me), 38.67 (Me), 21.26 (Me, Aryl), 19.28 (Me, Aryl), 18.80 (Me, Aryl); ¹⁹F NMR (C₆D₆) δ -77.92 (OTf). Anal. Calcd. for C₂₉H₄₆F₃N₃O₄SZr: C, 51.15; H, 6.81; N, 6.17. Found: C, 51.01; H, 6.74; N, 6.08.

* **[MesN₂NMe]ZrMe₂. Method A:** MeMgI (0.14 mL, 3 M in diethyl ether, 0.42 mmol, 2 equiv.) was added to a diethyl ether solution (3 mL) of [MesN₂NMe]ZrI₂ (137 mg, 0.197 mmol) at -30 °C. The reaction mixture was stirred at room temperature for 40 min and 1,4-dioxane (5 drops) was added. Insoluble materials were removed by filtration through Celite and washed with diethyl ether (2 mL). The filtrate was concentrated *in vacuo* until the volume was ~1 mL. The concentrated solution was cooled to -30 °C for 3 h to give a colorless crystalline solid. The supernatant was decanted and the product was dried *in vacuo*; yield 63 mg (68%). **Method B:** MeLi (0.15 mL, 1.4 M in diethyl ether, 0.21 mmol) was added to a diethyl ether suspension (3 mL) of [MesN₂NH]ZrMe₂ (98 mg, 0.21 mmol) at -30 °C. The cloudy and white suspension became homogeneous, pale yellow immediately. The solution was stirred at room temperature for 1 h and cooled to -30 °C. MeI (45 mg, 0.32 mmol, 1.5 equiv.) was added to the cold solution and the reaction mixture was stirred at room temperature for 1 h. All volatile components were removed *in vacuo*. The solid residue was extracted with toluene (5 mL) and the toluene extract was filtered through Celite. Toluene was removed from the filtrate *in vacuo* and the solid residue was partially dissolved in pentane (10 mL). The volume of the pentane solution was reduced *in vacuo* until the volume was ~2 mL to afford a colorless crystalline solid. The concentrated solution was cooled to -30 °C for 2 h. The supernatant was decanted and the product was dried *in vacuo*; yield 64 mg (63%). **Method C:** MeLi (1.44 mL, 2.12 M in diethyl ether, 3.05 mmol, 3.1 equiv.) was added to a diethyl ether solution (10 mL) of [MesN₂NH]Zr(NMe₂)₂ (507 mg, 0.981 mmol) at -30 °C. The reaction mixture was stirred at room temperature for 2 h and cooled to

-30 °C. MeOTf (0.43 mL, 3.920 mmol, 4 equiv.) was added to the cold solution. The reaction mixture was stirred at room temperature for 15 min and the solvent was removed *in vacuo*. The solid residue was triturated and extracted with pentane (20 mL x 3). The extract was filtered through Celite and concentrated *in vacuo* to give a white crystalline solid; yield 181 mg (39%).

Method D: MeLi (0.08 mL, 1.4 M in diethyl ether, 0.112 mmol) was added to a diethyl ether solution (3 mL) of [MesN₂NMe]ZrMe(OTf) (71 mg, 0.117 mmol) at -30 °C. The reaction mixture was stirred at room temperature for 1 h and the solvent was removed *in vacuo*. The solid residue was extracted with pentane (10 mL) and stirred at room temperature for 30 min. Insoluble materials were removed by filtration through Celite and washed with pentane (1 mL). The filtrate was concentrated *in vacuo* until the volume was ~1 mL. The concentrated solution was cooled to -30 °C to give a colorless crystalline solid. The supernatant was decanted and the product was dried *in vacuo*; yield 38 mg (69%).

Method E: This method can be regarded as a combination of the Method C of [MesN₂NH]ZrMe₂ and the Method B of [MesN₂NMe]ZrMe₂. MeMgBr (5 equiv.) was added to a diethyl ether suspension of {H₂[MesN₂NH]}ZrCl₄ to give [MesN₂NMe]ZrMe₂ on a scale of 8 g; yield 95%.¹⁷² X-ray quality crystals were grown from a saturated solution of diethyl ether and pentane at -30 °C: ¹H NMR (C₆D₆) δ 6.99 (s, 2, H_m), 6.95 (s, 2, H_m), 3.62 (m, 2, CH₂), 2.98 (m, 2, CH₂), 2.66 (m, 2, CH₂), 2.47 (s, 6, *Me*-Aryl), 2.44 (s, 6, *Me*-Aryl), 2.20 (s, 6, *Me*-Aryl), 2.12 (m, 2, CH₂), 2.01 (s, 3, NMe), 0.26 (s, 3, ZrMe), 0.23 (s, 3, ZrMe); ¹H NMR (toluene-*d*₈) δ 6.89 (s, 2, H_m), 6.86 (s, 2, H_m), 3.58 (m, 2, CH₂), 3.01 (m, 2, CH₂), 2.68 (m, 2, CH₂), 2.43 (s, 6, *Me*-Aryl), 2.37 (s, 6, *Me*-Aryl), 2.19 (m, 2, CH₂), 2.14 (s, 6, *Me*-Aryl), 2.08 (s, 3, NMe), 0.15 (s, 3, ZrMe), 0.06 (s, 3, ZrMe); ¹H NMR (C₆D₅Br) δ 6.87 (s, 2, H_m), 6.84 (s, 2, H_m), 3.71 (m, 2, CH₂), 3.06 (m, 2, CH₂), 2.94 (m, 2, CH₂), 2.49 (m, 2, CH₂), 2.40 (s, 6, *Me*-Aryl), 2.34 (s, 6, *Me*-Aryl), 2.28 (s, 3, NMe), 2.14 (s, 6, *Me*-Aryl), 0.04 (s, 3, ZrMe), -0.03 (s, 3, ZrMe); ¹³C NMR (C₆D₆) δ 146.13 (C, Aryl), 136.63 (C, Aryl), 136.08 (C, Aryl), 134.32 (C, Aryl), 130.36 (C_m), 130.05 (C_m), 61.14 (CH₂), 55.89 (CH₂), 43.31 (Me), 40.62 (Me), 37.10 (Me), 21.42 (Me, Aryl), 19.20 (Me, Aryl), 19.09 (Me,

Aryl). Anal. Calcd. for $C_{25}H_{39}N_3Zr$: C, 63.51; H, 8.31; N, 8.89. Found: C, 63.26; H, 8.14; N, 8.85.

[MesN₂NMe]ZrBn₂. $\{H_2[MesN_2NH]\}ZrCl_4$ was synthesized by heating a toluene suspension of $H_2[MesN_2NH]$ and $ZrCl_4$ at 80 °C overnight. Solid $\{H_2[MesN_2NH]\}ZrCl_4$ was filtered, washed with toluene, and dried *in vacuo*. Solid $PhCH_2K$ (227 mg, 1.743 mmol, 5 equiv.) was added in portions to a white suspension of $\{H_2[MesN_2NH]\}ZrCl_4$ (200 mg, 0.349 mmol) in diethyl ether (4 mL) at -30 °C. The orange suspension was stirred at room temperature for 1 h, during which time the orange color faded gradually to become pale yellow. The pale yellow suspension was cooled to -30 °C and a diethyl ether solution (2 mL) of MeI (50 mg, 0.352 mmol) at -30 °C was added. The reaction mixture was stirred at room temperature for 45 min. All volatile materials were removed *in vacuo*. The solid residue was triturated with pentane (5 mL) and filtered through Celite. The solvent was removed from the filtrate to give an oily residue. The oil was redissolved in diethyl ether (1 mL) and the solution was cooled to -30 °C overnight to give yellow crystals. The supernatant was decanted and the crystals were dried *in vacuo*; yield 49 mg (22%): 1H NMR (C_6D_6) δ 7.09 (t, 2, Aryl), 7.02 (t, 2, Aryl), 6.97 (s, 2, Aryl), 6.94 (s, 2, Aryl), 6.89 (t, 2, Aryl), 6.22 (d, 2, Aryl), 6.50 (d, 2, Aryl), 3.33 (m, 2, CH₂), 3.27 (m, 2, CH₂), 2.80 (m, 2, CH₂), 2.50 (s, 6, *Me*-Aryl), 2.44 (s, 6, *Me*-Aryl), 2.19 (s, 6, *Me*-Aryl), 2.16 (m, 2, CH₂), 2.05 (s, 3, NMe), 1.80 (s, 2, ZrCH₂Ph), 1.70 (s, 2, ZrCH₂Ph); ^{13}C NMR (C_6D_6) δ 147.85, 135.67, 134.69, 130.76, 130.22, 129.87, 129.45, 127.58, 123.01, 122.28, 65.24 (ZrCH₂Ph), 64.15 (ZrCH₂Ph), 58.05 (NCH₂CH₂N), 55.34 (NCH₂CH₂N), 42.98 (NMe), 21.32 (Me, Aryl), 20.40 (Me, Aryl), 19.78 (Me, Aryl). Anal. Calcd. for $C_{37}H_{47}N_3Zr$: C, 71.10; H, 7.58; N, 6.72. Found: C, 70.88; H, 7.50; N, 6.67.

[MesN₂NBn]Zr(NMe₂)₂ and [MesN₂NBn]ZrCl₂. MeLi (0.12 mL, 2.12 M in diethyl ether, 0.254 mmol) was added to a diethyl ether solution (3 mL) of $[MesN_2NH]Zr(NMe_2)_2$ (130 mg, 0.252 mmol) at -30 °C. The reaction mixture was stirred at room temperature for 2 h and cooled to -30 °C. To this cold solution was added a cold diethyl ether solution (3 mL, -30 °C) of $PhCH_2Br$ (0.03 mL, 0.252 mmol). The reaction mixture was stirred at room temperature for 2 h,

at which time a reaction aliquot was analyzed by ^1H NMR spectroscopy which showed quantitative formation of $[\text{MesN}_2\text{NBn}]\text{Zr}(\text{NMe}_2)_2$: ^1H NMR (C_6D_6) δ 7.14 (m, 2, Ph), 7.02 (m, 3, Ph), 6.98 (s, 2, H_m , Mes), 6.96 (s, 2, H_m , Mes), 4.12 (s, 2, NCH_2Ph), 3.37 (m, 2, $\text{NCH}_2\text{CH}_2\text{N}$), 3.27 (m, 2, $\text{NCH}_2\text{CH}_2\text{N}$), 3.19 (s, 6, ZrNMe), 2.74 (m, 4, $\text{NCH}_2\text{CH}_2\text{N}$), 2.57 (s, 6, *Me*-Aryl), 2.50 (s, 6, *Me*-Aryl), 2.42 (s, 6, ZrNMe), 2.23 (s, 6, *Me*-Aryl). All volatile materials were removed *in vacuo* and toluene (3 mL) was added. Me_3SiCl (0.1 mL, 0.756 mmol, 3 equiv.) was added to this toluene suspension at room temperature with stirring. The reaction was monitored by analyzing a reaction aliquot by ^1H NMR spectroscopy which showed quantitative formation of $[\text{MesN}_2\text{NBn}]\text{ZrCl}_2$ in 2 days. All volatile components were removed *in vacuo* and the product was extracted with CH_2Cl_2 (5 mL). LiBr was removed by filtration through Celite and the solvent was removed *in vacuo*. The colorless crystalline solid was washed with pentane (2 mL) and dried *in vacuo*; overall yield 123 mg (83%): ^1H NMR (C_6D_6 ; chemical shifts may vary within ~ 0.3 ppm depending on the concentration) δ 7.07 (m, 3, Ph), 6.91 (s, 2, H_m , Mes), 6.86 (s, 2, H_m , Mes), 6.77 (m, 2, Ph), 4.36 (s, 2, NCH_2Ph), 3.41 (m, 2, $\text{NCH}_2\text{CH}_2\text{N}$), 3.17 (m, 2, $\text{NCH}_2\text{CH}_2\text{N}$), 2.70 (m, 2, $\text{NCH}_2\text{CH}_2\text{N}$), 2.69 (s, 3, *Me*-Aryl), 2.68 (s, 3, *Me*-Aryl), 2.63 (m, 2, $\text{NCH}_2\text{CH}_2\text{N}$), 2.46 (s, 3, *Me*-Aryl), 2.44 (s, 3, *Me*-Aryl), 2.41 (s, 6, *Me*-Aryl); ^{13}C NMR (C_6D_6) δ 146.58 (C, Aryl), 135.78 (C, Aryl), 134.45 (C, Aryl), 134.11 (C, Aryl), 132.27 (CH, Aryl), 132.02 (C, Aryl), 130.61 (CH, Aryl), 130.25 (CH, Aryl), 129.18 (CH, Aryl), 129.01 (CH, Aryl), 59.60 (NCH_2Ph), 55.56 (NCH_2), 52.73 (NCH_2), 21.31 (*Me*-Aryl), 19.84 (*Me*-Aryl), 19.40 (*Me*-Aryl). Anal. Calcd. for $\text{C}_{29}\text{H}_{37}\text{Cl}_2\text{N}_3\text{Zr}$: C, 59.06; H, 6.32; N, 7.12. Found: C, 58.89; H, 6.30; N, 7.04.

$[\text{MesN}_2\text{NBn}]\text{ZrMe}_2$. MeLi (0.48 mL, 1.4 M in diethyl ether, 0.672 mmol) was added to a diethyl ether solution (10 mL) of $[\text{MesN}_2\text{NH}]\text{ZrMe}_2$ (306 mg, 0.667 mmol) at -30°C . The solution was stirred at room temperature for 1 h and cooled to -30°C . To this cold solution was added a diethyl ether solution (2 mL) of PhCH_2Br (114 mg, 0.667 mmol) at -30°C . The clear solution became yellow and cloudy in 10 seconds. The reaction mixture was stirred at room temperature for 30 min. (**Note:** Longer reaction time led to the decomposition of

[MesN₂NBn]ZrMe₂.) The volatile components were removed *in vacuo* and the residue was extracted with dichloromethane (20 mL). The extract was filtered through Celite and the solvent was completely removed *in vacuo* to give a colorless solid. The solid product was washed with pentane (2 mL x 2) and dried *in vacuo*; yield 255 mg (70%): ¹H NMR (C₆D₆) δ 7.11-6.99 (m, 9, Aryl), 3.96 (s, 2, NCH₂Ph), 3.90 (m, 2, NCH₂CH₂N), 3.13 (m, 2, NCH₂CH₂N), 2.61 (m, 2, NCH₂CH₂N), 2.58 (s, 6, *Me*-Aryl), 2.51 (m, 2, NCH₂CH₂N), 2.47 (s, 6, *Me*-Aryl), 2.21 (s, 6, *Me*-Aryl), 0.38 (s, 3, ZrMe), 0.27 (s, 3, ZrMe); ¹H NMR (toluene-*d*₈; the intensities of the aromatic resonances are not certain due to their overlap with residual C₇H₈ signals) δ 7.11 (m, Aryl), 6.98 (m, Aryl), 6.94 (s, 2, Aryl), 6.93 (s, 2, Aryl), 3.96 (s, 2, NCH₂Ph), 3.85 (m, 2, NCH₂CH₂N), 3.13 (m, 2, NCH₂CH₂N), 2.65 (m, 2, NCH₂CH₂N), 2.56 (s, 6, *Me*-Aryl), 2.51 (m, 2, NCH₂CH₂N), 2.43 (s, 6, *Me*-Aryl), 2.19 (s, 6, *Me*-Aryl), 0.30 (s, 3, ZrMe), 0.13 (s, 3, ZrMe); ¹³C NMR (toluene-*d*₈; the assignment of aromatic signals and mesityl methyl signals is incomplete due to their overlap with residual C₇H₈ signals) δ 145.82, 136.05, 135.55, 133.97, 132.02, 130.05, 129.95, 110.36, 104.35, 55.33 (CH₂), 54.55 (CH₂), 43.43 (CH₂), 40.37 (ZrMe), 35.00 (ZrMe), 19.15 (*Me*-Aryl), 18.75 (*Me*-Aryl). Anal. Calcd. for C₃₁H₄₃N₃Zr: C, 67.83; H, 7.90; N, 7.66. Found: C, 67.62; H, 8.03; N, 7.59.

[MesN₂NBn^F]Zr(NMe₂)₂ and [MesN₂NBn^F]ZrCl₂. MeLi (0.16 mL, 1.4 M in diethyl ether, 0.224 mmol) was added to a diethyl ether solution (5 mL) of [MesN₂NH]Zr(NMe₂)₂ (121 mg, 0.234 mmol) at -30 °C. The reaction mixture was stirred at room temperature for 1 h and cooled to -30 °C. To this cold solution was added a diethyl ether solution (2 mL) of C₆F₅CH₂Br (61 mg, 0.234 mmol) at -30 °C and the solution was stirred at room temperature for 2 h to give [MesN₂NBn^F]Zr(NMe₂)₂ quantitatively according to the ¹H and ¹⁹F NMR spectra: ¹H NMR (C₆D₆) δ 6.94 (s, 4, H_m), 4.01 (s, 2, NCH₂C₆F₅), 3.40 (m, 2, NCH₂CH₂N), 3.24 (m, 2, NCH₂CH₂N), 3.18 (s, 6, ZrNMe), 2.62 (m, 4, NCH₂CH₂N), 2.50 (s, 6, *Me*-Aryl), 2.48 (s, 6, ZrNMe), 2.36 (s, 6, *Me*-Aryl), 2.19 (s, 6, *Me*-Aryl); ¹⁹F NMR (C₆D₆) δ -134.19 (d, 2, F_o), -153.87 (t, 1, F_p), -162.38 (t, 2, F_m). All volatile materials were removed *in vacuo* and toluene (3 mL) was added. To this toluene solution was added Me₃SiCl (0.09 mL, 0.702 mmol, 3 equiv.)

and the mixture was stirred at room temperature. The reaction was monitored by analyzing an aliquot of its ^1H NMR spectrum which showed quantitative formation of $[\text{MesN}_2\text{NBn}^{\text{F}}]\text{ZrCl}_2$ in 24 h. LiBr was removed by filtration with Celite and the filtrate was concentrated *in vacuo* (at $\sim 50^\circ\text{C}$) until the volume was ~ 0.5 mL. Pentane (2 mL) was added to the concentrated toluene solution to precipitate a white solid. The supernatant was decanted and the solid was dried *in vacuo*; overall yield 120 mg (75%): ^1H NMR (C_6D_6) δ 6.90 (s, 2, H_m), 6.83 (s, 2, H_m), 4.30 (s, 2, $\text{NCH}_2\text{C}_6\text{F}_5$), 3.47 (m, 2, $\text{NCH}_2\text{CH}_2\text{N}$), 3.25 (m, 2, $\text{NCH}_2\text{CH}_2\text{N}$), 2.66 (m, 4, $\text{NCH}_2\text{CH}_2\text{N}$), 2.57 (s, 6, *Me*-Aryl), 2.46 (s, 6, *Me*-Aryl), 2.14 (s, 6, *Me*-Aryl); ^{19}F NMR (C_6D_6) δ -137.72 (d, 2, F_o), -152.09 (t, 1, F_p), -161.83 (t, 2, F_m); ^{13}C NMR (C_6D_6) δ 145.86 (C, Aryl), 136.07 (C, Aryl), 134.36 (C, Aryl), 133.95 (C, Aryl), 130.74 (C_m), 130.53 (C_m), 55.34 (CH_2), 52.75 (CH_2), 46.67 (CH_2), 21.30 (Me, Aryl), 19.72 (Me, Aryl), 19.47 (Me, Aryl), CF not found. Anal. Calcd. for $\text{C}_{29}\text{H}_{32}\text{Cl}_2\text{F}_5\text{N}_3\text{Zr}$: C, 51.25; H, 4.75; N, 6.18. Found: C, 51.32; H, 4.70; N, 6.24.

$[\text{MesN}_2\text{NBn}^{\text{F}}]\text{ZrMe}_2$. MeLi (0.37 mL, 1.4 M in diethyl ether, 0.518 mmol) was added to a diethyl ether solution (10 mL) of $[\text{MesN}_2\text{NH}]\text{ZrMe}_2$ (240 mg, 0.523 mmol) at -30°C . The solution was stirred at room temperature for 1 h and cooled to -30°C . To this cold solution was added a diethyl ether solution (3 mL) of $\text{C}_6\text{F}_5\text{CH}_2\text{Br}$ (136 mg, 0.521 mmol) at -30°C . The reaction mixture was stirred at room temperature for 2 h. All volatile components were removed *in vacuo*. The residue was extracted with toluene (10 mL) and the extract was filtered through Celite. The solvent was completely removed *in vacuo* to give an orange solid. The solid was gently washed with cold pentane (2 mL x 2) to give pale a yellow solid; yield 301 mg (90%): ^1H NMR (C_6D_6) δ 6.96 (s, 2, H_m), 6.95 (s, 2, H_m), 3.85 (s, 2, $\text{NCH}_2\text{C}_6\text{F}_5$), 3.62 (m, 2, $\text{NCH}_2\text{CH}_2\text{N}$), 3.30 (m, 2, $\text{NCH}_2\text{CH}_2\text{N}$), 2.61 (s, 6, *Me*-Aryl), 2.48 (m, 4, $\text{NCH}_2\text{CH}_2\text{N}$), 2.41 (s, 6, *Me*-Aryl), 2.18 (s, 6, *Me*-Aryl), 0.42 (s, 3, ZrMe), 0.05 (s, 3, ZrMe); ^{19}F NMR (C_6D_6) δ -138.18 (d, 2, F_o), -153.07 (t, 1, F_p), -161.96 (t, 2, F_m); ^{13}C NMR (C_6D_6) δ 145.31 (C, Aryl), 136.00 (C, Aryl), 135.53 (C, Aryl), 134.86 (C, Aryl), 130.50 (C_m), 130.28 (C_m), 55.48 (CH_2), 54.18 (CH_2), 44.29 (CH_2), 42.43 (ZrMe), 38.85 (ZrMe), 21.59 (Me, Aryl), 19.76 (Me, Aryl),

19.49 (Me, Aryl), CF not found. Anal. Calcd. for $C_{31}H_{38}F_5N_3Zr$: C, 58.28; H, 6.00; N, 6.58. Found: C, 58.35; H, 6.10; N, 6.47.

* **[MesN₂NH]TiMe₂**. Solid $TiCl_4(THF)_2$ (97 mg, 0.290 mmol) was added to a THF solution (5 mL) of $H_2[MesN_2NH]$ (99 mg, 0.291 mmol) at -30 °C with vigorous stirring. The reaction mixture immediately became dark red. The solution was stirred at room temperature for 50 min and cooled to -30 °C. MeMgI (0.39 mL, 3 M in diethyl ether, 1.17 mmol, 4 equiv.) was added to this cold solution. Gas evolved immediately and the red solution lightened in color. The solution was stirred at room temperature for 10 min and all volatile components were removed *in vacuo*. The solid residue was extracted with pentane (8 mL) and the extract was filtered through Celite. The filtrate was concentrated *in vacuo* until the volume was ~ 1 mL and the concentrated solution was cooled to -30 °C for 6 h to give a red crystalline solid. The supernatant was decanted and the solid was dried *in vacuo*; yield 41 mg (34%): ¹H NMR (C_6D_6) δ 7.03 (s, 2, H_m), 6.93 (s, 2, H_m), 3.55 (m, 2, CH₂), 3.20 (m, 2, CH₂), 2.72 (s, 6, Me-Aryl), 2.37 (m, 4, CH₂), 2.34 (s, 6, Me-Aryl), 2.21 (s, 6, Me-Aryl), 1.03 (br s, 1, NH), 0.84 (s, 3, TiMe), 0.49 (s, 3, TiMe); ¹³C NMR (C_6D_6) δ 151.61 (C, Aryl), 134.22 (C, Aryl), 133.78 (C, Aryl), 133.11 (C, Aryl), 130.08 (C_m), 129.98 (C_m), 63.55 (TiMe), 58.89 (CH₂), 48.83 (TiMe), 48.02 (CH₂), 21.38 (Me, Aryl), 19.75 (Me, Aryl), 19.35 (Me, Aryl). Anal. Calcd. for $C_{24}H_{37}N_3Ti$: C, 69.38; H, 8.98; N, 10.11. Found: C, 69.03; H, 8.81; N, 10.26.

[MesN₂NMe]TiMe₂. MeLi (0.1 mL, 1.4 M in diethyl ether) was added to a diethyl ether solution (5 mL) of $[MesN_2NH]TiMe_2$ (56 mg, 0.135 mmol) at -30 °C. The orange solution was stirred at room temperature for 1 h and cooled to -30 °C. MeI (29 mg, 0.204 mmol, 1.5 equiv.) was added to the cold solution and the reaction mixture was stirred at room temperature for 4 h, at which time a reaction aliquot was analyzed by ¹H NMR spectroscopy which showed quantitative formation of $[MesN_2NMe]TiMe_2$. All volatile components were removed *in vacuo*. The residue was extracted with pentane (5 mL) and filtered through Celite. The filtrate was concentrated *in vacuo* until the volume was ~1 mL. The concentrated solution was cooled to -30 °C to give a yellow crystalline solid. The supernatant was decanted and the solid was dried *in*

vacuo; yield 55 mg (96%): ^1H NMR (C_6D_6) δ 7.02 (s, 2, H_m), 6.94 (s, 2, H_m), 3.56 (m, 2, CH_2), 3.38 (m, 2, CH_2), 2.75 (s, 6, *Me*-Aryl), 2.58 (m, 2, CH_2), 2.35 (s, 6, *Me*-Aryl), 2.21 (s, 6, *Me*-Aryl), 2.15 (m, 2, CH_2), 1.90 (s, 3, NMe), 0.96 (s, 3, TiMe), 0.58 (s, 3, TiMe); ^{13}C NMR (C_6D_6) δ 151.57 (C, Aryl), 134.33 (C, Aryl), 133.91 (C, Aryl), 133.17 (C, Aryl), 130.21 (C_m), 130.06 (C_m), 65.87 (TiMe), 57.25 (CH_2), 56.95 (CH_2), 50.93 (NMe), 43.87 (TiMe), 21.36 (Me, Aryl), 19.82 (Me, Aryl), 19.32 (Me, Aryl). Anal. Calcd. for $\text{C}_{25}\text{H}_{39}\text{N}_3\text{Ti}$: C, 69.92; H, 9.15; N, 9.78. Found: C, 69.82; H, 9.21; N, 9.72.

* **[MesN₂NH]HfMe₂**. Solid HfCl_4 (66 mg, 0.206 mmol) was added to a diethyl ether solution (3 mL) of $\text{H}_2[\text{MesN}_2\text{NH}]$ (70 mg, 0.206 mmol) at -30°C with vigorous stirring. The reaction mixture was stirred at room temperature for 50 min, cooled to -30°C , and treated with MeMgI (0.28 mL, 3 M in diethyl ether, 0.84 mmol, 4 equiv.). Gas evolved immediately. The solution was stirred at room temperature for 8 min and 1,4-dioxane (4 drops) was added. Insoluble materials were removed by filtration through Celite to give a pale yellow solution. The solution was concentrated *in vacuo* until the volume was ~ 1 mL and cooled to -30°C for 1 h to give colorless crystals. The supernatant was decanted and the crystals were dried *in vacuo*. The crystals contained 2 equiv. of diethyl ether per Hf according to the ^1H NMR spectrum and elemental analysis; yield 47 mg (33%): ^1H NMR (C_6D_6) δ 6.99 (s, 2, H_m), 6.95 (s, 2, H_m), 3.45 (q, 8, OCH_2CH_3), 3.35 (m, 2, $\text{NCH}_2\text{CH}_2\text{N}$), 3.19 (m, 2, $\text{NCH}_2\text{CH}_2\text{N}$), 2.56 (s, 6, *Me*-Aryl), 2.44 (s, 6, *Me*-Aryl), 2.32 (m, 4, $\text{NCH}_2\text{CH}_2\text{N}$), 2.21 (s, 6, *Me*-Aryl), 1.17 (br s, 1, NH), 0.84 (t, 12, OCH_2CH_3), 0.15 (s, 3, HfMe), -0.23 (s, 3, HfMe); ^{13}C NMR (C_6D_6) δ 147.12 (C, Aryl), 135.70 (C, Aryl), 135.49 (C, Aryl), 133.93 (C, Aryl), 130.26 (C_m), 129.96 (C_m), 66.82 (OCH_2CH_3), 57.06 ($\text{NCH}_2\text{CH}_2\text{N}$), 54.87 (HfMe), 49.56 ($\text{NCH}_2\text{CH}_2\text{N}$), 48.40 (HfMe), 21.39 (Me, Aryl), 19.41 (Me, Aryl), 19.29 (Me, Aryl), 14.45 (OCH_2CH_3). Anal. Calcd. for $\text{C}_{24}\text{H}_{37}\text{HfN}_3(\text{OEt}_2)_2$: C, 55.36; H, 8.27; N, 6.05. Found: C, 55.48; H, 8.21; N, 6.11.

Polymerization of 1-hexene using activated [MesN₂NH]ZrMe₂ (Table 3.2).

Stock solutions of [MesN₂NH]ZrMe₂ (6.54 mM in chlorobenzene) and $[\text{Ph}_3\text{C}][\text{B}(\text{C}_6\text{F}_5)_4]$ (5.96 mM in chlorobenzene) were freshly prepared and employed for each polymerization. The molarity

of the two stock solutions was arbitrarily controlled in a ratio of 1.1:1 with the limiting reagent being $[\text{Ph}_3\text{C}][\text{B}(\text{C}_6\text{F}_5)_4]$. A 100 mL one-necked round-bottom flask was charged with a magnetic stir bar, a rubber septum cap, and a solution of $[\text{Ph}_3\text{C}][\text{B}(\text{C}_6\text{F}_5)_4]$ (1.5 mL, 8.94 μmol). The solution was cooled to 0 °C and a solution of $[\text{MesN}_2\text{NH}]\text{ZrMe}_2$ (1.5 mL, 9.81 μmol) was added. The mixture was stirred at 0 °C for ~10 seconds. The yellowish orange solution was kept at 0 °C and a stoichiometric amount of 1-hexene (0.15 mL, 134 equiv.; 0.35 mL, 313 equiv.; 0.70 mL, 626 equiv.) was added into this solution with an air-free syringe. After one hour, the polymerization reaction was quenched with HCl (1 mL, 1 M in diethyl ether). All volatile components were removed *in vacuo* (100 mTorr, 70 °C) until the product weight did not change (~20 h). Yields were essentially quantitative in each experiment.

Polymerization of 1-hexene using activated $[\text{MesN}_2\text{NMe}]\text{ZrMe}_2$ (Table 3.2). The procedures were all identical to those employing $[\text{MesN}_2\text{NH}]\text{ZrMe}_2$ as the catalyst precursor. The concentrations of the stock solutions for $[\text{MesN}_2\text{NMe}]\text{ZrMe}_2$ and $[\text{Ph}_3\text{C}][\text{B}(\text{C}_6\text{F}_5)_4]$ in chlorobenzene were 6.34 mM and 5.75 mM, respectively. The volume of the stock solutions employed in each experiment was 1.5 mL. The mixture of $[\text{MesN}_2\text{NMe}]\text{ZrMe}_2$ and $[\text{Ph}_3\text{C}][\text{B}(\text{C}_6\text{F}_5)_4]$ was either kept at 0 °C (runs 6-8, 10, 13-14) or gradually warmed to 20 °C (runs 9, 11, and 12). The amounts of 1-hexene employed were 0.15 mL (139 equiv.), 0.35 mL (325 equiv.), and 0.70 mL (649 equiv.), respectively. Yields were all quantitative for each experiment.

Polymerization of 1-hexene using activated $[\text{MesN}_2\text{NMe}]\text{ZrMe}_2$ (Table 3.3). The concentrations of the stock solutions for both $[\text{MesN}_2\text{NMe}]\text{ZrMe}_2$ and $[\text{Ph}_3\text{C}][\text{B}(\text{C}_6\text{F}_5)_4]$ were the same as those employed in Table 3.2. A stoichiometric amount of 1-hexene was added to the catalyst solution at 20 °C in all runs. The temperature change was monitored by a thermometer with an error of 1 °C. After a pause (in a condition as specified in Table 3.3), a second stoichiometric amount of 1-hexene was added and the solution temperature was monitored by a thermometer. The polymerization was quenched and the poly(1-hexene) isolated as described above. Yields were quantitative in runs 1-5 and ~ 60% in runs 6-9.

Appendix

X-ray Crystallographic data: Structural Parameters and Atomic Coordinates.

The single crystals were grown under the conditions that were described in the Experimental Sections of each chapter. All X-ray data were collected on a Siemens SMART/CCD diffractometer with $\lambda(\text{MoK}\alpha) = 0.71073 \text{ \AA}$ using ω scans at temperatures specified (see Tables below). The structures were solved using a full-matrix least squares refinement on F^2 . No absorption correction was applied. All non-hydrogen atoms were refined anisotropically.

Table A.1. Crystal data and structure refinement for [MesNON]HfNp₂, [BdeNON][BdeNON']Zr₂(CH₂SiMe₃)₂, and [Ar^FN₂N]TaMe₂.

compound	HfNp ₂	Zr ₂	TaMe ₂
identification code	99086	98042	96205
formula	C ₄₀ H ₅₂ HfN ₂ O	C ₄₄ H ₆₈ N ₄ O ₂ Si ₆ Zr ₂	C ₁₈ H ₁₄ F ₁₀ N ₃ Ta
formula weight	755.33	1036.00	643.27
crystal size (mm)	0.20 x 0.20 x 0.20	0.28 x 0.24 x 0.13	0.33 x 0.32 x 0.28
crystal system	Monoclinic	Triclinic	Monoclinic
space group	<i>P</i> 2 ₁ / <i>c</i>	<i>P</i> $\bar{1}$	<i>P</i> 2 ₁ / <i>n</i>
<i>a</i> (Å)	9.82720(10)	13.328(4)	10.70300(10)
<i>b</i> (Å)	20.25430(10)	14.964(4)	14.83590(10)
<i>c</i> (Å)	18.5991(3)	18.212(3)	12.98420(10)
α (°)	90	100.217(12)	90
β (°)	100.7380(10)	103.932(14)	111.4020(10)
γ (°)	90	114.90(2)	90
<i>V</i> (Å ³)	3637.20(7)	3032.9(13)	1919.57(3)
<i>Z</i>	4	2	4
density calcd. (Mg/ m ³)	1.379	1.134	2.226
μ (mm ⁻¹)	2.899	0.494	5.832
<i>F</i> (000)	1544	1080	1224
<i>T</i> (K)	181(2)	188(2)	183(2)
θ range (ω scans)	1.50 to 23.26°	1.58 to 23.26°	2.12 to 23.25°
limiting indices	-9 ≤ <i>h</i> ≤ 10 -18 ≤ <i>k</i> ≤ 21 -20 ≤ <i>l</i> ≤ 10	-14 ≤ <i>h</i> ≤ 14 -13 ≤ <i>k</i> ≤ 16 -20 ≤ <i>l</i> ≤ 16	-11 ≤ <i>h</i> ≤ 9 -7 ≤ <i>k</i> ≤ 16 -13 ≤ <i>l</i> ≤ 14
reflections collected	11381	12202	6076
independent reflections	4935	8370	2716
<i>R</i> _{int}	0.0480	0.0357	0.0416
data / restr. / parameters	4931 / 0 / 417	8361 / 0 / 523	2716 / 0 / 290
goodness-of-fit on <i>F</i> ²	1.276	0.936	1.126
<i>R</i> 1 / <i>wR</i> 2 [<i>I</i> > 2σ(<i>I</i>)]	0.0477 / 0.0912	0.0431 / 0.1174	0.0292 / 0.0750
<i>R</i> 1 / <i>wR</i> 2 (all data)	0.0570 / 0.0970	0.0548 / 0.1415	0.0306 / 0.0775
extinction coefficient	0.00069(11)	---	0.0049(3)
max / min peaks (eÅ ⁻³)	0.588 / -1.046	0.546 / -0.455	0.916 / -2.064

Table A.2. Crystal data and structure refinement for {[Ar^FN₂NH]TaMe₂} {MeB(C₆F₅)₃} (toluene solvate), [MesN₂NH]ZrMe₂, and [MesN₂NMe]ZrMe₂.

compound	TaMe ₂ ⁺	[MesN ₂ NH]ZrMe ₂	[MesN ₂ NMe]ZrMe ₂
identification code	96212	98213	98186
formula	C ₄₄ H ₂₅ BF ₂₅ N ₃ Ta	C _{34.50} H ₄₉ N ₃ Zr	C ₂₅ H ₃₉ N ₃ Zr
formula weight	1262.43	596.99	472.81
crystal size (mm)	0.21 x 0.18 x 0.13	0.24 x 0.12 x 0.08	0.12 x 0.12 x 0.12
crystal system	Orthorhombic	Monoclinic	Orthorhombic
space group	<i>Pbca</i>	<i>P2₁/c</i>	<i>Pnma</i>
a (Å)	24.1706(5)	18.740(11)	13.1319(8)
b (Å)	15.1650(2)	10.874(5)	24.1909(14)
c (Å)	24.4337(5)	17.541(7)	7.9669(5)
α (°)	90	90	90
β (°)	90	110.54(4)	90
γ (°)	90	90	90
V (Å ³)	8956.1(3)	3347(3)	2530.9(3)
Z	8	4	4
density calcd. (Mg/ m ³)	1.873	1.185	1.241
μ (mm ⁻¹)	2.597	0.353	0.449
F (000)	4904	1268	1000
T (K)	183(2)	183(2)	192(2)
θ range (ω scans)	1.67 to 20.00°	2.20 to 19.99°	1.68 to 23.27°
limiting indices	-26 ≤ h ≤ 18 -16 ≤ k ≤ 14 -27 ≤ l ≤ 26	-20 ≤ h ≤ 18 -12 ≤ k ≤ 12 -14 ≤ l ≤ 19	-14 ≤ h ≤ 14 -26 ≤ k ≤ 16 -8 ≤ l ≤ 8
reflections collected	25514	9623	9643
independent reflections	4182	3122	1869
R _{int}	0.0641	0.1190	0.0990
data / restr. / parameters	4154 / 0 / 663	2977 / 0 / 353	1867 / 0 / 140
goodness-of-fit on F ²	1.463	1.118	1.130
R1 / wR2 [I > 2σ(I)]	0.0775 / 0.1525	0.0692 / 0.1565	0.0526 / 0.1244
R1 / wR2 (all data)	0.0842 / 0.1621	0.0945 / 0.1759	0.0814 / 0.1543
extinction coefficient	0.00002(3)	0.0031(5)	0.0000(8)
max / min peaks (eÅ ⁻³)	0.981 / -1.162	0.577 / -0.354	0.428 / -0.390

Table A.3. Atomic coordinates ($\times 10^4$) and equivalent isotropic displacement parameters ($\text{\AA}^2 \times 10^3$) for [MesNON]HfNp₂. $U(\text{eq})$ is defined as one third of the trace of the orthogonalized U_{ij} tensor.

Atom	x	y	z	$U(\text{eq})$
Hf	2141(1)	2036(1)	889(1)	22(1)
O	3353(5)	2488(3)	41(3)	27(1)
N(1)	1445(6)	3006(3)	607(3)	25(1)
N(2)	4186(6)	1692(3)	1102(3)	24(1)
C(1)	910(8)	1312(4)	150(4)	27(2)
C(2)	945(8)	1082(4)	-646(4)	29(2)
C(3)	-283(9)	650(4)	-937(4)	42(2)
C(4)	2270(9)	679(4)	-658(5)	42(2)
C(5)	901(9)	1678(4)	-1143(4)	38(2)
C(6)	1568(8)	1926(4)	1985(4)	34(2)
C(7)	472(9)	1518(5)	2254(4)	38(2)
C(8)	389(10)	1661(5)	3048(4)	52(3)
C(9)	-848(24)	1440(13)	1783(11)	55(8)
C(10)	430(48)	820(16)	2130(24)	168(29)
C(11)	372(8)	3319(4)	931(4)	27(2)
C(12)	-1018(9)	3245(4)	579(4)	33(2)
C(13)	-2055(9)	3528(5)	898(5)	40(2)
C(14)	-1753(9)	3901(4)	1535(5)	39(2)
C(15)	-362(10)	3983(4)	1846(4)	39(2)
C(16)	711(9)	3696(4)	1571(4)	32(2)
C(21)	2081(8)	3429(4)	160(4)	26(2)
C(22)	1718(9)	4081(4)	-2(4)	37(2)
C(23)	2466(10)	4456(4)	-414(5)	45(2)
C(24)	3580(10)	4187(5)	-663(5)	45(2)
C(25)	3947(8)	3528(5)	-523(4)	37(2)
C(26)	3173(8)	3161(4)	-131(4)	27(2)
C(31)	4955(7)	1683(4)	531(4)	25(2)
C(32)	-4493(7)	2100(4)	-61(4)	30(2)
C(33)	4981(8)	2072(4)	-712(4)	34(2)
C(34)	6074(9)	1638(4)	-751(5)	42(2)
C(35)	6607(8)	1249(4)	-156(5)	38(2)
C(36)	6062(8)	1271(4)	483(4)	33(2)
C(41)	4872(7)	1397(4)	1789(4)	22(2)
C(42)	4817(8)	713(4)	1913(4)	31(2)
C(43)	5526(8)	461(4)	2573(4)	33(2)
C(44)	6288(8)	855(4)	3103(4)	36(2)
C(45)	6318(8)	1530(4)	2967(4)	35(2)
C(46)	5633(8)	1810(4)	2320(4)	31(2)
C(121)	-1404(9)	2867(5)	-130(5)	43(2)
C(141)	-2891(10)	4213(5)	1866(6)	58(3)
C(161)	2201(9)	3793(4)	1934(5)	43(2)
C(421)	4024(10)	251(4)	1340(5)	48(2)
C(441)	7101(9)	561(5)	3801(5)	48(2)
C(461)	5730(10)	2536(4)	2192(5)	49(3)
C(9')	1310(30)	809(18)	2326(21)	61(8)
C(10')	-883(27)	1942(20)	1842(19)	104(13)

Table A.4. Atomic coordinates ($\times 10^4$) and equivalent isotropic displacement parameters ($\text{\AA}^2 \times 10^3$) for $[\text{BdeNON}][\text{BdeNON}']\text{Zr}_2(\text{CH}_2\text{SiMe}_3)_2$. $U(\text{eq})$ is defined as one third of the trace of the orthogonalized U_{ij} tensor.

Atom	x	y	z	$U(\text{eq})$
Zr(1)	-2665(1)	9598(1)	7690(1)	31(1)
Zr(2)	-1796(1)	8128(1)	6345(1)	32(1)
Si(1)	-5730(1)	8654(1)	6957(1)	46(1)
Si(2)	-3758(1)	7403(1)	7484(1)	36(1)
Si(3)	-1571(1)	11571(1)	6915(1)	48(1)
Si(4)	787(1)	10497(1)	6870(1)	45(1)
Si(5)	-3970(1)	7290(1)	4387(1)	55(1)
Si(6)	-1211(1)	5946(1)	5648(1)	54(1)
O(1)	-730(2)	10048(2)	8485(2)	32(1)
O(2)	-2673(2)	10419(2)	8928(2)	37(1)
N(1)	-4261(3)	9657(3)	7432(2)	41(1)
N(2)	-3129(3)	8500(3)	8306(2)	33(1)
N(3)	-1451(3)	11133(3)	7737(2)	38(1)
N(4)	-241(3)	9470(3)	7086(2)	38(1)
C(1)	-5415(4)	6808(4)	7099(3)	51(1)
C(2)	-5910(4)	7324(4)	6568(3)	49(1)
C(3)	-200(5)	11957(4)	6654(3)	63(1)
C(4)	44(5)	11104(4)	6269(3)	60(1)
C(5)	-2413(4)	8113(4)	5089(3)	47(1)
C(6)	-1820(4)	6595(3)	6235(3)	41(1)
C(11)	35(3)	11140(3)	8794(2)	32(1)
C(12)	-407(3)	11695(3)	8408(3)	37(1)
C(13)	260(4)	12775(4)	8733(3)	50(1)
C(14)	1313(4)	13254(4)	9370(3)	55(1)
C(15)	1737(4)	12663(4)	9712(3)	51(1)
C(16)	1101(4)	11592(3)	9425(2)	40(1)
C(17)	-6495(4)	8620(5)	7692(3)	66(2)
C(18)	-6487(5)	8858(5)	6038(3)	69(2)
C(21)	-206(3)	9410(3)	8444(2)	29(1)
C(22)	95(3)	9176(3)	7775(2)	34(1)
C(23)	643(4)	8556(4)	7792(3)	46(1)
C(24)	824(4)	8157(4)	8411(3)	56(1)
C(25)	472(4)	8370(4)	9039(3)	48(1)
C(26)	-42(4)	9005(3)	9053(2)	39(1)
C(27)	-3319(5)	6414(4)	7712(3)	52(1)
C(28)	-3126(3)	8106(3)	6818(2)	36(1)
C(31)	-3441(3)	8686(3)	8971(2)	33(1)
C(32)	-3232(3)	9695(3)	9306(2)	37(1)
C(32)	-2878(5)	11979(4)	9226(3)	54(1)
C(33)	-3547(4)	9959(4)	9947(3)	47(1)
C(34)	-4091(5)	9202(4)	10273(3)	55(1)
C(35)	-4304(4)	8210(4)	9963(3)	50(1)
C(36)	-3982(4)	7950(4)	9317(3)	43(1)
C(37)	-1838(6)	12717(5)	7053(4)	78(2)
C(38)	-2895(5)	10490(4)	6076(3)	65(2)
C(41)	-3220(4)	11016(3)	8706(3)	41(1)

Appendix

C(43)	-3415(5)	12536(4)	8987(4)	63(1)
C(44)	-4258(5)	12149(5)	8240(4)	70(2)
C(45)	-4563(5)	11212(4)	7710(3)	57(1)
C(46)	-4049(4)	10606(4)	7930(3)	43(1)
C(47)	2021(4)	11478(5)	7783(3)	70(2)
C(48)	1359(5)	9924(5)	6194(3)	69(2)
C(51)	-4815(5)	8014(5)	4441(4)	87(2)
C(52)	-4740(5)	6051(4)	4613(3)	66(2)
C(53)	-4038(6)	6890(6)	3331(3)	101(3)
C(61)	-1736(8)	5817(7)	4570(4)	112(3)
C(62)	-1718(8)	4591(6)	5674(5)	107(3)
C(63)	412(6)	6634(7)	6048(6)	154(5)

Table A.5. Atomic coordinates ($\times 10^4$) and equivalent isotropic displacement parameters ($\text{\AA}^2 \times 10^3$) for $[\text{Ar}^{\text{F}}\text{N}_2\text{N}]\text{TaMe}_2$. $U(\text{eq})$ is defined as one third of the trace of the orthogonalized U_{ij} tensor.

Atom	x	y	z	$U(\text{eq})$
Ta(1)	1338(1)	2096(1)	1138(1)	27(1)
F(11)	904(4)	3158(2)	2415(3)	40(1)
F(12)	387(4)	4117(2)	3980(3)	46(1)
F(13)	23(4)	3256(3)	5716(3)	49(1)
F(14)	157(4)	1417(3)	5806(3)	57(1)
F(15)	646(4)	464(3)	4302(3)	54(1)
F(21)	1174(4)	3659(2)	591(3)	39(1)
F(22)	1310(4)	5355(2)	-97(3)	51(1)
F(23)	2009(4)	5654(3)	-1908(3)	60(1)
F(24)	2517(4)	4205(3)	-2988(3)	59(1)
F(25)	2362(4)	2538(3)	-2353(3)	49(1)
N(1)	1169(5)	1360(3)	2450(4)	32(1)
N(2)	1681(5)	2189(3)	-334(4)	33(1)
N(3)	1618(5)	839(3)	790(4)	34(1)
C(1)	1217(8)	381(4)	2422(5)	47(2)
C(2)	1842(8)	118(5)	1597(6)	54(2)
C(3)	1736(7)	1350(4)	-932(5)	39(1)
C(4)	2095(7)	605(4)	-105(5)	42(2)
C(5)	3274(6)	2683(5)	2153(5)	40(1)
C(6)	-830(6)	2374(5)	439(5)	44(2)
C(11)	722(6)	2711(4)	3286(5)	32(1)
C(12)	467(6)	3215(4)	4065(5)	33(1)
C(13)	285(6)	2786(4)	4939(5)	35(2)
C(14)	365(6)	1864(5)	4978(5)	38(1)
C(15)	630(6)	1370(4)	4179(5)	35(1)
C(16)	853(5)	1777(4)	3283(5)	32(1)
C(21)	1508(6)	3791(4)	-329(4)	33(1)
C(22)	1557(6)	4659(4)	-657(5)	37(1)
C(23)	1890(6)	4812(4)	-1576(5)	42(2)
C(24)	2150(6)	4072(5)	-2109(5)	43(2)
C(25)	2080(6)	3201(5)	-1759(5)	36(1)
C(26)	1759(6)	3021(4)	-822(5)	29(1)

Table A.6. Atomic coordinates ($\times 10^4$) and equivalent isotropic displacement parameters ($\text{\AA}^2 \times 10^3$) for $\{[\text{Ar}^{\text{F}}\text{N}_2\text{NH}]\text{TaMe}_2\}\{\text{MeB}(\text{C}_6\text{F}_5)_3\}(\text{toluene})$. $U(\text{eq})$ is defined as one third of the trace of the orthogonalized U_{ij} tensor.

Atom	x	y	z	$U(\text{eq})$
Ta(1)	1557(1)	2732(1)	3741(1)	42(1)
F(12)	616(6)	4275(8)	4518(5)	79(4)
F(13)	-473(6)	4222(11)	4726(5)	118(6)
F(14)	-970(5)	2657(13)	4958(5)	128(6)
F(15)	-365(6)	1140(10)	4961(5)	109(5)
F(16)	719(5)	1220(7)	4741(5)	79(4)
F(22)	2097(4)	1260(7)	2600(4)	66(3)
F(23)	2087(4)	1399(8)	1504(5)	82(4)
F(24)	2218(4)	3033(8)	1036(4)	72(3)
F(25)	2337(4)	4461(9)	1668(4)	72(3)
F(26)	2336(4)	4319(7)	2768(4)	59(3)
F(32)	150(5)	2282(8)	7655(4)	80(4)
F(33)	-385(7)	1992(10)	8591(5)	119(5)
F(34)	-1355(6)	2810(9)	8819(5)	104(4)
F(35)	-1799(5)	3904(9)	8039(5)	88(4)
F(36)	-1322(4)	4111(8)	7084(5)	74(3)
F(43)	892(5)	5662(8)	7690(5)	94(4)
F(44)	1530(5)	5915(8)	6799(6)	98(4)
F(45)	90(4)	4469(7)	7693(4)	70(3)
F(45)	1379(5)	4884(9)	5895(5)	87(4)
F(46)	599(4)	3653(8)	5889(4)	69(3)
F(52)	919(4)	2450(5)	6780(5)	64(3)
F(53)	1171(5)	790(8)	6525(6)	105(5)
F(54)	398(5)	-330(8)	6139(5)	77(3)
F(55)	-658(5)	247(7)	6023(5)	80(4)
F(56)	-938(4)	1869(7)	6304(4)	66(3)
N(1)	1289(5)	2756(10)	4500(5)	44(4)
N(2)	2242(5)	2706(10)	3296(5)	45(4)
N(3)	2297(6)	2822(19)	4317(7)	126(10)
C(1)	1602(8)	2824(15)	5023(8)	70(6)
C(1S)	2104(8)	1(12)	4926(9)	55(5)
C(2)	2181(8)	2690(13)	4869(7)	54(5)
C(2S)	1971(8)	4(15)	4401(10)	67(6)
C(3)	2816(8)	2708(18)	3487(8)	85(8)
C(3S)	2334(14)	148(16)	3995(10)	84(8)
C(4)	2817(7)	2664(12)	4086(7)	50(5)
C(4S)	2876(15)	323(13)	4130(14)	92(11)
C(5)	1139(7)	3789(11)	3363(7)	46(5)
C(5S)	3020(9)	310(14)	4665(16)	86(9)
C(6S)	2639(11)	160(13)	5059(10)	71(6)
C(6)	1134(7)	1635(12)	3430(8)	59(6)
C(7S)	1691(9)	-176(16)	5366(10)	100(8)
C(11)	693(7)	2727(14)	4599(6)	42(5)
C(12)	387(8)	3485(18)	4611(7)	59(6)
C(13)	-171(12)	3476(21)	4710(7)	77(8)
C(14)	-428(10)	2736(27)	4850(9)	83(8)

C(15)	-151(10)	1939(17)	4853(7)	58(6)
C(16)	428(9)	1960(12)	4733(7)	50(5)
C(21)	2200(6)	2809(13)	2729(8)	43(5)
C(22)	2143(6)	2078(12)	2383(10)	51(5)
C(23)	2144(7)	2142(20)	1817(10)	68(7)
C(24)	2223(8)	2916(24)	1593(8)	78(10)
C(25)	2275(7)	3677(16)	1916(11)	62(6)
C(26)	2261(7)	3590(13)	2475(8)	41(5)
C(31)	-569(7)	3155(12)	7309(6)	41(5)
C(32)	-354(8)	2628(13)	7725(8)	51(5)
C(33)	-613(9)	2516(11)	8211(8)	50(5)
C(34)	-1111(9)	2934(12)	8327(9)	56(6)
C(35)	-1327(8)	3443(13)	7928(8)	51(5)
C(36)	-1068(7)	3549(12)	7439(8)	47(5)
C(41)	290(7)	3991(12)	6795(7)	44(5)
C(43)	814(8)	5167(13)	7251(10)	60(6)
C(44)	1124(8)	5276(12)	6797(11)	62(6)
C(45)	1056(8)	4765(15)	6349(9)	60(6)
C(45)	403(7)	4527(12)	7234(8)	46(5)
C(46)	640(7)	4140(12)	6362(7)	44(5)
C(51)	-21(7)	2303(11)	6527(7)	37(4)
C(52)	510(7)	1925(11)	6579(7)	43(5)
C(53)	646(8)	1057(14)	6456(9)	63(6)
C(54)	264(8)	515(13)	6245(8)	52(5)
C(55)	-272(8)	799(13)	6204(8)	52(5)
C(56)	-389(7)	1652(14)	6341(7)	47(5)
B	-234(8)	3282(14)	6721(9)	46(6)
C(7)	-615(7)	3707(12)	6229(7)	54(5)

Table A.7. Atomic coordinates ($\times 10^4$) and equivalent isotropic displacement parameters ($\text{\AA}^2 \times 10^3$) for $[\text{MesN}_2\text{NH}]\text{ZrMe}_2$. $U(\text{eq})$ is defined as one third of the trace of the orthogonalized U_{ij} tensor.

Atom	x	y	z	$U(\text{eq})$
Zr(1)	2621(1)	5782(1)	4566(1)	34(1)
N(1)	2552(4)	6419(6)	5666(4)	38(2)
N(2)	2666(4)	6465(6)	3465(4)	35(2)
N(3)	2390(5)	7950(6)	4486(4)	54(2)
C(1)	2602(5)	8509(8)	5286(5)	39(2)
C(2)	2411(6)	7681(8)	5863(5)	56(3)
C(3)	2665(6)	8552(8)	3905 (5)	48(3)
C(4)	2546(6)	7741(8)	3186(6)	59(3)
C(5)	3663(5)	4581(8)	4995(5)	48(3)
C(6)	1667(6)	4387(8)	4160(6)	56(3)
C(11)	2603(5)	5592(8)	6329(5)	37(2)
C(12)	3307(6)	5353(8)	6925(6)	43(2)
C(13)	3355(6)	4526(8)	7551(5)	43(3)
C(14)	2737(7)	3951(8)	7603(5)	51(3)
C(15)	2037(6)	4206(8)	7020(6)	44(2)
C(16)	1950(5)	5028(8)	6385(5)	41(2)
C(21)	2756(5)	5640(7)	2866(5)	32(2)
C(22)	3504(5)	5367(8)	2871(5)	38(2)
C(23)	3569(6)	4550(8)	2283(6)	46(3)
C(24)	2950(6)	3980(7)	1712(5)	38(2)
C(25)	2240(6)	4287(8)	1710(5)	44(2)
C(26)	2124(5)	5094(8)	2267(5)	33(2)
C(121)	4012(6)	6014(9)	6924(5)	62(3)
C(141)	2809(7)	3046(9)	8297(6)	73(4)
C(161)	1167(6)	5325(10)	5794(6)	69(3)
C(221)	4183(5)	6006(10)	3451(6)	60(3)
C(241)	3063(6)	3072(9)	1114(6)	65(3)
C(261)	1315(5)	5447(9)	2188(6)	58(3)
C(1S)	-702(7)	4872(12)	1088(11)	89(4)
C(2S)	-643(7)	4460(18)	1867(9)	88(4)
C(3S)	-366(10)	3299(25)	2114(11)	125(7)
C(4S)	-199(9)	2531(19)	1605(17)	136(7)
C(5S)	-265(8)	2906 (17)	835(12)	104(5)
C(6S)	-523(6)	4068(15)	589(7)	74(4)
C(7S)	-956(8)	6078(13)	832(10)	133(6)
C(8S)	5068(8)	3839(20)	9622(10)	117(6)
C(9S)	5321(8)	5067(23)	9406(10)	115(6)
C(10S)	5245(10)	6133(20)	9787(13)	125(7)
C(11S)	5105(17)	2831(24)	9321(18)	88(9)

Table A.8. Atomic coordinates ($\times 10^4$) and equivalent isotropic displacement parameters ($\text{\AA}^2 \times 10^3$) for $[\text{MesN}_2\text{NMe}]\text{ZrMe}_2$. $U(\text{eq})$ is defined as one third of the trace of the orthogonalized U_{ij} tensor.

Atom	x	y	z	$U(\text{eq})$
Zr(1)	8124(1)	7500	1251(1)	41(1)
N(1)	8595(3)	6685(2)	816(5)	49(1)
N(2)	9648(4)	7500	-348(7)	46(2)
C(1)	7925(6)	7500	4044(9)	59(2)
C(2)	6503(6)	7500	283(11)	60(2)
C(3)	9292(6)	7500	-2138(10)	85(3)
C(4)	10238(4)	6999(3)	-29(9)	74(2)
C(5)	9525(4)	6501(2)	-4(8)	60(2)
C(11)	7949(4)	6239(2)	1356(6)	49(1)
C(12)	8056(4)	6008(2)	2954(7)	54(1)
C(13)	7389(6)	5598(3)	3473(8)	70(2)
C(14)	6621(5)	5401(2)	2463(9)	65(2)
C(15)	6546(4)	5612(2)	850(8)	60(2)
C(16)	7197(4)	6021(2)	280(7)	52(1)
C(121)	8917(5)	6182(3)	4105(8)	82(2)
C(141)	5886(5)	4964(3)	3096(10)	99(2)
C(151)	7090(5)	6216(3)	-1524(7)	70(2)

Symmetry transformations used to generate equivalent atoms:

#1 $x, -y+3/2, z$

References

- (1) Wilkinson, G.; Rosenblum, M.; Whiting, M. C.; Woodward, R. B. *J. Am. Chem. Soc.* **1952**, *74*, 2125.
- (2) Wilkinson, G. *J. Organomet. Chem.* **1975**, 273.
- (3) Janiak, C.; Schumann, H. *Adv. Organomet. Chem.* **1991**, *33*, 291-393.
- (4) Jordan, R. F. *Adv. Organomet. Chem.* **1991**, *32*, 325.
- (5) Macomber, D. W.; Hart, W. P.; Rausch, M. D. *Adv. Organomet. Chem.* **1982**, *21*, 1.
- (6) Bochmann, M. *Comprehensive Organometallic Chemistry II*; Abel, E. W., Stone, F. G. A. and Wilkinson, G., Ed.; Pergamon: Oxford; Vol. 4, pp 221-271.
- (7) Bochmann, M. *Organometallics 2. Complexes with Transition Metal-Carbon π -Bonds.*; Oxford University: Oxford, 1994, pp 42-65.
- (8) Long, N. J. *Metallocenes: An Introduction to Sandwich Complexes.*; Blackwell Science: Oxford, 1998.
- (9) Binger, P.; Podubrin, S. *Comprehensive Organometallic Chemistry II*; Abel, E. W., Stone, F. G. A. and Wilkinson, G., Ed.; Pergamon: Oxford; Vol. 4, pp 439-464.
- (10) Winter, M. J. *Adv. Organomet. Chem.* **1989**, *29*, 101.
- (11) Jutzi, P. *Chem. Rev.* **1986**, *86*, 983.
- (12) Oconnor, J. M.; Casey, C. P. *Chem. Rev.* **1987**, *87*, 307.
- (13) Poli, R. *Chem. Rev.* **1991**, *91*, 509.
- (14) Halterman, R. L. *Chem. Rev.* **1992**, *92*, 965.
- (15) Tilley, T. D. *Acc. Chem. Res.* **1993**, *26*, 22.
- (16) Heyhawkins, E. *Chem. Rev.* **1994**, *94*, 1661.
- (17) Jutzi, P.; Burford, N. *Chem. Rev.* **1999**, *99*, 969.
- (18) *Ferrocenes: Homogeneous Catalysis, Organic Synthesis, Materials Science.*; Togni, A. and Hayashi, T., Ed.; VCH: Weinhiem, 1995.

- (19) *Metallocenes*; Togni, A., Ed.; Wiley: Weinheim, 1998.
- (20) Chisholm, M. H.; Rothwell, I. P. *Comprehensive Coordination Chemistry*; Wilkinson, G., Gillard, R. D. and McCleverty, J. A., Ed.; Pergamon: Oxford, 1987; Vol. 2, pp 161-188.
- (21) Trofimenko, S. *Chem. Rev.* **1993**, 93, 943.
- (22) Grimes, R. N. *Pure Appl. Chem.* **1987**, 59, 847.
- (23) Fryzuk, M. D. *Can. J. Chem.* **1992**, 70, 2839.
- (24) Schrock, R. R. *Acc. Chem. Res.* **1997**, 30, 9.
- (25) Verkade, J. G. *Acc. Chem. Res.* **1993**, 26, 483.
- (26) Pinkas, J.; Wang, T. L.; Jacobson, R. A.; Verkade, J. G. *Inorg. Chem.* **1994**, 33, 5244.
- (27) Duan, Z. B.; Young, V. G.; Verkade, J. G. *Inorg. Chem.* **1995**, 34, 2179.
- (28) Friedrich, S.; Gade, L. H.; Scowen, I. J.; McPartlin, M. *Angew. Chem., Int. Ed. Engl.* **1996**, 35, 1338.
- (29) Memmler, H.; Gade, L. H.; Lauher, J. W. *Inorg. Chem.* **1994**, 33, 3064.
- (30) Hellmann, K. W.; Gade, L. H.; Gevert, O.; Steinert, P.; Lauher, J. W. *Inorg. Chem.* **1995**, 34, 4069.
- (31) Hellmann, K. W.; Gade, L. H.; Li, W. S.; Mcpartlin, M. *Inorg. Chem.* **1994**, 33, 5974.
- (32) Bochmann, M. *J. Chem. Soc., Dalton Trans.* **1996**, 255.
- (33) Brintzinger, H. H.; Fischer, D.; Mulhaupt, R.; Rieger, B.; Waymouth, R. M. *Angew. Chem., Int. Ed. Engl.* **1995**, 34, 1143.
- (34) Kaminsky, W.; Arndt, M. *Adv. Polym. Sci.* **1997**, 127, 144.
- (35) Sinclair, K. B.; Wilson, R. B. *Chem. Ind.* **1994**, 857.
- (36) Brand, H.; Arnold, J. *J. Am. Chem. Soc.* **1992**, 114, 2266.
- (37) Kim, H.-J.; Whang, D.; Kim, K.; Do, Y. *Inorg. Chem.* **1993**, 32, 360.
- (38) Brand, H.; Capriotti, J. A.; Arnold, J. *Organometallics* **1994**, 13, 4469.
- (39) Uhrhammer, R.; Black, D. G.; Gardner, T. G.; Olsen, J. D.; Jordan, R. F. *J. Am. Chem. Soc.* **1993**, 115, 8493.

- (40) Black, D. G.; Swenson, D. C.; Jordan, R. F.; Rogers, R. D. *Organometallics* **1995**, *14*, 3539.
- (41) Giannini, L.; Solari, E.; Angelis, S. D.; Ward, T. R.; Floriani, C.; Chiesi-Villa, A.; Rizzoli, C. *J. Am. Chem. Soc.* **1995**, *117*, 5801.
- (42) Dunn, S. C.; Batsanov, A. S.; Mountford, P. *J. Chem. Soc., Chem. Commun.* **1994**, 2007.
- (43) Tjaden, E. B.; Swenson, D. C.; Jordan, R. F.; Petersen, J. L. *Organometallics* **1995**, *14*, 371.
- (44) Male, N. A. H.; Thornton-Pett, M.; Bochmann, M. *J. Chem. Soc., Dalton Trans.* **1997**, 2487.
- (45) Corazza, F.; Solari, E.; Floriani, C.; Chiesi-Villa, A.; Guastini, C. *J. Chem. Soc., Dalton Trans.* **1990**, 1335.
- (46) Solari, E.; Floriani, C.; Chiesi-Villa, A.; Rizzoli, C. *J. Chem. Soc., Dalton Trans.* **1992**, 367.
- (47) Aoyagi, K.; Gantzel, P. K.; Kalai, K.; Tilley, T. D. *Organometallics* **1996**, *15*, 923.
- (48) Cozzi, P. G.; Gallo, E.; Floriani, C.; Chiesivilla, A.; Rizzoli, C. *Organometallics* **1995**, *14*, 4994.
- (49) Walther, D.; Fischer, R.; Gorls, H.; Koch, J.; Schweder, B. *J. Organomet. Chem.* **1996**, *508*, 13.
- (50) McKnight, A. L.; Waymouth, R. M. *Chem. Rev.* **1998**, *98*, 2587.
- (51) Scollard, J. D.; McConville, D. H. *J. Am. Chem. Soc.* **1996**, *118*, 10008.
- (52) Baumann, R.; Davis, W. M.; Schrock, R. R. *J. Am. Chem. Soc.* **1997**, *119*, 3830.
- (53) Baumann, R.; Schrock, R. R. *J. Organomet. Chem.* **1998**, *557*, 69.
- (54) Schrock, R. R. *Pure Appl. Chem.* **1997**, *69*, 2197.
- (55) Mösch-Zanetti, N. C.; Schrock, R. R.; Davis, W. M.; Wanninger, K.; Seidel, S. W.; O'Donoghue, M. B. *J. Am. Chem. Soc.* **1997**, *119*, 11037.

- (56) Schrock, R. R.; Seidel, S. W.; Mösch-Zanetti, N. C.; Shih, K.-Y.; O'Donoghue, M. B.; Davis, W. M.; Reiff, W. M. *J. Am. Chem. Soc.* **1997**, *119*, 11876.
- (57) Schrock, R. R.; Seidel, S. W.; Mösch-Zanetti, N. C.; Dobbs, D. A.; Shih, K.-Y.; Davis, W. M. *Organometallics* **1997**, *16*, 5195.
- (58) Greco, G. E.; Popa, A. I.; Schrock, R. R. *Organometallics* **1998**, *17*, 5591.
- (59) Cummins, C. C.; Lee, J.; Schrock, R. R.; Davis, W. M. *Angew. Chem., Int. Ed. Engl.* **1992**, *31*, 1501.
- (60) Rosenberger, C.; Schrock, R. R.; Davis, W. M. *Inorg. Chem.* **1997**, *36*, 123.
- (61) Shih, K.-Y.; Schrock, R. R.; Kempe, R. *J. Am. Chem. Soc.* **1994**, *116*, 8804.
- (62) Kol, M.; Schrock, R. R.; Kempe, R.; Davis, W. M. *J. Am. Chem. Soc.* **1994**, *116*, 4382.
- (63) O'Donoghue, M. B.; Zanetti, N. C.; Schrock, R. R.; Davis, W. M. *J. Am. Chem. Soc.* **1997**, *119*, 2753.
- (64) O'Donoghue, M. B.; Davis, W. M.; Schrock, R. R. *Inorg. Chem.* **1998**, *37*, 5149.
- (65) Cummins, C. C. *Prog. Inorg. Chem.* **1998**, *47*, 685.
- (66) Cummins, C. C. *J. Chem. Soc., Chem. Commun.* **1998**, 1777.
- (67) Odom, A. L.; Arnold, P. L.; Cummins, C. C. *J. Am. Chem. Soc.* **1998**, *120*, 5836.
- (68) Johnson, A. R.; Davis, W. M.; Cummins, C. C.; Serron, S.; Nolan, S. P.; Musaev, D. G.; Morokuma, K. *J. Am. Chem. Soc.* **1998**, *120*, 2071.
- (69) Laplaza, C. E.; Cummins, C. C. *Science* **1995**, *268*, 861.
- (70) Laplaza, C. E.; Johnson, M. J. A.; Peters, J. C.; Odom, A. L.; Kim, E.; Cummins, C. C.; George, G. N.; Pickering, I. J. *J. Am. Chem. Soc.* **1996**, *118*, 8623.
- (71) Schrock, R. R.; Schattenmann, F.; Aizenberg, M.; Davis, W. M. *Chem. Commun.* **1998**, 199.
- (72) Aizenberg, M.; Turculet, L.; Davis, W. M.; Schattenmann, F.; Schrock, R. R. *Organometallics* **1998**, *17*, 4795.
- (73) Baumann, R., Ph.D. Thesis, Massachusetts Institute of Technology, **1998**.
- (74) Micovic, I. V.; Ivanovic, M. D.; Piatak, D. M.; Bojic, V. D. *Synthesis* **1991**, 1043.

- (75) Knops, P.; Sendhoff, N.; Mekelburger, H.-B.; Vogtle, F. *Topic Curr. Chem.* **1991**, *161*, 1.
- (76) Wolfe, J. P.; Wagaw, S.; Buchwald, S. L. *J. Am. Chem. Soc.* **1996**, *118*, 7215.
- (77) Wolfe, J. P.; Wagaw, S.; Marcoux, J.-F.; Buchwald, S. L. *Acc. Chem. Res.* **1998**, *31*, 805.
- (78) Benzing, E.; Kornicker, W. *Chem. Ber.* **1961**, *94*, 2263.
- (79) Diamond, G. M.; Rodewald, S.; Jordan, R. F. *Organometallics* **1995**, *14*, 5.
- (80) Martin, J. L.; Martin, G. J.; Delpuech, J. J. *Practical NMR Spectroscopy*; Heyden, London, 1980, pp 295-299.
- (81) Sandström, J. *Dynamic NMR Spectroscopy*; Academic Press: London, 1982, pp 25-28.
- (82) Collier, M. R.; Lappert, M. F.; Pearce, R. *J. Chem. Soc., Dalton Trans.* **1973**, 445.
- (83) Graf, D. D.; Schrock, R. R.; Davis, W. M.; Stumpf, R. *Organometallics* **1999**, *18*, 843.
- (84) Planalp, R. P.; Andersen, R. A.; Zalkin, A. *Organometallics* **1983**, *2*, 16.
- (85) Davies, G. R.; Jarvis, J. A. J.; Kilbourn, B. T.; Pioli, J. P. *J. Chem. Soc., Chem. Commun.* **1971**, 677.
- (86) Margl, P.; Deng, L. Q.; Ziegler, T. *J. Am. Chem. Soc.* **1999**, *121*, 154.
- (87) Resconi, L.; Piemontesi, F.; Camurati, I.; Balboni, D.; Sironi, A.; Moret, M.; Rychlicki, H.; Zeigler, R. *Organometallics* **1996**, *15*, 5046.
- (88) Resconi, L.; Piemontesi, F.; Camurati, I.; Sudmeijer, O.; Nifant'ev, I. E.; Ivchenko, P. V.; Juz'mina, L. G. *J. Am. Chem. Soc.* **1998**, *120*, 2308.
- (89) Cummins, C. C.; Schrock, R. R.; Davis, W. M. *Organometallics* **1992**, *11*, 1452.
- (90) Simpson, S. J.; Andersen, R. A. *Inorg. Chem.* **1981**, *20*, 3627.
- (91) Simpson, S. J.; Andersen, R. A. *Inorg. Chem.* **1981**, *20*, 2991.
- (92) Huheey, J. E. *Inorganic Chemistry: Principles of Structure and Reactivity.*; 3rd ed.; Harper & Row: New York, 1983, pp A28-A44.
- (93) Negishi, E.; Takahashi, T. *Acc. Chem. Res.* **1994**, *27*, 124.

- (94) Negishi, E.; Nguyen, T.; Maye, J. P.; Choueiri, D.; Suzuki, N.; Takahashi, T. *Chem. Lett.* **1992**, 2367.
- (95) van der Heijden, H.; Hessen, B. *J. Chem. Soc., Chem. Commun.* **1995**, 145.
- (96) Busico, V.; Cipullo, R.; Chadwick, J. C.; Modder, J. F.; Sudmeijer, O. *Macromolecules* **1994**, 27, 7538.
- (97) Busico, V.; Cipullo, R.; Talarico, G. *Macromolecules* **1998**, 31, 2387.
- (98) Busico, V.; Cipullo, R.; Talarico, G.; Segre, A. L.; Caporaso, L. *Macromolecules* **1998**, 31, 8720.
- (99) Guerra, G.; Longo, P.; Cavallo, L.; Corradini, P.; Resconi, L. *J. Am. Chem. Soc.* **1997**, 119, 4394.
- (100) Pangborn, A. B.; Giardello, M. A.; Grubbs, R. H.; Rosen, R. K.; Timmers, F. J. *Organometallics* **1996**, 15, 1518.
- (101) Randall, J. J.; Lewis, C. E.; Slagan, P. M. *J. Org. Chem.* **1962**, 27, 4098.
- (102) Bradley, D. C.; Thomas, I. M. *J. Chem. Soc.* **1960**, 3857.
- (103) Zucchini, U.; Albizzati, E.; Giannini, U. *J. Organomet. Chem.* **1971**, 26, 357.
- (104) Davidson, P. J.; Lappert, M. F.; Pearce, R. *J. Organomet. Chem.* **1973**, 57, 269.
- (105) Diamond, G. M.; Jordan, R. F.; Petersen, J. L. *Organometallics* **1996**, 15, 4030.
- (106) Schrock, R. R.; Fellmann, J. D. *J. Am. Chem. Soc.* **1978**, 100, 3359.
- (107) Schrock, R. R.; Sancho, J.; Pederson, S. F. *Inorg. Synth.*; Kaesz, H. D., Ed.; John Wiley & Sons: New York; Vol. 26, pp 44-51.
- (108) Uhrhammer, R.; Crowther, D. J.; Olson, J. D.; Swenson, D. C.; Jordan, R. F. *Organometallics* **1992**, 11, 3098.
- (109) Uhrhammer, R.; Su, Y. X.; Swenson, D. C.; Jordan, R. F. *Inorg. Chem.* **1994**, 33, 4398.
- (110) Mashima, K.; Fujikawa, S.; Nakamura, A. *J. Am. Chem. Soc.* **1993**, 115, 10990.
- (111) Bazan, G. C.; Donnelly, S. J.; Rodriguez, G. *J. Am. Chem. Soc.* **1995**, 117, 2671.
- (112) Bazan, G. C.; Rodriguez, G. *Polyhedron* **1995**, 14, 93.

- (113) Sperry, C. K.; Cotter, W. D.; Lee, R. A.; Lachicotte, R. J.; Bazan, G. C. *J. Am. Chem. Soc.* **1998**, *120*, 7791.
- (114) Rodriguez, G.; Bazan, G. C. *J. Am. Chem. Soc.* **1995**, *117*, 10155.
- (115) Rodriguez, G.; Graham, J. P.; Cotter, W. D.; Sperry, C. K.; Bazan, G. C.; Bursten, B. E. *J. Am. Chem. Soc.* **1998**, *120*, 12512.
- (116) Rodriguez, G.; Sperry, C. K.; Bazan, G. C. *J. Mol. Catal. A-Chem.* **1998**, *128*, 5.
- (117) Mashima, K.; Fujikawa, S.; Urata, H.; Tanaka, E.; Nakamura, A. *J. Chem. Soc., Chem. Commun.* **1994**, 1623.
- (118) Spannenberg, A.; Fuhrmann, H.; Arndt, P.; Baumann, W.; Kempe, R. *Angew. Chem., Int. Ed. Engl.* **1998**, *37*, 3363.
- (119) Freundlich, J. S.; Schrock, R. R.; Davis, W. M. *J. Am. Chem. Soc.* **1996**, *118*, 3643.
- (120) Freundlich, J. S.; Schrock, R. R.; Davis, W. M. *Organometallics* **1996**, *15*, 2777.
- (121) Guérin, F.; McConville, D. H.; Payne, N. C. *Organometallics* **1996**, *15*, 5085.
- (122) Guérin, F.; McConville, D. H.; Vittal, J. J. *Organometallics* **1997**, *16*, 1491.
- (123) Guérin, F.; McConville, D. H.; Vittal, J. J. *Organometallics* **1996**, *15*, 5586.
- (124) Guérin, F.; Del Vecchio, G.; McConville, D. H. *Polyhedron* **1998**, *17*, 917.
- (125) Guérin, F.; McConville, D. H.; Vittal, J. J.; Yap, G. A. P. *Organometallics* **1998**, *17*, 5172.
- (126) Guérin, F.; McConville, D. H.; Vittal, J. J. *Organometallics* **1995**, *14*, 3154.
- (127) Guérin, F.; McConville, D. H.; Vittal, J. J.; Yap, G. A. P. *Organometallics* **1998**, *17*, 1290.
- (128) Cai, S.; Schrock, R. R. *Inorg. Chem.* **1991**, *30*, 4105.
- (129) Schrock, R. R.; Lee, J.; Liang, L.-C.; Davis, W. M. *Inorg. Chim. Acta* **1998**, *270*, 353.
- (130) Bradley, D. C.; Thomas, I. M. *Can. J. Chem.* **1962**, *40*, 1355.
- (131) Schrock, R. R.; Meakin, P. *J. Am. Chem. Soc.* **1974**, *96*, 5288.
- (132) Schrock, R. R. *J. Organomet. Chem.* **1976**, *122*, 209.
- (133) Juvinal, G. L. *J. Am. Chem. Soc.* **1964**, *86*, 4202.

- (134) Fowles, G. W. A.; Rice, D. A.; Wilkins, J. D. *J. Chem. Soc., Dalton Trans.* **1973**, 961.
- (135) Schrock, R. R.; Cummins, C. C.; Wilhelm, T.; Kol, M.; Lin, S.; Reid, S.; Davis, W. M. *Organometallics* **1996**, *15*, 1470.
- (136) Shannon, R. D. *Acta Crystallogr.* **1976**, *A32*, 751.
- (137) Dewan, J. C.; Edwards, A. J.; Calves, J. Y.; Guerchais, J. E. *J. Chem. Soc., Dalton Trans.* **1977**, 978.
- (138) Roesky, H. W.; Schruppf, F.; Noltemeyer, M. *J. Chem. Soc., Dalton Trans.* **1990**, 713.
- (139) Clark, H. C. S.; Cloke, F. G. N.; Hitchcock, P. B.; Love, J. B.; Wainwright, A. P. *J. Organomet. Chem.* **1995**, *501*, 333.
- (140) Horton, A. D.; de With, J.; van der Linden, A. J.; van de Weg, H. *Organometallics* **1996**, *15*, 2672.
- (141) Manzer, L. E. *Inorg. Synth.* **1982**, *21*, 135.
- (142) Schrock, R. R. *J. Am. Chem. Soc.* **1975**, *97*, 6577.
- (143) Schrock, R. R.; Sharp, P. R. *J. Am. Chem. Soc.* **1978**, *100*, 2389.
- (144) Neuner, B.; Schrock, R. R. *Organometallics* **1996**, *15*, 5.
- (145) Reid, S. M.; Neuner, B.; Schrock, R. R.; Davis, W. M. *Organometallics* **1998**, *17*, 4077.
- (146) Lee, J.; Schrock, R. R. , unpublished results.
- (147) Schrock, R. R.; Seidel, S. W.; Schrodi, Y.; Davis, W. M. *Organometallics* **1999**, *118*, 428.
- (148) Ruchardt, C. *Angew. Chem., Int. Ed. Engl.* **1970**, *9*, 830.
- (149) Carey, F. A.; Sundberg, R. J. *Advanced Organic Chemistry. Part A: Structure and Mechanisms.*; 2nd ed.; Plenum: New York, 1984, pp 640-641.
- (150) Scoles, L.; Minhas, R.; Duchateau, R.; Jubb, J.; Gambarotta, S. *Organometallics* **1994**, *13*, 4978.
- (151) Minhas, R. K.; Scoles, L.; Wong, S.; Gambarotta, S. *Organometallics* **1996**, *15*, 1113.
- (152) Hunter, W. E.; Hrnecir, D. C.; Bynum, V.; Penttila, R. A.; Atwood, J. L. *Organometallics* **1983**, *2*, 750.

- (153) Schrock, R. R. *Alkylidene Complexes of the Earlier Transition Metals*; Braterman, P. R., Ed.; Plenum: New York, 1986.
- (154) Lappert, M. F.; Milne, C. R. C. *J. Chem. Soc., Chem. Commun.* **1978**, 925.
- (155) Schaefer, W. P.; Quan, R. W.; Bercaw, J. E. *Acta Crystallogr. C-Cryst. Str.* **1993**, *49*, 878.
- (156) Schaefer, W. P.; Quan, R. W.; Bercaw, J. E. *Acta Crystallogr. C-Cryst. Str.* **1992**, *48*, 1610.
- (157) Yang, X.; Stern, C. L.; Marks, T. J. *J. Am. Chem. Soc.* **1991**, *113*, 3623.
- (158) Yang, X.; Stern, C. L.; Marks, T. J. *J. Am. Chem. Soc.* **1994**, *116*, 10015.
- (159) Hlatky, G. G.; Turner, H. W.; Eckman, R. R. *J. Am. Chem. Soc.* **1989**, *111*, 2728.
- (160) Hlatky, G. G.; Eckman, R. R.; Turner, H. W. *Organometallics* **1992**, *11*, 1413.
- (161) Freundlich, J.; Schrock, R. R.; Cummins, C. C.; Davis, W. M. *J. Am. Chem. Soc.* **1994**, *116*, 6476.
- (162) Albright, T. A.; Burdett, J. K.; Whangbo, M.-H. *Orbital Interactions in Chemistry*; John Wiley & Sons: New York, 1985, pp 381-401.
- (163) Cloke, F. G. N.; Hitchcock, P. B.; Love, J. B. *J. Chem. Soc., Dalton Trans.* **1995**, 25.
- (164) Horton, A. D.; de With, J. *J. Chem. Soc., Chem. Commun.* **1996**, 1375.
- (165) Schattenmann, F.; Schrock, R. R.; Davis, W. M. *Organometallics* **1998**, *17*, 989.
- (166) Friedrich, S.; Schubart, M.; Gade, L. H.; Scowen, I. J.; Edwards, A. J.; McPartlin, M. *Chem. Ber. Rec.* **1997**, *130*, 1751.
- (167) Hartwig, J. F. *Angew. Chem., Int. Ed. Engl.* **1998**, *37*, 2046.
- (168) Hong, Y.; Senanayake, C. H.; Xiang, T.; Vandenbossche, C. P.; Tanoury, G. J.; Bakale, R. P.; Wald, S. A. *Tetrahedron Lett.* **1998**, *39*, 3121.
- (169) Scollard, J. D.; McConville, D. H.; Vittal, J. J. *Organometallics* **1995**, *14*, 5478.
- (170) Johnson, A. R.; Wanandi, P. W.; Cummins, C. C.; Davis, W. M. *Organometallics* **1994**, *13*, 2907.
- (171) Bates, R. B.; Taylor, S. R. *J. Org. Chem.* **1993**, *58*, 4469.

- (172) Schrock, R. R.; McConville, D. H. , collaborative results with Exxon Chemical Corporation.
- (173) Friedrich, S. G. L. E. A. M. M. *J. Chem. Soc., Dalton Trans.* **1993**, 2861.
- (174) Jordan, R. F.; Bajgur, C. S.; Scott, B.; Willett, R. *J. Am. Chem. Soc.* **1986**, *108*, 7410.
- (175) Jordan, R. F.; Dasher, W. E.; Echols, S. F. *J. Am. Chem. Soc.* **1986**, *108*, 1718.
- (176) Bochmann, M.; Lancaster, S. J.; Hursthouse, M. B.; Malik, K. M. A. *Organometallics* **1994**, *13*, 2235.
- (177) Gomez, R.; Green, M. L. H.; Haggitt, J. L. *J. Chem. Soc., Chem. Commun.* **1994**, 2607.
- (178) Gomez, R.; Green, M. L. H.; Haggitt, J. L. *J. Chem. Soc., Chem. Commun.* **1996**, 939.
- (179) von H. Spence, R. E.; Parks, J. D.; Piers, W. E.; MacDonald, M.-A.; Zaworotko, M. J.; Rettig, S. J. *Angew. Chem., Int. Ed. Engl.* **1995**, *34*, 1230.
- (180) Pauling, L. *The Nature of the Chemical Bond.*; 3rd ed.; Cornell University Press: Ithaca, N.Y., 1960, p 93.
- (181) Allred, A. L. *J. Inorg. Nucl. Chem.* **1961**, *17*, 215.
- (182) Lochmann, L.; Trekoval, J. *J. Organomet. Chem.* **1987**, *326*, 1.

Acknowledgments

First of all, I would like to thank Professor Richard Schrock for being providing me an excellent environment for doing chemistry and showing me the way he does science with careful attitude and great enthusiasm, which has been truly inspiring to me for the last four years. I believe that what I learned from Dick will continue to reward me by not only enjoying fundamentally important chemistry but also directing it to a practical application. It is Dick who shows me how to approach scientific questions from the very basic foundation. I would also like to thank him for bringing lots of intelligent chemists into his group. Discussion about chemistry with people in the Schrock group is always enjoyable.

I would like to thank my thesis committee, Professors Stephen Lippard and Christopher Cummins, for an instructive defense. I not only saw the way they thought of a question from my thesis, but also knew what would be potentially interesting chemistry stemming from my research results.

Thanks to my first Inorganic Chemistry mentor, Professor Wen-Shu Hwang, who showed me how interesting and important Organometallic Chemistry can be. I knew I would pursue the chemistry further after his guidance. It was also him who encouraged me to come to MIT. Thanks goes to Professors Dick Schrock, Kit Cummins, Alan Davison, Dietmar Seyferth, and Hans-Conrad zur Loye for providing classes in my first year at MIT. Being a TA with Professors Robert Field, Allen Davison, and Kit Cummins is an wonderful experience. Thanks also to 5.11 TAs in the Fall of 1995, I would never forget the heart-warming card and gift they prepared for my son, Jia-Yu.

I would also like to thank Dr. William Davis for solving all the crystal structures in my thesis. Thanks to Ms. Li Li for her operation of the High Resolution Mass Spectrometer. Drs. Jesse Lee and David Graf were my first two labmates. I am grateful for working with them. Without knowing anything about handling the drybox before I came, I have been used to doing oxygen- and moisture-sensitive chemistry in these years, thanks to them. Dave was also a terrific English mentor, who showed me slang English and American culture which I did not really know that much about. Drs. Tim Warren, Scott Seidel, Robert Baumann, and Arturo Casado are all great chemists to talk to. Discussion with them is usually informative. Thanks to John Alexander; John and I are Dick's twin students. We came together, we leave together. Good luck at Cornell. Denyce Wicht, Sherry Zhu, Hsiu-Fu Hsu, Jennifer Jamieson, and Jonathan Goodman deserve the credit for proofreading my thesis. Thanks also goes to Sarah Aeilts, Parisa Mehrkhodavandi, and Connie Lu, who shared the same lab space with me in the last several months. Thanks to Gretchen

Kappelmann, who has been doing a terrific job in getting administrative things done. I was grateful for the home-made dessert from her for my 4th-year seminar, although I actually did not get a chance to try a piece. Special thanks to Denyce for spending time playing with my son. Inside the Chemistry Department, I would like to thank Susan Brighton and Launa Johnston for being really helpful in providing information when I first came. I was also really excited when I heard two more students coming from my hometown in 1997. Good luck to James Tsai and Bruce Yu. I would also like to thank everyone I met in the past four years both inside and outside the Schrock group. Life could have been boring without you all. Thanks to everyone.

My research would not go well if my ordinary life did not get balanced. I would like to sincerely thank my wife, Hsiu-Ling, for her long-term support and care for what I like to pursue, which is always encouraging to me. My son, Jia-Yu, has been a mature boy to understand when I need to work, although he is only 3 years and 9 months old. Thanks also to Yi-Shan Yang for being a long-term friend of ours and caring for Jia-Yu. He really enjoys reading the books she sent. Thanks to Jane Chang for providing me information I needed before I came to MIT. Yung-Chin Hsiao showed me around the MIT and helped me settle down when I came, which is really appreciated. Special thanks to Chih-Jen Sun and Philip Chao. I will never forget the three of us working together in the Army and applying together for graduate schools in the US, then coming together for the advanced study. Chih-Hao Ho, Long-Sheng Kuo, Bruce Kuo, Ginger Wang, Chien-Ning Yu, Jung-Chi Liao, Jiun-Yu Lai, and Yu-Hsuan Su have been good friends of ours in the MIT community. Good luck to you all.

I would like to regard this thesis as a remark for my staying at MIT. I would also like to expand the spirit that I learned from here to my entire career. After all, I would like to thank my Dad, Mom, brothers, and my only sister from the bottom of my heart. Without their love and care, the journey to my career goal would not be so fruitful.

Lan-Chang Liang
Cambridge, Massachusetts
June 28, 1999